NOUS TERMOESTABLES EPOXÍDICS MODIFICATS AMB ESTRUCTURES DENDRÍTIQUES DE TIPUS HIPERRAMIFICAT I ESTRELLA

Mireia Morell Bel

Dipòsit Legal: T. 155-2012

UNIVERSITAT ROVIRA I VIRGILI
NOUS TERMOESTABLES EPOXÍDICS MODIFICATS AMB ESTRUCTURES DENDRÍTIQUES DE TIPUS HIPERRAMIFICAT I ESTRELLA
Mireia Morell Bel
DL:T. 155-2012

UNIVERSITAT ROVIRA I VIRGILI
NOUS TERMOESTABLES EPOXÍDICS MODIFICATS AMB ESTRUCTURES DENDRÍTIQUES DE TIPUS HIPERRAMIFICAT I ESTRELLA
Mireia Morell Bel
DL:T. 155-2012

Mireia Morell i Bel

NOUS TERMOESTABLES EPOXÍDICS MODIFICATS AMB ESTRUCTURES DENDRÍTIQUES DE TIPUS HIPERRAMIFICAT I ESTRELLA

TESI DOCTORAL

dirigida per la Dra. Àngels Serra i Albet i
el Dr. Xavier Ramis i Juan

Departament
de Química Analítica i Orgànica

UNIVERSITAT ROVIRA I VIRGILI

Tarragona, Octubre del 2011

UNIVERSITAT ROVIRA I VIRGILI
NOUS TERMOESTABLES EPOXÍDICS MODIFICATS AMB ESTRUCTURES DENDRÍTIQUES DE TIPUS HIPERRAMIFICAT I ESTRELLA
Mireia Morell Bel
DL:T. 155-2012

UNIVERSITAT ROVIRA I VIRGILI

DEPARTAMENT DE QUIMICA ANALITICA I QUIMICA ORGANICA

C/ Marcel.lí Domingo s/n
Campus Sescelades
43007 Tarragona
Tel. 34 977 55 97 69
Fax 34 977 55 84 46
e-mail: secqaqo@urv.net

La Dra. Àngels Serra i Albet, catedràtica d'Universitat del Departament de Química Analítica i Orgànica de la Universitat Rovira i Virgili i el Dr. Xavier Ramis i Juan, catedràtic d'Universitat del Departament de Màquines i Motors Tèrmics de la Universitat Politècnica de Catalunya, CERTIFIQUEN QUE:

La Mireia Morell i Bel, llicenciada en Química per la Universitat de Girona, ha desenvolupat sota la nostra supervisió i direcció el treball d'investigació que porta per nom:

"Nous termoestables epoxídics modificats amb estructures dendrítiques de tipus hiperramificat i estrella"

que es presenta en aquesta memòria per optar al Grau de Doctor en Química amb Menció Europea.

I perquè consti a efectes legals, signen aquest certificat.

Tarragona, 20 d'Octubre de 2011

Dra. Àngels Serra i Albet Dr. Xavier Ramis i Juan

UNIVERSITAT ROVIRA I VIRGILI
NOUS TERMOESTABLES EPOXÍDICS MODIFICATS AMB ESTRUCTURES DENDRÍTIQUES DE TIPUS HIPERRAMIFICAT I ESTRELLA
Mireia Morell Bel
DL:T. 155-2012

UNIVERSITAT ROVIRA I VIRGILI
NOUS TERMOESTABLES EPOXÍDICS MODIFICATS AMB ESTRUCTURES DENDRÍTIQUES DE TIPUS HIPERRAMIFICAT I ESTRELLA
Mireia Morell Bel
DL:T. 155-2012

AGRAÏMENTS

Tot va començar un bon dia que em vaig convèncer a mi mateixa: "has de ser valenta Mireia". Amb tan sols una petita empenta de la meva família ja estava preparant les maletes per començar una nova etapa, lluny d'ells, dels meus amics i de la meva ciutat. Doncs bé, ja han passat casi quatre anys des d'aquell moment i avui estic escrivint aquestes línies que posen punt i final a aquell viatge. Haig de reconèixer que no ha estat tan difícil, al final ha resultat ser una experiència única i enriquidora tan professionalment com personal.

És per aquests bons anys que he passat fent el doctorat que voldria donar les gràcies a la Universitat Rovira i Virgili i especialment al Grup de Polímers. He disposat de nombrosos recursos i de bons equipaments sense els quals no hagués realitzat en tan bones condicions aquest treball. En segon lloc, estic sincerament agraïda d'haver estat acompanyada en aquest trajecte d'un enorme grup de bons professionals i magnífiques persones. És per això, que no vull acomiadar-me de tots ells sense escriure'ls una petita mostra de tot el meu agraïment.

Per mil raons m'agradaria donar les gràcies als meus directors de tesi, la Dra. Àngels Serra i el Dr. Xavier Ramis. Els agraeixo que m'hagin iniciat en aquest esplèndid i difícil món de la investigació. Gràcies per trobar tots els moments dins i fora la universitat per discutir i resoldre qualsevol dubte que tingués per petit fos. Gràcies per la confiança, la llibertat i el recolzament científic que m'heu mostrat quan he emprés certs camins, crec que fer un doctorat requereix iniciativa pròpia. Finalment, també us vull agrair la paciència, la comprensió i l'empatia que m'heu mostrat al llarg d'aquests anys, sobretot en l'últim tram del doctorat que per certes circumstàncies se m'ha fet una mica més feixuc del compte.

També m'agradaria mostrar el meu agraïment al Dr. Francesc Ferrando del Departament d'Enginyeria Mecànica de l'Escola Tècnica Superior d'Enginyeria Química (ETSEQ) per omplir de coneixement el racó de la física de polímers que tan se'ns escapa als químics.

Vull donar les gràcies a la resta de professors del Grup de Polímers de la URV, la Dra. Ana Mantecón, el Dr. Toni Reina, la Dra. Virgina Cádiz, la Dra. Marina Galià, el Dr. Joan Carles Ronda i el Dr. Gerard Lligadas. I també, als professors del Grup de Sucres completant l'Àrea de Química Orgànica, el Dr. Sergio Castillón, la Dra. Yolanda Díaz i la Dra. Maribel Matheu per la seva cordialitat.

I would like to thank Prof. Brigitte Voit, Dr. Albena Lederer and Dr. Hartmut Komber from the Leibniz-Institut für Polymerforshung (Dresden) for giving me the possibility to be part of IPF for several months and learn a lot about polymer synthesis and characterization. Of

course thanks also for your good scientific advices and for the great experience I lived when I was there.
Of course, I cannot forget my Russian friend Dr. Anna Khalyavina for her kindly attention and for being part of my life since my stay in Dresden. Big thanks also to Susanne Boye, Dr. Michael Erber, Ulrike Georgi, Frank Däbritz and the rest of the staff for helping me in every problem I had and for being so kind with me.

Gràcies a tots els companys de l'Àrea de Química Orgànica, tan els que encara hi són com els que ja han marxat. Especialment a la Marta i la Marisa, per haver compartit els meus primers anys doctorat i fer-me de "germanes grans" al pis; a la Mercè, en Lucas i en Quique; a la Patri i en David, a tots dos, per animar els dinars a la ETSE durant els meus inicis; a en Javi, pel seu bon rotllo; a l'Isidre i en Pep. I gràcies també als nou vinguts per suportar-me durant l'última etapa de la tesi: l'Asta, en Suryakant, en Camilo, la Mariluz, la Zeinep, l'Asev, la Cristina, sempre recordaré aquell JIP plujós acompanyades d'un molt bon ambient i del "Tuneti"; a en Rodolfo, por ser uno de mis favoritos y el que mejor baila; y l'Adrián, por saber ir por la vida poco a poco, tengo que aprender más de ti en ese aspecto.

A més a més, vull agrair especialment aquells companys del Laboratori 330 amb els que he compartit moments de tots colors i amb els que sempre he trobat suport. Silvana gràcies per compartir alegries i penes i per escoltar-me quan ho he necessitat, desitjo que acabis el doctorat perquè t'ho mereixes i que siguis molt feliç amb el petit Marco. Marjorie eres una gran amiga y te deseo lo mejor a ti y al capitán Enrique. Xavier gràcies per estar sempre disposat a treballar i a discutir sobre els comportaments extranys que molt sovint presenten els materials. Cristina hace poco que estás por aquí pero te he cogido mucho cariño y espero que cojas con fuerza este camino que es el doctorado y que te vaya muy bien. David, que t'haig de dir a tu? Jo crec que gaire res que no t'hagi dit ja. Saps que has sigut molt important per mi. Tu vas ser el primer en acollir a "la Gironina", a treure-la a passejar per Tarragona i ser el primer en escoltar "anem cap *allà*" o "*en* Busi", vaja a escoltar el català de veritat. Has sabut aguantar-me en les meves crisis existencials i jo finalment, he pogut lidiar amb el teu desordre al laboratori. Crec que mai hagués pogut desitjar tenir un company de doctorat millor que tu així que saps perfectament que et trobaré a faltar moltíssim i et desitjo tot el millor en la teva nova etapa a Itàlia.

Finalment i amb moltíssima estima m'agradaria donar les gràcies a les meves amigues Irene (la "sucrera") i Cristina (la "quimiomètrica") per ser això: amigues. Per estar allà sempre que ho he necessitat, escoltant els meus dubtes i les meves inquietuds. Per compartir aquells moments en els que tot era negre i el camí cap a la tesi semblava una tortura. Per motivar-nos mútuament i compartir alegries i èxits. Per intentar dilucidar el

nostre futur dins i fora de la URV. Simplement, gràcies per haver entrat a la meva vida i estar al meu cantó en aquest moment.
També vull mencionar especialment,
A les meves químiques, Ester, Alícia, Imma i Àngels pels anys que portem juntes i que tot i estar lluny de vosaltres durant aquests últims anys no us heu oblidat mai de mi. Espero que continuem juntes molts més anys.
A l'Albert, per trobar sempre algun foradet per veure'ns quan pujava a Girona i preocupar-se per mi.
A l'Anna per preguntar-me sempre com m'anava i a la Gemma per donar-me tot el suport i oferir-se a dissenyar la meravellosa portada d'aquesta tesi.
Als pares d'en Pau, Maria i Narcís, pel seu interès i les mostres d'ànim que he rebut sempre.
A la colla d'amics, en Carles, els Xaviers Pont i Bonet, la Bibi, l'Esther, l'Adrià, l'Albert Morera, l'Anna i l'Edu per interessar-se per l'evolució d'aquesta tesi en cada sopar o trobada que hem fet.

I per acabar, un agraïment molt especial a la meva família i sobretot als meus pares, Josep Maria i Montserrat, que sempre m'han recolzat en cada decisió que he pres. M'heu ensenyat que només treballant i amb sacrifici s'aconsegueixen les coses i que no m'ha de fer por el que vingui sinó el que ja no pugui tornar mai més. M'heu ensenyat anar endavant i així ho estic fent. Gràcies al meu germà el qual li tinc una admiració especial pel talent que té i per la bona persona que és, no canviïs mai Albert. També donar les gràcies a la meva àvia Encarna per la seva preocupació envers el meu futur i pels seus ànims. I un record especial als meus avis Pepita, Josep Maria i Bernat a qui sempre tindré presents, que si haguessin pogut veure aquesta tesi de ben segur haguessin estat orgullosos de mi. I, finalment, donar les gràcies a en Pau per estar al meu costat any rere any, mes a mes, dia a dia. Gràcies per creure en mi, per animar-me a ser cada dia millor amb el què faig i per estimar-me tant.

Si ara hagués de tornar enrere, no en tinc cap dubte, de ben segur que tornaria a preparar les maletes.

Moltes gràcies a tots,

Mireia

UNIVERSITAT ROVIRA I VIRGILI
NOUS TERMOESTABLES EPOXÍDICS MODIFICATS AMB ESTRUCTURES DENDRÍTIQUES DE TIPUS HIPERRAMIFICAT I ESTRELLA
Mireia Morell Bel
DL:T. 155-2012

UNIVERSITAT ROVIRA I VIRGILI
NOUS TERMOESTABLES EPOXÍDICS MODIFICATS AMB ESTRUCTURES DENDRÍTIQUES DE TIPUS HIPERRAMIFICAT I ESTRELLA
Mireia Morell Bel
DL:T. 155-2012

UNIVERSITAT ROVIRA I VIRGILI
NOUS TERMOESTABLES EPOXÍDICS MODIFICATS AMB ESTRUCTURES DENDRÍTIQUES DE TIPUS HIPERRAMIFICAT I ESTRELLA
Mireia Morell Bel
DL:T. 155-2012

ÍNDEX

UNIVERSITAT ROVIRA I VIRGILI
NOUS TERMOESTABLES EPOXÍDICS MODIFICATS AMB ESTRUCTURES DENDRÍTIQUES DE TIPUS HIPERRAMIFICAT I ESTRELLA
Mireia Morell Bel
DL:T. 155-2012

CAPÍTOL

Introducció general i objectius

UNIVERSITAT ROVIRA I VIRGILI
NOUS TERMOESTABLES EPOXÍDICS MODIFICATS AMB ESTRUCTURES DENDRÍTIQUES DE TIPUS HIPERRAMIFICAT I ESTRELLA
Mireia Morell Bel
DL:T. 155-2012

I.1 INTRODUCCIÓ GENERAL

Els polímers termoestables són materials de gran interès i amb una àmplia versatilitat en el món industrial degut a les seves excel·lents propietats elèctriques, mecàniques i tèrmiques. Es solen formar a través d'una reacció de curat a partir de precursors multifuncionals de baix pes molecular generant-se xarxes polimèriques entrecreuades. Els materials que n'esdevenen resulten insolubles i infusibles [1].

I.1.1 Conceptes generals dels materials termoestables epoxídics

La primera síntesi d'una reïna epoxi basada en el bisfenol A va ser descrita pel suís P. Castan i el nord-americà S.O. Greenlee el 1936 [2]. El diglicidilèter de bisfenol A (DGEBA) va esdevenir la primera reïna epoxi comercial el 1940 i des de llavors ha estat una de les més emprades industrialment. La seva principal via d'obtenció es basa en fer reaccionar bisfenol A amb epiclorohidrina en medi bàsic fort [3]. En funció de la relació epiclorohidrina/bisfenol A emprada es poden obtenir pre-polímers amb diferent grau de polimerització (*n*).

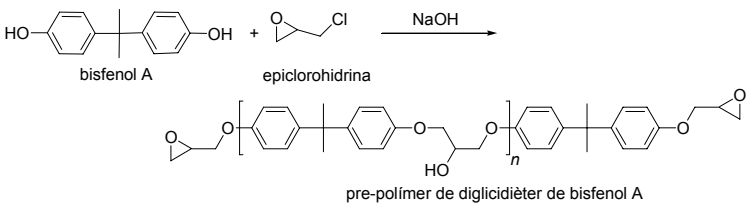

Esquema I-1 Obtenció de la reïna de diglicidilèter de bisfenol A

Les reïnes epoxi constitueixen uns dels materials termoestables més emprats avui en dia doncs presenten múltiples aplicacions en recobriments, adhesius i en la fabricació de compòsits (mescles de reïnes epoxi amb fibres, generalment de vidre o carboni) [4].

I.1.2 Mecanismes de polimerització en termoestables epoxídics

Les reïnes epoxi poden polimeritzar a través de dos mecanismes, la polimerització per passos i la polimerització en cadena.

La polimerització per passos procedeix a través de reaccions elementals, pas a pas, entre els grups oxirà de la reïna i el grups reactius de l'agent de curat multifuncional. En aquests casos, els agents de curat, que poden ser amines

[1] Stevens, M.P., *Polymer Chemistry. An Introduction*, 2nd ed., Oxford University Press, Oxford, **1990**.
[2] Lee, H., Neville, K., *Handbook of Epoxy Resins*, McGraw-Hill, New York, **1967**.
[3] Potter, W.G., *Epoxy Resins* Plastic Institute, New York, **1970**.
[4] May, C. A., ed., *Introduction to Epoxy Resins* in *Epoxy Resins Chemistry and Technology*, 2nd ed., Marcel Dekker, New York, **1988**.

primàries o secundàries, alcohols, àcids, anhídrids o isocianats, entre d'altres, són emprats en quantitats estequiomètriques o properes a l'estequiomètrica ja que actuen com a reactiu donant lloc a l'entrecreuament de les molècules de reïna a través d'ells mateixos.

En canvi, la propagació a través d'un mecanisme de polimerització en cadena és degut a la reacció directa d'una espècie (iniciador), en proporcions catalítiques, amb una molècula de monòmer. L'iniciador, que sol ser un catió o un anió, queda unit a l'extrem i es converteix en un cadena de polímer en creixement (centre actiu) que es va alimentant de molècules de reïna presents al medi.

El sistema més clàssic d'obtenció de termoestables epoxídics és mitjançant la polimerització per passos, concretament emprant com a agent de curat una diamina primària [5].

Després de les amines, els anhídrids són els reactius més emprats per curar reïnes epoxi. Entre els anhídrids més comuns destaquen, l'anhídrid ftàlic (PA), l'anhídrid tetrahidroftàlic (THPA), l'anhídrid metil nàdic (NMA) i l'anhídrid metiltetrahidroftàlic (MTHPA) les estructures dels quals es mostren a l'**Esquema I-2**.

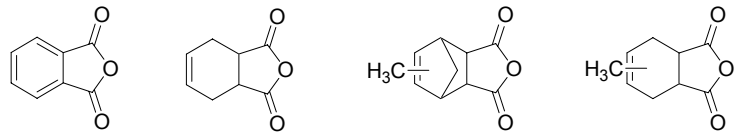

Esquema I-2 Estructures químiques dels anhídrids més emprats com agents de curat

La reacció directa d'aquests compostos amb reïnes epoxi no és ràpida. La reacció de policondensació, sense la presència d'un catalitzador es duu a terme a temperatures elevades (entre 190 i 310 ºC), normalment acompanyada d'una certa degradació tèrmica del material [6]. Per aquesta raó, es sol requerir la presència d'un accelerador per tal de facilitar el procés com poden ser traces d'aigua, o bé grups reactius com ara hidroxils, amines terciàries o imidazoles.

A l'**Esquema I-3** es mostra el mecanisme de reacció del curat d'un sistema epoxi/anhídrid sense catalitzador. Com es pot observar és un procés complex que s'inicia amb la presència de grups hidroxil en el medi (**A**). La propagació es duu a terme per reacció de l'intermedi contenint un grup àcid carboxílic format amb un anell oxirà (**B**) i continua per reacció de grups hidroxil formats o existents al medi

[5] Pascault, J. P., Sautereau, H., Verdu, J., Williams, R. J. J., *Chemistry of Crosslinked Polymer Synthesis* in *Thermosetting Polymers*, Marcel Dekker, New York, **2002**.
[6] Montserrat, S.; Flaqué, C.; Calafell, M.; Andreu, G.; Málek, J. *Influence of the accelerator concentration on the curing reaction of an epoxy-anhydride system* Termochim. Acta **1995**, 269, 213-229.

amb una molècula d'anhídrid (**C**). A més a més, existeixen reaccions laterals que poden ocòrrer durant el procés. Concretament és el cas de l'eterificació produïda per grups hidroxils formats o existents al medi (**D**).

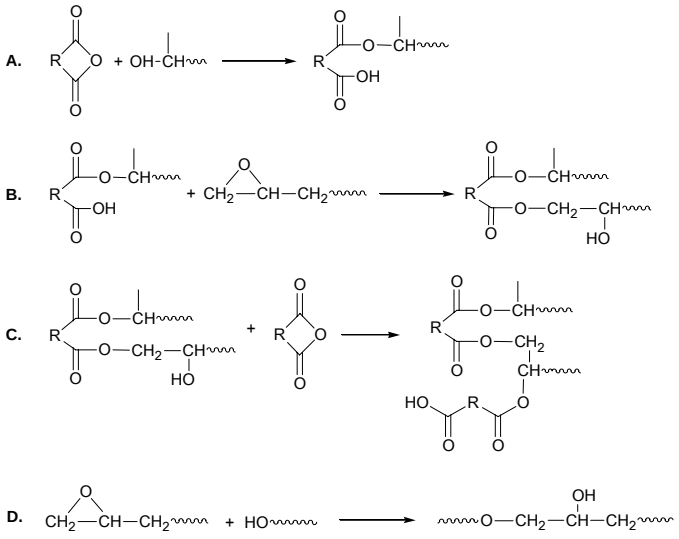

Esquema I-3 Mecanisme de reacció d'un sistema epoxi/anhídrid no catalitzat [7]

Com s'ha comentat anteriorment, la reactivitat d'un sistema simple epoxi/anhídrid és lenta. Per tant, l'addició d'un catalitzador en una proporció d'un 0.5 a un 3 % en pes ajuda a reduir el temps de curat i per tant a prevenir la degradació del termoestable [8].

El mecanisme catalitzat (**Esquema I-4**), es produeix a través d'una polimerització en cadena. En primer lloc, el catalitzador, com per exemple una amina terciària, reacciona amb un anell oxirà per formar un intermedi zwitteriònic contenint un catió amoni i un anió alcòxid (**A**). Aquest, ràpidament reacciona amb una molècula d'anhídrid generant un grup carboxilat (**B**). La propagació té lloc a través de la reacció entre el grup carboxilat de l'espècie formada i un altre grup epoxi formant-se un grup alcòxid nou (**C**). Aquesta espècie pot començar una reacció de copolimerització alternada (**D**). No existeixen evidències clares respecte a l'etapa de terminació de la polimerització i si l'amina terciària queda permanentment enllaçada durant el transcurs de la reacció. Alguns autors

[7] Rocks, J.; Rintoul, L.; Vohwinkel, F.; George, G. *The kinetics and mechanism of cure of an amino-glycidyl epoxy resin by a co-anhydride as studied by FT-Raman spectroscopy* Polymer **2004**, 45, 6799-6811.
[8] Petrie, E.M. *Epoxy adhesive formulations* McGraw-Hill, New York, **2006**.

descriuen l'enllaç permanent d'aquesta [9] mentre que altres contradiuen aquest fet [10].

Depenent de la proporció d'amina terciària emprada així com de les condicions de curat seleccionades, el procés no catalitzat pot competir amb el procés catalitzat.

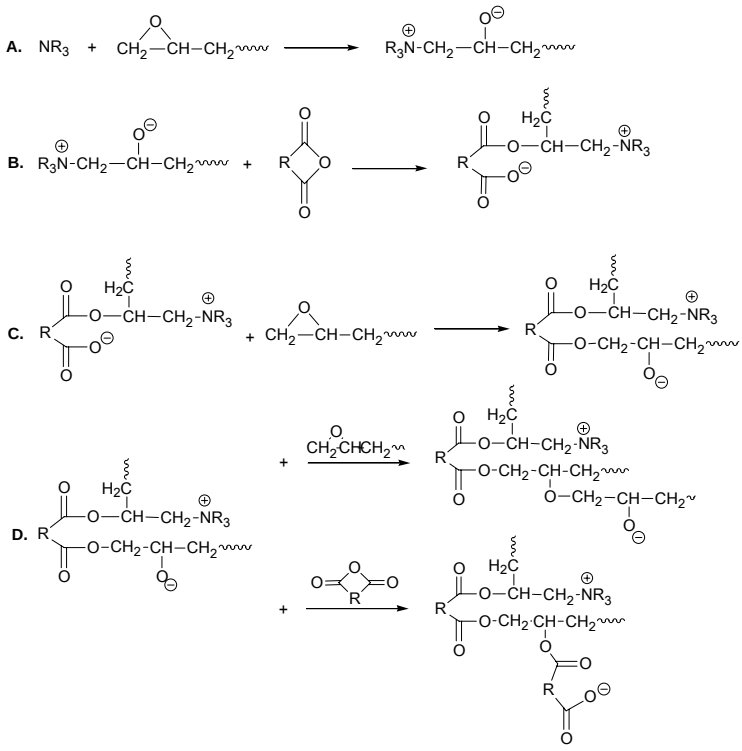

Esquema I-4 Mecanisme de reacció d'un sistema epoxi/anhídrid catalitzat per una amina terciària

Una altra manera d'obtenir materials termoestables a partir de reïnes epoxi consisteix en la reacció d'eterificació per obertura d'anell, mitjançant polimerització catiònica (tèrmica o fotoquímica) o aniònica. En la present tesi, només es farà referència al curat tèrmic emprant iniciadors catiònics i aniònics.

Pel que fa a la polimerització catiònica [11], l'espècie en propagació està formada per un ió oxoni, on l'electrofília dels dos carbonis de l'anell es veu

[9] Leukel, J.; Burchard, W.; Krüguer, R.P.; Munch H.; Schulz, G. *Mechanism of the anionic copolymerization of anhydride-cured epoxies – analyzed by matrix-assisted laser desorption ionization time-of-flight mass spectrometry (MALDI-TOF-MS)* Macromol. Rapid. Commun. **1996**, 17, 359-366.
[10] Fedtke, M.; Domaratius, F. *Curing of epoxide resins by anhydrides of dicarboxylic acids: model reactions* Polym. Bull. **1986**, 15, 13-19.

augmentada de tal manera que poden ser atacats per l'oxigen oxiránic d'una altra unitat monomèrica, tot i la seva pobra nucleofília, o pel parell d'electrons d'un oxigen d'una altra espècie present en el medi de reacció. L'atac nucleòfil pot realitzar-se sobre ambdós carbonis de l'anell (posicions *α* i *β*). No existeix una preferència clara de l'atac nucleòfil sobre el carboni menys substituït ja que en la propagació de la cadena el mecanisme adoptat és el S_N2 border-line (**Esquema I-5**).

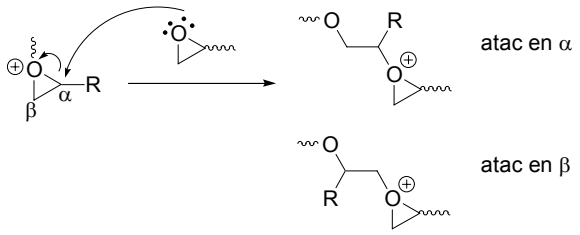

Esquema I-5 Polimerització catiònica de compostos epoxídics

Aquest mecanisme es dóna quan s'usen iniciadors amb un fort caràcter d'àcid de Brönsted, l'anió dels quals no ha de ser bon nucleòfil com per exemple el bisulfat, el perclorat o el bifosfat. També quan s'usen àcids de Lewis els quals poden actuar sols o conjuntament amb un compost pròtic que actuï de coiniciador. Un dels iniciadors més emprats en polimeritzacions catiòniques de compostos epoxídics és el sistema BF_3·amina on en aquest cas l'amina actua de coiniciador cedint un protó [12]. Els inconvenients que presenta l'ús d'aquest sistema és la seva elevada higroscòpia que fa que es deteriorin les propietats elèctriques dels materials sobretot a temperatures i humitats elevades. A més a més, els materials obtinguts presenten una elevada fragilitat.

Alternativament el nostre grup de recerca ha desenvolupat uns agents de curat catiònics nous com són els triflats de terres rares. Aquests iniciadors són àcids de Lewis molt forts degut a l'acidesa del catió la qual es veu potenciada pel caràcter electroatraient que presenta el grup trifluorometansulfonil $(OTf)_3$ [13]. Els cations lantànids (Ln(III)) són durs segons la terminologia de Pearson i presenten una elevada capacitat de coordinació [14].

[11] May, C. A., ed., *Curing Reactions* in *Epoxy Resins Chemistry and Technology*, 2nd ed., Marcel Dekker, New York, **1988**.
[12] Ghaemy, M.; Khandani, M.H. *Kinetics of curing reaction of DGEBA with BF_3-amine complexes using isothermal DSC technique* Eur. Polym. J. **1998**, 34, 477-486.
[13] Kobayashi, S. *Lanthanides: Chemistry and Use in Organic Synthesis*, Springer, Berlin, **1999**.
[14] a) Pearson, R.G. *Hard and soft acids and bases* J. Am. Chem. Soc. **1963**, 85, 3533-3539. b) Kobayashi, S.; Hachiya, I. *Lanthanide triflates as water-tolerant Lewis acids. Activation of commercial formaldehyde solution and use in the aldol reaction of silyl enol ethers with aldehydes in aqueous media* J. Org. Chem. **1994**, 59, 3590-3596.

Aquest catalitzadors presenten certs avantatges respecte altres àcids de Lewis com el $AlCl_3$, BF_3 o el $TiCl_4$ com ara:

- Són tolerants a l'aigua doncs no reaccionen ni es desactiven en medis aquosos [14b].
- Són estables a l'aire.
- Són relativament solubles en dissolvents orgànics, la qual cosa permet obtenir mescles homogènies.
- Presenten una toxicitat menor que la dels triflats de metalls de transició i similar a la dels metalls alcalins.

En treballs anteriors del nostre grup es va realitzar un estudi de l'activitat de diferents triflats de lantànid en la polimerització del diglicidilèter de bisfenol A (DGEBA) i es va poder observar que el procés de curat esdevenia més eficaç que l'ús del sistema convencional BF_3·amina [15].

És conegut que les reïnes epoxi homopolimeritzen per via catiònica a través de dos mecanismes: el propagació a través del monòmer activat (AM) i el de final de cadena activa (ACE) [16] tal com es mostra a l'**Esquema I-6**. El primer és un mecanisme el qual requereix la presència de grups hidroxil al medi per tal de reaccionar amb un monòmer activat generant un catió oxoni secundari amb un hidrogen actiu. Posteriorment aquest catió transfereix un protó a un altre monòmer donant lloc a un altre monòmer actiu, produint-se una transferència de cadena. El procés pot continuar per reacció del monòmer actiu per propagació mitjançant el mecanisme ACE o bé pot tornar a reaccionar amb una altre compost hidroxíl·lic. El mecanisme ACE per la seva banda, es basa en la propagació de la reacció de polimerització a través d'un catió oxoni que és atacat pel parell d'electrons d'un oxigen oxiránic.

[15] a) Castell, P.; Galià, M.; Serra, A.; Salla, J.M.; Ramis, X. *Study of lanthanide triflates as new curing initiators for DGEBA* Polymer **2000**, 41, 8465-8474. b) García, S.J.; Ramis, X.; Serra, A.; Suay, J. *Addition effect of erbium (III) trifluoromethanesulfonate in the homopolymerization kinetics of a DGEBA resin* Termochim. Acta **2006**, 441, 45-52. c) García, S.J.; Ramis, X.; Serra, A.; Suay, J. J. *Cationic crosslinking of solid DGEBA resins with ytterbium(III) trifluoromethanesulfonate as initiator* J. Therm. Anal. Calorim. **2006**, 83, 429-438.
[16] Kubisa, P.; Penczek, S. *Cationic activated monomer polymerization of heterocyclic monomers* Prog. Polym. Sci. **1999**, 24, 1409-1437.

Monòmer Activat - AM

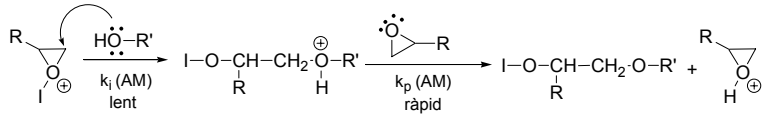

Final de cadena actiu - ACE

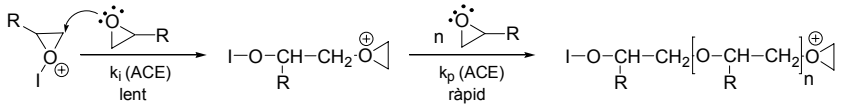

Esquema I-6 Mecanisme de propagació a través del monòmer activat – AM i mecanisme de final de cadena activa – ACE en l'homopolimerització catiònica de reïnes epoxi

La competència entre els mecanismes AM i ACE ve determinada per les concentracions relatives de monòmer epoxi i d'agents de transferència com ara aigua o compostos hidroxílics en general. S'accepta que, durant la polimerització de grups epoxi, aquest balanç és més favorable cap al mecanisme AM a conversions altes, degut a la baixa concentració de grups epoxi sense reaccionar [16]. Tanmateix també s'ha observat que el mecanisme AM pot tenir lloc a l'inici del procés i pot estar afavorit per un augment en la proporció d'iniciador i de grups hidroxil al medi [17].

Dels diferents triflats de lantànid que s'han utilitzat en treballs anteriors al grup de recerca, com ara el $Sm(OTf)_3$, el $Yb(OTf)_3$ o el $La(OTf)_3$ val a dir que el $Yb(OTf)_3$ és el que més accelera el procés de curat i per tant el que permet dur a terme el curat isotèrmic a temperatures més baixes [18]. Aquests fet es pot atribuir a la major acidesa de Lewis i duresa de Pearson del Yb^{3+} en comparació amb els altres cations [14a]. A més a més, els materials obtinguts emprant el $Yb(OTf)_3$ presenten valors superiors de T_g als obtinguts emprant el $La(OTf)_3$ i una degradabilitat tèrmica també superior [19]. Per aquestes raons, en la present tesi únicament s'ha fet ús d'aquest iniciador quan la via d'obtenció dels materials termoestables seleccionada ha sigut la polimerització catiònica.

Pel que fa a la polimerització aniònica es dóna quan intervenen iniciadors amb fort caràcter nucleòfil o amb fortes característiques bàsiques. Entre els iniciadors aniònics més emprats en el curat de reïnes epoxi trobem les amines

[17] a) Matejka, L.; Chabanne, P.; Tighzert, L.; Pascault, J.P. *Cationic polymerization of diglycidyl ether of bisphenol A* J. Polym. Sci., Part A: Polym. Chem. **1994**, 32, 1447-1458. b) Salla, J.M.; Fernández-Francos, X.; Ramis, X.; Mas, C.; Mantecón, A.; Serra, A. *Influence of the proportion of ytterbium triflate as initiator on the mechanism of copolymerization of DGEBA epoxy resin and γ-butyrolactone* J. Therm. Anal. Calorim. **2008**, 91, 385-393. c) Foix, D.; Erber, M.; Voit, B.; Lederer, A.; Ramis, X.; Mantecón, A.; Serra, A. *New hyperbranched polyester modified DGEBA thermosets with improved chemical reworkability* Polym. Degrad. Stab. **2010**, 95, 445-452.
[18] Mas, C.; Mantecón, A.; Serra, A.; Ramis, X.; Salla, J.M. *Influence of lanthanide triflate compounds on formation of networks from DGEBA and γ-butyrolactone* J. Polym. Sci., Part A: Polym. Chem. **2004**, 42, 3782-3791.
[19] González, L.; Ramis, X.; Salla, J.M.; Mantecón, A.; Serra, A. *New poly(ether-ester) thermosets obtained by cationic curing of DGEBA and 7,7-dimethyl-6,8-dioxaspiro[3.5]nonane-5,9-dione with several Lewis acids as initiators* J. Polym. Sci., Part A: Polym. Chem. **2008**, 46, 1229-1239.

terciàries [20]. Entre aquestes les més utilitzades són la 4-(*N*,*N*-dimetilamino)piridina (DMAP) i els imidazoles *N*-substituïts [21].

El curat amb amines terciàries consisteix en una polimerització en cadena iniciada per l'amina terciària i propagada per un anió alcòxid, tal i com apareix de manera simplificada a l'**Esquema I-7**.

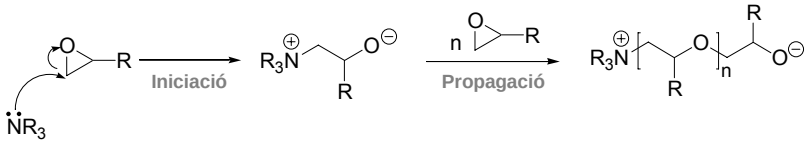

Esquema I-7 Mecanisme de l'homopolimerització aniònica de reïnes epoxi iniciada per una amina terciària

Tant les etapes d'iniciació com de propagació segueixen el mecanisme S_N2 i per tant l'obertura de l'anell oxirà es dóna a la posició menys substituïda obtenint-se polímers regiorregulars.

En anteriors estudis es va poder observar que en les polimeritzacions aniòniques iniciades amb amines terciàries la concentració de grups hidroxil al medi influïa significativament tant en el procés de curat [22] com en el de gelificació [23]. En primer lloc, a l'augmentar la proporció de grups hidroxil s'observava una acceleració en el procés de curat, especialment durant l'etapa d'iniciació. Aquest fet va ser atribuït a la formació d'un major nombre d'espècies actives degut a l'ajut de les espècies donadores de protons les quals poden interaccionar amb l'oxigen oxiránic, incrementant la càrrega positiva del carboni de l'anell epoxi i facilitant l'atac de l'amina terciària sobre aquest. Com a conseqüència es forma un alcòxid procedent del compost hidroxílic i un catió amoni quaternari a partir de l'amina i el grup epoxi (**Esquema I-8**).

[20] May, C. A., ed., *Curing Agents and Modifiers* in *Epoxy Resins Chemistry and Technology*, 2nd ed., Marcel Dekker, New York, **1988**.
[21] a) Ricciardi, F.; Romanchick, W.A.; Joullie, M.M. Mechanism of imidazole catalysis in the curing of epoxy resins J. Polym. Sci. Polym. Chem. Ed. **1983**, 21, 1475-1490. b) Dell'Erba, I.E.; Williams, R.J.J. *Homopolymerization of epoxy monomers initiated by 4- (dimethylamino)pyridine* Polym. Eng. Sci. **2006**, 46, 351-359.
[22] Rozenberg, B.A. *Kinetics, thermodynamics and mechanism of reactions of epoxy oligomers with amines* Adv. Polym. Sci. **1986**, 75, 113-165.
[23] Fernández-Francos, X.; Cook, W.D.; Salla, J.M.; Serra, A.; Ramis, X. *Crosslinking of mixtures of diglycidylether of bisphenol-A with 1,6-dioxaspiro[4.4]nonan-2,7-dione initiated by tertiary amines: III. Effect of hydroxyl groups on network formation* Polym. Int. **2009**, 58, 1401-1410.

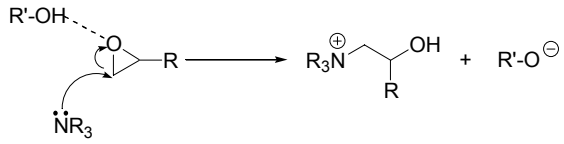

Esquema I-8 Mecanisme postulat d'iniciació catalitzada per espècies donadores de protons

D'altra banda, Ooi *i col.* varen observar tres pics exotèrmics durant el curat isotèrmic per calorimetria diferencial d'escombrat (DSC) del DGEBA amb diferents imidazoles, establint que el procés de curat era més complex que el que es mostra a l'**Esquema I-7** on només explicaria el primer (iniciació) i el segon (propagació) pic exotèrmic observat [24]. El tercer pic es va associar a la regeneració de l'amina terciària a través de dos possibles mecanismes de *N*-dealquilació i *β*-eliminació tal i com es mostra a l'**Esquema 1-9**.

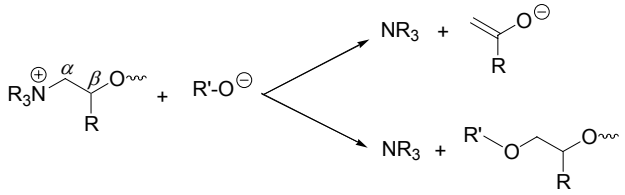

Esquema I-9 Regeneració de l'amina terciària per *β*-eliminació (a dalt) i *N*-dealquilació (a baix) (adaptat de [24]).

Fernández-Francos *i col.*, del nostre grup d'investigació apunta que la presència de grups hidroxil que poden generar espècies alcòxid al medi no només faria més eficient la iniciació, per un increment en el nombre d'espècies actives, sinó que en cas d'haver reaccions de regeneració durant el curat, la reiniciació també seria més eficient [25].

Pel que fa al procés de gelificació, es coneix que la conversió al punt de gel en una xarxa formada per polimerització en cadena depèn del nombre de monòmers entrecreuables, *kinetic chain length* (KCL), principalment influit per dos factors [26]: 1. una alta concentració d'iniciador incrementa el nombre de cadenes actives i redueix la KCL, per tant incrementa la conversió a la gelificació i 2. la presència de reaccions de transferència de cadena, com es mostra a l'**Esquema I-10**, també redueix la KCL i fa pujar la conversió a la gelificació. El nombre de cadenes està determinat, doncs, per la quantitat d'iniciador i d'espècies donadores de protons.

[24] Ooi, S.K.; Cook, W.D.; Simon, G.P.; Such, C.H. *DSC studies of the curing mechanisms and kinetics of DGEBA using imidazole curing agents* Polymer, **2000**, 41, 3639-3649.
[25] Fernández-Francos, X.; Cook, W.D.; Serra, A.; Ramis, X.; Liang, G. G.; Salla, J.M. *Crosslinking of mixtures of DGEBA with 1,6-dioxaspiro[4,4]nonan-2,7-dione initiated by tertiary amines. Part IV. Effect of hydroxyl groups on initiation and curing kinetics* Polymer **2010**, 51, 26-34.
[26] Odian, G.G. *Principles of polymerization*, 4th ed., Wiley Interscience, New York, **2004**.

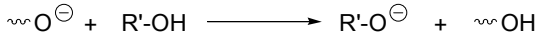

Esquema I-10 Transferència de cadena entre un anió alcòxid i una espècie donadora de protons

En un treball del nostre grup, es va observar que al incrementar la proporció de grups hidroxil la conversió a la gelificació augmentava. Aquest fet es pot argumentar per l'existència de reaccions de transferència que són l'element determinant ja que es redueix la longitud de les cadenes i n'augmenta el nombre, incrementant per tant la conversió a la gelificació [23].

Finalment, es va poder establir que tant el procés de curat com les propietats finals dels materials obtinguts emprant 1-metilimidazole (1MI) com a iniciador líquid eren similars als termoestables obtinguts usant l'iniciador sòlid 4-(*N*,*N*-dimetilamino)piridina (DMAP) [27]. És per això que en la present tesi, s'ha emprat únicament el 1-metilimidazole (1MI) ja que al ser un reactiu líquid ha facilitat la preparació i homogeneïtzació de les mescles reactives.

I.1.3 Propietats dels materials termoestables epoxídics

L'ús de reïnes epoxi requereix la formació d'una estructura tridimensional entrecreuada unida per mitjà d'enllaços covalents. Val a dir que l'estructura química, la morfologia i l'homogeneïtat de l'estructura tridimensional així com la densitat d'entrecreuament són paràmetres que venen determinats per l'agent de curat emprat, el mecanisme de polimerització i la cinètica del procés de curat [28].

L'ús de reïnes epoxi comercials en algunes aplicacions, per exemple com a recobriments en el camp de la microelectrònica, es veu limitat pel fet de presentar un cert nombre d'inconvenients (**Figura I-1**).

Figura I-1 Principals limitacions de les reïnes epoxi comercials

En primer lloc, durant el procés de curat es produeix una contracció que influeix negativament sobre les propietats finals i la durabilitat del material, ja que

[27] Fernández-Francos, X.; Salla, J.M.; Mantecón, A.; Serra, A.; Ramis, X. *Crosslinking of mixtures of DGEBA with 1,6-dioxaspiro[4.4]nonan-2,7-dione initiated by tertiary amines, Part II: Thermo-mechanical properties and reworkability* Polym. Degrad. Stab. **2008**, 93, 760-769.
[28] a) Wu, S.; Soucek, M.D. *Kinetic modeling of crosslinking reactions for cycloaliphatic epoxides with hydroxyl- and carboxyl-functionalized acrylic copolymers: 1. pH and temperature effects* Polymer **1998**, 39, 5747-5759. b) May, C. A., ed., *Physical, Mechanical Properties of Cured Resins* in *Epoxy Resins Chemistry and Technology*, 2nd ed., Marcel Dekker, New York, **1988**. c) Pascault, J.N., Sautereau, H., Verdu, J., Williams, R.J.J. *Termosetting polymers,* Marcel Dekker, New York, **2002**.

durant aquest procés es poden formar microescletxes, microporus o tensions mecàniques que amb el temps poden evolucionar cap a la fatiga mecànica del material i a una possible pèrdua d'adherència. Aquesta pèrdua d'adherència o les lesions presents al recobriment poden facilitar la penetració d'humitat, accelerant la corrosió dels components metàl·lics arribant fins hi tot, a la destrucció del dispositiu electrònic encapsulat [29].

Per tal de reduir la contracció durant el procés de curat s'han dut a terme vàries aproximacions com ara l'addició de càrregues inorgàniques com per exemple sílica, quars o càrregues orgàniques de poliuretà, poliestirè o PVC. Tanmateix, aquestes càrregues perjudiquen en certs aspectes ja que augmenten significativament la viscositat de la mescla, dificultant el processat i a més a més redueixen la transparència del recobriment. Els materials que s'obtenen presenten una elevada rigidesa i fragilitat i al ser heterogenis les propietats elèctriques es veuen deteriorades [2].

Una alternativa a l'addició de càrregues és l'ús de monòmers capaços de polimeritzar sense contracció o fins i tot amb expansió [30]. Aquest fet és atribuible al mode de polimertització per obertura d'anell on per cada distància de Van der Waals (**3**) que passa a una distància d'enllaç covalent (**3a**) almenys hi ha dues distàncies d'enllaç covalent (**1**, **2**) que passen a distàncies properes a la de Van der Waals (**1a**, **2a**) i un enllaç covalent senzill (**4**) que passa a un de doble (**4a**) segons l'**Esquema I-11**.

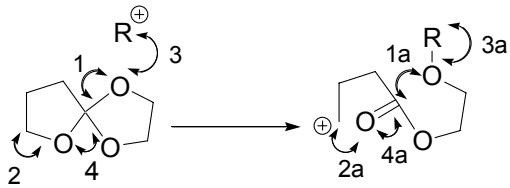

Esquema I-11 Canvis d'enllaços durant la iniciació en l'homopolimertització d'un monòmer expandible (espiroortoester, SOE)

Així doncs, l'ús de monòmers expandibles com ara els SOEs o els espiroortocarbonats (SOCs) (**Esquema I-12**) com a modificants de sistemes

[29] Chung, K.; Takata, T.; Endo, T. *Anionic ring-opening copolymerization of bicyclic bis(γ-lactone)s with mono- and bifunctional epoxides via double ring-opening isomerization of the bis(γ-lactone)s and volume change during copolymerization* Macromolecules **1995**, 28, 3048-3054.
[30] Sadhir, R.K., Luck, M.R., ed., *Expanding Monomers: Synthesis, Characterization and Applications*, CRC Press: Boca Raton, FL, **1992**.

termostables és una estratègia per a reduir la contracció química durant el curat [31].

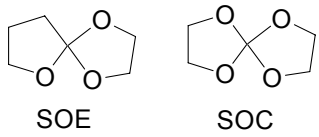

Esquema I-12 Estructura de diferents monòmers expandibles

A través de l'estudi de la reacció de grups epoxi amb monolactones en un medi catiònic, com per exemple la *γ*-butirolactona (*γ*-BL), es va observar com abans de la gelificació l'encongiment era bastant elevat degut a la formació del SOE intermedi, entre el grup epoxi i el carbonil de l'ester cíclic i la homopolimerització dels grups epòxid. En canvi, després de la gelificació l'encongiment es veia certament reduït degut a la polimerització dels grups SOE [31a,32]. El fet que la major part de la contracció tingués lloc abans de la gelificació no dóna cap problema ja que el material és un fluid mentre que després de la gelificació, quan el moviment es veu restringit, l'encongiment pot generar tensions internes en el material i portar a la formació d'escletxes i pèrdua d'adherència. En posteriors estudis, emprant bislactones, com ara les derivades de l'àcid de Meldrum, espirobislactones com la 1,6-dioxaspiro[4.4]nonan-2,7-diona (s(*γ*-BL)) o bislactones condensades com les derivades de la 2,8-dioxabiciclo[3.3.0]octan-3,7-diona, es va aconseguir reduir la contracció global durant el procés de curat tant en medis catiònics com aniònics [33]. A l'**Esquema I-13** es mostren les principals estructures contenint esters cíclics emprades al nostre grup de recerca.

[31] a) Mas, C.; Ramis, X.; Salla, J.M.; Mantecon, A.; Serra, A. *Copolymerization of diglycidyl ether of bisphenol A with γ-butyrolactone catalyzed by ytterbium triflate: Shrinkage during curing* J. Polym. Sci., Part A: Polym. Chem. **2003**, 41, 2794-2808. b) Chikaoka, S.; Takata, T.; Endo, T. *Cationic ring-opening polymerization of spiroorthoester. Polymer structure, polymerization mechanism, and volume change on polymerization* Macromolecules, **1992**, 25, 625-628.
[32] Gonzalez, S.; Fernández-Francos, X.; Salla, J.M.; Serra, A.; Mantecón, A.; Ramis, X. *New thermosets obtained by the cationic copolymerization of diglycidyl ether of bisphenol A with γ-caprolactone with an improvement in the shrinkage. I. Study of the chemical processes and physical characteristics* J. Polym. Sci., Part A: Polym. Chem. **2007**, 45, 1968-1979.
[33] a) González, L.; Ramis, X.; Salla, J.M.; Mantecon, A.; Serra, A. *Reduction of the shrinkage of thermosets by the cationic curing of mixtures of diglycidyl ether of bisphenol A and 6,6-dimethyl-(4,8-dioxaspiro[2.5]octane-5,7-dione)* J. Polym. Sci., Part A: Polym. Chem. **2006**, 44, 6869-6879. b) Fernández-Francos, X.; Salla, J.M.; Cadenato, A.; Morancho, J.M.; Mantecón, A.; Serra, A.; Ramis, X. *Novel thermosets obtained by UV-induced cationic copolymerization of DGEBA with an spirobislactone* J. Polym. Sci., Part A: Polym. Chem. **2007**, 45, 5446-5458. c) Arasa, M.; Ramis, X.; Salla, J.M.; Mantecón, A.; Serra, A. *Anionic copolymerization of DGEBA with two derivatives of a bicyclic bis(γ-lactone)s using tertiary amines as initiators* Polymer **2009**, 50, 2228-2236.

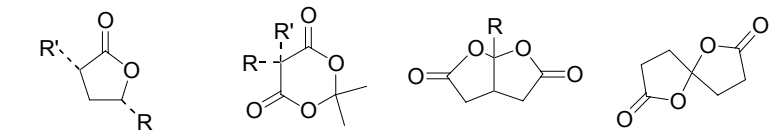

Esquema I-13 Estructura de diverses mono i bis(*γ*-lactones) estudiades

L'utilització de monolactones per a reduir l'encongiment, malgrat els seus beneficis, presenta com a principal inconvenient que el SOE que s'expandirà durant el curat prèviament s'ha de formar dins del medi de reacció i aquest procés és difícil de controlar. La situació òptima és que els grups SOE es formin abans de la gelificació i que polimeritzin després d'aquesta. L'alternativa d'introduir directament monòmers expandibles, com ara bislactones, dins del medi de reacció evita el problema de la formació del monòmer expandible durant el curat però té com a principal inconvenient el seu elevat cost, tant els que són comercials com els sintetitzats. A més a més, la copolimerització del DGEBA amb mono- o bislactones augmenta la flexibilitat de la xarxa polimèrica i per tant la T_g del material termoestable diminueix considerablement.

En quant als termoestables epoxídics no modificats, l'elevada densitat d'entrecreuament fa que aquests materials presentin una elevada rigidesa però alhora una elevada fragilitat la qual cosa compromet l'adherència com a conseqüència de fractures fràgils que pot patir el recobriment [8]. Entre les estratègies emprades per millorar la tenacitat de les reïnes epoxi l'ús d'additius plastificants, com ara termoplàstics lineals flexibles o elastòmers, capaços d'absorbir l'energia de fractura a través de deformacions plàstiques, segueix sent la més utilitzada a nivell tecnològic [34]. No obstant, la introducció d'estructures flexibles a la xarxa polimèrica produeix una disminució de la T_g la qual cosa pot limitar la temperatura d'ús del material.

Una altra estratègia emprada per tal millorar aquesta propietat, es la generació d'una nova fase dins la matriu expoxídica. Aquesta es sol dur a terme mitjançant la tècnica que s'anomena *reaction induced phase separation* (RIPS) o *chemical induced phase separation* (CIPS) i que es basa en partir d'una mescla homogènia de reïna epoxi i agent modificant. Durant el procés de curat, el pes molecular de la reïna va creixent i l'agent modificant, degut a la contribució

[34] a) Manzione, L.T.; Gillham, J.K.; McPherson, C.A. *Rubber-modified epoxies: I. Transition and morphology* J. Appl. Polym. Sci. **1981**, 26, 889-905. b) Garg, A.C.; Mai, Y.W. *Failure mechanism in toughened epoxy resins- A review* Comp. Sci. Tech. **1988**, 31, 179-223.

entròpica desfavorable, es separa formant una segona fase a escala micro- o nanomètrica [35].

A nivell científic s'han continuat desenvolupant noves vies per tal de millorar aquesta propietat sense afectar negativament les propietats termomecàniques. Noves aproximacions, seguint la tècnica anteriorment descrita, involucren l'ús d'una gran varietat de copolímers de bloc els quals es caracteritzen en què un dels blocs, durant el procés de curat, forma una fase a nivell nanomètric mentre l'altre part de l'estructura polimèrica queda unida o resta miscible amb la matriu epoxídica [36]. De totes maneres, tot i millorar significativament la tenacitat del materials [37], en certs casos, la nanoestructuració tampoc assegura mantenir les propietats termomecàniques [38]. Tanmateix, l'ús d'estructures lineals, perjudica considerablement el processat de la mescla reactiva degut a un augment dràstic de la viscositat [39].

Finalment, s'ha de tenir en compte que les reïnes epoxi entrecreuades són termoestables i per tant la seva eliminació, un cop acabada la seva funció, és molt dificultosa ja que són materials insolubles i infusibles. Es parla de termoestables reciclables quan aquests es poden eliminar i es pot recuperar el dispositiu recobert encara que el recobriment no pugui tornar a ser emprat. La introducció de grups tèrmica o químicament làbils és la manera més utilitzada per obtenir recobriments degradables. En concret, la degradació tèrmica és un dels mètodes més emprats ja que ens ofereix un procés relativament ràpid i net.

Entre els diferents treballs que s'han trobat a la literatura sobre la degradació tèrmica de materials termoestables, la introducció de grups carbonat [40] o ester són les estratègies més seguides doncs permeten obtenir materials que poden ser degradats a temperatures entre 200 i 250 ºC. Aquesta temperatura disminueix a mesura que augmenta la substitució en el C_α degut a un major nombre d'hidrògens

[35] a) Hwang, J.F.; Manson, J.A.; Hertzberg, R.W.; Miller, G.A.; Sperling, L.H. *Structure-property relationships in rubber-toughened epoxies* Prog. Eng. Sci. **2004**, 29, 1466-1476. b) Bagheri, R.; Marouf, B.T.; Pearson, R.A. *Rubber-toughned epoxies: A critical review* J. Macromol. Sci., Part C: Polym. Rev. **2009**, 49, 201-225.
[36] Ruiz-Pérez, L.; Royston, G.J.; Fairclough, J.P.A.; Ryan, A.J. *Toughening by nanostructure* Polymer **2008**, 49, 4475-4488.
[37] Pascault, J.P., Williams, R.J.J. *Polymer Blends*, Paul, D.R., Bucknall, C.B. eds.; Wiley Interscience, New York, **2000**.
[38] a) Fan, W.; Wang, L.; Zheng, S. *Nanostructures in thermosetting blends of epoxy resin with polydimethylsiloxane-block-poly(ε-caprolactone)-block-polystyrene ABC triblock copolymer* Macromolecules **2009**, 42, 327-336. b) Fan, W.; Wang, L.; Zheng, S. *Double reaction-induced microphase separation in epoxy resin containing polystyrene-block-poly(ε-caprolactone)-block-poly(n-butyl acrylate) ABC triblock copolymer* Macromolecules **2010**, 43, 10600-10611.
[39] a) Cicala, G.; Recca, G. *Studies on epoxy blends modified with a hyperbranched polyester* Polym. Eng. Sci. **2008**, 48, 2382-2388. b) Corcione, C.E.; Frigione, M. *A novel procedure able to predict the rheological behavior of trifunctional epoxy resin/hyperbranched aliphatic polyester mixtures* Polym. Test. **2009**, 28, 830-835.
[40] a) Wang, L.; Li, H.; Wong, C.P. *Syntheses and characterizations of thermally reworkable epoxy resins. Part I* J. Polym. Sci., Part A: Polym. Chem. **1999**, 37, 2991-3001. b) Wang, L.; Li, H.; Wong, C.P. *Syntheses and characterizations of thermally reworkable epoxy resins II* J. Polym. Sci., Part A: Polym. Chem. **2000**, 38, 3771-3782.

en *γ* la qual cosa afavoreix l'eliminació pirolítica mitjançant un mecanisme de *β*-eliminació (**Esquema I-14**) [41].

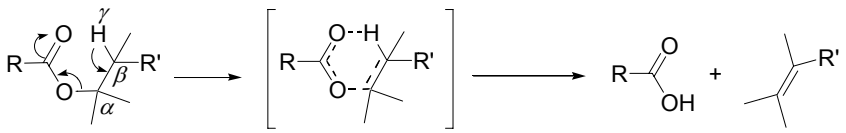

Esquema I-14 Mecanisme d'eliminació pirolítica d'esters (*β*-eliminació)

I.1.4 Estructura i propietats generals dels polímers dendrítics

Des de la dècada dels anys 80 els polímers dendrítics, macromolècules altament ramificades, representen una de les àrees més interessants en el camp de la ciència i l'enginyeria de polímers. Apart de les arquitectures polimèriques clàssiques com són les: lineal, ramificada, entrecreuada, cíclica, estrella i escala, s'han desenvolupat altres noves subclasses de polímers dendrítics (**Figura I-2**) [42].

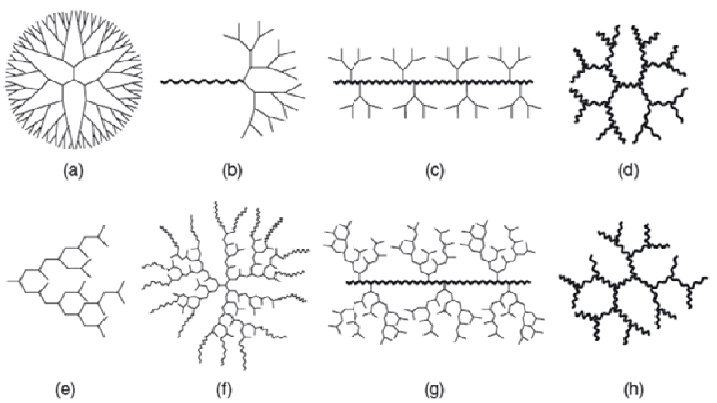

Figura I-2 Polímers dendrítics amb diferents estructures: (a) dendrímer, (b) híbrid lineal-dendrític, (c) polímer dendronitzat, (d) híbrid estrella-dendrímer, (e) polímer hiperramificat, (f) polímer estrella, (g) HBP empeltat en una cadena de polímer lineal, i (h) híbrid estrella-hiperramificat

Els dendrímers (**a**) així com estructures híbrides relacionades (**b-d**) són molècules perfectament definides amb un alt grau de ramificació en comparació amb els polímer hiperramificats (**e**) o les estructures híbrides contenint l'arquitectura hiperramificada (**f-h**). Per contrapartida, la seva obtenció és

[41] a) Chen, J.S.; Ober, C.K.; Poliks, M.D. *Characterization of thermally reworkable thermosets: materials for environmentally friendly processing and reuse* Polymer **2002**, 43, 131-139. b) Chen, J.S.; Ober, C.K.; Poliks, M.D.; Zhang, Y.; Wiesner, U.; Cohen, C. *Controlled degradation of epoxy networks: analysis of crosslink density and glass transition temperature changes in thermally reworkable thermosets* Polymer **2004**, 45, 1939-1950.
[42] Yan, D., Gao, C., Frey, H. eds., *Hyperbranched polymers. Synthesis, properties and applications*, 1st ed., Wiley Interscience, Hoboken, **2011**.

dificultosa i requereix un cost elevat ja que normalment s'involucren diferents etapes de síntesi així com llargues etapes de purificació. Això fa que la seva aplicació científica i tecnològica estigui certament limitada a camps com la nanotecnologia o la biomedicina. En canvi, els polímers hiperramificats i els seus derivats, anàlegs als dendrímers, es poden sintetitzar per mitjà de mètodes relativament senzills, normalment en una o dues etapes, la qual cosa facilita la seva disponibilitat, el seu cost i per tant permet el seu ús en un ampli ventall d'aplicacions com per exemple com additius per tintes d'impremta [43], compostos estabilitzants de la llum UV [44], així com per obtenir nanocompòsits híbrids (orgànic-inorgànic) [45] o millorar propietats tèrmiques i mecàniques de polímers termoplàstics o termoestables [46,47].

En termes estructurals un polímer hiperramificat preparat a partir d'un monòmer de tipus AB_2 està compost, generalment, de tres tipus de subunitats repetitives lineal (*L*), dendrítica (*D*) i terminal (*T*) (**Figura I-3**). Addicionalment, en funció del mètode sintètic emprat per obtenir el HBP podem diferenciar una altra subunitat corresponent al grup focal o inicial (*I*) o al nucli (*core*) que indica el punt on s'ha iniciat el creixement del polímer.

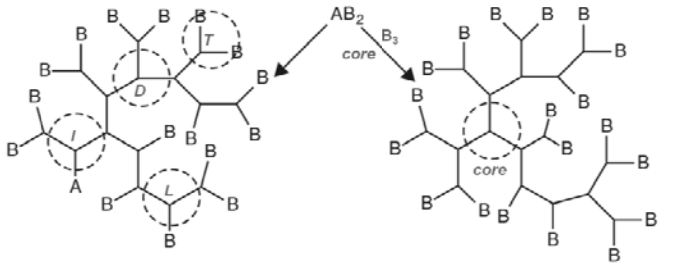

Figura I-3 Estructura esquematitzada d'un polímer hiperramificat obtingut per polimerització d'un monòmer de tipus AB_2

[43] Bruchmann, B. *Dendritic polymers based on urethane chemistry – Syntheses and applications* Macromol. Mater. Eng. **2007**, 292, 981-992.
[44] Bergenudd, H.; Eriksson, P.; DeArmitt, C., Stenberg, B.; Malmstroem, E. *Synthesis and evaluation of hyperbranched phenolic antioxidants of three different generations* Polym. Degrad. Stab. **2002**, 76, 503-509.
[45] Americo, E., Sangermano, M.; Mallucelli, G.; Priola, A.; Rizza, G. *Preparation and characterization of hyperbranched polymer/silica hybrid nanocoatings by dual-curing process* Macromol. Mater. Eng. **2006**, 291, 1287-1292.
[46] Voit, B. *Hyperbranched polymers - All problems solved after 15 years of research?* J. Polym. Sci., Part A: Polym. Chem. **2005**, 43, 2679-2699.
[47] Fan, Z.; Jähnichen, K.; Desbois, Ph.; Häussler, L.; Vogel, R.; Voit, B. *Blends of different linear polyamides with hyperbranched aromatic AB_2 and A_2 + B_3 polyesters* J. Polym. Sci., Part A: Polym. Chem. **2009**, 47, 3558-3572.

Per tal de correlacionar quantitativament les subunitats descrites anteriorment i donar un valor fiable de la ramificació, Fréchet *i col.* al mateix temps que Kim i Webster van descriure el grau de ramificació (*DB*) com [48,49]:

$$DB = \frac{n^o\ unitats\ dendrítiques + n^o\ unitats\ terminals}{n^o\ total\ unitats} = \frac{D+T}{D+T+L} \qquad \text{(I-1)}$$

on *D* és el nombre total d'unitats dendrítiques, *T* el nombre total d'unitats terminals i *L* el nombre total d'unitats lineals.

El *DB* generalment és determinat per espectroscòpia de RMN comparant les intensitats de les senyals de les respectives subunitats dendrítiques. En el cas de tenir una molècula perfectament dendrítica, com en el cas dels dendrímers, el *DB* és 1. L'equació I-1 és totalment vàlida per polímers dendrítics de pes molecular alt. De totes maneres, en aquelles estructures de pes molecular elevat contenint una proporció d'unitats dendrítiques aproximadament similar a la d'unitats terminals o bé, en macromolècules de baix pes molecular una nova aproximació descrita per Frey *i col.* i Yan *i col.* resulta més adient per determinar el *DB* [50,51]:

$$DB = \frac{2D}{2D+L} \qquad \text{(I-2)}$$

Aquest paràmetre és un dels més importants per caracteritzar HBPs doncs està estretament lligat amb les propietats d'aquests com ara el volum lliure, l'empaquetament de cadenes, el radi de gir promig (R_g), la temperatura de transició vítria (T_g), el grau de cristal·lització o la rigidesa mecànica, entre d'altres [52].

Els dendrímers, els HBPs i els altres anàlegs dendrítics presenten una sèrie de característiques i propietats úniques les quals els fan seriosos competidors enfront a polímers amb la topologia clàssica lineal (**Taula I-1**). Els dendrímers per la seva part, presenten una estructura globular, perfectament ramificada i regular, amb un *DB* igual a 1 i una polidispersitat inferior a 1.05. En quant a les seves propietats, degut a la seva topologia globular, pràcticament no presenten empaquetament molecular la qual cosa comporta que la seva viscositat sigui molt baixa, siguin molt solubles i presentin una funcionalitat i una reactivitat molt

[48] Hawker, C.J.; Lee, R.; Fréchet, J.M.J. *One-step synthesis of hyperbranched dendritic polyesters* J. Am. Chem. Soc. **1991**, 113, 4583-4588.
[49] Kim, Y.H.; Webster, O.W. *Hyperbranched polyphenylenes* Macromolecules **1992**, 25, 5561-5572.
[50] Hölter, D.; Burgath, A.; Frey, H. *Degree of branching in hyperbranched polymers* Acta Polym. **1997**, 48, 30-35.
[51] Lin, Q.; Long, T.E. *Polymerization of A_2 and B_3 monomers. A facile approach to hyperbrached poly(aryl-ester)s* Macromolecules **2003**, 36, 9809-9816.
[52] a) Gong, W.; Mai, Y.; Zhou, Y.; Qi, N.; Wang, B., Yan, D. *Effect of the degree of branching on atomic-scale free volume in hyperbranched poly[3-ethyl-3-(hydroxymethyl)oxetane]. A positron study* Macromolecules **2005**, 38, 9644-9649. b) Khalyavina, A.; Schallausky, F.; Komber, H.; Al Samman, M.; Radke W.; Lederer A. *Aromatic−aliphatic polyesters with tailored degree of branching based on AB/AB_2 and ABB^*/AB_2 monomers* Macromolecules **2010**, 43, 3268-3276.

elevades. Els HBPs, amb una estructura menys definida que els dendrímers, presenten unes propietats molt similars però amb els avantatges que no només són més fàcils d'obtenir, com s'ha comentat anteriorment, sinó que a més a més, actualment existeix una gran varietat d'estructures polimèriques comercialment disponibles [42,53].

Taula I-1 Comparació de les característiques estructurals i de les propietats d'un polímer lineal, hiperramificat i d'un dendrímer

Polímer	Lineal	Hiperramificat	Dendrímer
Topologia	1D, lineal	3D, el·lipsoïdal	3D, globular
Síntesi	Fàcil, 1 etapa	Cost baix, 1 etapa	Tediós, vàries etapes
Purificació	Precipitació	Precipitació	Cromatografia
PDI	> 1.1	> 3.0	1.0 (< 1.05)
DB	0	0.4 – 0.5	1.0
Empaquetament	Fort	Feble	Molt feble
Viscositat	Elevada	Baixa	Molt baixa
Solubilitat	Baixa	Elevada	Molt elevada
Funcionalitat	Als extrems	A les subunitats lineals i terminals	A les subunitats terminals
Reactivat	Baixa	Elevada	Molt elevada

Pel què fa als polímers estrella, en termes estructurals estan compostos per un nucli amb una funcionalitat superior a 3 i braços polimèrics lineals. Els polímers estrella "*senzills*" és a dir, amb un nombre reduït de braços, han sigut àmpliament estudiats tan pel què fa a la seva obtenció com a la seva aplicació [54].

En canvi, els polímers estrella "*complexes*" (**Figura I-2**, exemple f), contenint un nombre relativament alt de cadenes lineals (braços) degut a l'elevada funcionalitat del nucli, han pres recentment especial rellevància en l'àmbit científic [55]. Així doncs en la present tesi, l'utilització del terme *polímer estrella* es referirà a tota aquella estructura complexa que contingui un nucli polifuncional i un nombre de braços superior a 20. El fet que hagin estat obtinguts a partir de nuclis hiperramificats, els polímers estrella sintetitzats presenten dispersitat en quant al nombre de braços.

Gràcies a la gran varietat de mètodes de polimerització, HBPs i monòmers disponibles es pot controlar, d'una manera eficaç, la longitud dels braços així com

[53] Voit, B.; Lederer, A. *Hyperbranched and highly branched polymer architecture – Synthetic strategies and major characterization aspects* Chem. Rev. **2009**, 109, 5924-5973.
[54] Hadjichristidis, N., Pitsikalis, M., Iatrou, H. *Polymers with Star-related Structures* in *Macromolecular Engineering. Precise Synthesis, Materials Properties, Applications.* Matyjaszewski, K., Gnanou, Y.; Leibler, L., eds., 1st ed., Wiley-VCH, Weinheim, **2007**.
[55] Gao, H.; Matyjaszewski, K. *Synthesis of functional polymers with controlled architecture by CRP of monomers in the presence of cross-linkers: From stars to gels* Prog. Polym. Sci. **2009**, 34, 317-350.

es poden obtenir un gran ventall de polímers estrella amb nuclis i braços amb estructures moleculars ben diferents [56].

En quant a les seves característiques i propietats els podríem situar, topològicament, entre els dendrímers (3D, globular) i els polímers hiperramificats (3D, el·lipsoïdal) sempre i quant el nombre de braços per molècula sigui superior a 20 [57]. La seva interacció potencial és altament repulsiva i per tant són molècules poc deformables, comparables amb esferes rígides, díficils d'entortolligar-se entre elles. Això fa que presentin un empaquetament molecular molt baix la qual cosa comporta que la seva viscositat sigui molt baixa i siguin molt solubles. Aquest lleuger empaquetament sorgeix per la capacitat que tenen els extrems dels braços, més lliures en quant a moviment, d'interpenetrar amb altres extrems dels braços de molècules veïnes (**Figura I-4**) [58]. A més a més, degut al elevat nombre de braços per molècula, fa que presentin una funcionalitat i una reactivitat molt elevades.

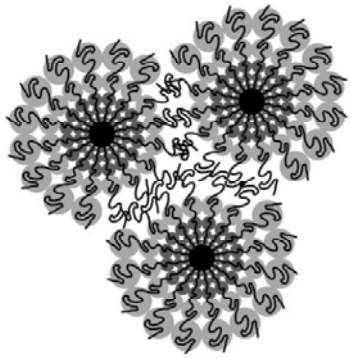

Figura I-4 Dibuix il·lustratiu de tres molècules de polímer estrella en solució lleugerament interpenetrades a través dels extrems dels braços

Un dels comportaments típics que els caracteritza és la viscositat la qual resta pràcticament constant al augmentar el pes molecular del polímer, contràriament al que ocorre amb polímers lineals o hiperramificats (**Figura I-5**) [42,53,58].

[56] a) Knischka, R.; Lutz, P.J.; Sunder, A.; Mülhaupt, R.; Frey, H. *Functional poly(ethylene oxide) multiarm star polymers: core-first synthesis using hyperbranched polyglycerol initiators* Macromolecules **2000**, 33, 315-320. b) Liu, C.; Zhang, Y.; Huang, J. *Well-defined star polymers with mixed-arms by sequential polymerization of atom transfer radical polymerization and reverse addition-fragmentation chain transfer on a hyperbranched polyglycerol core* Macromolecules **2008**, 41, 325-331.
[57] Mishra, M.K., Kobayashi, S. eds, *Star and hyperbranched polymers.* 1st ed., Marcel Dekker, Inc., New York, **1999**.
[58] Erwin, B.M.; Cloitre, M.; Gauthier, M.; Vlassopoulos, D. *Dynamics and rheology of colloidal star polymers* Soft Matter, **2010**, 6, 2825-2833.

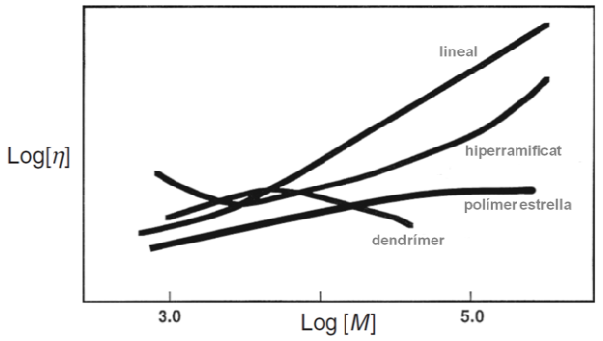

Figura I-5 Relació entre la viscositat intrínseca (log [*η*]) i el pes molecular (log [*M*]) per diferents topologies polimèriques

Per tant els polímers estrella també poden resultar bons candidats per ser emprats tant científica- com industrialment en múltiples aplicacions doncs presenten propietats molt similars als dendrímers i la seva obtenció continua sent més assequible.

I.1.5 Principals mètodes de síntesi de polímers hiperramificats (HBPs) i estrella

Els polímers hiperramificats (HBPs) es poden obtenir a través de tres vies diferents: *bottom-up* (polimerització dels monòmers), *top-down* (degradació d'una xarxa polimèrica o una biomacromolècula) i *middle-upon* (modificació d'un polímer hiperramificat precursor) (**Figura I-6**) [42].

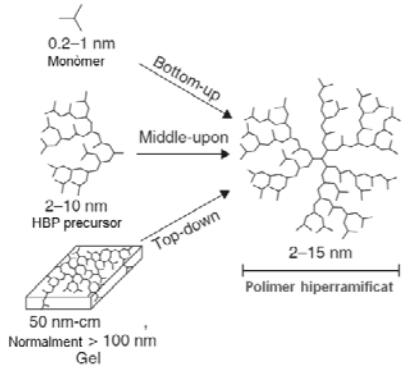

Figura I-6 Principals vies d'obtenció d'un polímer hiperramificat

La majoria d'estructures actualment disponibles s'obtenen per mitjà de la via *bottom-up*. Dins d'aquesta via podem distingir dues categories principals: mètodes on s'empra un únic monòmer (**SMM**, *single-monomer methodology*) on es sintetitza

el polímer a partir de la polimerització de monòmers AB_n o AB_n latents. En funció del mecanisme de reacció, aquesta categoria inclou cinc aproximacions:

1. Policondensació de monòmers AB_n.
2. Autopolicondensació vinílica (SCVP, *self-condensing vinyl polymerization*).
3. Polimerització per obertura d'anell (ROP, *ring-opening polymerization*).
4. Polimerització radicalària per transferència atòmica (ATRP, *atom-transfer radical polymerization*).
5. Polimerització per transferència de protó (PTP, *proton-transfer polymerization*).

L'altre categoria conté mètodes on s'empra més d'un monòmer (**CMM**, *couple-monomer methodology*) i el polímer es sintetitza per polimerització directa de dos monòmers funcionalment simètrics (per exemple: A_2 + B_3) o no simètrics (per exemple: A_2 +BB'_2). A la **Taula I-2** es mostren les principals metodologies sintètiques i aproximacions per obtenir HBPs [59].

En la present tesi, s'explicarà en detall les metodologies de polimerització de monòmers A* + B_n o CB_n (apartat **III.1.1**) i monòmers AB* per obertura d'anell (apartat **IV.1.1**) i per autopolicondensació vinílica (apartat **IV.1.2**) ja que són amb les que s'ha treballat.

Taula I-2 Metodologies i aproximacions sintètiques per obtenir HBPs

Estratègia	Metodologia	Aproximació	Característiques
SMM	Polimerització AB_n	Condensació	Risc de gelificació nul Monòmers poc disponibles
	Polimerització AB*	**SCVP** ATRP **ROP** PTP	Monòmers disponibles Elevat control del DB en copolimeritzacions
CMM	Monòmers simètrics	A_2 + B_3	Monòmers disponibles Risc de gelificació alt
	Monòmers no simètrics	A_2 + CB_n **A* + CB_n** **A* + B_n** AA' + B'_2 ($B'B_2$) ABA + CD_n	Monòmers disponibles Risc de gelificació nul

[59] Gao, Y.; Yan, D. *Hyperbranched polymers: from synthesis to applications* Prog. Polym. Sci. **2004**, 29, 183-275.

Respecte als polímers estrella, existeixen dues vies d'obtenció: *core-first* (el nucli HBP actua de macroiniciador i es fa polimeritzar el monòmer directament [60]) i *arm-first* (els braços es sintetitzen prèviament i posteriorment s'incorporen químicament al nucli HBP [61] o bé, un extrem dels braços té la capacitat de polimeritzar juntament amb altres extrems i crear un nucli entrecreuat [55]).

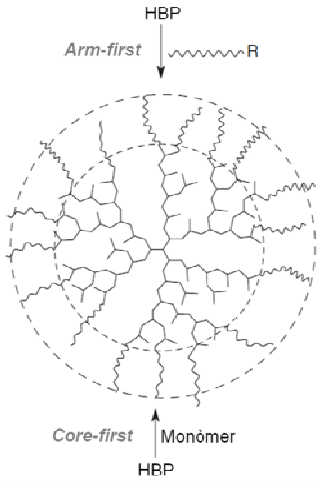

Figura I-7 Principals vies d'obtenció d'un polímer estrella

Per mitjà de la via *arm-first* l'obtenció de polímers estrella és bastant complexa. En primer lloc, no es pot controlar eficaçment el nombre de braços que s'incorporen a l'estrella, el que comporta que s'origini una distribució ampla de molècules amb nombre de braços diferents. A més a més, la incorporació dels braços no és completa i per tant calen processos de purificació tediosos com són la precipitació fraccionada o la diàlisis en vàries etapes per tal de separar els braços de l'estrella formada. L'altre via, *core-first*, permet la preparació de polímers estructuralment ben definits amb un nombre precís de braços. Els rendiments solen ser alts i el procés de purificació senzill ja que simplement cal eliminar el monòmer residual del cru de reacció. De totes maneres, l'obtenció d'estructures amb més de 30 braços tampoc és senzilla ja que és necessària l'obtenció prèvia del macroiniciador (per exemple: HBP), el pes molecular dels braços només es pot determinar per mètodes indirectes i si s'utilitzen mètodes de polimerització radicalària controlada cal optimitzar les condicions de reacció per tal d'evitar l'acoblament estrella-estrella (*star-star coupling)* [55]. Actualment aquest procediment ha resultat ser una àrea d'especial interès. La majoria de polimeritzacions, radicalària controlada, per obertura d'anell, aniònica o catiònica,

[60] Maier, S.; Sunder, A.; Frey, H.; Mülhaupt, R. *Synthesis of poly(glycerol)-block-poly(methyl acrylate) multi-arm star polymers* Macromol. Rapid Commun. **2000**, 21, 226-230.
[61] Comanita, B.; Noren, B.; Roovers, J. *Star poly(ethylene oxide)s from carbosilane dendrimers* Macromolecules **1999**, 32, 1069-1072.

es poden aplicar emprant un HBP com a macroiniciador. Entre els nuclis hiperramificats més utilitzats destaquen els polièsters [62], els polièters (per exemple: el poliglicidol) [63] o la polietilenimina [64].

I.1.6 Termoestables epoxídics modificats amb polímers hiperramificats (HBPs) i polímers estrella

Els HBPs han estat recentment molt emprats en aplicacions tecnològiques perquè, com s'ha comentat anteriorment, poden ser obtinguts a nivell industrial amb relativa facilitat. La seva estructura ramificada fa que aquests continguin un nombre elevat de grups reactius al final de cada ramificació. A més a més, degut a la seva topologia el·lipsoïdal presenten unes propietats a nivell de processat molt bones en comparació amb els seus anàlegs lineals.

El primer HBP emprat com a modificant d'un sistema epoxídic va ser el polièster alifàtic hiperramificat basat en l'àcid 2,2-bis(hidroximetil)propiònic (BHMPA) descrit per Hult *i col.* [65], i comercialitzat per Perstop amb el nom de Boltorn®. Boogh *i col.* [66], varen ser els primers en estudiar l'efecte de l'addició d'aquesta estructura (Boltorn H30) (**Esquema I-15**), prèviament modificada amb grups epoxi terminals, en un sistema clàssic reïna epoxi i amina.

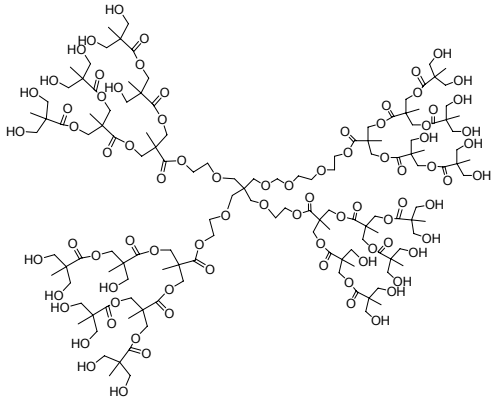

Esquema I-15 Estructura idealitzada del poliester hiperramificat (Boltorn H30)

[62] a) Xia, W.; Jiang, G.; Chen, W. *Synthesis and drug-release properties of hyperbranched polyesters grafted with biocompatible poly(ε-caprolactone)* J. Appl. Polym. Sci. **2008**, 109, 2089-2094. b) Xia, C.; Ding, X.; Sun, Y.; Liu, H.; Li, Y. *Hyperbranched-upon-dendritic macromolecules as unimolecular hosts for controlled release* J. Polym. Sci., Part A: Polym. Chem. **2010**, 48, 4013-4019.
[63] Zhang, X.; Cheng, J.; Wang, Q.; Zhong, Z.; Zhuo, R. *Miktoarm copolymers bearing one poly(ethylene glycol) chain and several poly(ε-caprolactone) chains on a hyperbranched polyglycerol core* Macromolecules **2010**, 43, 6671-6677.
[64] Adeli, M.; Haag, R. *Multiarm star nanocarriers containing a poly(ethylene imine) core and polylactide arms* J. Polym. Sci., Part A: Polym. Chem. **2006**, 44, 5740-5749.
[65] Hult, A.; Johansson, M.; Malmström, E.; Roovers, J. *Hyperbranched Polymers* Adv. Polym. Sci. **1999**, 143, 1-34.
[66] Boogh, L; Petterson, B.; Månson, J.A.E. *Dendritic hyperbranched polymers as toughening for epoxy resins* Polymer **1999**, 40, 2249-2261.

Més tard Ratna *i col.* [67], varen utilitzar el mateix polímer sense modificar, és a dir, contenint grup hidroxil terminals. En ambdós estudis, es produïa una separació de fases durant el procés de curat generant partícules micromètriques disperses en la matriu contínua. Tanmateix, com a resultat de la segregació del HBP i la flexibilitat inherent de l'estructura dendrítica es generava un augment de la tenacitat de fins al 300 % depenen del grau de modificació del polímer hiperramificat, el percentatge de modificant emprat i del cicle de curat seguit. Com a contrapartida, el mòdul elàstic i la temperatura de transició vítria es veien disminuïts mentre que la viscositat de la mescla reactiva augmentava considerablement amb el percentatge de modificant introduït en comparació amb el material no modificat. Resultats similars es varen obtenir en estudis posteriors realitzats per Cicala *i col.* i Frigione *i col.* [39,68,69].

Yang *i col.* [70], en canvi, varen obtenir materials homogenis al emprar el Boltorn H30 en un sistema epoxi/anhídrid i varen relacionar la millora en la resistència al impacte així com en l'elongació i la resistència a la ruptura amb un augment del volum lliure dins la matriu generat pel HBP demostrat per PALS (*positronium annihilation lifetime spectroscopy*).

Altres estructures hiperrafimicades també han estat utilitzades com a modificants de reïnes epoxi com és el cas dels polièters alifàtics. Mülhaupt *i col.* [71], varen emprar varis polièters-poliols amb grups estearat, hidroxi-benzoat i epoxi terminals en un sistema epoxi/anhídrid. En els tres casos s'observaven micropartícules d'uns 12 μm indicant que es produïa separació de fases. De totes maneres en aquest cas, les propietats mecàniques no es veien pràcticament millorades, la viscositat de la mescla reactiva augmentava considerablement al afegir només un 5 % en pes de modificant i les propietats termomecàniques es veien certament afectades.

En l'estudi realitzat per Varley *i col.* es va emprar el Boltorn E1, basat en el poliester Boltorn H30 modificat amb cadenes alifàtiques contenint grups oxirà interns, com agent modificant d'un sistema epoxi/anhídrid [72]. En aquest cas, la viscositat de la mescla al afegir diferent proporcions de HBP no es veia pràcticament alterada. A més a més, la resistència al impacte augmentava

[67] Ratna, D.; Simon, G.P. *Thermomechanical properties and morphology of blends of a hydroxyl-functionalized hyperbranched polymer and epoxy resin* Polymer **2001**, 42, 8833-8839.
[68] Cicala, G.; Recca, A.; Restuccia, C. *Influence of hydroxyl functionalized hyperbranched polymers on the thermomechanical and morphological properties of epoxy resins* Polym. Eng. Sci. **2005**, 45, 225-237.
[69] Frigione, M.E.; Calò, E. *Influence of an hyperbranched aliphatic polyester on the cure kinetic of a trifunctional epoxy resin* J. Appl. Polym. Sci. **2008**, 107, 1744-1758.
[70] Yang, J.P.; Chen, Z.K.; Yang, G., Fu, S.Y.; Ye, L. *Simultaneous improvements in the cryogenic tensile strength, ductility and impact strength of epoxy resins by a hyperbranched polymer* Polymer **2009**, 49, 3168-3175.
[71] Fröhlich, J.; Kautz, H.; Thomann, R.; Frey, H.; Mülhaupt, R. *Reactive core/shell hyperbranched blockcopolyethers as new liquid rubber for epoxy toughening* Polymer **2004**, 45, 2155-2164.
[72] Varley, R.J.; Tian, W. *Toughening of an epoxy anhydride resin system using an epoxidized hyperbranched polymer* Polym. Int. **2004**, 53, 69-77.

progressivament al augmentar la proporció de HBP, arribant a un 100 % de millora amb un 20 % en pes de modificant, sense afectar molt negativament les propietats termomecàniques. El sistema presentava una separació de fases amb partícules nanomètriques d'uns 200 nm.

En treballs realitzats recentment pel nostre grup d'investigació també s'han obtingut resultats positius al emprar polièsters hiperramificats com a modificants de sistemes epoxi. En primer lloc, la modificació del DGEBA amb Boltorn H30 en presència de triflat d'iterbi ($Yb(OTf)_3$) com a iniciador catiònic permetia incorporar químicament l'agent modificant a través de reaccions de transferència induïdes pels grups hidroxil terminals del HBP. A la vegada, a l'augmentar la proporció de HBP la contracció global es veia reduïda substancialment degut a un augment en el volum lliure dins la matriu epoxídica. A més a més, la conversió a la gelificació (α_{gel}) augmentava, degut a un augment de reaccions de transferència que redueixen la longitud de les cadenes i n'augmenta el nombre, incrementant α_{gel}. Ambdós fenòmens són positius ja que ajuden a disminuir les tensions internes que es generen durant el procés de curat. Finalment, els materials contenint HBP podien ser degradats a una temperatura més baixa que el material no modificat degut a la presència d'esters a l'estructura hiperramificada [73].

En un altre treball dut a terme per Foix *i col.* es van obtenir resultats similars emprant el mateix polímer com agent modificant en un sistema epoxi/anhídrid. Apart d'evidenciar per mitjà d'espectroscòpia d'infrarroig (FTIR) la incorporació química del HBP a través, en aquest cas, de reaccions de condensació, van observar que l'addició de Boltorn H30 incrementava la T_g quan la proporció d'aquest al material no superava el 15 % en pes. Cal destacar que tot i observar una millora de les propietats termomecàniques els materials resultaren totalment homogenis [74].

En un treball posterior, emprant Boltorn H30 modificat amb grups undecenoat i undecenoat amb grups epoxi terminals van poder demostrar que el fet d'introduir cadenes alifàtiques llargues no reactives al HBP permetia obtenir materials microestructurats per separació del HBP dins la matriu epoxídica. Pel contrari, quan les cadenes alifàtiques llargues estaven modificades amb grups oxirà terminals aquests podien reaccionar amb la reïna generant en aquest cas, materials homogenis. En ambdós casos, la T_g es veia lleugerament disminuïda

[73] Fernández-Francos, X.; Salla, J.M.; Cadenato, A.; Morancho, J.M.; Serra, A.; Mantecón, A.; Ramis, X. A *New strategy for controlling shrinkage of DGEBA resins cured by cationic copolymerization with hydroxyl-terminated hyperbranched polymers and ytterbium triflate as an initiator* J. Appl. Polym. Sci. **2009**, 111, 2822-2829.
[74] Foix, D.; Yu, Y.; Serra, A.; Ramis, X.; Salla, J.M. *Study on the chemical modification of epoxy/anhydride thermosets using a hydroxyl terminated hyperbranched polymer* Eur. Polym. J. **2009**, 45, 1454-1466.

encara que pel material microestructurat aquesta disminució no fos sensible al percentatge de polímer dins la matriu [75].

També s'han obtingut millores en quant a la reciclabilitat del materials termoestables modificats amb HBPs en un sistema catiònic. Concretament, per mitjà de tractament químic com és la hidròlisi bàsica, es va aconseguir fragmentar els materials modificats amb un polièster hiperramificat alifàtic-aromàtic provinent de la condensació de l'àcid 4,4-bis(4-hidroxifenil)valèric (**Esquema I-16**) [17c].

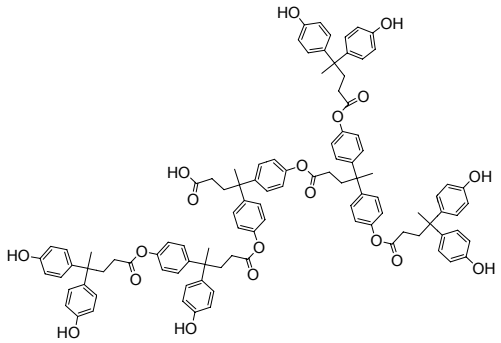

Esquema I-16 Estructura teòrica del poliester aromàtic hiperramificat derivat de l'àcid 4,4-bis(4-hidroxifenil)valèric

En quant a l'ús de polímers estrella com a modificants de sistemes epoxídics, podem trobar el treball de Meng *i col.* [76], els quals han sigut els primers en estudiar el seu efecte en un sistema epoxi/amina. Concretament varen obtenir materials nanoestructurats mitjançant la modificació del DGEBA amb un polímer estrella, contenint el nucli de poliestirè i els braços d'un copolímer poli(òxid d'etilè)-*b*-poliestirè (PEO-*b*-PS/P(DVB-St)) (**Esquema I-17**). Com a resultat destacat, val a dir que la T_g dels materials modificats amb un 5 o un 10 % en pes de polímer estrella mostraven un valor 10 ºC superior a la reïna base però no es va evaluar la seva influència en les propietats mecàniques dels materials.

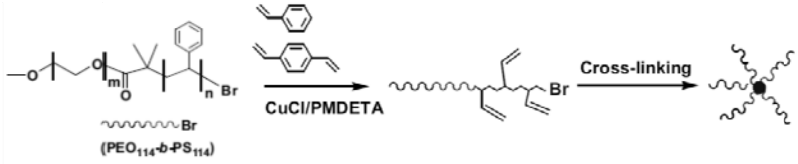

Esquema I-17 Ruta sintètica seguida per l'obtenció del polímer estrella PEO-*b*-PS/P(DVB-St) a través de la via "*arm-first*"

[75] Fernández-Francos, X.; Foix, D.; Serra, A.; Salla, J.M.; Ramis, X. *Novel thermosets based on DGEBA and hyperbranched polymers modified with vinyl and epoxy end groups* Funct. React. Polym. **2010**, 70, 798-806.
[76] Meng, Y.; Zhang, X.H.; Du, B.Y.; Zhou, B.X.; Zhou, X.; Qi, G.R. *Thermosets with core–shell nanodomain by incorporation of core crosslinked star polymer into epoxy resin* Polymer **2011**, 52, 391-399.

I.2 OBJECTIUS

L'objectiu final d'aquest treball és la millora de propietats de materials termoestables epoxídics obtinguts a partir d'una reïna comercial, el diglicidilèter de bisfenol A (DGEBA), a través de la modificació amb polímers dendrítics de tipus hiperramificat i estrella.

Tenint en compte els precedents descrits en el **Capítol I**, apartat **I.1.6**, s'han establert els objectius concrets següents:

En primer lloc, l'ús de HBPs comercials, de tipus poliester alifàtic, com agents modificants de reïnes epoxi ha demostrat ser una de les estratègies més emprades per tal de millorar la tenacitat d'aquests materials en els últims temps. Així doncs, el primer objectiu és l'estudi de nous HBPs, comercials o prèviament sintetitzats, per tal de provar la seva eficiència principalment en la disminució de la fragilitat així com en la contracció durant el procés de curat i la degradabilitat dels materials.

Concretament, es proposa l'ús de poli(ester-amide)s hiperramificades comercials o sintetitzades com modificants d'un sistema epoxi/anhídrid (**Esquema I-18**). A més a més, s'estudia l'efecte del pes molecular del HBP en les propietats finals dels materials.

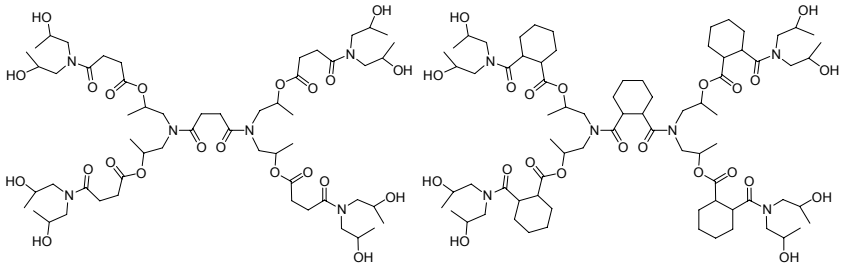

Esquema I-18 Estructures idealitzades de les poli(ester-amide)s hiperramificades comercials emprades

Addicionalment, es descriu la síntesi d'un nou poli(amino-ester) hiperramificat polihidroxíl·lic (PAE) per tal d'estudiar la seva influència com a modificant reactiu del diglicidilèter de bisfenol A iniciat aniònicament (**Esquema I-19**).

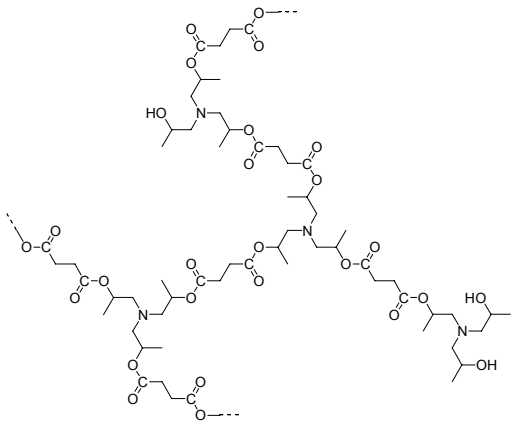

Esquema I-19 Estructura idealitzada del poli(amino-ester) hiperramificat sintetitzat (PAE) i emprat com a agent modificant d'un sistema epoxi aniònic

Els resultats obtinguts es recullen al **Capítol III** - *"Ús de HBPs com a modificants del diglicidilèter de bisfenol A (DGEBA)".*

La recerca de noves topologies dendrítiques com a possibles candidates en la millora de propietats de termoestables de base epoxi resulta de gran importància i a la vegada poc explorada. Entre elles, els polímers de tipus "estrella" resulten actualment de gran interès degut a les seves característiques similars als dendrímers. Per tant, el segon objectiu plantejat és l'obtenció de polímers estrella variant el nucli hiperramificat així com l'estructura química dels braços i posteriorment emprar-los per modificar sistemes epoxídics tan catiònics com aniònics. El disseny estructural de les estrelles sintetitzades s'ha dut a terme jugant amb dos paràmetres: rigidesa/flexibilitat i caràcter polar/apolar combinant els dos paràmetres entre les dues parts constituents del polímer estrella, el nucli i els braços.

Inicialment es descriu la síntesi i la caracterització de polímers estrella multibraços contenint nuclis hiperramificats de tipus polièter – *polar i flexible* - (PGOH) o poliestirè - *apolar i rígid* - (PSOH) i braços de poli(*ε*-caprolactona) - *apolar i flexible* - (PCL) mitjançant polimerització per obertura d'anell (**Esquema I-20**).

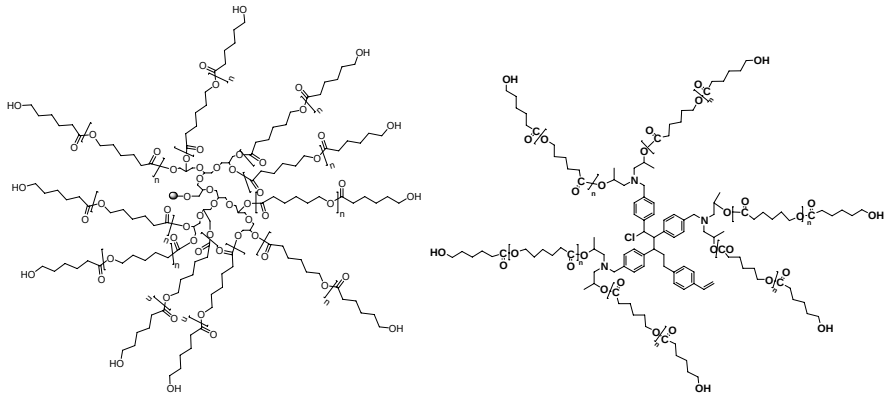

Esquema I-20 Polímers estrella sintetitzats a través de polimerització per obertura d'anell i emprats com agent modificants del DGEBA. Esquerra (PGOH-*b*-PCL) i dreta (PSOH-*b*-PCL)

En segon lloc, s'estudia l'efecte d'aquesta nova topologia en els processos de curat i gelificació així com en la viscositat de les mescles i les propietats finals dels materials. A més, s'estudia l'efecte de la longitud dels braços del polímer estrella i es compara els avantatges que proporciona l'ús d'aquesta nova topologia amb la topologia lineal clàssica.

Els resultats obtinguts es recullen al **Capítol IV** - *"Síntesi de polímers estrella mitjançant ROP i el seu ús com a modificants del DGEBA"*.

Finalment, es descriu la síntesi de polímers estrella contenint com a nucli hiperramificat un polièter - *polar i flexible* - i braços de poli(metil metacrilat) - *apolar i rígid* - (PGOH-*b*-PMMA) o poliestirè - *apolar i rígid* - (PGOH-*b*-PS) mitjançant polimerització radicalària controlada així com el seu ús com a modificants d'un sistema epoxídic aniònic (**Esquema I-21**).

Concretament, s'ha proposat primerament la síntesi de varis polímers estrella (PGOH-*b*-PMMA) contenint diferent nombre de braços i llargada per tal d'avaluar l'efecte d'aquests dos paràmetres en les propietats reològiques de les estructures.

Seguidament, s'avalua la influència de l'addició d'aquestes estructures, PGOH-*b*-PMMA i PGOH-*b*-PS, en els processos de curat i gelificació així com en la morfologia i les propietats finals dels materials termoestables obtinguts.

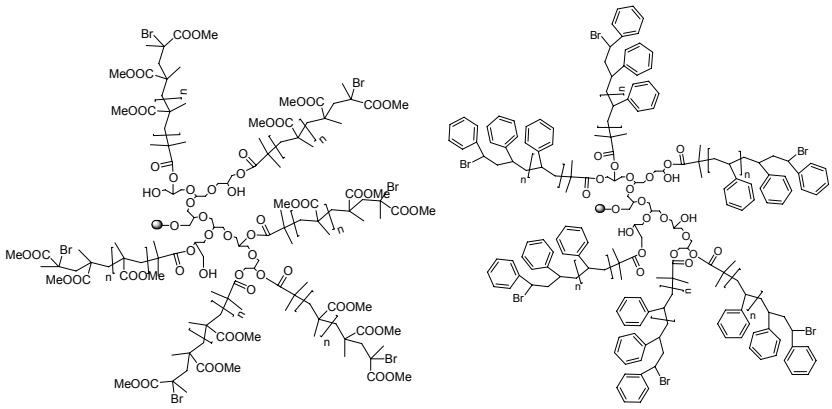

Esquema I-21 Polímers estrella sintetitzats a través de polimerització radicalària controlada i emprats com agent modificants del DGEBA. Esquerra (PGOH-*b*-PMMA) i dreta (PGOH-*b*-PS)

Els resultats obtinguts es recullen al **Capítol V** - *"Síntesi de polímers estrella per ATRP i el seu ús com a modificants del DGEBA"*.

CAPÍTOL II

Tècniques i mètodes d'anàlisi

UNIVERSITAT ROVIRA I VIRGILI
NOUS TERMOESTABLES EPOXÍDICS MODIFICATS AMB ESTRUCTURES DENDRÍTIQUES DE TIPUS HIPERRAMIFICAT I ESTRELLA
Mireia Morell Bel
DL:T. 155-2012

II.1 CALORIMETRIA DIFERENCIAL D'ESCOMBRAT (DSC)

S'han fet servir dos calorímetres Mettler DSC821e i DSC822e calibrats amb Indi. El DSC821e equipat amb un braç robòtic TSO801RO i operant entre 30 ºC i 300 ºC. El DSC822e operant entre -150 ºC i 250 ºC. A la **Figura II-1** es mostren els calorímetres Mettler emprats.

Figura II-1 Calorímetres DSC821e i DSC822e (esquerra) i detall del braç robòtic TSO801RO del DSC821e (dreta)

Cinètica de curat

L'estudi de la cinètica mitjançant DSC parteix de la base que el calor després o absorbit durant una reacció és proporcional al grau de conversió de reactius a productes [1]. Per tant, la velocitat de reacció, $d\alpha / dt$, entesa com la velocitat de conversió d'una espècie de referència, serà proporcional a la calor alliberadaque mesurem dH / dt . La integració d'aquest senyal, el calor mesurat durant el procés de curat (ΔH) serà equivalent a la calor alliberada durant el curat, que podrà ser completa (ΔH_{total}) o no. En el cas de processos senzills, amb una sola reacció implicada, es compleixen totes aquestes assumpcions. En processos complexes, on tinguin lloc més reaccions, no és estrictament cert, de totes maneres en molts casos es pot considerar que el calor mesurat és principalment degut a la reacció d'un dels components del sistema i per tant es pot fer servir com a mesura de la reacció d'aquest [1,2]. La velocitat de reacció i la conversió es poden calcular com:

$$\frac{d\alpha}{dt} = \frac{dH / dt}{\Delta H_{total}} = \frac{dh / dt}{\Delta h_{total}} \qquad \text{(II-1)}$$

$$\alpha = \frac{\Delta H_t}{\Delta H_{total}} = \frac{\Delta h_t}{\Delta h_{total}} \qquad \text{(II-2)}$$

[1] Turi, E.A., ed., *Thermal Characterization of Polymeric Materials*, 2n ed., San Diego: Academic Press, CA, **1997**.
[2] Fernandez, X.; Ramis, X.; Salla, J.M. *Cationic copolymerization of cycloaliphatic epoxy resin with a spirobislactone with lanthanum triflate as initiator: Kinetics of the curing process.* Thermochim. Acta, **2005**, 438, 144-154.

on dh/dt i Δh_{total} són la velocitat d'alliberament de calor i la calor total de reacció, respectivament, normalitzats respecte a la massa de la mostra, ΔH_t, és la calor alliberada fins a un temps *t*, i Δh_t és aquesta calor normalitzada respecte a la massa de la mostra, la qual es pot expressar en *J/g*, o de manera més útil respecte als equivalents d'espècie reactiva en *kJ/eq* o (*kJ/mol*).

La cinètica de curat es pot estudiar de manera isotèrmica monitoritzant la calor alliberada (dh/dt) a temperatura constant o mitjançant experiències no isotèrmiques a través d'un escombrat de temperatures a velocitat d'escalfament constant. Aquest últim mètode presenta l'avantatge que no es perd informació a l'inici de l'experiment i que la reacció sempre és completa ja que per les velocitats d'escalfament usuals la temperatura de la mostra sempre és superior a la T_g del material [1] i conseqüentment, al final de la reacció, superior a la seva $T_{g\infty}$. En aquest cas, el grau de conversió es pot calcular com:

$$\alpha = \frac{\Delta H_T}{\Delta H_{dyn}} = \frac{\Delta h_T}{\Delta h_{dyn}} \qquad \text{(II-3)}$$

on ΔH_{dyn} és el calor total de reacció a través d'una experiència dinàmica i Δh_{dyn} és aquest calor normalitzat respecte a la massa de la mostra, ΔH_T, és el calor alliberat fins a una temperatura T a través d'una experiència dinàmica i Δh_T és aquesta calor normalitzada respecte a la massa de la mostra.

II.2 TERMOGRAVIMETRIA (TGA)

S'ha emprat una termobalança Mettler TGA/SDTA851e/LF/1100 (**Figura II-2**) per analizar l'estabilitat tèrmica dels diferents materials mitjançant experiències dinàmiques a 10 ºC/min des de 30 a 800 ºC en atmosfera de nitrogen (100 cm^3/min mesurats en condicions normals). L'inici de la descomposició tèrmica, que es pot definir a partir d'un percentatge de pèrdua de massa (normalment el 2 o el 5 %), és un indicador de l'estabilitat límit del material. La temperatura de màxima velocitat de degradació s'associa a l'estructura del reticle i la seva estabilitat.

Figura II-2 Termobalança Mettler TGA/SDTA851e/LF/1100

II.3 ANÀLISI TERMODINAMOMECÀNICA (DMTA)

Les mesures enregistrades als laboratoris de la Universitat Rovira i Virgili (Tarragona) s'han realitzat emprant un analitzador DMTA 2980 de TA instruments (**Figura II-3**, esquerra) per l'anàlisi dinàmica a 3 ºC/min i 1 Hz en la modalitat de deformació en tres punts *three-point bending* o flexió en un o dos punts *single*/*dual cantilever* (**Figura II-3**, dreta). Les mesures fetes als laboratoris de la Universitat Politècnica de Catalunya (Barcelona) s'han realitzat mitjançant un analitzador PL-DMTA MKIII de Rheometrics (equip antic) o un analitzador DMA Q800 de TA instruments (equip nou) per l'anàlisi dinàmica a 3 ºC/min i 1 Hz en la modalitat de flexió en un o dos punts *single/dual cantilever*.

Figura II-3 DMTA 2980 de TA instruments (esquerra) i detall del suport en la modalitat de flexió en un o dos punts *single*/*dual cantilever* (dreta)

S'han emprat mostres prismàtiques amb una geometria resultant 20 x 5 x 1.5 mm^3. Les mostres s'han preparat a partir d'un motllo de tefló amb un gruix de 1.5 mm col·locat al mig de dues plaques metàl·liques, recorbertes d'una fina capa de silicona, formant un sandvitx. La mescla líquida s'introdueix mitjançant una pipeta Pasteur a través del motlle fins que aquest queda totalment omplert. Posteriorment, el motlle es introduït a l'estufa i es procedeix a seguir el cicle de curat i post-curat establert. Un cop desemmotllada, es llimen els laterals de la mostra amb paper de vidre per tal d'aconseguir que aquesta sigui perfectament paral·lela. La deformació

de les mostres s'ha situat al 0.5 %, dins del límits recomanats pel fabricant, sense sobrepassar l'interval de viscoelasticitat lineal.

Principis de l'anàlisi termodinamomecànica

L'anàlisi termodinamomecànica mesura la resposta mecànica dels materials polimèrics sotmesos a una deformació oscil·latòria a una freqüència determinada o a diferents freqüències [1]. Degut a la viscoelasticitat dels polímers, la tensió sinusoïdal de resposta mesurada pel DMTA es caracteritza per presentar un desplaçament δ respecte la deformació sinusoïdal aplicada. Es defineix un mòdul complex E^* com $E^* = E' + iE''$ on $E' = E^* \cdot \cos \delta$, que és la component elàstica i indica l'habilitat del material per guardar energia mecànica i $E'' = E^* \cdot \sin \delta$ és la component viscosa o de pèrdues i indica l'habilitat del material per dissipar energia.

Les propietats mecàniques d'un polímer termoestable depenen entre d'altres paràmetres de la temperatura a la qual es fa l'assaig. En funció d'aquest paràmetre es pot establir una resposta viscoelàstica general (**Figura II-4**).

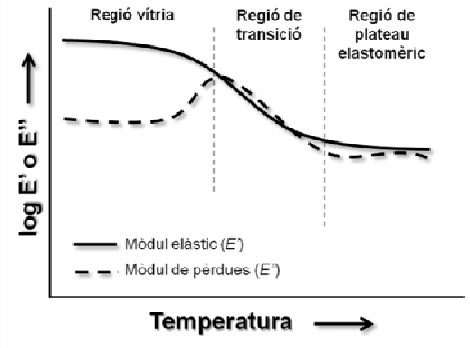

Figura II-4 Resposta viscoelàstica general d'un material entrecreuat

S'acostuma a fer servir el màxim de la relació tan $\delta = E''/E'$ o el màxim de E'' com a indicadors de la transició vítria, tot i que ambdues determinacions estan condicionades per la freqüència a la qual es realitza l'experiment. L'amplada del senyal de tan δ es relaciona amb la homogeneïtat dels materials. En canvi, la seva alçada o àrea té a veure amb l'energia dissipada de manera irreversible per fregament viscós durant la transició vítria així com amb les propietats amortidores que presenta el material [1,3].

[3] Chern, Y.C.; Tseng, S.M.; Hsieh, K.H. *Damping properties of interpenetrating polymer networks of polyurethane-modified epoxy and polyurethanes.* J. Appl. Polym. Sci. **1999**, 74, 328-335.

II.4 ANÀLISI TERMOMECÀNICA (TMA)

S'ha fet servir un analitzador tèrmic-mecànic Mettler TMA 40 per estudiar la dilatació tèrmica dels materials completament curats i fer el seguiment del procés de curat per determinar el punt de gelificació i monitoritzar la contracció (**Figura II-5**, esquerra).

Per a l'estudi de la dilatació tèrmica s'han fet servir les mostres preparades en l'apartat anterior (anàlisi termodinamomecànica) tallades convenientment i suportades entre dos discs de quars. Els coeficients d'expansió tèrmica lineal (*CTE*) en els estats vitri i gomós s'han determinat per mitjà d'experiències dinàmiques a 10 ºC/min, aplicant una força constant de 0.01 N.

Pel seguiment del procés de curat (gelificació i contracció), s'ha fet servir un disc de fibra de vidre silanitzada impregnat de mostra líquida (formulació abans de curar), entre dos discs de quars (**Figura II-5**, dreta). El procés de gelificació s'ha monitoritzat dinàmicament a 5 ºC/min, aplicant una força periòdica entre 0.0025 i 0.01 N en cicles de 12 segons. Pel seguiment de la contracció durant el procés de curat s'ha dut a terme experiències isotèrmiques a 120 ºC emprant una força de 0.01 N.

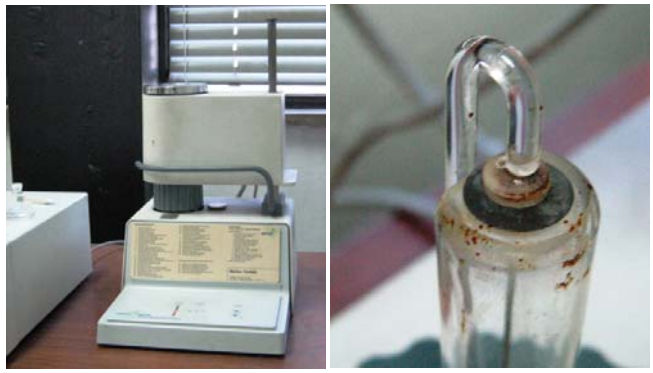

Figura II-5 Analitzador Mettler TMA 40 (esquerra) i detall de la sonda amb una mostra suportada en fibra de vidre entre dos discs de quars (dreta)

Principis de l'anàlisi termomecànica

L'anàlisi termomecànica mesura canvis dimensionals (gruix) d'una mostra sotmesa a una lleugera tensió en funció de la temperatura o del temps [1].

Els coeficients d'expansió tèrmica lineal (*CTE*, K^{-1}) en els estats vitri i gomós es poden calcular com:

$$CTE = \frac{1}{L_0}\cdot\frac{dL}{dT} = \frac{1}{L_0}\cdot\frac{dL/dt}{dT/dt} \qquad \text{(II-4)}$$

on, L és el gruix de la mostra, L_0 és la longitud inicial, t és el temps i T és la temperatura.

L'estudi de la dilatació tèrmica permet la caracterització de la temperatura de transició vítria (T_g) degut a l'augment en el coeficient de dilatació quan passen la relaxació vítria (**Figura II-6**) [1].

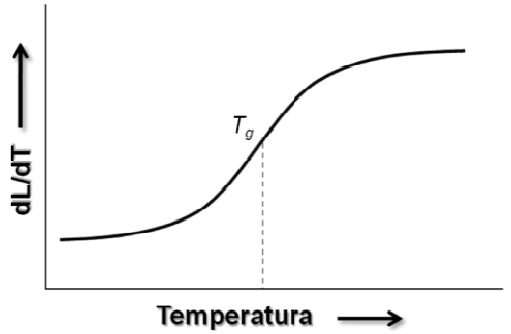

Figura II-6 Corba del coeficient de dilatació durant una experiència dinàmica d'un material completament curat

El procés de contracció també es pot seguir, com s'ha comentat anteriorment, per mitjà d'aquesta tècnica. En tots els casos, aquest encongiment es dóna en dues etapes ben diferenciades. La primera abans de gelificar i la segona després. Entre ambdues etapes (punt d'inflexió) es produeix el fenomen de la gelificació a partir del qual el material es torna parcialment insoluble (**Figura II-7**) [18,4,5].

[4] Mas, C.; Ramis, X.; Salla, J.M.; Mantecón, A.; Serra, A. *Copolymerization of diglycidyl ether of bisphenol A with γ-butyrolactone catalyzed by ytterbium triflate: Shrinkage during curing.* J. Polym. Sci., Part A: Polym. Chem. **2003**, 41, 2794-2808.
[5] Mas, C.; Mantecón, A.; Serra, A.; Ramis, X.; Salla, J.M. *Improved thermosets obtained from cycloaliphatic epoxy resins and γ-butyrolactone with lanthanide triflates as initiators. I. Study of curing by differential scanning calorimetry and fourier transform infrared.* J. Polym. Sci., Part A: Polym. Chem. **2005**, 43, 2337-2347.

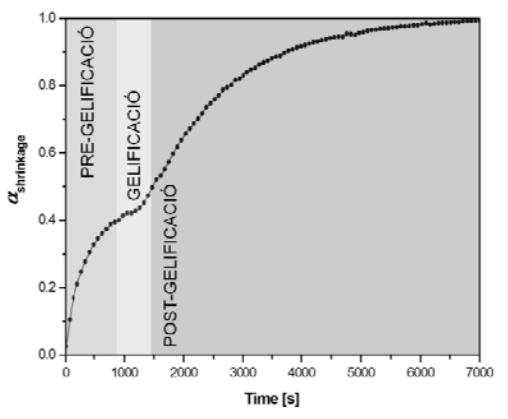

Figura II-7 Evolució del grau de contracció ($\alpha_{shrinkage}$) en funció dels temps mitjançant TMA de la formulació DGEBA/MTHPA contenint un 10 % en pes de S1200. Experiència isotèrmica a 120 ºC (força 0.01 N)

El grau de contracció ($\alpha_{shrinkage}$) es pot calcular com:

$$\alpha_{shrinkage} = \frac{L_t - L_0}{L_\infty - L_0} \qquad \text{(II-5)}$$

on L_t, L_0 i L_∞ representen, respectivament, el gruix de la mostra a temps *t,* a l'inici del procés i al final de la reacció.

La gelificació es pot determinar per TMA de diferents maneres. Per una banda per mitjà d'experiències isotèrmiques, com s'ha descrit anteriorment, en les quals aquesta es manifesta com el punt on no existeix contracció durant el procés de curat. Un altre mode de determinació és a partir de la reducció en l'amplitud de les oscil·lacions de la sonda quan s'aplica una força oscil·latòria. Mentre encara es troba en estat líquid, la formulació pot fluir lliurement dins del suport de fibra de vidre. Per tant, la força dinàmica aplicada per la sonda provoca una gran deformació de la mostra. Un cop la mostra gelifica no pot continuar fluint i l'amplitud de les deformacions disminueix. Aquest mètode, ja emprat anteriorment pel nostre grup de recerca [6], permet determinar tant el temps de gelificació (t_{gel}) com la conversió a la gelificació (α_{gel}), en combinació amb un escombrat dinàmic per DSC, per mitjà del calor residual (Δh_{res}) de la mostra gelificada segons l'equació següent (**Figura II-8**):

[6] a) Cadenato, A.; Salla, J.M.; Ramis, X.; Morancho, J.M.; Marroyo, L.M.; Martin, J.L. *Determination of gel and vitrification times of thermoset curing process by means of TMA, DMTA and DSC techniques TTT diagram* J. Therm. Anal. **1997**, 49, 269-279. b) Ramis, X.; Salla, J.M. *Time-temperature transformation (TTT) cure diagram of an unsaturated polyester resin* J. Polym. Sci., Part B: Polym. Phys. **1997**, 35, 371-388.

$$\alpha_{gel} = \frac{\Delta h_{total} - \Delta h_{res}}{\Delta h_{total}} \qquad \text{(II-6)}$$

on Δh_{total} és el calor total de reacció normalitzada respecte a la massa de la mostra.

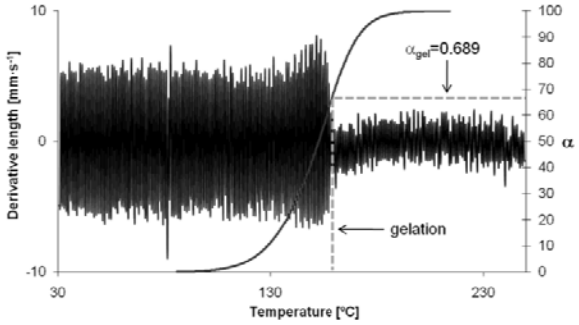

Figura II-8 Determinació del punt de gelificació per TMA i DSC de la mescla DGEBA/MTHPA amb un 10 % en pes de H30000 i 0.5 % en pes de BDMA (bencil-*N,N*-dimetilamina)

II.5 REOMETRIA

S'ha fet servir un reòmetre de tensió controlada ARG2 de TA instruments equipat amb un sistema Peltier amb plats paral·lels de mida 25 mm (**Figura II-9**). Els diferents experiments s'han dut a terme a temperatura constant i dins de l'interval de viscoelasticitat lineal.

Principis de l'anàlisi reomètrica

La mesura de la deformació de resposta respecte a la tensió oscil·latòria aplicada permet la determinació de la viscositat i el mòdul de cisalla *G*. Com amb DMTA, la viscoelasticitat dels polímers es manifesta en un desfasament *δ* entre la tensió i la deformació. Es defineix un mòdul complex *G** com $G^* = G' + iG''$ amb un component elàstic $G' = G^* \cdot \cos \delta$ i un component viscós $G'' = G^* \cdot \sin \delta$. L'evolució de *G'*, *G"* i tan *δ* permet identificar els processos d'entrecreuament, gelificació i vitrificació durant un procés de curat.

Figura II-9 Reòmetre ARG2 de TA instruments (esquerra) i detall dels plats paral·lels entre els quals es col·loca la mostra (dreta)

En primer lloc, s'ha estudiat la gelificació durant el curat isotèrmic a través d'un escombrat en el temps i en la modalitat d'oscil·lació multiona (*multiwave oscillation*). Aquesta modalitat és similar a la d'oscil·lació simple emprant una única freqüència però en aquest cas el material és exposat simultàniament a oscil·lacions de dos o més freqüències. Aquestes oscil·lacions al passar a través del material actuen de manera independent però la deformació del material resultant és la suma de les deformacions causades per cada oscil·lació individualment. Així doncs, el resultat obtingut és el mateix que en mode multifreqüència però amb l'avantatge que es redueix molt més el temps de l'assaig ja que les oscil·lacions es generen al mateix temps i en multifreqüència es genera una corba per cada freqüència en diferents temps. Això fa que es puguin analitzar processos que es donen en un període de temps relativament curt.

Es duu a terme la determinació del temps de gelificació (t_{gel}) com el creuament de les corbes de tan δ, que és invariant respecte la freqüència tal com es mostra a la **Figura II-10**, i que generalment es troba abans del creuament de les corbes G' i G'', una determinació de la gelificació que sí depèn de la freqüència i per tant no és del tot correcte tenint en compte que la gelificació és un fenomen químic [7].

Com que la viscositat del sistema canvia significativament al llarg del procés de curat s'ha establert un programa de control per tal d'adequar l'amplitud de l'oscil·lació amb la tensió aplicada cada vegada més elevada. D'aquesta manera, es pot registrar tot el procés de curat des de la mescla inicialment líquida fins que el material esdevé totalment entrecreuat. La conversió a la gelificació (α_{gel}) així com la T_g al punt de gelificació (T_{gel}) s'han determinat aturant l'experiment just al punt on

[7] Pascault, J.P., Sautereau, H., Verdu, J., Williams, R.J.J., *Rheological and Dielectric Monitoring of Network Formation* in *Thermosetting Polymers*, Marcel Dekker, New York, **2002**.

s'assoleix la gelificació, congelant la mostra instantàniament amb nitrogen líquid i realitzant un escombrat dinàmic per DSC de la mostra gelificada. El grau de conversió a la gelificació es calcula a partir de l'equació (II-6).

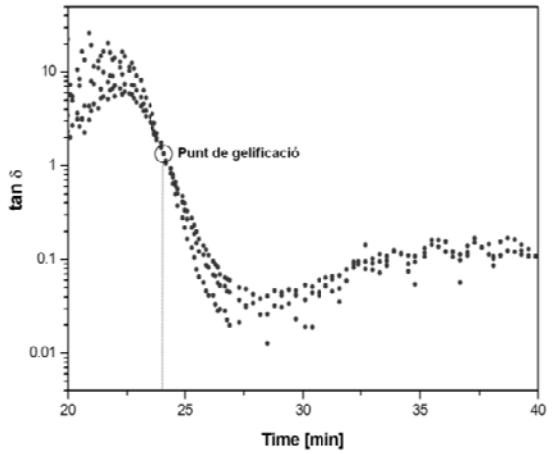

Figura II-10 Evolució de la tan *δ* durant el procés de curat a 80 ºC d'una formulació DGEBA/1MI contenint un 5 % en pes de PGOH-*b*-PCL_{30}

En segon lloc, per la determinació de la contracció després de la gelificació (S_{gel}) s'ha dut a terme un assaig a temperatura constant relativament elevada per tal d'evitar que el material vitrifiqui i es pugui perdre informació. Establint la força normal a 0 es segueix l'evolució del *gap* (distància entre els dos plans paral·lels) a partir del punt de gelificació i fins que aquest esdevé pràcticament constant. S_{gel} es pot determinar a partir de la següent equació, segons Shah *i col.* [8]:

$$S_{gel} = \left[\left(1 + \frac{1}{3} \left(\frac{h - h_0}{h_0} \right) \right)^3 - 1 \right] x100 \qquad \text{(II-7)}$$

on h_0 és el gap inicial al punt de gelificació, h és el gap final quan aquest esdevé constant.

Per tal d'emprar l'equació anterior cal tenir en compte dos supòsits: el primer que les deformacions de la reïna horitzontalment són negligibles i el segon que la mostra resulta incompressible.

[8] Shah, D.U.; Schubel, P.J. *Evaluation of cure shrinkage measurement techniques for thermosetting resins* Polym. Test. **2010**, 29, 629-639.

Finalment, el seguiment de la viscositat complexa (η^*) tant de les mescles abans de curar com de films polimèrics s'ha realitzat en funció de la freqüència angular establint una deformació constant.

II.6 ESPECTROSCÒPIA INFRA-ROJA PER TRANSFORMADA DE FOURIER (FTIR)

S'ha fet servir un espectrofotòmetre FTIR-680PLUS de Jasco amb una resolució de 4 cm^{-1} dotat d'un dispositiu de reflectància total atenuada amb control de temperatura (Golden Gate Heated Single Reflection Diamond ATR, Specac-Teknokroma). La **Figura II-11** mostra l'equip emprat i un detall del dispositiu ATR.

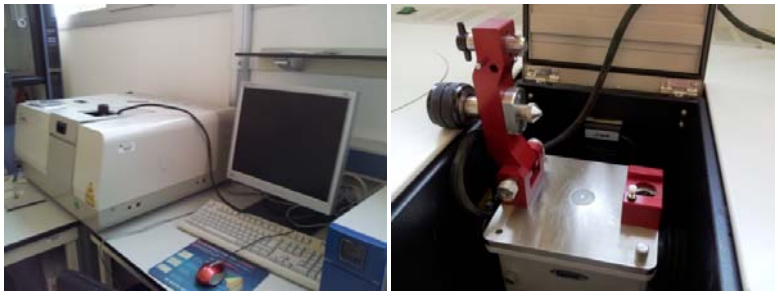

Figura II-11 Espectrofotòmetre FTIR-680PLUS (esquerra) i detall del dispositiu ATR amb placa tèrmica incorporada (dreta)

D'acord amb la llei de Lambert-Beer, $A=\varepsilon \cdot c \cdot l$, l'absorbància A d'una espècie a una freqüència determinada és proporcional a la seva absortivitat ε i a la seva concentració c. El seguiment de l'absorbància a freqüències que es puguin identificar els grups reactius pertanyents a alguna espècie determinada permet estudiar la concentració d'aquesta espècie durant un procés químic. Per tal de compensar variacions en el camí òptic l o canvis físics que puguin afectar els senyals de diferents mostres o d'espectres adquirits en línia durant un procés químic s'ha de dur a terme una normalització dels espectres fent servir un senyal de referència corresponent a alguna espècie la concentració de la qual romangui inalterable.

Es defineix, per tant, una absorbància normalitzada ($\overline{A}$) com:

$$\overline{A} = \frac{A}{A_{ref}} \qquad \text{(II-8)}$$

on A_{ref} és l'absorbància de la senyal de referència.

Es pot calcular la conversió d'una espècie que desapareix com:

$$\alpha(t) = 1 - \left(\frac{\overline{A}^t}{\overline{A}^0} \right) \quad \text{(II-9)}$$

on $\overline{A}^0$ és l'absorbància normalitzada de l'espècie a l'inici del procés i $\overline{A}^t$ és l'absorbància normalitzada en un instant de temps *t*.

En el cas d'una espècie que es forma, la conversió es pot calcular com:

$$\alpha(t) = \left(\frac{\overline{A}^t}{\overline{A}^\infty} \right) \quad \text{(II-10)}$$

on $\overline{A}^\infty$ és la màxima 'absorbància normalitzada de l'espècie.

II.7 MESURA DE DENSITATS I CONTRACCIÓ GLOBAL

El càlcul de la contracció global implica conèixer els valors dels volums específics o densitats dels materials abans ($\rho_{monomer}$) i després de curar ($\rho_{polymer}$) a les condicions de procés. Per tant, en la present tesi s'ha fet ús d'un picnòmetre d'heli AccuPyc 1330 de Micromeritics per tal de determinar les densitats corresponents a una temperatura de 30 ºC (**Figura II-12**) i posteriorment aplicant la següent equació s'ha pogut determinar la contracció global (*Shrinkage*):

$$Shrinkage = \left[\frac{\rho_{polymer} - \rho_{monomer}}{\rho_{polymer}} \right] x100 \quad \text{(II-11)}$$

Figura II-12 Picnòmetre d'heli AccuPyc 1330 emprat

II.8 RESSONÀNCIA MAGNÈTICA NUCLEAR (RMN)

L'enregistrament dels espectres de RMN de ^1H i ^{13}C a la Universitat Rovira i Virgili s'han dut a terme en un espectròmetre Varian Gemini 400 amb una resolució

de 400 MHz i 100.6 MHz, respectivament. Al Leibniz-Institut für Polymerforschung a Dresden, s'ha emprat un espectròmetre Bruker DRX 500 amb una resolució de 500.13 MHz (^{1}H) i 125.75 MHz (^{13}C). Com a dissolvents s'han emprat: $CDCl_3$, DMSO-d_6, acetona-d_6, C_6D_6 i diclorometà (CD_2Cl_2). La calibració interna s'ha dut a terme per mitjà dels pics residuals dels dissolvents: $CDCl_3$ δ (^{1}H) = 7.26 ppm, δ (^{13}C) = 77.16 ppm; DMSO-d_6 δ (^{1}H) = 2.50 ppm, δ (^{13}C) = 39.52 ppm; acetona-d_6 δ (^{1}H) = 2.05 ppm, δ (^{13}C) = 29.84, 206.3 ppm; C_6D_6 δ (^{1}H) = 7.16 ppm, δ (^{13}C) = 128.06 ppm i CD_2Cl_2 δ (^{1}H) = 5.32 ppm, δ (^{13}C) = 54.00 ppm.

Les mesures quantitatives de ^{13}C s'han enregistrat amb 8 segons de temps de espera entre polsos i amb la seqüència *inverse gated decoupling*.

S'han dut a terme experiments per mesurar el temps de relaxació spin-spin (T_2) per tal d'identificar indirectament el nucli en aquells polímers estrella els quals els senyals del nucli eren molt amples i resultaven parcialment cobertes per els senyals dels braços. Basant-se en la diferent mobilitat que existeix en diverses zones d'una molècula, que afecten als T_2 es poden filtrar alguns senyals. En polímers estrella, els spins nuclears de les regions amb una movilitat restringida (nucli) presenten una difusivitat rotacional més petita que aquells que estàn en regions amb més moviment i per tant presenten un temps de relaxació T_2 spin-spin més baix i es mostren com a senyals amples.

Emprant seqüències de magnetització consecutives es van filtrant aquells spins nuclears que tenen més tendència a perdre la coherència de fase i que per tant no entren en el nou cicle de magnetització per no trobar-se en fase. Aquests spins nuclears corresponen als nuclis amb un moviment més restringit dins la molècula. Això es tradueix a l'espectre en una eliminació progressiva dels senyals amples i per tant es pot identificar parts de l'estructura amb diferent grau de moviment.

Per realitzar aquests experiments, s'ha emprat un espectròmetre Bruker Avance III 600 operant a una freqüència de protó de 600.20 MHz. Les mesures del temps de relaxació T_2 s'ha dut a terme mitjançant una seqüència de magnetització o filtre de tipus CPMG (Carr-Purcell-Meiboom-Gill) entre 40.7 i 1220 ms.

Els T_2 corresponents al nucli i als braços s'han determinat mitjançant la següent equació [9]:

$$I_{2\tau} = I_0 \cdot exp\ (-2\tau/T_2) \qquad \text{(II-12)}$$

[9] Friebolin, H. *Basic One- and Two-Dimensional NMR Spectroscopy*, 4th ed., Wiley-VCH, Weinheim, **2005**.

on I_0 i $I_{2\tau}$ són l'àrea de la senyal al inici de l'experiment i després de cada seqüència CPMG i 2τ correspon a la duració del filtre. El T_2 s'obté del pendent de la recta al graficar $\ln[I_{2\tau}/I_0]$ respecte 2τ.

II.9 CROMATOGRAFIA D'EXCLUSIÓ MOLECULAR (SEC)

La determinació de pesos moleculars promig i la seva distribució s'ha dut a terme en dos cromatògrafs d'exclusió moleculars. En primer lloc, als laboratoris de la Universitat Rovira i Virgili (URV) s'han emprat dos equips: un cromatògraf Waters equipat amb un detector d'índex de refracció (RI) Waters 510 (RID-6A from Shimadzu) i amb una combinació de columnes Waters SHODEX en sèrie (K80M, Gel 5 μm MIXED-D, Gel 3 μm MIXED-E) o un cromatògraf Agilent 1200 equipat amb un detector RI Agilent 1100 series i amb una combinació de columnes en sèrie PLgel 3 μm MIXED-E, PLgel 5 μm MIXED-D i PLgel 20 μm MIXED-A (**Figura II-13**). La calibració s'ha dut a terme amb patrons de poliestirè o poli(metil metacrilat) en funció de l'estructura a analitzar i les mesures s'han dut a terme emprant un cabal de 1 mL/min. En ambdós equips s'ha emprat THF com eluent.

Figura II-13 Cromatògraf Agilent 1200 amb detector d'índex de refracció (RI)

D'altra banda, als laboratoris del Leibniz-Institut für Polymerforschung a Dresden, s'ha emprat un Agilent 1200 equipat amb un detector de dispersió de llum làser multiangular (MALLS) Tristar MiniDawn (Wyatt Technology) i un detector de refracció de llum (RI) Knauer, emprant DMAc amb 3 g/L de LiCl com eluent i una columna PolarGel-M-column de Polymer Laboratories. L'ús del detector MALLS permet determinar el pes molecular absolut ja que no està influenciat per l'arquitectura molecular del polímer. A més a més, no és necessària la calibració amb patrons.

En aquest cas, l'evaluació dels pesos moleculars promig ($\overline{M_w}$, $\overline{M_n}$) i el radi de gir ($R_{g,z}$) s'han determinat per mitjà del software ASTRA 4.9 de Wyatt Technologies.

Primerament, s'ha determinat el valor del *dn/dc*, que és l'índex de refracció diferencial específic el qual depèn de cada polímer i del solvent emprat. S'ha dut a terme, analitzant el pic cromatogràfic i assumint una conversió de la massa completa. L'obtenció d'aquest valor és necessari per tal de poder conèixer acuradament els paràmetres abans esmentats ja que la constant òptica (*K*) (equació II-13) que apareix en l'equació de Rayleigh (equació II-14), que expressa la llum dispersada d'una solució diluïda de partícules, és proporcional al quadrat del *dn/dc* i per tant si hi ha un error en aquest paràmetre es produeix el doble d'error en la determinació del pes molecular.

$$K = \frac{16\pi^2}{\lambda_0^4 N_A} n_0^2 \left(\frac{dn}{dc}\right)^2 \qquad \text{(II-13)}$$

on *dn/dc* és l'índex de refracció diferencial específic; N_A és el número d'Avogadro; n_0 és l'índex de refracció del solvent i λ_0 és la longitud d'ona en el buit.

$$\frac{Kc}{R_\theta} = \frac{1}{M_w} * \left[\left(1 + \frac{1}{3} * \left\langle S^2 \right\rangle_z * q^2\right) + 2A_2 M_w c\right] \qquad \text{(II-14)}$$

on R_θ és la intensitat de la dispersió normalitzada a l'angle de dispersió θ; *c* és la concentració en g/cm^3; *q* és la magnitud del vector de dispersió relacionat a l'angle θ i $<S^2>_z$ és la distància promig de totes les conformacions possibles on l'índex *z* és el promig en *z* respecte la distribució de pesos moleculars.

El $R_{g,z}$ s'ha determinat pel mètode de Zimm [10]:

$$R_{g,z} = \sqrt{< S^2 >_z} \qquad \text{(II-15)}$$

II.10 CROMATOGRAFIA DE GASOS (GC)

Per tal de determinar la conversió de monòmer en les polimeritzacions radicalàries s'ha emprat un cromatògraf de gasos 6890 equipat amb un espectròmetre de masses 5973 i una columna capil·lar HP-5MS d'Agilent Technologies (Palo Alto) (**Figura II-14**).

El gas portador, heli de puresa 99.999 %, s'ha emprat a un cabal de 1 mL/min. El volum de mostra injectat era de 1 μL en mode split. El monòmers es van quantificar a partir del seus pic principal corresponents a l'ió de massa m/z més abundant.

[10] a) Zimm, B.H. *The scattering of light and the radial distribution function of high polymer solutions* J. Chem. Phys. **1948**, 16, 1093-1099. b) Zimm, B.H. *Apparatus and methods for measurement and interpretation of the angular variation of light scattering; Preliminary results on polystyrene solutions* J. Chem. Phys. **1948**, 16, 1099-1116.

Prèviament a la mesura de les mostres, es va dur a terme una calibració externa emprant patrons comercials de l'anàlit i cobrint l'interval de concentracions de 50 a 1000 ppm. Posteriorment, les mostres diluïdes van ser analitzades sota les mateixes condicions que els patrons i la concentració de l'anàlit extreta per interpolació a la recta de calibrat.

Figura II-14 Cromatògraf de gasos 6890 equipat amb un espectròmetre de masses 5973 (GC-MS)

II.11 MICROSCÒPIA ELECTRÒNICA D'ESCOMBRAT

Per mitjà de la microscòpia electrònica d'escombrat es pot observar i caracteritzar la superfície de materials inorgànics i orgànics, obtenint informació de la morfologia del material. En aquest treball, s'ha fet ús de dos tipus de microscopis electrònics d'escombrat, un microscopi electrònic d'escombrat convencional (SEM) Jeol JSM 6400 amb una resolució de 3.5 nm i un microscopi electrònic d'escombrat ambiental (ESEM) model FEI Quanta 600 (**Figura II-15**). En el cas d'emprar el SEM s'han recobert prèviament les mostres amb una capa fina d'or.

Figura II-15 Microscopi electrònic d'escombrat (SEM) Jeol JSM 6400 (esquerra) i microscopi electrònic d'escombrat ambiental (ESEM) FEI Quanta 600 (dreta)

Principis de la microscòpia electrònica d'escombrat (Figura II-16)

Es fa incidir un feix prim d'electrons accelerats sobre una mostra gruixuda opaca als electrons. Aquest feix es focalitza sobre la superfície de la mostra de tal

manera que es realitza un escombrat d'aquesta seguint una trajectòria de línies paral·leles.

La interacció del feix d'electrons amb la mostra genera dos radiacions principals: els electrons secundaris i els electrons retrodispersats. Els primers són electrons de baixa energia que es generen de l'emissió per part dels àtoms constituents de la mostra (els que estàn més aprop de la superfície). Amb els electrons secundaris s'obté una imatge de l'apariència tridimensional de la mostra. En canvi, els electrons retrodispersats són electrons del feix incident que han interaccionat amb els àtoms de la mostra i han sigut reflectits. La intensitat de les dues radiacions varia en funció de l'angle que forma el feix incident i la superfície del material, és a dir, depén de la topografia de la mostra.

El senyal emés pels electrons i les radiacions resultants de l'impacte es recull mitjançant un detector i s'amplifica per cada posició de la sonda. Les variacions de la intensitat del senyal que es produeixen mentre la sonda escombra la superfície de la mostra, s'utilitzen per variar la intensitat del senyal en un tub de raigs catòdics que es va desplaçant en sincronia amb la sonda. El resultat és una imatge topogràfica molt ampliada de la mostra.

Si la mostra no és bona conductora s'acostuma a recobrir-la amb una pel·lícula conductora metàl·lica o de carboni per evitar que aquesta es carregui quan sigui irradiada. En el cas del microscopi electrònic d'escombrat ambiental no és necessari recobrir la mostra ja que es treballa amb un buit baix contràriament als microscopis electrònics convencionals on es treballa amb un buit alt i les mostres han de ser conductores.

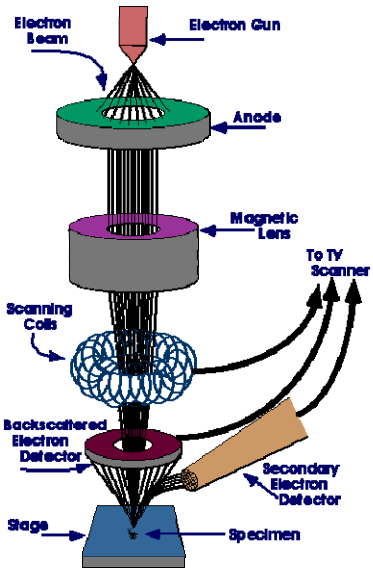

Figura II-16 Diagrama del funcionament d'un microscopi electrònic d'escombrat

II.12 MICROSCÒPIA ELECTRÒNICA DE TRANSMISSIÓ

Per mitjà de la microscòpia electrònica de trasmissió es pot estudiar l'estructura interna dels materials. En aquest treball, s'ha fet ús d'un microscopi electrònic de transmissió (TEM) Jeol 1011 (**Figura II-17**).

Les mostres dels materials termoestables observades per mitjà del TEM van ser prèviament tallades emprant un ultramicròtom a temperatura ambient i observades sense necessitat de tinció.

Figura II-17 Microscopi electrònic de transmissió (TEM) Jeol 1011

Principis de la microscòpia electrònica de transmissió

Els microscopis electrònics més senzills consten de dues lents formadores de la imatge de manera molt similar als microscopis òptics convencionals. La il·luminació prové d'un canó d'electrons emesos per un filament de W o LaB_6. Els electrons són accelerats a l'aplicar un potencial negatiu (100 kV - 1000 kV) i focalizats mitjançant dos lents condensadores sobre una mostra fina, transparent als electrons.

Després de passar a través de la mostra els electrons són recollits i focalizats per la lent objectiu dins d'una imatge ampliada. La imatge s'amplia encara més gràcies a les lents projectores les quals controlen l'ampliació de la imatge a la pantalla fluorescent. La imatge final es projecta sobre una pantalla fluorescent o una pel·lícula fotogràfica.

II.13 MICROSCÒPIA DE FORCES ATÒMIQUES

S'ha utilitzat un microscopi de forces atòmiques Agilent 5500 AFM/SPM en mode de contacte i emprant una punta de silici (**Figura II-18**, dreta).

Principis de la microscòpia de forces atòmiques

Aquest microscopi utilitza un cantilever amb una punta fina al seu extrem com a sensor per rastrejar la superfície de la mostra ja siguin materials o molècules individuals dipositades sobre superfícies llises, com per exemple sílica. El sistema, a més a més, presenta un feix de llum làser que es reflexa sobre la superfície llisa posterior del cantilever fins al fotodetector. Mitjançant la variació de l'alçada de la punta, mentre aquesta es desplaça sobre la superfície, el feix de llum làser varia la seva inclinació i per tant la seva posició al fotodetector creant-se una imatge del relleu de la mostra.

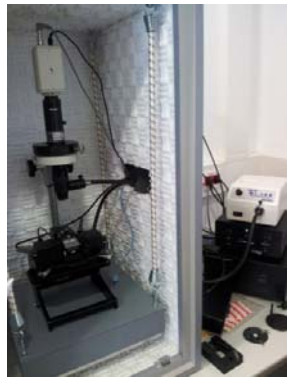

Figura II-18 Microscopi de forces atòmiques (AFM) Agilent 5500 AFM/SPM (dreta)

II.14 PROPIETATS MECÀNIQUES

Les propietats mecàniques dels materials obtinguts en la present tesi s'han assajat al Departament d'Enginyeria Mecànica de la Universitat Rovira i Virgili, sota la supervisió del Dr. Francesc Ferrando.

II.14.1 Resistència a l'impacte (Izod)

El pèndol d'impacte permet mesurar l'energia absorbida pel trencament d'una mostra de dimensions controlades, en relació amb l'energia màxima del pèndol.

S'ha fet servir un pèndol d'impacte Izod 5110 d'acord amb dues normatives diferents (**Figura II-19**).

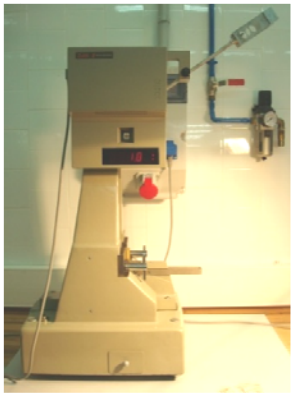

Figura II-19 Pèndol d'impacte Izod 5110

Els primers estudis es van realitzar segons la normativa ASTM 256-05a en mostres rectangulars de 70 x 12 x 4 mm^3 amb una energia de pèndol de 1 J (apartat **III.2**) i 2.75 J (apartat **III.3**), respectivament. Estudis posteriors s'han realitzat seguint la normativa ASTM D 4508-05 (2008), en mostres rectangulars de 25 x 12 x 2 mm^3 amb una energia de pèndol de 1 J (apartats **IV.3** i **V.3**) i 0.56 J (apartat **V.4**), respectivament.

L'energia d'impacte (impact strength, I.S., kJ/m^2) es calcula com:

$$I.S. = \frac{E - E_{blanc}}{A \cdot G} \cdot E_{max} \cdot 10 \qquad \text{(II-16)}$$

on E i E_{blanc} són el % d'energia perduda pel pèndol amb mostra i en buit respectivament, E_{max} és l'energia màxima del pèndol, i A i G són l'amplada i el gruix de la mostra.

II.14.2 Microduresa (Knoop)

La microduresa ha estat mesurada amb un microindentador Wilson Wolpert (Micro-Knoop 401 MAV) segons la normativa ASTM D1494-98 (2002) (**Figura II-20**). La microduresa Knoop ha estat determinada segons l'equació següent:

$$HKN = L/A_p = L/l^2 \cdot C_p \qquad \text{(II-17)}$$

on L és la força aplicada a través de l'indentador (Kg), A_p és l'àrea projectada de la indentació (mm^2), l és la longitud mesurada de la diagonal llarga de la indentació (mm), C_p és la constant de l'indentador que relaciona l^2 amb A_p.

Figura II-20 Microindentador Wilson Wolpert (Micro-Knoop 401 MAV) (esquerra) i detall de la mesura de la microduresa d'un material termoestable (dreta)

II.14.3 Mòdul d'elasticitat

El mòdul d'elasticitat es determina normalment, mitjançant un assaig dinàmic i s'aïlla a partir del pendent de la secció en línia recta d'un diagrama tensió-deformació. En funció del tipus de càrrega representada pel diagrama d'esforç-deformació, el mòdul elàstic es pot especificar com:

- Mòdul elàstic de compressió
- Mòdul elàstic de flexió
- Mòdul elàstic tallant
- Mòdul elàstic de tracció
- Mòdul elàstic de torsió

El mòdul que s'utiliza individualment sol referir-se al mòdul elàstic de tracció. El mòdul tallant quasi sempre és igual al mòdul de torsió i ambdós es coneixen com mòdul de rigidesa. En canvi, els mòduls elàstics de tracció i de compressió són aproximadament iguals i es coneixen com mòdul de Young.

S'ha emprat un màquina d'assajos mecànics universal Houndsfield 10ks. Al primer estudi (apartat **III.2**) es va determinar el mòdul elàstic a través d'un assaig de tracció, emprant mostres cilíndriques de 70 x 12 x 4 mm^3. Al segon estudi (apartat **III.3**) es va determinar el mòdul elàstic a través d'un assaig de flexió. En aquesta configuració la tensió màxima a la secció central de la proveta és:

$$\sigma = \frac{3FL}{2bd^2} \qquad \text{(II-17)}$$

i la corresponent deformació és:

$$\varepsilon = \frac{6Dd}{L^2} \qquad \text{(II-18)}$$

del pendent de la corba es pot aïllar el mòdul d'elasticitat segons:

$$E_B = \frac{\Delta\sigma}{\Delta\varepsilon} \qquad \text{(II-19)}$$

on E_B és el mòdul d'elasticitat en flexió (N/mm^2), L és la longitud entre els suports (mm), b és l'amplada de la proveta (mm), d és l'alçada de la proveta (mm), D és la desviació de la proveta (mm) i F és la tensió aplicada (N).

A l'estudi de l'apartat **V.4** s'ha determinat el mòdul d'elasticitat a flexió mitjançant un assaig dinàmic emprant el DMTA.

II.15 ANÀLISI CINÈTICA ISOCONVERSIONAL

La cinètica del procés de curat s'ha estudiat per tal de descriure el comportament dels diferents sistemes. Els resultats poden ser utilitzats per a determinar la influència del catalitzador, analitzar l'efecte de l'addició de diferents proporcions d'un comonòmer així com determinar l'efecte de la temperatura en el procés [11].

Per la seva facilitat, el procediment més emprat per tal d'obtenir els paràmetres cinètics d'un sistema reactiu (factor pre-exponencial, A; energia d'activació, E_a; i la funció integral del grau de conversió $g(\alpha)$) consisteix en realitzar curats dinàmics en el DSC. A partir dels termogrames DSC es poden obtenir les corbes grau de conversió enfront a la temperatura a diferents velocitats d'escalfament constant i a partir d'aquestes els paràmetres cinètics.

Per tal de determinar els paràmetres cinètics s'ha emprat un mètode isoconversional integral [12]. Aquest mètode pressuposa que la velocitat de la reacció a una conversió determinada és funció únicament de la temperatura.

L'anàlisi cinètica d'una reacció no isotèrmica es pot descriure a través de l'equació de velocitat, assumint que la dependència de la velocitat de reacció amb la temperatura segueix l'equació d'Arrhenius:

$$\frac{d\alpha}{dt} = \beta\frac{d\alpha}{dT} = Af(\alpha)exp\left(-\frac{E_a}{RT}\right) \qquad \text{(II-20)}$$

on $\frac{d\alpha}{dt}$ és la velocitat de conversió, α és el grau de conversió, T és la temperatura absoluta, β és la velocitat d'escalfament lineal, A és el factor pre-exponencial, E_a és

[11] Salla, J.M.; Ramis, X.; Morancho, J.M.; Cadenato, A. *Isoconversional kinetic analysis of a carboxyl terminated polyester resin crosslinked with triglycidyl isocyanurate (TGIC) used in powder coatings from experimental results obtained by DSC and TMDSC* Termochim. Acta **2002**, 388, 355-370.
[12] Vyazovkin, S.; Sbirrazzuoli, N. *Isoconversional Kinetic Analysis of Thermally Stimulated Processes in Polymers* Macromol. Rapid Commun. **2006**, 27, 1515-1532.

l'energia d'activació, *R* és la constant dels gasos ideals i *f(α)* és la funció diferencial del grau de conversió.

Reordenant l'equació II-20 es pot obtenir l'anomenada integral de temperatura:

$$g(\alpha) = \int_0^{\alpha} \frac{d\alpha}{f(\alpha)} = \frac{A}{\beta} \int_0^{T} e^{-(Ea/RT)} dT \qquad \text{(II-21)}$$

on $g(\alpha) = \int_0^{\alpha} \frac{d\alpha}{f(\alpha)}$ és la funció integral del grau de conversió.

Per tal de resoldre la integral de la temperatura es pot emprar l'aproximació de Coats-Redfern [13] i considerant que $2RT/E_a$ és molt inferior a 1, s'obté l'anomenada equació de Kissinger-Akahira-Sunose [14]:

$$ln \frac{\beta}{T^2} = ln\left[\frac{AR}{g(\alpha)E}\right] - \frac{E_a}{RT} \qquad \text{(II-22)}$$

Per cada grau de conversió, la representació lineal de $ln \frac{\beta}{T^2}$ enfront T^1 permet determinar E_a i $ln\left[\frac{AR}{g(\alpha)E}\right]$ a partir del pendent i l'ordenada a l'origen. Si es coneix el model cinètic que s'adequa a la reacció es pot determinar també per cada grau de conversió, el factor pre-exponencial.

Per determinar el model cinètic *g(α)* per cada sistema estudiat, s'ha utilitzat l'equació de Coats-Redfern:

$$ln \frac{g(\alpha)}{T^2} = ln\left[\frac{AR}{\beta E}\right] - \frac{E_a}{RT} \qquad \text{(II-23)}$$

Per cada velocitat d'escalfament i model cinètic es representa $ln\left[\frac{g(\alpha)}{T^2}\right]$ enfront de T^1 i a partir del pendent i l'ordenada a l'origen es pot obtenir respectivament l'energia d'activació i el factor pre-exponencial.

En aquest treball s'ha seleccionat, pel mètode de Coats-Redfern, el model cinètic que dona millor coeficient de correlació i una energia d'activació més propera a la determinada isoconversionalment, que es considera la vertadera ja que la seva determinació no requereix cap hipòtesis sobre el model cinètic. Una

[13] Coats, A.W.; Redfern, J.P. *Kinetic parameters from thermogravimetric data* Nature, **1964**, 201, 68-69.
[14] Kissinger, H.E. *Reaction kinetics in differential thermal analysis* Anal. Chem. **1957**, 29, 1702-1706.

vegada s'ha seleccionat el model cinètic, es pot determinar el factor pre-exponencial *A* a una conversió concreta a través del pendent i l'ordenada a l'origen de l'equació II-22.

A la **Taula II-1**, es mostren els models cinètics utilitzats per tal de seleccionar quin és el que s'ajusta millor al procés estudiat.

Taula II-1 Expressions algebràiques de *f(α)* i *g(α)* de diferents models cinètics

Model	*f(α)*	*g(α)*
Diffusion D_1	$1/2(1-\alpha)^{-1}$	α^2
Diffusion D_2	$-ln(1-\alpha)$	$(1-\alpha)ln(1-\alpha)+\alpha$
Diffusion D_3	$3/2(1-\alpha)^{2/3}[-1-(1-\alpha)^{-1/3}]$	$[1-(1-\alpha)^{1/3}]^2$
Diffusion D_4	$3/2(1-\alpha)^{1/3}[-1-(1-\alpha)^{-1/3}]$	$(1-2/3\alpha)(1-\alpha)^{2/3}$
Avrami-Erofeev A_2	$2(1-\alpha)[-ln(1-\alpha)]^{1/2}$	$[-ln(1-\alpha)]^{1/2}$
Avrami-Erofeev A_3	$3(1-\alpha)[-ln(1-\alpha)]^{2/3}$	$[-ln(1-\alpha)]^{1/3}$
Avrami-Erofeev A_4	$4(1-\alpha)[-ln(1-\alpha)]^{3/4}$	$[-ln(1-\alpha)]^{1/4}$
Avrami-Erofeev $A_{3/2}$	$(3/2)(1-\alpha)[-ln(1-\alpha)]^{1/3}$	$[-ln(1-\alpha)]^{2/3}$
Power	$2\alpha^{1/2}$	$\alpha^{1/2}$
F_1 or n=1	$(1-\alpha)$	$-ln(1-\alpha)$
Phase-boundary-controlled reaction R_2	$2(1-\alpha)^{1/2}$	$1-(1-\alpha)^{1/2}$
Phase-boundary-controlled reaction R_3	$3(1-\alpha)^{2/3}$	$1-(1-\alpha)^{1/3}$
n=2	$(1-\alpha)^2$	$-1+(1-\alpha)^{-1}$
n=3	$(1-\alpha)^3$	$2^{-1}[-1+(1-\alpha)^{-2}]$
n=1.5	$(1-\alpha)^{1.5}$	$[1-(1-\alpha)^{-0.5}/0.5]$
n=1.5, m=0.5	$\alpha^{0.5}(1-\alpha)^{1.5}$	$[(1-\alpha)\alpha^{-1}]^{-0.5}(0.5)^{-1}$

Finalment, es pot determinar la constant de velocitat *k(T)* a una temperatura determinada per mitjà de l'equació d'Arrhenius:

$$ln\ k(T) = ln\ A - \frac{E_a}{RT} \qquad \text{(II-24)}$$

on *R* és la constant dels gasos ideals, *T* és la temperatura seleccionada, *A* és el factor pre-exponencial i E_a és l'energia d'activació. Els dos últims paràmetres s'obtenen de l'anàlisi isoconversional a una conversió concreta.

II.16 DETERMINACIÓ DEL NOMBRE DE GRUPS HIDROXILS (N_{OH})

El nombre de grups hidroxil d'alguns polímers hiperramificats s'ha determinat seguint la norma ISO 2554-1974.

En primer lloc, es procedeix a preparar una dissolució acetilant dissolent 11.8 mL d'anhídrid acètic en 100 mL de piridina. Seguidament, es dissolen 0.4-0.6 g del polímer a analitzar curosament pesats, en 5 mL de dissolució acetilant. La mescla s'agita durant 20 minuts a 130 ºC. Transcorregut aquest temps, s'agafeixen 8 mL d'aigua per tal d'hidrolitzar l'excés d'anhídrid acètic. Finalment, la solució es valora emprant una dissolució etanòlica de KOH 1N per tal de determinar el punt d'equivalència.

Anàlogament, es porta a terme el mateix procediment anterior però sense polímer i amb el mateix volum de solució acetilant. El nombre de grups hidroxil (N_{OH}) es determina a partir del resultat de les dues valoracions emprant la següent equació:

$$N_{OH} = \frac{(V_0 - V_1)C \cdot M_{KOH}}{m} + AN \qquad \text{(II-25)}$$

on V_0 i V_1 són els volums gastats de KOH 1N fins al punt d'equivalència en les valoracions del blanc i de la mostra (mL), respectivament; C és la concentració de la dissolució de KOH (eq/L); M_{KOH} és el pes molecular del KOH (g/mol); m és la massa de polímer (g); i AN és el nombre de grups àcids que conté el polímer.

II.17 DETERMINACIÓ DE L'ABSORCIÓ D'AIGUA PER IMMERSIÓ

S'ha determinat l'absorció d'aigua segons la normativa ASTM D 570-98. Per tal de dur a terme l'experiment s'han emprat tres mostres de cada material termoestables de mides 10 x 10 x 1 mm^3.

Primerament, les mostres s'acondicionen durant 24 hores a 50 ± 1 ºC en una estufa. Es deixen refredar i es pesen immediatament per tal determinar el pes inicial. Seguidament, les mostres es submergeixen en aigua a 50 ± 1 ºC i es procedeix a pesar cada mostra en repetides ocasions fins que el pes es manté constant o l'increment d'aquest és inferior al 1 % durant dues setmanes. L'absorció d'aigua (*I.W.*) es pot determinar mitjançant la següent equació:

$$I.W.,\% = \frac{pes_{mullat} - pes_{inicial}}{pes_{inicial}} x100 \qquad \text{(II-26)}$$

La cinètica d'absorció i deabsorció en reïnes epoxi, segueix generalment un comportament pseudo Fickià. Les característiques de la difusió que segueix un comportament Fickià són les següents:

- Les corbes d'absorció són lineals durant l'inici del procés.
- Per sobre el comportament lineal inicial, les corbes d'absorció i deabsorció són còncaves a l'abscissa.
- Quan les corbes d'absorció reduïdes es representen per diferents films polimèrics de gruix diferent, aquestes es poden superposar.

Quan un film de polímer s'exposa a un fluid, la variació de la concentració (*C*) d'una substància en funció del temps (*t*) i la posició (*x*) es pot explicar per la segona llei de Fick [15]:

$$\frac{\partial C}{\partial t} = D\frac{\partial^2 C}{\partial x^2} \qquad \text{(II-27)}$$

on *D* és el coeficient de difusió. Si el material té una concentració inicial de difusió uniforme (C_0) i la superfície manté constant la concentració de saturació C_{max}, la solució de l'equació II-27 és la següent:

$$\frac{C - C_0}{C_{max} - C_0} = 1 - \frac{4}{\pi}\sum_{n=0}^{\infty}\frac{(-1)^n}{2n+1} exp\left[-D(2n+1)^2\pi^2 t / L^2\right] cos\frac{(2n+1)\pi x}{L} \qquad \text{(II-28)}$$

La quantitat total de substància que difon a través del film polimèric (*M*) en funció del temps es genera a partir de la integral de l'equació II-28 a través del gruix del film (*L*):

$$\frac{M}{M_{max}} = 1 - \frac{8}{\pi^2}\sum_{n=0}^{\infty}\frac{1}{(2n+1)^2} exp\left[-D(2n+1)^2\pi^2 t / L^2\right] \qquad \text{(II-29)}$$

on M_{max} és la quantitat màxima de substància que ha pogut difondre. Una expressió simplificada de l'equació II-29, només vàlida per valors M/M_{max} inferiors a 0.6, té la següent forma:

$$\frac{M}{M_{max}} = \frac{4}{L\sqrt{\pi}}\sqrt{Dt} \qquad \text{(II-30)}$$

Representant M/M_{max} per valors inferiors a 0.6 enfront $\frac{\sqrt{t}}{L}$ es pot determinar el coefficient de difusió *D* a través del pendent.

[15] a) Crank, J.J. *The mathematics of diffusion* Clarendon Press, UK, **1975**. b) Hayward, D.; Hollins, E.; Johncock, P.; McEwan, I.; Pethrick, R.A.; Pollock, E.A. *The cure and diffusion of water in halogen containing epoxy/amine thermosets* Polymer **1997**, 38, 1151-1168.

CAPÍTOL III

Ús de HBPs com a modificants del diglicidilèter de bisfenol A (DGEBA)

UNIVERSITAT ROVIRA I VIRGILI
NOUS TERMOESTABLES EPOXÍDICS MODIFICATS AMB ESTRUCTURES DENDRÍTIQUES DE TIPUS HIPERRAMIFICAT I ESTRELLA
Mireia Morell Bel
DL:T. 155-2012

III.1 INTRODUCCIÓ

Com s'ha comentat al capítol I (apartat **I.1.5**), existeixen dues categories principals d'obtenció de polímers hiperramificats a través de la via *bottom-up*. SMM (*single-monomer methodology*) on es sintetitza el polímer a partir de la polimerització de monòmers AB_n o AB_n latents i CMM *(couple-monomer methodology)* on el polímer es sintetitza per polimerització directa de dos monòmers funcionalment simètrics o no simètrics.

III.1.1 Polímers hiperramificats obtinguts per polimerització de monòmers no simètrics (A* + CB_n i A* + B_n)

Segons la teoria de Flory sobre la gelificació [1], la polimerització ideal entre monòmers simètrics A_2 i B_3 es basa en tres assumpcions: i) els grups A i B tenen la mateixa reactivitat durant el transcurs de la reacció; ii) no existeixen reaccions laterals; i iii) no es poden generar ciclacions o terminacions de cadena durant el procés. Si la primera assumpció resulta invàlida, com és el cas de la categoria CMM emprant monòmers no simètrics, es poden obtenir HBPs, sense perill que el sistema gelifiqui i arribant a valors de pes molecular elevats. L'ús de monòmers no simètrics permet diferenciar la reactivitat entre els grups funcionals del monòmer. A la **Figura III-1** es mostren els principis bàsics de les categories d'obtenció d'HBPs, SMM i CMM (aproximació $A_2 + B_3$ (monòmers simètrics) i AA' + B'B_2 (monòmers no simètrics).

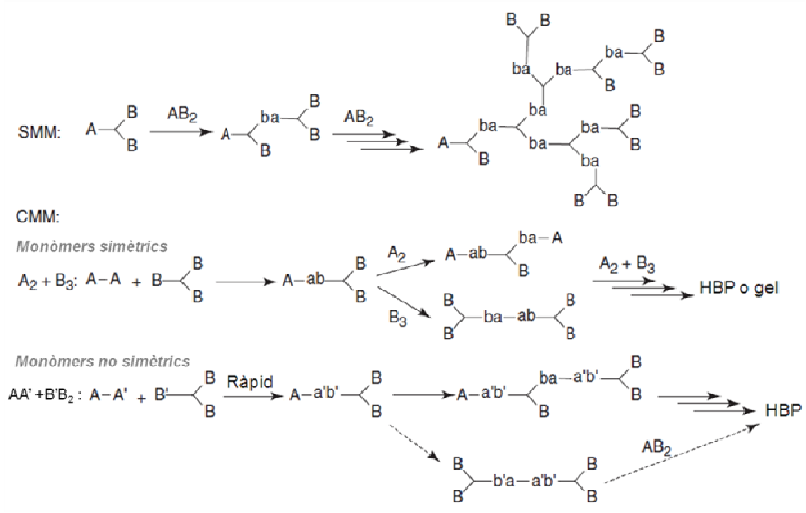

Figura III-1 Il·lustració esquemàtica de la preparació de polímers hiperramificats a través de les vies SMM i CMM amb monòmers simètrics ($A_2 + B_3$) i monòmers no simètrics

[1] Flory, P.J. *Molecular size distribution in three dimensional polymers. VI. Branched polymers containing A-R-B_{f-1} type units* J. Am. Chem. Soc. **1952**, 74, 2718-2723.

En les policondensació de monòmers AB_2 o AB_2 latents es formen oligòmers i posteriorment macromolècules contenint un grup funcional A per cada molècula. D'aquesta manera, es prevé totalment la gelificació ja que no es pot formar cap xarxa polimèrica. En canvi, en les polimeritzacions entre monòmers simètrics (A_2 + B_3), inicialment es formen espècies AB_2 però aquestes poden reaccionar lateralment amb traces de monòmers residuals A_2 o B_3 formant d'espècies A_xB_y ($x \geq 2$, $y \geq 2$) susceptibles de formar cicles intramoleculars i xarxes polimèriques gelificant el sistema. L'única manera d'obtenir HBPs solubles a través d'aquesta aproximació és aturar la reacció a una conversió inferior per tal de no arribar a la gelificació. En comparació, emprant monòmers no simètrics es formen intermedis AB_n els quals poden polimeritzar generant HBPs sense risc de gelificació com s'ha comentat anteriorment.

Froehling *i col.* [2,3], investigadors de DSM, van ser els primers en emprar la via CMM amb monòmers no simètrics per obtenir poli(ester-amide)s hiperramificades. Concretament, varen emprar l'aproximació A* + CB_n on A* era l'anhídrid 1,2-ciclohexandicarboxíl·lic (CHDA) i el monòmer CB_n la bis(*2*-hidroxipropil)amina (DIPA). Li *i col.*, també varen obtenir HBPs utilitzant la mateixa estratègia [4,5].

Anàlogament, s'han preparat altres poli(ester-amide)s per policondensació directa d'anhídrid ftàlic (PA), anhídrid succínic (SA), anhídrid diglicòlic (DGA) o anhídrid glutàric (GA) i dietanolamina (DEOA) o bis(*2*-hidroxipropil)amina (DIPA) en condicions similars obtenint-se en tots els casos pesos moleculars relativament baixos 680 - 6.000 g/mol (determinat per SEC-DV).

Algunes de les poli(ester-amide)s hiperramificades esmentades anteriorment s'han aconseguit produir a gran escala i comercialitzar com és el cas d'Hybrane® (DSM) [6].

Un monòmer A* (o també anomenat AA') conté dos grups funcionals latents; un grup A es forma per reacció de A* amb el grup C del monòmer CB_n, generant intermedis AB_n Seguidament, la autopolicondensació d'aquests intermedis generen l'HBP.

---

[2] Froehling, P.E.; Brackman, J. *Properties and applications of poly(propylene imine) dendrimers and poly(ester amide) hyperbranched polymers* Macromol. Symp. **2000**, 151, 581-589.
[3] van Benthem, R.A.T.M.; Meijerink, N.; Geladé, E.; de Koster, C.G.; Muscat, D.; Froehling, P.E.; Hendriks, P.H.M.; Vermeulen, C.J.A.A.; Zwartkruis, T.J.G. *Synthesis and characterization of bis(2-hydroxypropyl)amide-based hyperbranched polyesteramides* Macromolecules **2001**, 34, 3559-3566.
[4] Li, X.; Zhan, J.; Li, Y.S. *Facile syntheses and characterization of hyperbranched poly(ester amide)s from commercially available aliphatic carboxylic anhydride and multihydroxyl primary amine* Macromolecules **2004**, 37, 7584-7594.
[5] Li, X.; Zhan, J.; Lin, Y.; Li, Y.G.; Li, Y.S. *Facile synthesis and characterization of aromatic and semiaromatic hyperbranched poly(ester amide)s* Macromolecules **2005**, 38, 8235-8243.
[6] Froehling, P.E. *Development of DSM's hybrane® hyperbranched polyesteramides* J. Polym. Sci., Part A: Polym. Chem. **2004**, 42, 3110-3115.

La condensació de CHDA amb DIPA normalment origina espècies AB_2 contenint un grup àcid carboxíl·lic i dos grups hidroxil. Els enllaços ester es formen posteriorment, a pressió reduïda i temperatura alta (180 ºC), a través d'un intermedi iònic oxazolini-carboxilat generant la corresponent poli(ester-amida) hiperramificada amb grups hidroxils terminals, tal com es mostra a l'**Esquema III-1**.

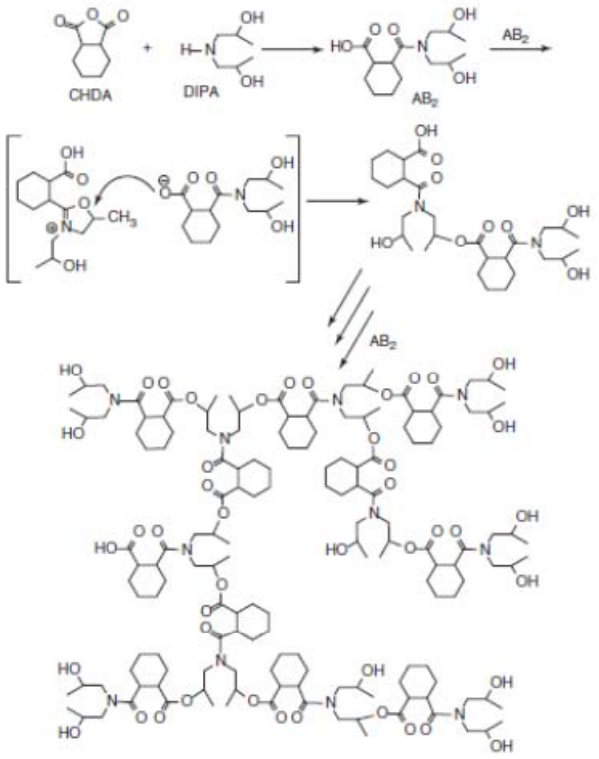

Esquema III-1 Obtenció d'una poli(ester-amida) hiperramificada a través de l'aproximació A* + CB_n

La determinació del *DB* es sol dur a terme per RMN de ^{13}C emprant compostos model per tal d'identificar les diferents subunitats repetitives. Per aquest tipus de polímers el *DB* es situa entre 0.30 i 0.60 en funció principalment del volum estèric dels grups funcionals dels monòmers els quals poden dificultar la formació de subunitats dendrítiques [4].

Emprant una estratègia similar a la descrita anteriorment per les poli(ester-amide)s hiperramificades s'han obtingut poliesters hiperramificats [7]. En aquest cas, a partir de polialcohols (B_n) i anhídrids cíclics (A*) com ara, el trimetilolpropà (TMP o TMOP) i l'anhídrid succínic (SA) com es mostra a l'**Esquema III-2**.

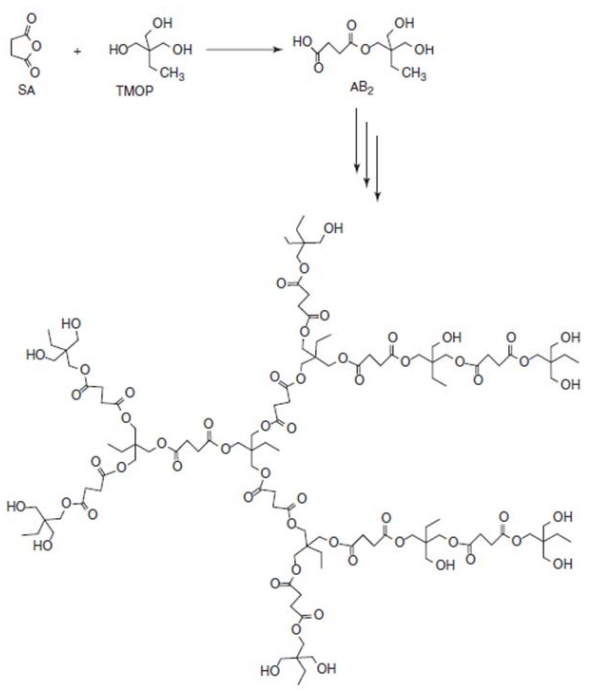

Esquema III-2 Obtenció d'un poliester hiperramificada a través de l'aproximació A* + B_n

Com que cada grup hidroxil del monòmer B_n té la mateixa reactivitat, existeix un elevat risc de gelificació. Per tant, és necessari eliminar l'aigua del cru de reacció durant l'inici d'aquesta per tal d'evitar l'entrecreuament.

En el present capítol, es descriu l'ús com a modificants reactius del diglicidilèter de bisfenol A, de poli(ester-amides) hiperramificades comercials obtingudes a través de l'estratègia A* + CB_n així com d'un nou poli(amino-ester) hiperramificat sintetitzat per mitjà de la via A* + B_n la qual fins ara no ha sigut explorada en aquest últim tipus de polímer.

[7] Yan, D., Gao, C., Frey, H. eds., *Hyperbranched polymers. Synthesis, properties and applications*, 1st ed., Wiley Interscience, Hoboken, **2011**, p. 123.

III.2

NEW IMPROVED THERMOSETS OBTAINED FROM DGEBA AND A HYPERBRANCHED POLY(ESTER-AMIDE)

Mireia Morell, Xavier Ramis, Francesc Ferrando, Yingfeng Yu, Àngels Serra

*Polymer **2009**, 50, 5374 - 5383*

UNIVERSITAT ROVIRA I VIRGILI
NOUS TERMOESTABLES EPOXÍDICS MODIFICATS AMB ESTRUCTURES DENDRÍTIQUES DE TIPUS HIPERRAMIFICAT I ESTRELLA
Mireia Morell Bel
DL:T. 155-2012

Polymer **2009**, 50, 5374-5383

NEW IMPROVED THERMOSETS OBTAINED FROM DGEBA AND A HYPERBRANCHED POLY(ESTER-AMIDE)

Mireia Morell,[1] Xavier Ramis,[2] Francesc Ferrando,[3] Yingfeng Yu,[1,4] Àngels Serra[1]

[1] Department of Analytical and Organic Chemistry, University Rovira i Virgili, C/ Marcel·lí Domingo s/n, Tarragona 43007, Spain.
[2] Thermodynamics Laboratory, ETSEIB University Politècnica de Catalunya, C/ Av. Diagonal 647, Barcelona 08028, Spain.
[3] Department of Mechanical Engineering, University Rovira i Virgili, C/ Països Catalans 26, Tarragona 43007, Spain.
[4] The Key Laboratory of Molecular Engineering of Polymers, Ministry of Education, Department of Macromolecular Science, Fudan University, Shanghai 200433, China.

Abstract

The influence on the curing process of a commercial hydroxy-functionalized hyperbranched poly(ester-amide) (HBP) Hybrane® S1200 on diglycidylether of bisphenol A (DGEBA) was studied. By Differential Scanning Calorimetry (DSC) and Fourier Transform Infrared Spectroscopy (FTIR) the curing reaction was studied and the covalent incorporation of the modifier in the matrix was proved. By Thermomechanical Analysis (TMA) the reduction of the contraction after gelation on changing the S1200 proportion was observed. The incorporation of S1200 increased the glass transition temperature (T_g) and reduced the overall shrinkage, especially after gelation. The modified materials were more thermally degradable than neat DGEBA thermosets. Thermal expansion coefficient, Young's modulus, impact strength and microhardness were improved without compromising the thermomechanical characteristics. The water uptake behavior was also evaluated.

Keywords: epoxy resin; hyperbranched; anhydrides

Introduction

In some epoxy resins applications such as coatings for electronic encapsulations, properties such as toughness and low shrinkage are necessary [1,2]. During the curing process the volume is usually reduced, which tends to originate deformations and cracks, decreasing the adhesion and consequently the protective capacity of the coating. Degradability is required when the reworkability of the electronic devices is desired. The improvement on this property could be achieved with the introduction of labile groups such as esters of secondary or tertiary alkyl groups in the network [3,4]. It is well known that thermosetting materials cannot be recycled but they can be brokendown under controlled conditions to remove them from the substrate, enabling the repairing or recycling of electronic devices assembled with such materials [5].

Toughness is also needed to prevent the loss of adhesion and the damage of the electronic devices caused by brittle fractures. During the past decades considerable efforts have been made to improve it. One of the most successful approaches to decrease the brittleness of epoxy resins is to blend them with rubbers or elastomers able to stand energy absorption mechanisms [6,7]. However,

using these modifiers, some thermomechanical properties can be strongly affected and some problems arise in terms of processing.

Hyperbranched polymers (HBP)s, dendritic macromolecules with a large number of functional groups at the end of the branches, are a new class of modifiers for epoxy resins, which have the advantage of reducing the viscosity of the reactive mixture and can improve the mechanical properties [8,9]. Most of the commercial HBPs used have hydroxyl groups at the end of the branches, but up till now, there are few reports concerning the role of these HBPs on the toughness of epoxy resins [10,11]. Although some improvements on this property were observed, the covalent incorporation of the HBP in the matrix was not completely clarified.

Anhydrides are common curing agents for epoxy resins but they have been scarcely employed in the modification of diglycidylether of bisphenol A (DGEBA) with hydroxyl HBPs (Boltorn® H30) [11,12]. Anhydrides can react with both epoxy and hydroxyl groups forming ester linkages, which is advantageous to increase reworkability.

In the present work, we selected as HBP the hydroxyl-ended commercial hyperbranched poly(ester-amide) Hybrane® S1200 as reactive modifier of DGEBA and methyltetrahydrophthalic anhydride (MTHPA) with a tertiary amine as curing agent. The addition of S1200 to this curing system should allow improving the thermal reworkability through the presence of secondary ester groups. It was also expected a reduction of the shrinkage after gelation as we saw in previous studies [12,13]. In addition, the flexibility of the HBP structure can improve the toughness of the thermosets.

Experimental

Materials

Diglycidylether of bisphenol A (DGEBA) Epikote Resin 827 was provided by Shell Chemicals (epoxide equivalent weight (EEW) = 182.1 g/eq, n = 0.082). Methyltetrahydrophthalic anhydride (MTHPA) (Ciba-Huntsman) (HY918) and *N*,*N*-dimethylbenzylamine (BDMA) (Aldrich) were used as received. The hydroxyl terminated hyperbranched poly(ester-amide) Hybrane® S1200 (DSM) was used as modifier. The average molecular weight, as reported on data sheet, is about 1,200 g/mol and the theoretical number of OH groups/molecule is 8. T_g value is 45 ºC.

Preparation of DGEBA/MTHPA/HBP mixtures

The mixtures were prepared by adding the required amount of S1200 into the epoxy resin. The initial mixture with the selected proportion of DGEBA and S1200 was heated until the HBP was dissolved and the solution became clear. Then, MTHPA was added and the resulting solution was stirred and degassed under vacuum for 15 min at 70 ºC. Finally, BDMA was added and the mixture was stirred and cooled down to -10 ºC maintaining it at this temperature until use to prevent

Polymer **2009**, 50, 5374-5383

polymerization. The mixtures containing 0 - 20 wt.% (by weight) of HBP were prepared and the equivalent stoichiometric relation between MTHPA, DGEBA and HBP was kept for all materials. When amine (BDMA) was added, the amine/anhydride molar ratio was kept unchanged. The compositions of the formulations studied are collected in **Table 1**.

Table 1 Composition of the formulations with different weight percentage of S1200. In percentage by total weight (wt.%) of the mixture and in equivalent ratio, (Xeq)

Formulation	DGEBA		MTHPA		BDMA		OH from HBP	
(% S1200)	Xeq	wt.%	Xeq	wt.%	Xeq	wt.%	Xeq	wt.%
DGEBA/MTHPA	1	52.0	1	48.0	0.0065	0.53	-	-
DGEBA/MTHPA/5%	0.93	48.1	1.07	46.9	0.0061	0.50	0.14	5
DGEBA/MTHPA/10%	0.88	44.2	1.14	45.8	0.0061	0.50	0.26	10
DGEBA/MTHPA/15%	0.83	40.3	1.21	44.7	0.0061	0.50	0.38	15
DGEBA/MTHPA/20%	0.75	38.2	1.33	42.8	0.0061	0.50	0.58	20

Characterization techniques

Calorimetric analyses were carried out on a Mettler DSC-821e thermal analyzer. Samples of approximately 5 mg in weight were cured in aluminium pans in a nitrogen atmosphere. The calorimeter was calibrated using an indium standard (heat flow calibration) and an indium-lead-zinc standard (temperature calibration).

In the dynamic curing process the degree of conversion by DSC (α_{DSC}) was calculated as follows:

$$\alpha_{DSC} = \frac{\Delta H_T}{\Delta H_{dyn}} \quad (1)$$

where ΔH_T is the heat released up to a temperature T, obtained by integration of the calorimetric signal up to this temperature, and ΔH_{dyn} is the total reaction heat associated with the complete conversion of all reactive groups.

The glass transition temperatures (T_gs) were calculated after complete curing, by means of a second scan at 20 ºC/min as the temperature of the half-way point of the jump in the heat capacity when the material changed from glassy to the rubbery state under N_2 atmosphere.

A FTIR spectrophotometer FTIR-680PLUS from JASCO with a resolution of 4 cm^{-1} in the absorbance mode was used to monitor the isothermal curing process at 120 ºC. This device was equipped with an attenuated-total-reflection accessory with thermal control and a diamond crystal (Golden Gate heated single-reflection diamond ATR, Specac-Teknokroma). The disappearance of the absorbance peak at 913 cm^{-1} was used to monitor the epoxy equivalent conversion. The consumption of the reactive carbonyl group of anhydride was evaluated by the absorbance at

1777 cm^{-1}. The peak at 1508 cm^{-1} of the phenyl group was chosen as an internal standard. Conversions of the different reactive groups, epoxy and anhydride, were determined by the Lambert-Beer law from the normalized changes of absorbance at 913 and 1777 cm^{-1}:

$$\alpha(t)_{epoxy} = 1 - \left(\frac{\bar{A}^t_{913}}{\bar{A}^0_{913}} \right) \quad (2)$$

$$\alpha(t)_{anhydride} = 1 - \left(\frac{\bar{A}^t_{1777}}{\bar{A}^0_{1777}} \right) \quad (3)$$

where $\bar{A}^0$ and $\bar{A}^t$ are respectively the normalized absorbance of the reactive group before curing and after a reaction time *t*.

From these conversions and taken into account the equivalent formulation of the mixtures, the equivalent evolution of the reactive groups which participates in the curing can be obtained:

$$eq(t)_{epoxy} = eq_{initial} \cdot \alpha(t)_{epoxy} \quad (4)$$

$$eq(t)_{anhydride} = eq_{initial} \cdot \alpha(t)_{anhydride} \quad (5)$$

Thermomechanical analyses were carried out on a Mettler TMA40 thermomechanical analyzer. The samples were supported by two small circular ceramic plates and silanized glass fibers, which were impregnated with the samples. Isothermal experiments at 120 ºC were undertaken using TMA by application of a force of 0.01 N in order to monitor contraction during the curing process. The degree of shrinkage ($\alpha_{shrinkage}$) can be calculated as follows:

$$\alpha_{shrinkage} = \frac{L_t - L_0}{L_\infty - L_0} \quad (6)$$

where L_t, L_0 and L_∞ represent, respectively, the thickness of the sample at time *t*, at the onset and at the end of the reaction.

The conversion at the gel point was evaluated by means of non-isothermal experiments performed between 40 and 225 ºC at a heating rate of 5 ºC/min applying a periodic force that change (cycle time = 12 s) from 0.0025 to 0.01 N. The gel point was taken in TMA as the temperature at which a sudden decrease in the amplitude of the oscillations was observed. The gel conversion, α_{gel}, was determined as the DSC conversion at the temperature gelled in TMA in a non-isothermal experiment.

The linear thermal expansion coefficients in the glassy and rubbery states measurements of the cured samples were performed using samples with a size of

Polymer **2009**, 50, 5374-5383

(4 x 4 x 2 mm^3). The samples were mounted on the TMA and heated at a rate of 10 ºC/min. The coefficient of thermal expansion (*CTE*) can be determined as:

$$CTE = \frac{1}{L_0}\frac{dL}{dT} = \frac{1}{L_0}\frac{dL/dt}{dT/dt} \quad (7)$$

where, L is the thickness of the sample, L_o the initial length, t the time and T the temperature.

The glass transition temperature (T_gs) of the cured samples was also determined by non-isothermal TMA experiment as the cross of the tangents between the glassy and rubbery states.

The overall shrinkage was calculated from the densities of the materials before and after curing, which were determined using a Micromeritics AccuPyc 1330 Gas Pycnometer thermostatized at 30 ºC.

Thermogravimetric analyses (TGAs) were carried out in a Mettler TGA/SDTA 851e thermobalance. Cured samples with an approximate mass of 8 mg were degraded between 30 and 800 ºC at a heating rate of 10 ºC/min in N_2 (100 cm^3/min measured in normal conditions).

Thermal-dynamic-mechanical analyses (DMTAs) were carried out with a Rheometrics PL-DMTA MKIII analyser. The samples were cured isothermally in a mould at 150 ºC for 4 h and then post-cured for 2 h at 200 ºC. Single cantilever bending at 1Hz was performed at 3 ºC/min, from 30 ºC to 200 ºC on prismatic rectangular samples (20 x 5 x 1.5 mm^3).

Young's modulus was measured with the Universal Testing Machine Hounsfield 10-KS. Tensile tests were performed on cylindrical samples of 8 mm of diameter. The gauge length was 50 mm and the test cross-head speedy was 1 mm/min. For each material 6 determinations were made with a confidence level of 95 %.

The impact test was performed at 23 ºC by means of an Izod 5110 impact tester, according to ASTM 256-05a using V-notched rectangular samples. The pendulum employed had a kinetic energy of 1 J. The fracture area of the specimens for impact tests was observed with scanning electron microscope (SEM). The samples were metalized with gold and observed with a Jeol JSM 6400 with a 3.5 nm resolution.

Microhardness was measured with a Wilson Wolpert (Micro-Knoop 401MAV) device following the ASTM D1474-98 (2002) standard procedure. For each material 10 determinations were made with a confidence level of 95 %. The Knoop microhardness (HKN) was calculated from the following equation:

$$HKN = L/A_p = L/l^2 C_p \quad (8)$$

where, L is the load applied to the indenter (0.025 Kg), A_p is the projected area of indentation in mm^2, l is the measured length of long diagonal of indentation in mm, C_p is the indenter constant (7.028×10^{-2}) relating l^2 to A_p. The values were obtained from 10 determinations with the calculated precision (95 % of confidence level).

Water uptake was evaluated by immersion tests according to ASTM D 570-98. To carry out this test three square samples of each thermoset (1 x 1 x 0.1 cm^3) were cut and thermally conditioned at 50 ± 1 ºC during 24 hours in an oven. Then, the samples were cooled and immediately weighed to get the initial weight. The samples were immersed under water at 50 ± 1 ºC during the selected times and then were dried with a dry cloth and weighed. The weightings were repeated until constant weight, at which the specimens can be considered substantially saturated. The increase in weight can be calculated as follows:

$$\text{Increase in weight},\% = \frac{\text{weight}_{\text{wet}} - \text{weight}_{\text{initial}}}{\text{weight}_{\text{initial}}} \times 100 \quad (9)$$

Diffusion coefficient determination

Water uptake has been modeled by Fick's second law [14,15]:

$$\frac{\partial C}{\partial t} = D\frac{\partial^2 C}{\partial x^2} \quad (10)$$

where D is the diffusion coefficient. If the material has a uniform initial diffusant concentration (C_0) and the surface kept at a constant concentration C_{max} the solution of Eq. (10) is:

$$\frac{C - C_0}{C_{max} - C_0} = 1 - \frac{4}{\pi}\sum_{n=0}^{\infty}\frac{(-1)^n}{2n+1} exp\left[-D(2n+1)^2\pi^2 t / L^2\right] cos\frac{(2n+1)\pi x}{L} \quad (11)$$

The total amount of substance diffusing in the polymeric material (M) as a function of time is given by the integral of Eq. (11) across the thickness (L):

$$\frac{M}{M_{max}} = 1 - \frac{8}{\pi^2}\sum_{n=0}^{\infty}\frac{1}{(2n+1)^2} exp\left[-D(2n+1)^2\pi^2 t / L^2\right] \quad (12)$$

where M_{max} is the maximum quantity of the diffusing substance at infinite time. A simplified form of Eq. (12) for values M/M_{max} lower than 0.6 has the form:

$$\frac{M}{M_{max}} = \frac{4}{L\sqrt{\pi}}\sqrt{Dt} \quad (13)$$

Representing M/M_{max} for values lower than 0.6 in front of $\frac{\sqrt{t}}{L}$ enables D to be determined from the slope.

Polymer **2009**, 50, 5374-5383

Results and discussion

Amongst the hyperbranched polymers used as thermoset toughners the aliphatic polyesters based on *bis*-hydroxymethyl propionic acid, commercially available from Perstorp polyols (Boltorn®) are the most reported [8,9,11,16,17]. However there are some other commercially available hyperbranched polymers which can be employed to improve the properties of an epoxy thermoset. Concretely, in this study an aliphatic poly(ester-amide) hyperbranched polymer (HBP) Hybrane® S1200 has been used to modify DGEBA. The idealized chemical structure of this modifier is shown in **Scheme 1**.

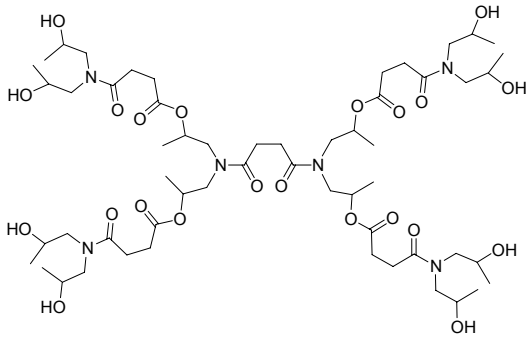

Scheme 1 Idealized chemical structure of Hybrane® S1200

The structure of S1200 presents some advantages: the hydroxylic groups at the chain ends allow the covalent bonding of the HBP to the matrix, the aliphatic structure can flexibilize the network while maintaining the T_g value by the high functionality of the HBP, and the presence of secondary alkyl esters can help to increase the thermal degradability of the materials.

The reaction of DGEBA with anhydrides as curing agents has been broadly studied in terms of its reactivity and mechanism [1,18,19]. The reactive process is complex and it involves higher temperatures with several competing reactions capable to taking place; particularly etherification takes an important role in non-catalyzed systems. The most significant reaction mechanisms are shown in **Scheme 2** (**a**), which corresponds to a polycondensation initiated by hydroxyl groups.

Because of the epoxy/anhydride reaction is slow an accelerator is often used to initiate the process at lower temperatures. This catalyzed mechanism is represented in **Scheme 2** (**b**) and follows a ring-opening pathway. It is important to note that the introduction of the HBP in an epoxy/anhydride system can contribute to the non-catalyzed mechanism favoring the polycondensation mechanism. To know the influence of the HBP in the reaction kinetics and mechanism, the curing process was studied by means of DSC and FTIR.

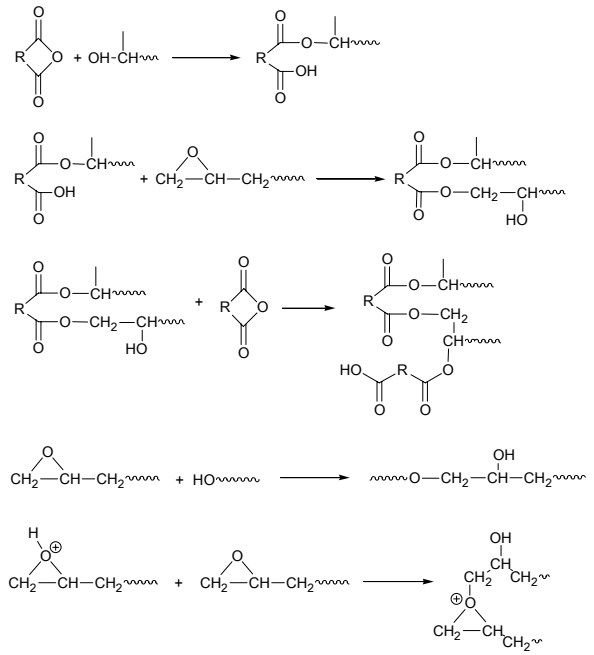

Scheme 2 (**a**) Reaction mechanisms of the curing of epoxides with anhydrides

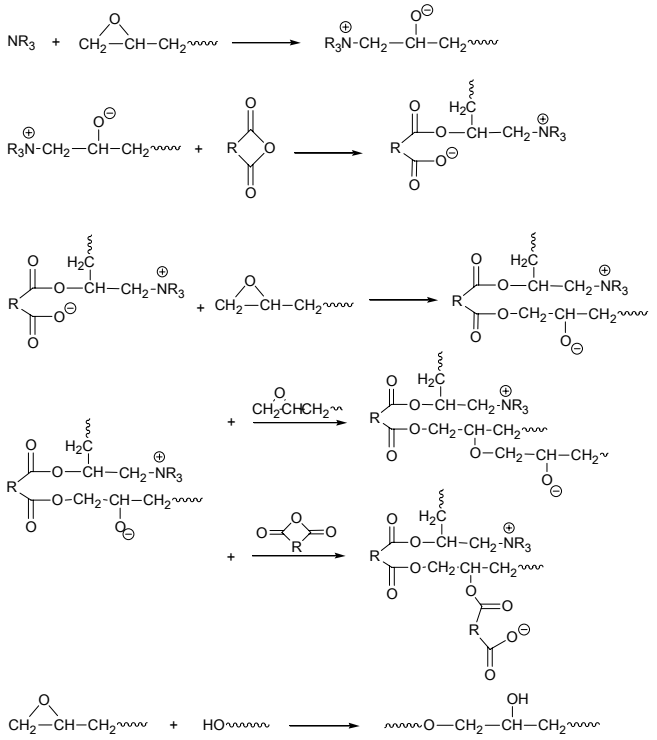

Scheme 2 (**b**) Reactions mechanisms of the curing epoxides with anhydrides, catalized by a tertiary amine

Polymer **2009**, 50, 5374-5383

Calorimetric studies of DGEBA/MTHPA/BDMA with several S1200 proportions

In a previous work [12] we determined that the maximum degree of curing was reached when one anhydride reacted either with an epoxide or with two hydroxyl groups of the HBP and a 0.5 wt.% BDMA was employed in all the formulations prepared. This optimal formulation has been selected to prepare the formulations studied, which are collected in **Table 1**.

Figure 1 shows the DSC exotherms and the conversion degrees against temperature recorded at 10 ºC/min of neat DGEBA/MTHPA and DGEBA/S1200/MTHPA formulations.

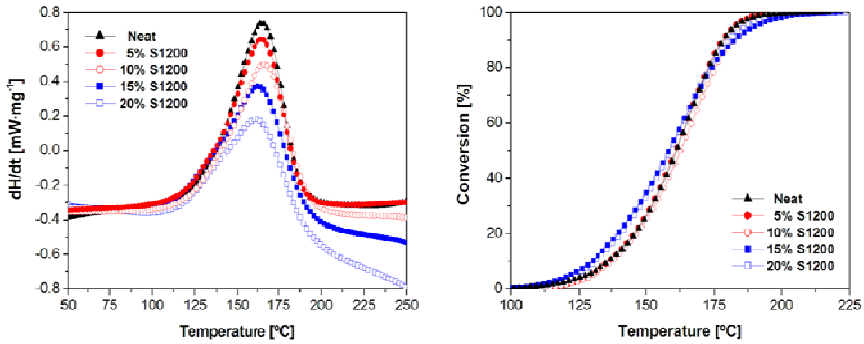

Figure 1 DSC scanning curves and conversion degrees against temperature of the curing of DGEBA/MTHPA and DGEBA/MTHPA mixtures containing different weight percentages of S1200 at a heating rate of 10 ºC/min

It can be observed, that there is no much influence on the shape of the crosslinking exotherm on changing the proportion of S1200 in the reactive mixture, since all of them exhibit a unimodal curve. The addition of little percentages of HBP does not accelerate the curing process but the addition of 15 wt.% or 20 wt.% produces an accelerative effect in the first stages of curing. This fact could be attributed to the high proportion of hydroxyl groups in S1200 which can favor the non-catalyzed mechanism at the beginning of the curing process. These mixtures show a delay at higher temperatures and higher conversions due to the concurrence of the different reactive processes. A similar behaviour was observed in a previous study on the curing of DGEBA/Boltorn® H30/anhydride/BDMA mixtures [12].

In **Table 2** the calorimetric data of the curing process of the formulations studied are collected.

Table 2 Calorimetric data of DGEBA/MTHPA/BDMA mixtures with different percentages of S1200

Formulation (% S1200)	Δh (J/g)	T_{max} [a] (ºC)	T_g [b] (ºC)
DGEBA/MTHPA/0%	245	165	92
DGEBA/MTHPA/5%	220	165	97
DGEBA/MTHPA/10%	216	167	97
DGEBA/MTHPA/15%	210	163	97
DGEBA/MTHPA/20%	190	162	95

a. Temperature of the maximum of the curing exotherm.
b. Glass transition temperature obtained by DSC. Second scan after dynamic curing.

The reaction enthalpy is mainly due to the opening of epoxy group because of the strained ring. For that reason, it is shown that the enthalpy is decreased as the amount of HBP is increased, since the proportion of DGEBA in the formulation is going down. It can be also commented that there are not many differences on the maximum of the curing exotherm on adding HBP to the epoxy resin. The presence of S1200 in the material leads to an increase in the T_g, but this value is not affected by the percentage of modifier in the material. This can be explained by the opposite effects arising from the flexibility of the structure and its high functionality.

FTIR studies of DGEBA/MTHPA/BDMA with 20 wt.% of S1200

By FTIR the evolution of the characteristic functional groups taking part in the curing process was followed. **Figure 2** shows the initial and final spectra of the 20 wt.% S1200 DGEBA/MTHPA mixture with 0.5 wt.% of BDMA at 120 ºC. In the initial spectrum, we can observe two main carbonyl bands at 1777 and 1859 cm^{-1} attributable to the unsymmetrical and the symmetrical stretching vibration of the cyclic anhydride, respectively. Moreover, the shoulder at 1729 cm^{-1} can be attributed to the ester groups of the S1200 structure. In the region between 950 and 850 cm^{-1} the deformation of the C-O-C bond of epoxy group at 913 cm^{-1} can be observed. The disappearance of the absorptions of the anhydride and epoxide indicates the complete consumption of these groups. During curing the ester band at 1729 cm^{-1} increases because of the reaction of anhydride with epoxides and hydroxyl groups.

Polymer **2009**, 50, 5374-5383

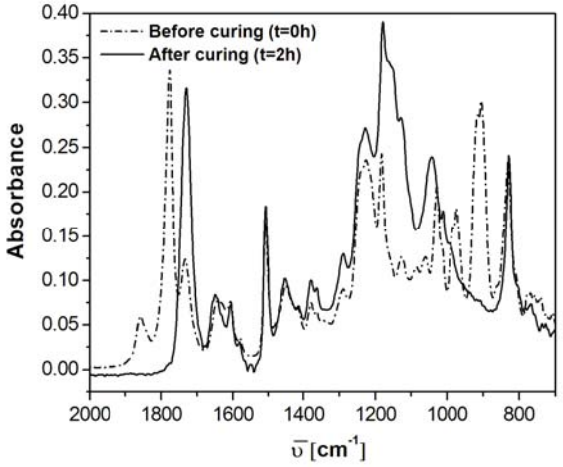

Figure 2 ATR-FTIR spectra of the mixture DGEBA/MTHPA with 20 wt.% of S1200 and 0.5 wt.% of BDMA before and after curing at 120 ºC

To monitor the disappearance of the hydroxyl groups during curing we followed the different consumption of anhydride and epoxy groups in terms of equivalents, which are represented in **Figure 3** (**a**). We can observe that anhydride groups disappear faster than epoxide in the first stages of the curing, which implies an initial reaction of hydroxyl groups with anhydride. The different evolution can be emphasized by representing the equivalent consumption of epoxy, anhydride and hydroxyl groups in a 20 wt.% S1200 formulation during the first minutes of curing, which is shown in **Figure 3** (**b**).

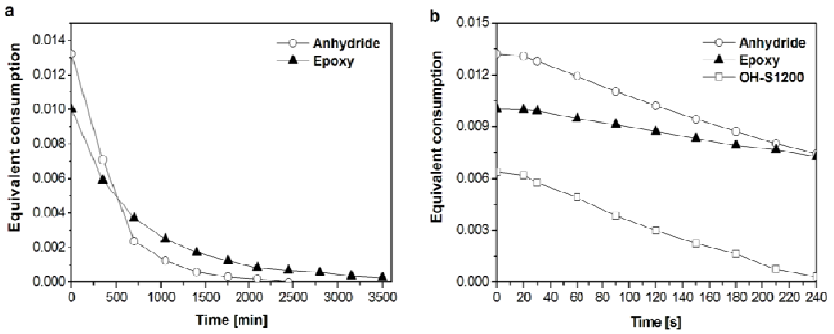

Figure 3 a - Epoxy (913 cm^{-1}) and anhydride (1777 cm^{-1}) equivalent evolution versus time for the mixture DGEBA/MTHPA with 20 wt.% of S1200 and 0.5 wt.% of BDMA during all the curing process at 120 ºC by ATR-FTIR. **b** - Epoxy, anhydride and OH-HBP equivalent evolution versus time for the same mixture during the 4 first minutes of curing at 120 ºC by ATR-FTIR

Thus, epoxides and anhydrides can react by both mechanisms represented in **Scheme 2**, but hydroxyl groups only participates in the polycondensation mechanism, **Scheme 2** (**a**). These results indicate that S1200 becomes covalently

linked to the growing network from the very beginning of its formation, acting as a true reactive modifier.

Study of the gelation process and shrinkage of the formulations

It is known that internal stresses in thermosets mainly appear when the network loses its mobility. For this reason it is desirable to advance the gelation until higher conversions. Experimentally, one can determine the gelation point by using TMA starting at a region in which contraction is not observed between two contraction steps in the sample. When the material reaches sufficient mechanical stability (gelation) the TMA measuring probe deforms less the sample and the amplitude of the oscillations is reduced. The gel conversion, α_{gel}, can be determined as the DSC conversion at the temperature gelled in TMA in a non-isothermal experiment. **Figure 4** shows the signal derivative from which the conversion at the gelation can be determined.

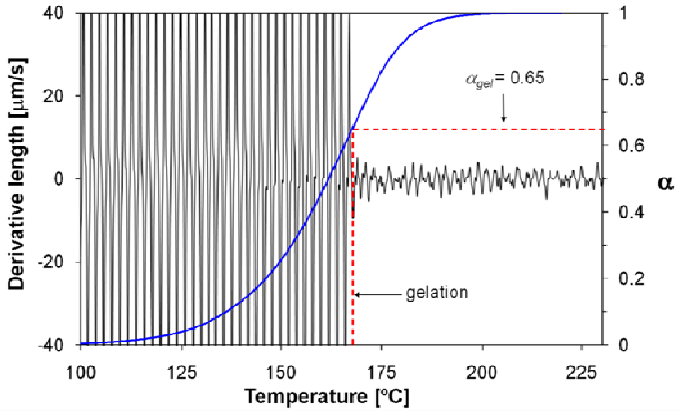

Figure 4 Gel point determination using combined TMA and DSC for the mixture DGEBA/MTHPA with 20 wt.% of S1200 and 0.5 wt.% of BDMA

By isothermal TMA the degree of shrinkage, $\alpha_{shrinkage}$, during curing at 120 ºC has been determined. Experimentally, one can detect the gelation point by using TMA starting at a region in which contraction is not observed between two contraction steps in the sample. In previous papers [20,21] we demonstrated, by solubility test and DMTA essays at different forces, how this point can be associated with the gel point.

Figure 5 shows the plot of the shrinkage evolution during the curing at 120 ºC against time for all the formulations studied, obtained by isothermal TMA.

Polymer **2009**, 50, 5374-5383

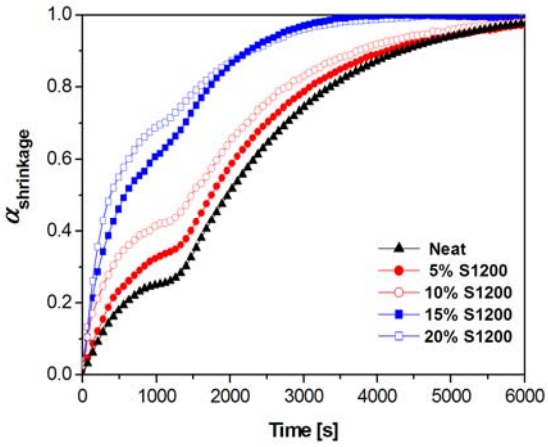

Figure 5 Degree of shrinkage, $\alpha_{shrinkage}$ vs time of the curing in TMA at 120 ºC of mixtures DGEBA/MTHPA and DGEBA/MTHPA/S1200 in different weight percentages

The first stage of contraction, before gelation, increases with the percentage of S1200, but this is not detrimental because the materials have enough mobility to stand deformations. The higher shrinkage before gelation can be explained by the polycondensation mechanism, with a high shrinkage, which takes place between the hydroxyl groups of the HBP and the anhydride. After gelation shrinkage clearly decreases with the addition of S1200, which is beneficial from the point of view of the appearance of internal stresses. TMA only allows determining the relative contraction before and after gelation during the curing process but it does not allow quantifying the global shrinkage. We evaluate it by determining the density of all the formulations before and after curing by gas pycnometry.

In **Table 3** the values for the conversion at the gelation (α_{gel}), gelation time (t_{gel}), global shrinkage and shrinkage before and after gelation of DGEBA/MTHPA with different proportions of S1200 are collected.

Table 3 Gelation data, densities and shrinkage of the systems studied

Formulation (% S1200)	α_{gel} [a]	t_{gel} [b] (min)	$\alpha_{shrinkage}$ [c]	ρ_{mon} (g/cm^3)	ρ_{pol} (g/cm^3)	S [d] (%)	S_{gel} [e]
DGEBA/MTHPA/0%	0.64	21.5	0.27	1.182	1.214	2.64	1.93
DGEBA/MTHPA/5%	0.59	21.9	0.36	1.182	1.214	2.64	1.69
DGEBA/MTHPA/10%	0.65	19.8	0.43	1.186	1.214	2.35	1.34
DGEBA/MTHPA/15%	0.61	17.8	0.62	1.188	1.213	2.13	0.81
DGEBA/MTHPA/20%	0.59	18.4	0.70	1.194	1.213	1.54	0.46

a. Determined as the conversion reached by non-isothermal TMA and DSC tests at 10 ºC/min.
b. Determined by TMA at 120 ºC.
c. Degree of shrinkage before gelation determined by TMA at 120 ºC.
d. Shrinkage determined as $[(\rho_{polymer} - \rho_{monomer})/\rho_{polymer}]$.
e. Degree of shrinkage after gelation determined as $[\text{shrinkage}\cdot(1-\alpha_{shrinkage})]$.

From the values of the table we can observe that there is not an obvious tendency of the evolution of the conversion at the gelation but there is a little reduction of the gelation time when the modifier is incorporated, in accordance to

the accelerative effect at low temperatures observed by DSC studies. In a previous work [13], we could prove that the addition of a HBP to a DGEBA cationic curing system greatly increased the conversion at the gelation, which can be explained in the basis of a decrease in the global functionality of the system on adding HBP ($f \approx 4$ for the DGEBA and $f \approx 3$ for the HBP obtained from an AB_2 type monomer). In the present work, the average functionality of DGEBA/MTHPA system is 3 similarly to that of S1200, and for this reason the conversion at the gelation should not be influenced by the presence of S1200. In contrast, there is a big variation of the contraction after gelation on increasing the proportion of HBP from 0.73 to 0.30. The mixture densities increase with the percentage of HBP, whereas the densities of the cured materials slightly decrease in comparison to the neat formulation. As the result, global shrinkage decreases with the incorporation of the modifier, showing the lowest shrinkage the material containing 20 wt.% of S1200. From the degree of shrinkage and the global shrinkage we can estimate the contraction after gelation, which is notably reduced on increasing the proportion of S1200. These results can be explained if we consider that the use of this kind of modifiers increases the free volume due to the expandable effect that occurs during the chemical incorporation of these macromolecules into the matrix, such it was previously described [12,13,22]. Some authors [23] reported that the addition of HBP to epoxy systems leads to more dense thermosets with less free volume, but these differences can be attributed to the structure of epoxy resin and HBP and also to the curing mechanism selected.

Study of thermal degradability

To test if our modification procedure leads to more reworkable thermosets, our materials were analyzed by TGA. **Figure 6** shows the TGA and DTG curves for the cured materials.

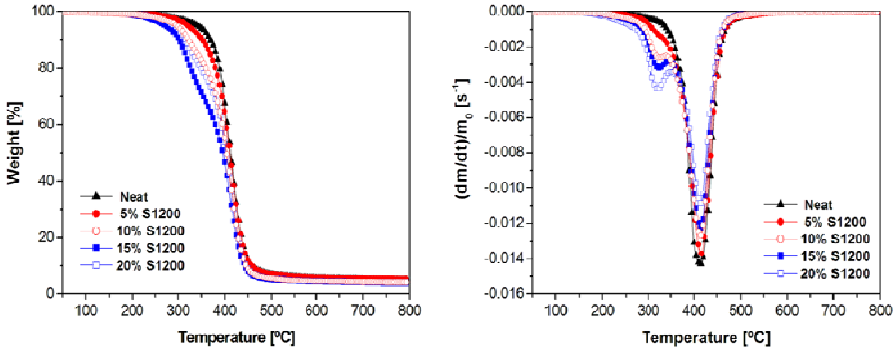

Figure 6 TG and DTG curves at 10 ºC/min in N_2 atmosphere of thermosetting materials obtained from DGEBA/MTHPA containing different proportions of S1200

In **Table 4** the thermogravimetric parameters are collected.

Table 4 TGA, TMA and DMTA data of the studied systems

Formulation (% S1200)	$T_{2\%}$[a] (ºC)	T_{max} (ºC)	% Char	CTE_{glass} $\cdot 10^6$ (K^{-1})	CTE_{rubber} $\cdot 10^6$ (K^{-1})	T_g[b] (ºC)	$T_{tan\,\delta}$[c] (ºC)	E'[d] (MPa)
DGEBA/MTHPA/0%	319	408	7	64.3	201.5	116	118	11.7
DGEBA/MTHPA/5%	282	415	6	64.1	201.4	119	132	17.8
DGEBA/MTHPA/10%	252	415	5	62.9	193.2	119	122	12.0
DGEBA/MTHPA/15%	250	414	4	62.1	191.5	119	116	8.8
DGEBA/MTHPA/20%	222	414	4	-	-	-	117	7.2

a. Temperature of a 2 % of weigth loss calculated by thermogravimetry.
b. Glass transition temperature obtained by TMA.
c. Temperature of the maximum of the tan δ.
d. Storage modulus of material at the rubbery region at a temperature of tan δ + 40 ºC.

DTG curves show that the addition of HBP leads to the appearance of a small peak at 325 ºC, which increases with the proportion of HBP and therefore can be attributed to the rupture of the secondary ester bonds of the S1200, because of they turn into little fragments which can be lost at this temperature. The main peak corresponds to the degradation of the crosslinked network and it remains similar for all materials. From TGA data it is observed that the onset of degradation is notably reduced when the proportion of S1200 is increased. It was reported, that the optimal temperatures for safe rework operations are in the range 230 - 250 ºC in nitrogen atmosphere, therefore, materials containing 15 wt.% to 20 wt.% of S1200 are able to be classified as reworkable thermosets [24].

Determination of thermal expansion coefficient

One of the most common causes of internal stresses in coatings is due to the mismatch in the thermal expansion coefficients (*CTE*s) between the coating and the substrate. **Table 4** collects the *CTE* values determined in the glassy and rubbery states of the materials prepared and the T_g determined as the cross of the tangents between both regions. It is interesting to note that on increasing the proportion of HBP the *CTE*s decrease. Usually, the introduction of flexible structures and the reduction of the crosslinking density increase this coefficient [25]. In these materials, flexible structures are introduced in the network and therefore the reduction of *CTE* should be attributed to a higher degree of crosslinking, due to the high number of functional groups in the HBP. It should be commented that the T_g has a major influence on the apparition of the internal stresses after curing. At the T_g the *CTE* changes from ~ 60 in the rubbery state to ~ 200 ppm/K in the glassy state and therefore the nearer the T_g to the curing temperature the less stresses are originated, when the coating is applied on the substrate.

Study of the thermomechanical properties

It has been observed by some authors [11,26], that the use of aliphatic hyperbranched polyesters as modifiers in epoxy resins leads to less densely crosslinked networks with an increased distance between crosslinks and therefore, mechanical properties of the material were affected in terms of strength. **Figures 7**

and **8** show the mechanical relaxation spectra and the tan *δ* plot of the different thermosets obtained.

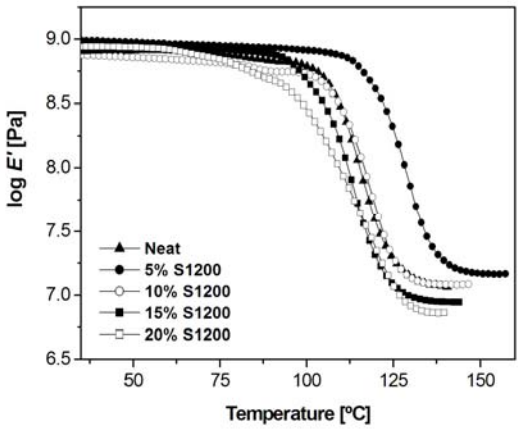

Figure 7 Storage modulus (*E'*) against temperature for the materials obtained

The tan *δ* curves are unimodal, which indicates that the materials are homogeneous, although the material containing 20 wt.% of S1200 shows a broader peak. The characteristic parameters associated to these spectra are shown in **Table 4**. As can be seen, the addition of a 5 wt.% of S1200 leads to the highest tan *δ* temperature. A further addition of S1200 slightly reduces this value. Tan *δ* temperatures correlate with T_g values determined by DSC.

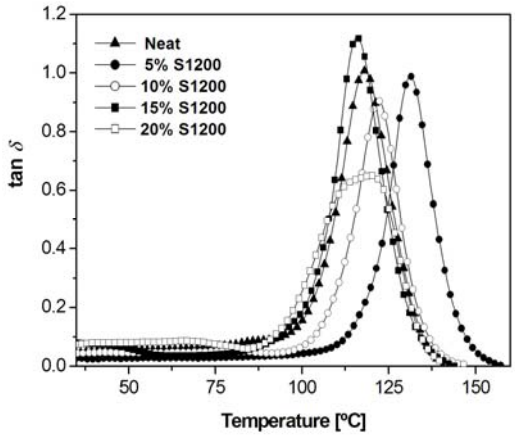

Figure 8 Tan *δ* against temperature for the materials obtained

The value of the relaxed modulus (*E'*) reaches also a maximum for the material with a 5 wt.% of S1200. Again, further addition of HBP reduces this parameter. From these studies we can state that the addition of percentages of S1200 until 10 wt.% increases the T_g and relaxed modulus in comparison to the neat epoxy, which can be explained by the higher density of crosslinking achieved

by the addition of the HBP, which can be considered as a whole as a multifunctional crosslinker.

Mechanical characterization

Boogh *et al.* [8] studied the effect of HBP as toughners in epoxy resins. Their system was based in the curing of an epoxy resin and epoxy functionalized HBPs with isophoronediamine. They could demonstrate that the addition of 10 wt.% of HBP to the material allows increasing 10-fold the toughness with a drop of the modulus of 10 %. The HBPs used were epoxy modified polyesters based in Boltorn®, which originated microphase separation. Yan *et al.* [11] observed a 20 % of improvement in impact strength by adding 10 wt.% of Boltorn® H30 to an epoxy resin/anhydride system with a high reduction of the Young modulus from 3.9 to 1.3 GPa. These materials did not show phase separation by SEM observation. Fu *et al.* [27] observed that the maximum impact strength was achieved by addition of 5 - 15 wt.% of a very flexible HBP to the DGEBA and in this way improvements of about 2 - 7 times in toughness were observed, although with a decrease in the T_g value. From these different results, it can be extracted that the structure of the components of the formulation and the mechanism selected are of capital importance in the mechanical behaviour.

The obtained values of Young's modulus, impact strength (I.S.) and Knoop microhardness (M.H.) for all the materials prepared are collected in **Table 5**.

Table 5 Mechanical properties and water uptake parameters evaluated of the systems studied

Formulation (% S1200)	Young's Modulus (GPa)	I.S. (kJ/m^2)	M.H. HKN	M_{max} (%)	$D\cdot10^{-8}$ (cm^2/s)
DGEBA/MTHPA/0%	3.8 (0.1)	1.3 (0.1)	19.7 (0.1)	1.0 ($2\cdot10^{-4}$)	4.3 (0.2)
DGEBA/MTHPA/5%	3.7 (0.2)	1.7 (0.1)	20.6 (0.1)	1.2 ($4\cdot10^{-4}$)	3.6 (0.0)
DGEBA/MTHPA/10%	4.3 (0.1)	2.1 (0.1)	20.4 (0.1)	1.7 ($7\cdot10^{-4}$)	2.9 (0.2)
DGEBA/MTHPA/15%	4.1 (0.3)	1.4 (0.1)	24.7 (0.2)	2.1 ($3\cdot10^{-4}$)	2.2 (0.1)
DGEBA/MTHPA/20%	4.0 (0.1)	1.5 (0.2)	21.3 (0.2)	2.6 ($6\cdot10^{-4}$)	1.7 (0.1)

The standard deviations are shown in parentheses.

It is observed that, in general, the addition of S1200 slightly increases the Young's modulus, reaching the maximum value for the material containing 10 wt.% of modifier (a 10 % of increase).

Impact resistance is a useful measure to evaluate the toughness or brittleness of a material. The addition of S1200 leads to a slight improvement on impact strength, also reaching the highest value for the thermoset containing 10 wt.% of HBP (60 % of improvement). Higher proportions of this modifier are detrimental, but in all cases the impact strength measured was higher than in the unmodified epoxy thermoset. This increase in toughness can be explained by the more flexible structure of S1200 introduced in the network [28].

Microhardness measurements are very useful in rating coatings on rigid substrates for their resistance to mechanical abuse, such as that produced by

blows, gouging and scratching. This technique is used in the industry to characterize the mechanical properties related to resistance and hardness of materials and it measures their capability to resist static loads or applied at low rates. As we can see, the addition of HBP slightly increases the microhardness in reference to pure cured DGEBA. This property, generally, is related with the final mechanical properties of the material: elongation at break and strength at break. In materials presenting higher values for these properties, the microhardness should be also higher.

In previous studies of our research group on the copolymerization of DGEBA with lactones [25,29] it was observed that the flexibilization of the network structure led to a decrease of the microhardness, modulus and T_g values. The use of S1200 in epoxy/anhydride systems leads to improvements of all the mechanical properties studied while maintaining the thermomechanical characteristics.

Morphology analysis by SEM

The toughness behaviour of DGEBA/MTHPA and the S1200 modified thermosets can be explained in terms of morphology observed by SEM. The fracture surfaces after impact tests were investigated by this technique and the most representative micrographs are shown in **Figure 9**.

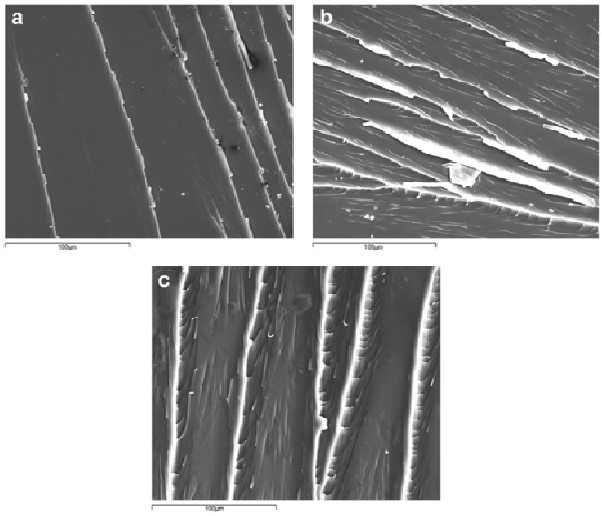

Figure 9 SEM micrographs for fracture surfaces of the following materials cured at 150 ºC: **a**) neat DGEBA/MTHPA; **b**) 5 wt.% S1200/DGEBA/MTHPA; **b**) 10 wt.% S1200/DGEBA/MTHPA

All the micrographs present a homogeneous appearance without any phase separation, although S1200 is a hydrophilic polymer and the epoxy matrix is hydrophobic. This homogeneity can be due to the fact that the particle size is too small to observe, which is attributed to the covalent bonding of the reactive groups of S1200 to anhydrides in the matrix. The smooth glassy fractured surface with little

Polymer **2009**, 50, 5374-5383

cracks in the unmodified material can be observed in **Figure 9** (**a**), without any sign of deformation, which accounts for its poor impact strength. In contrast, the fracture surface of the material with a 5 - 10 wt.% of S1200 **Figure 9** (**b**) and (**c**) is rougher than that of the unmodified material with more striations, suggesting that the impact specimens break more yieldingly. When the proportion of S1200 is increased again a brittle fracture is observed as a smooth surface. All these observations agree with the impact strength values measured (**Table 5**).

Water uptake behaviour

Epoxy resins are considered to be hardy polymers capable of stand deleterious conditions for considerable times. However, extended exposure to water can lead to damage. The main consequence of exposure to water is plasticisation, leading in turn to reduction of elastic modulus, strength and lowering the glass transition temperature [30]. Thus, the water absorption of the materials prepared is an important task to be studied.

The water absorption curves against time and the relative water gained against the root square of time at 50 ºC are shown in **Figure 10** for the thermosets obtained.

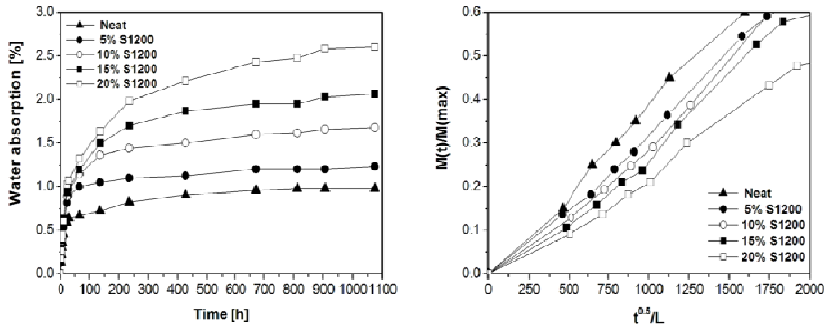

Figure 10 Water absorption curves against time and relative water weight gained as a function of root square of time at 50 ºC for DGEBA/MTHPA and DGEBA/MTHPA modified with different percentages of S1200

It is clear that HBP incorporation leads to an increase in the amount of absorbed water (M_{max}) due to the higher polarity of the thermosets containing the aliphatic poly(ester-amide) HBP compared with neat DGEBA/MTHPA system and to the increase in the free volume [31]. The equilibrium water uptake (M_{max}) was taken as the maximum values reached of the water absorption curves. The obtained values of this parameter and the corresponding diffusion coefficients determined for each material are collected in **Table 5**. The diffusion coefficient, calculated by the equations given in experimental part, on the contrary than the water uptake, decreases on adding HBP. This indicates that on adding S1200 the rate of absorption initially decreases but the equilibrium saturation percentages increases.

Conclusions

The addition of a hydroxyl ended HBP to epoxy/anhydride systems, in presence of a tertiary amine as catalyst, affects the mechanism of the curing process, favouring the non-catalyzed mechanism, which implies the reaction of hydroxyl and epoxy groups with anhydrides by a polycondensation process, leading to the covalent incorporation of the HBP to the network from the very beginning of the curing process.

Shrinkage after gelation is notably reduced on adding S1200. On increasing the proportion of modifier a progressive decrease of the global shrinkage is observed, which implies an increase in the free volume.

The thermal reworkability of the thermosets increases on adding a higher proportion of HBP.

By DMTA and SEM the homogeneous character of the materials prepared has been demonstrated. The tan δ value reaches a maximum for the material with a 5 wt.% of S1200. The addition of S1200 to DGEBA/MHTPA system increases the T_gs evaluated by DSC and TMA.

Thermal expansion coefficients in the glassy and rubbery states are slightly reduced on adding S1200 to the formulations.

Mechanical properties (Young's modulus, impact strength and microhardness) show little improvements on adding the HBPs tested to the material formulations. The proportion of 10 wt.% is the optimum one in order to achieve the best characteristics.

The presence of S1200 in the materials increases the water uptake, proportionally to the amount added, but decreases the diffusion coefficients.

Acknowledgements

DSM is acknowledged for hyperbranched polymer Hybrane® S1200 and Hunstman Advanced Materials for the HY918 (MTHPA) supply. The authors from the Universitat Rovira i Virgili and from Universitat Politècnica de Catalunya would like to thank CICYT (Comisión Interministerial de Ciencia y Tecnología) and FEDER (Fondo Europeo de Desarrollo Regional) (MAT2008-06284-C03-01 and MAT2008-06284-C03-02) for their financial support. M.M. acknowledges the grant FI-DGR 2009 from the Catalonian Government.

References

[1] May, C.A. editor. *Epoxy resins. Chemistry and technology*, 2nd ed., Marcel Dekker, New York, **1988** (Chapter 1).
[2] Petrie, E.M. *Epoxy Adhesive Formulations*, McGraw-Hill, New York, **2006**.
[3] Wang, L.; Li, H.; Wong, C.P. J. Polym. Sci., Part A: Polym. Chem. **2000**, 38, 3771-3782.
[4] Arasa, M.; Ramis, X.; Salla, J.M.; Mantecón, A.; Serra, A. Polym. Degrad. Stab. **2007**, 92, 2214-2222.
[5] Chen, J.S.; Ober, C.K.; Poliks, M.D. Polymer **2002**, 43, 131-139.

[6] Pascault, J.P.; Williams, R.J.J. In: Paul, D.R.; Bucknall, C.B. editors. *Polymer Blends*, vol.1., Wiley, New York, **2000**, 379-415.
[7] Thomas, R.; Durix, S.; Sinturel, C.; Omonov, T.; Goossens, S.; Groeninckx, G.; Moldenaers, P.; Thomas, S. Polymer **2007**, 48, 1695-1710.
[8] Boogh, L.; Pettersson, B.; Månson, J.A.E. Polymer **1999**, 40, 2249-2261.
[9] Ratna, D.; Varley, R.; Simon, G.P. J. Appl. Polym. Sci. **2003**, 89, 2339-2345.
[10] Wang, X.X.; Jiang, Z.G.; Zhang, Y.F. Chin. Chem. Lett. **2006**, 17, 125-128.
[11] Yang, J.P.; Chen, Z.K.; Yang, G.; Fu, A.Y.; Ye, L. Polymer **2008**, 49, 3168-3175.
[12] Foix, D.; Yu, Y.; Serra, A.; Ramis, X.; Salla, J.M. Eur. Polym. J. **2009**, 45, 1454-1466.
[13] Fernández-Francos, X.; Salla, J.M.; Cadenato, A.; Morancho, J.M.; Serra, A.; Mantecón, A.; Ramis X. J. Appl. Polym. Sci. **2009**, 111, 2822-2829.
[14] Crank, J.J. *The Mathematics of Diffusion*, Clarendon Press, UK, **1975**.
[15] Hayward, D.; Hollins, E.; Johncock, P.; McEwan, I.; Pethrick, R.A.; Pollock, E.A. Polymer **1997**, 38, 1151-1168.
[16] Frigione, M.; Calò, E. J. Appl. Polym. Sci. **2008**, 107, 1744-1758.
[17] Sangermano, M.; Amerio, E.; Di Gianni, A.; Priola, A.; Pospiech, D.; Voit B. Macromol. Symp. **2007**, 254, 9-15.
[18] Fisch, W.; Hofman, W.; Koskikallio, J. J. Appl. Chem. **1956**, 6, 429-441.
[19] O'Neill, L.A.; Cole, C.P. J. Appl. Chem. **1956**, 6, 356-364.
[20] Mas, C.; Ramis, X.; Salla, J.M.; Mantecón, A.; Serra A. J. Polym. Sci., Part A: Polym. Chem. **2003**, 41, 2794-2808.
[21] Mas C; Mantecón, A; Serra, A; Ramis, X; Salla, JM. J. Polym. Sci., Part A: Polym. Chem. **2004**, 42, 3782-3791.
[22] Lederer, A; Elrehim, M.A.; Schallausky, F.; Voigt, D; Voit, B. e-Polymers **2006**, 039, 1-14.
[23] Sangermano, M.; Priola, A.; Malucelli, G.; Bongiovanni, R.; Quaglia, A.; Amerio, E.; Voit, B.; Ziemer, A. Macromol. Mater. Eng. **2004**, 289, 442-446.
[24] Li, H.; Wong C.P. I.E.E.E.Trans. Adv. Packaging **2004**, 27, 165-172.
[25] Arasa, M.; Ramis, X.; Salla, J.M.; Ferrando, F.; Serra, A.; Mantecón, A. Eur. Polym. J. **2009**, 45, 1282-1292.
[26] Cicala, G.; Recca, A.; Restuccia, C. Polym. Eng. Sci. **2005**, 45, 225-237.
[27] Fu, J.F.; Shi, L.Y.; Yuan, S.; Hong, Q.D.; Zhang, D.S.; Chen, Y.; Wu, J. Polym. Adv. Technol. **2008**, 19, 1597-1607.
[28] Mezzenga, R.; Månson, J.A.E. J. Mater. Sci. **2001**, 36, 4883-4891.
[29] González, L.; Ferrando, F.; Ramis, X.; Salla, J.M.; Mantecón, A.; Serra, A. Prog. Org. Coat. **2009**, 65, 175-181.
[30] Popineau, S.; Rondeau-Mouro, C.; Sulpice-Gaillet, C.; Shanahan, M.E.R. Polymer **2005**, 46, 10733-10740.
[31] Case, S.L.; O'Brien, E.P.; Ward, T.C. Polymer **2005**, 46, 10831-10840.

UNIVERSITAT ROVIRA I VIRGILI
NOUS TERMOESTABLES EPOXÍDICS MODIFICATS AMB ESTRUCTURES DENDRÍTIQUES DE TIPUS HIPERRAMIFICAT I ESTRELLA
Mireia Morell Bel
DL:T. 155-2012

III.3

NEW EPOXY THERMOSETS MODIFIED WITH HYPERBRANCHED POLY(ESTER-AMIDE) OF DIFFERENT MOLECULAR WEIGHT

Mireia Morell, Michael Erber, Xavier Ramis, Francesc Ferrando, Brigitte Voit, Àngels Serra

European Polymer Journal ***2010****, 46, 1498 – 1509*

UNIVERSITAT ROVIRA I VIRGILI
NOUS TERMOESTABLES EPOXÍDICS MODIFICATS AMB ESTRUCTURES DENDRÍTIQUES DE TIPUS HIPERRAMIFICAT I ESTRELLA
Mireia Morell Bel
DL:T. 155-2012

European Polymer Journal **2010**, 46, 1498 – 1509

NEW EPOXY THERMOSETS MODIFIED WITH HYPERBRANCHED POLY(ESTER-AMIDE) OF DIFFERENT MOLECULAR WEIGHT

Mireia Morell,[1] Michael Erber,[2] Xavier Ramis,[3] Francesc Ferrando,[4] Brigitte Voit,[2] Angels Serra[1]

[1] Department of Analytical and Organic Chemistry, University Rovira i Virgili, C/ Marcel·lí Domingo s/n, Tarragona 43007, Spain.
[2] Leibniz-Institut für Polymerforschung Dresden, Hohe Strasse 6, Dresden 01069, Germany.
[3] Thermodynamics Laboratory, ETSEIB University Politècnica de Catalunya, C/ Av. Diagonal 647, Barcelona 08028, Spain.
[4] Department of Mechanical Engineering, University Rovira i Virgili, C/ Països Catalans 26, Tarragona 43007, Spain.

Abstract

The influence of hydroxy-functionalized hyperbranched poly(ester-amide) (HBP) of different molecular weight on the curing process of diglycidylether of bisphenol A (DGEBA) was studied using methyltetrahydrophthalic anhydride (MTHPA) as curing agent. By Differential Scanning Calorimetry (DSC) and Fourier Transform Infrared Spectroscopy (FTIR) the curing reaction was monitored and the covalent incorporation of the modifier in the matrix proved. By Thermomechanical Analysis (TMA) the reduction of the contraction after gelation on changing the HBP proportion was observed. The incorporation of HBP increased the glass transition temperature (T_g) and reduced the overall shrinkage, especially after gelation. The modified materials showed a higher thermally degradability than neat DGEBA thermosets. Thermal expansion coefficient, Young's modulus, impact strength and microhardness were improved without compromising the thermomechanical characteristics. The water uptake behaviour was also evaluated.

Keywords: epoxy resin; hyperbranched; crosslinking

Introduction

Epoxy resins are ideal materials for structural applications. However, when applied as coatings, they have some drawbacks such as brittleness and shrinkage, which reduce their performance and dimensional stability, leading to a final reduction of their protection capability [1]. During the past decades considerable efforts have been made to improve the toughness of these materials. One of the most successful approaches to decrease the brittleness of epoxy resins is to blend them with rubbers, elastomers or core-shell particles able to stand energy absorption mechanisms [2-4]. However, this results in a high increase in the viscosity of the uncured blends and/or to a decrease in the T_g of the thermosets. Some years ago, the use of hyperbranched polymers has been proposed to overcome the limitations of traditional modifiers [5] and a lot of research groups adopted this strategy to improve the mechanical characteristics [6-8]. It has been reported that the toughness increases while the Young's modulus and the glass transition temperature remained unaffected [5].

Another advantage of HBPs is their low viscosity compared to linear analogues, due to the low entanglement between molecules caused by their highly

branched architecture [5]. This characteristic allows improving the processability of HBP/epoxy thermosets, which is very important in the field of coatings.

One of the technological ways to reduce shrinkage during epoxy curing is the addition of fillers produces a great change on the mechanical properties and leads to the loss of transparency. Some authors proposed the use of expandable monomers, but a reduction of the T_g was always observed, because of their flexible structure [9-11]. As an alternative, the reduction of the shrinkage has been achieved by the addition of hyperbranched polymers [12,13] although in some papers the contrary behaviour has been described [14,15].

The improvement of the toughness in addition with the reduction of the shrinkage can minimize the generation of stresses during curing. Månson's group [16] investigated the applicability of HBPs as a stress-reducing agent in epoxy-based composite materials to prevent void formation. They observed that by adding a 10 wt.% of Boltorn E1, with a flexible polyester structure and epoxy groups at the chain ends, a reduction of 5 ºC in the T_g value and a strongly reduction of the shrinkage during curing and the internal stress level was achieved.

Apart from their structure, a parameter that should influence the effect of the HBPs on the characteristics of the thermosets is their average molar masses. If molar mass increases, maintaining the repetitive unit, the number of reactive chain ends increases as well. Some authors studied the mechanical properties of epoxy thermosets modified with HBPs of different molar masses [17,18]. They reported that the addition of HBP to the epoxy matrix improved tensile, flexural and impact strength and fracture toughness. These properties improve with the proportion of HBP and its molecular weight until reaching a maximum. This maximum should also depend, predictably, on the chemical structure of the HBP added and therefore this cannot be taken as a general trend.

In addition to that, one of the main limitations of the thermosetting materials is their low degradability. Coatings degradability is required when the reworkability of the coated electronic components is desired. The improvement on this property could be achieved by the introduction of labile groups such as esters of secondary or tertiary alkyl moieties in the network [19]. Ester groups can be thermally broken by a β-elimination process allowing removing the coating from the substrate. If their structure is appropriately selected, HBPs can help to solve this drawback. In previous studies we could increase the thermal degradability of epoxy thermosets by adding hyperbranched polyesters [13,20]. Besides, hyperbranched polymers have a large number of functional groups at the end of the branches, such as hydroxyls, which allow to covalently linking the modifier to the epoxy matrix by the use of anhydrides as curing agents. In the present work, we have selected as modifiers two hydroxyl-ended hyperbranched poly(ester-amide)s with cycloaliphatic rings in their structure. One of them is the commercial Hybrane® H1500 with a molecular weight ($\overline{M_n}$) of 1,500 g/mol and the other with a molecular weight of about 30,000 g/mol synthesized by us. The presence of cycloaliphatic rings in the

structure reduces the flexibility of the Hybrane® S1200, which affects the characteristics of the modified epoxy thermosets previously reported by us [20].

To our knowledge, there are not studies reported in literature related with the effect of adding these structures on diglycidylether of bisphenol A (DGEBA)/anhydride thermosets.

Experimental

Materials

Diisopropanolamine (DIPA) and *cis*-hexahydrophthalic anhydride (HHPA) were purchased from commercial sources (Fluka and Sigma-Aldrich respectively) and were used without further purification. Diglycidylether of bisphenol A (DGEBA) EPIKOTE RESIN 827 was provided by Shell Chemicals (epoxide equivalent weight (EEW) = 182.1 g/eq, n = 0.082). Methyltetrahydrophthalic anhydride (MTHPA) (Ciba-Huntsman) (HY918) and *N*,*N*-dimethylbenzylamine (BDMA) (Aldrich) were used as received. The hydroxyl terminated hyperbranched poly(ester-amide) Hybrane® H1500 (DSM) has an average molecular weight ($\overline{M_w}$), as reported on data sheet, of about 1,500 g/mol. The hydroxyl index of 402 mg KOH/g and the T_g value of 75 ºC were determined experimentally.

Xylene (mixture of isomers) was purified by vacuum distillation and dried over molecular sieves. Tetrahydrofuran (THF) and diethylether were used as received. All solvents were purchased from Scharlab.

Synthesis of hyperbranched H30000

The synthesis of hyperbranched polymer H30000 (represented in **Scheme 1**) was done similarly to the procedure described by Fang *et al.* [21].

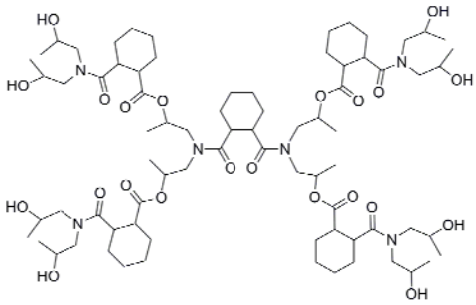

Scheme 1 Idealized chemical structure of the hyperbranched poly(ester-amide)s H1500 and H30000 studied

Diisopropanolamine (15.32 g, 0.115 mol) and xylene (50 mL) were introduced into a three-necked flask equipped with a thermometer, a single water dispenser and a gas inlet to fill the flask with nitrogen and (15.42 g, 0.10 mol) of *cis*-hexahydrophthalic anhydride dissolved in 50 mL xylene was added dropwise. The

reaction mixture was gradually heated in an oil bath to 80 °C and reacted for 6 hours under nitrogen at this temperature. For better stirring and mixing, small amounts of dry xylene were added if necessary. Then, the reaction mixture was heated to 180 °C until no more water could be azeotropically removed through the single water dispenser. To drive the reaction to higher conversion, vacuum (~ 5 mbar) was applied for further 15 min. After cooling, xylene was removed in vacuum yielding an almost colourless glassy substrate. The crude product was purified twice by precipitation from THF into diethylether and dried under vacuum at 50 °C. The yield of the resulting polymer was about 24.32 g (79 %).

^{1}H NMR ($CDCl_3$) *δ ppm*: 1.09-1.24 (complex m), 1.76 (broad s), 2.00-2.13 (broad s), 2.49 (complex m), 2.74 (complex m), 2.99 (complex m), 3.24 (complex m), 3.41-3.46 (complex m), 3.87 (complex m), 3.99 (complex m), 4.95-5.05 (complex m); ^{13}C NMR ($CDCl_3$) *δ ppm*: 15.39, 18.04, 21.29, 25.36, 28.94, 42.38, 44.85, 49.15-59.65 (broad), 65.98, 69.91, 174.6-177.25 (broad); FTIR (ATR) (cm^{-1}): 3429, 2930, 1727, 1660; Hydroxyl index: 754 mg KOH/g; $\overline{M_n}$ = 30,000 g/mol; $\overline{M_w} / \overline{M_n}$ = 3.1.

Preparation of DGEBA/MTHPA/HBP mixtures

The mixtures were prepared by adding the required amount of HBP (H1500 or H30000) into the epoxy resin. These mixtures were heated until the modifier was dissolved and the solutions became clear. Then, MTHPA was added and the resulting solutions were stirred and degassed under vacuum for 15 min at 70 ºC. Finally, BDMA was added and the mixtures were stirred and cooled down to -10 ºC maintaining them at this temperature until use to prevent polymerization. Mixtures containing 0 - 20 wt.% (by weight) of H1500 or 0 - 10 wt.% of H30000 were prepared and the equivalent stoichiometric relation between MTHPA, DGEBA and HBP was kept for all materials. When amine (BDMA) was added, the amine/anhydride molar ratio was kept unchanged. The compositions of the formulations studied are collected in **Table 1**.

Table 1 Composition of the formulations with different weight percentage of H1500 or H30000. In percentage by total weight (wt.%) of the mixture and in equivalent ratio, (Xeq)

Formulation (% HBP)	DGEBA		MTHPA		BDMA		OH from HBP	
	Xeq	wt.%	Xeq	wt.%	Xeq	wt.%	Xeq	wt.%
DGEBA/MTHPA	1	52.0	1	48.0	0.0065	0.53	-	-
H1500								
DGEBA/MTHPA/5%	0.95	48.5	1.05	46.5	0.0061	0.50	0.10	5
DGEBA/MTHPA/10%	0.90	44.8	1.11	45.2	0.0061	0.50	0.21	10
DGEBA/MTHPA/15%	0.85	40.8	1.18	44.2	0.0061	0.50	0.33	15
DGEBA/MTHPA/20%	0.80	37.2	1.24	42.8	0.0061	0.50	0.44	20
H30000								
DGEBA/MTHPA/5%	0.88	46.7	1.13	48.3	0.0062	0.50	0.23	5
DGEBA/MTHPA/10%	0.77	41.2	1.30	48.8	0.0061	0.50	0.47	10

Characterization techniques

^{1}H NMR and ^{13}C NMR measurements were carried out at 500.13 and 125.75 MHz, respectively, using a Bruker DRX 500 NMR spectrometer. $CDCl_3$ was used as solvent for all NMR measurements. For internal calibration the solvent signals of $CDCl_3$ were used: δ (^{13}C) = 77.0, δ (^{1}H) = 7.26 ppm. Quantitative ^{13}C NMR spectra were recorded using inverse gated decoupling and a relaxation delay of 8 s.

The determination of molecular weights and molecular weight distributions was carried out on a modular build SEC-system coupled with a multi-angle laser light scattering (MALLS) detector DAWN EOS (Wyatt Technologies, USA) and a refractive index (RI) detector (Knauer, Germany) in combination with a PL-GEL 5 mm mixed C column, 300 x 7.5 mm (Polymer Laboratories, UK) using a flow rate of 1 mL·min^{-1} and THF as the eluent. Calibration in the case of RI detection was performed using linear polystyrene standards.

The amount of hydroxyl groups was determined according to ISO 2554-1974. An acetylating solution was prepared by dissolving 11.8 mL of acetic anhydride in 100 mL of pyridine. About 0.4 - 0.6 g of the polymer sample was dissolved in 5 mL of the acetylating solution. The mixture was stirred for 20 min at 130 ºC. Thereafter, 8 mL of water was added in order to hydrolyze the excess acetic anhydride. Finally, the solution was titrated with 1 N ethanolic KOH solution to determine the equivalence point. An analogous “blank experiment” was performed without the polymer sample with exactly the same amount of the acetylating mixture. The hydroxyl number (N_{OH}) was calculated from the results of both titrations using the formula:

$$N_{OH} = \frac{(V_0 - V_1)C \cdot M_{KOH}}{m} + AN \quad (1)$$

where, V_0 and V_1 are the equivalence titration volume of KOH in mL from the blank experiment and from the sample titration, respectively; C is the concentration of KOH in eq/l; M_{KOH} is the molecular weight of KOH in g/mol; m is the mass of polymer sample in grams; and AN is the acid number, which has not been taken into account in this case because it is very low.

Calorimetric analyses were carried out on a Mettler DSC-821e thermal analyzer. Samples of approximately 5 mg in weight were cured in aluminum pans in a nitrogen atmosphere. The calorimeter was calibrated using an indium standard (heat flow calibration) and an indium-lead-zinc standard (temperature calibration).

In the dynamic curing process the degree of conversion by DSC (α_{DSC}) was calculated as follows:

$$\alpha_{DSC} = \frac{\Delta H_T}{\Delta H_{dyn}} \quad (2)$$

where ΔH_T is the heat released up to a temperature T, obtained by integration of the calorimetric signal up to this temperature, and ΔH_{dyn} is the total reaction heat associated with the complete conversion of all reactive groups.

The glass transition temperatures (T_gs) were calculated, after complete curing, by means of a second scan at 20 ºC/min as the temperature of the half-way point of the jump in the heat capacity when the material changed from glassy to the rubbery state under N_2 atmosphere.

An FTIR spectrophotometer FTIR-680PLUS from JASCO with a resolution of 4 cm^{-1} in the absorbance mode was used to monitor the isothermal curing process at 120 ºC. This device was equipped with an attenuated-total-reflection accessory with thermal control and a diamond crystal (Golden Gate heated single-reflection diamond ATR, Specac-Teknokroma). The disappearance of the absorbance peak at 913 cm^{-1} was used to monitor the epoxy equivalent conversion. The consumption of the reactive carbonyl group of anhydride was evaluated by the absorbance at 1777 cm^{-1}. The peak at 1508 cm^{-1} of the phenyl group was chosen as an internal standard. Conversions of the different reactive groups, epoxy and anhydride, were determined by the Lambert-Beer law as reported previously by us [12].

Thermomechanical analyses were carried out on a Mettler TMA40 thermomechanical analyzer. The samples were supported by two small circular ceramic plates and silanized glass fibers, which were impregnated with the samples. Isothermal experiments at 120 ºC were undertaken using TMA by application of a force of 0.01 N in order to monitor contraction during the curing process. The degree of shrinkage ($\alpha_{shrinkage}$) can be calculated as follows:

$$\alpha_{shrinkage} = \frac{L_t - L_0}{L_\infty - L_0} \tag{3}$$

where L_t, L_0 and L_∞ represent, respectively, the thickness of the sample at time t, at the onset and at the end of the reaction.

The conversion at the gel point was evaluated by means of non-isothermal experiments performed between 40 and 225 ºC at a heating rate of 5 ºC/min applying a periodic force that change (cycle time = 12 s) from 0.0025 to 0.01 N. The gel point was taken in TMA as the temperature at which a sudden decrease in the amplitude of the oscillations was observed. The gel conversion, α_{gel}, was determined as the DSC conversion at the temperature in which the gelation is observed in TMA in a non-isothermal experiment.

The linear thermal expansion coefficients in the glassy and rubbery states measurements of the cured samples were performed using samples with a size of (4 x 4 x 2 mm^3). The samples were mounted on the TMA and heated at a rate of 10 °C/min. The coefficient of thermal expansion (CTE) can be determined as:

$$CTE = \frac{1}{L_0}\frac{dL}{dT} = \frac{1}{L_0}\frac{dL/dt}{dT/dt} \quad (4)$$

where, L is the thickness of the sample, L_o the initial length, t the time and T the temperature.

The overall shrinkage was calculated from the densities of the materials before and after curing, which were determined using a Micromeritics AccuPyc 1330 Gas Pycnometer thermostatized at 30 ºC.

Thermogravimetric analyses (TGAs) were carried out in a Mettler TGA/SDTA 851e thermobalance. Cured samples with an approximate mass of 8 mg were degraded between 30 and 800 ºC at a heating rate of 10 ºC/min in N_2 (100 cm^3/min measured in normal conditions).

Thermal-dynamic-mechanical analyses (DMTAs) were carried out with a Rheometrics PL-DMTA MKIII analyzer. The samples were cured isothermally in a mould at 150 ºC for 4 h and then post-cured for 2 h at 200 ºC. Single cantilever bending at 1 Hz was performed at 2 ºC/min, from 30 ºC to 200 ºC on prismatic rectangular samples (20 x 5 x 1.5 mm^3).

The Izod impact test was performed at 23 ºC by means of a Zwick 5110 impact tester. The test specimens has a rectangular section according to ASTM 256-05a. The pendulum employed had a kinetic energy of 2.75 J.

The fracture area of the specimens for impact tests was observed with an environmental scanning electron microscope (ESEM) model FEI Quanta 600.

The modulus of elasticity was determined using a Houndsfield 10ks universal testing machine. The unnotched specimens were the same rectangular bars used in Izod test. A three point bending assembly has been constructed for this test in order to obtain flexural modulus of elasticity in a non destructive test. The tests were performed at a crosshead speed of 5 mm/min.

The modulus of elasticity is the ratio of stress to corresponding strain within the elastic limit, on the stress-strain curve. It is calculated using the slope of the stress-strain curve in accordance with Eq. 7. In this testing configuration, the maximum stress in central section of the beam is:

$$\sigma \equiv \frac{3FL}{2bd^2} \quad (5)$$

and the corresponding strain is:

$$\varepsilon \equiv \frac{6Dd}{L^2} \quad (6)$$

using a couple of points in the linear region, the slope of the curve and thus the modulus of elasticity can be obtained from:

$$E_B \equiv \frac{\Delta\sigma}{\Delta\varepsilon} \tag{7}$$

where, E_B is the modulus of elasticity in bending (N/mm^2), L (mm) is the support span, b (mm) is the width of beam tested, d (mm) is the depth of beam tested, D (mm) is the deflection of the beam, and F (N) is the force.

Microhardness was measured with a Wilson Wolpert (Micro-Knoop 401MAV) device following the ASTM D1474-98 (2002) standard procedure. For each material 10 determinations were made with a confidence level of 95 %. The Knoop microhardness (HKN) was calculated from the following equation:

$$\text{HKN} = L / A_p = L / l^2 \cdot C_p \tag{8}$$

where, L is the load applied to the indenter (0.025 Kg), A_p is the projected area of indentation in mm^2, l is the measured length of long diagonal of indentation in mm, C_p is the indenter constant (7.028 x 10^{-2}) relating l^2 to A_p. The values were obtained from 10 determinations with the calculated precision (95 % of confidence level).

Water uptake was evaluated by immersion tests according to ASTM D 570-98. To carry out this test three square samples of each thermoset (10 x 10 x 1 mm^3) were cut and thermally conditioned at 50 ± 1 ºC during 24 hours in an oven. Then, the samples were cooled and immediately weighed to get the initial weight. The samples were immersed under water at 50 ± 1 ºC during the selected times and then were dried with a dry cloth and weighed. The weightings were repeated until constant weight, at which the specimens can be considered substantially saturated. The increase in weight can be calculated as follows:

$$\text{Increase in weight},\% = \frac{\text{weight}_{\text{wet}} - \text{weight}_{\text{initial}}}{\text{weight}_{\text{initial}}} \text{ x } 100 \tag{9}$$

The diffusion coefficient was determined according to Ref. [20].

Results and discussion

Hyperbranched polymers have been studied as modifiers of epoxy thermosets with the commercial aliphatic polyester Boltorn® H30 being the most studied samples [5,6,13,15,22]. In a previous study [20], we selected as a HBP modifier the poly(ester-amide) Hybrane® S1200 obtained from succinic anhydride due to the presence of secondary alkyl esters in the structure which help to improve the thermal degradability of epoxy thermosets necessary for reworkability. Secondary alkyl ester groups are also present in the structure of Hybrane® H1500 (**Scheme 1**) and therefore, it can be interesting for the same purpose. Moreover this HBP, which derives from *cis*-hexahydrophthalic anhydride, contains cycloaliphatic units in the structure which can tailor several characteristics and this motivated us to initiate the present study and to extend it to the use of an analogous hyperbranched structure but with a higher molecular weight (H30000).

European Polymer Journal **2010**, 46, 1498 – 1509

As in the previous study we used a well established curing procedure: methyltetrahydrophthalic anhydride (MTHPA) as curing agent, catalyzed by a tertiary amine, benzyldimethylamine (BDMA) [20]. The presence of two reactive groups, epoxide and hydroxyl, leads to the adoption of a complex curing mechanism. In this mechanism polycondensation and ring-opening polymerization compete (**Scheme 2**) and the relative proportion of epoxy/hydroxyl groups in the curing mixture can favor one of them. This finally affects the morphology of the network and the characteristics of the final materials. The introduction of hydroxyl-ended HBPs in an epoxy/anhydride system favors the polycondensation mechanism [15,20]. To know the influence of the HBP in the reaction kinetics and mechanism, the curing process was studied by means of DSC and FTIR.

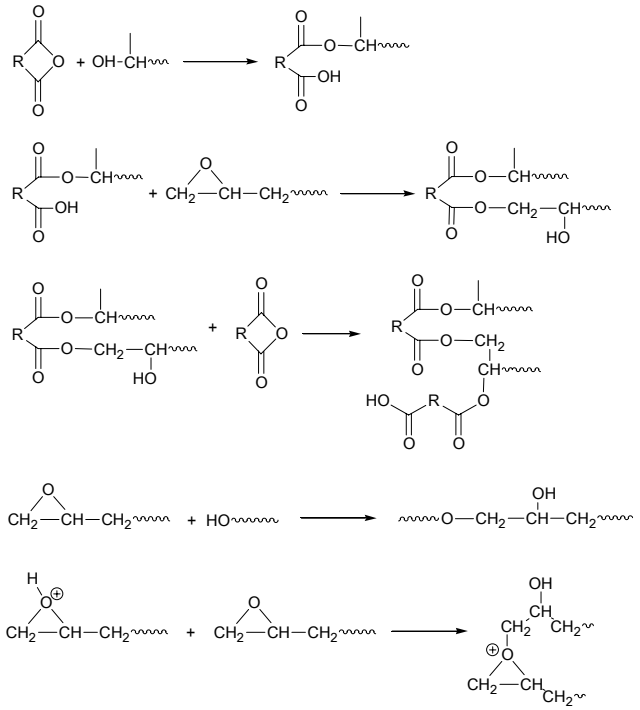

Scheme 2 (**a**) Reaction mechanisms of the curing of epoxides with anhydrides

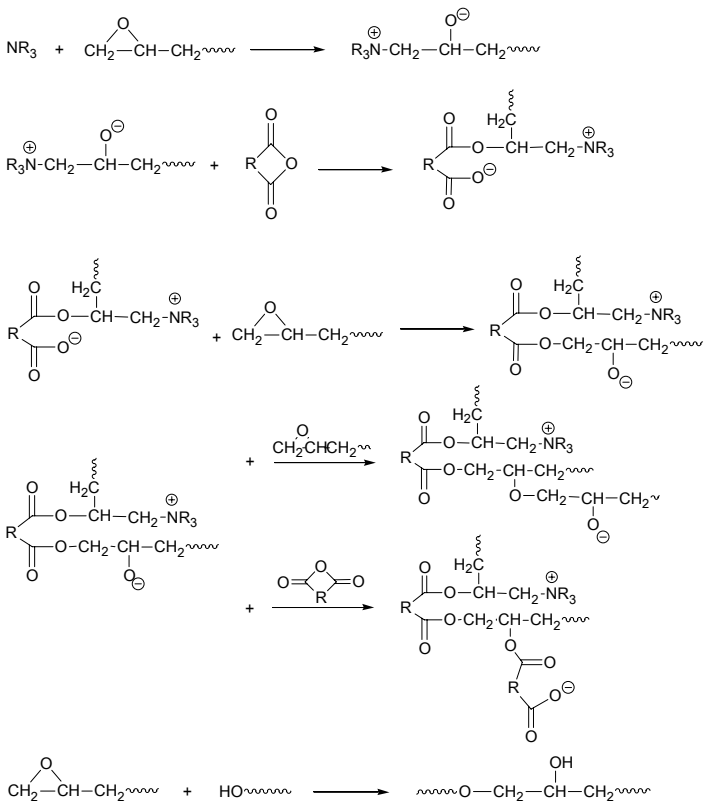

Scheme 2 (**b**) Reactions mechanisms of the curing epoxides with anhydrides, catalized by a tertiary amine

Studies on the curing of DGEBA/MTHPA/BDMA mixtures with several proportions of HBP

In a previous work [15] we determined that the maximum degree of curing was reached when one anhydride reacted either with an epoxide or with two hydroxyl groups of the HBP. In all the formulations prepared 0.5 wt.% of BDMA was added as a catalyst. This optimal ratio has been selected to prepare the formulations studied, which are collected in **Table 1**. As we can see in the table, on increasing the proportion of HBP in the formulation or/and the molecular weight of the HBP the hydroxyl/epoxy ratio increases as well.

The calorimetric curves of the curing process of all the formulations studied showed a unimodal shape, which seems to indicate that all the participating mechanisms take place simultaneously. However, there is a little difference among them, the addition of the HBPs generally leads to a slight increase in the conversion at a given temperature, especially until conversions of 80 %. **Figure 1** shows the plot of conversion degree against temperature recorded at 10 ºC/min of neat DGEBA/MTHPA and the formulations containing different proportions of H1500.

European Polymer Journal **2010**, 46, 1498 – 1509

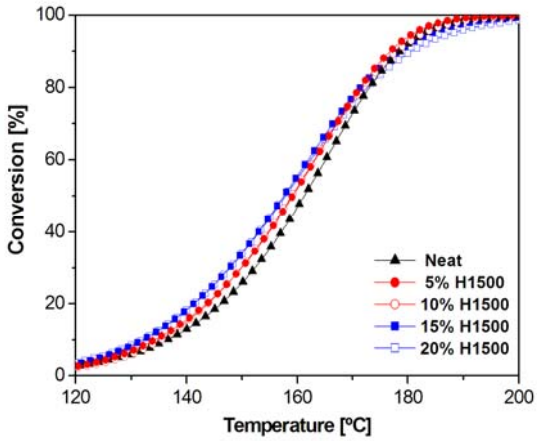

Figure 1 Conversion degree as determined by DSC against temperature of the curing of DGEBA/MTHPA and DGEBA/MTHPA mixtures containing different weight percentages of H1500 at a heating rate of 10 ºC/min

The monitoring along the curing process by FTIR spectroscopy allowed to confirm that anhydride groups disappeared faster than epoxides, which can be attributed to an initial esterification of hydroxyl groups by the mechanism depicted in **Scheme 2** (**a**) similarly as observed in previous studies [15,20]. The evolution of the characteristic functional groups taking part in the curing process confirmed the disappearance of the absorptions peaks of the anhydride (1777 and 1859 cm^{-1}) and epoxide (913 cm^{-1}) indicating the complete curing.

Table 2 collects the calorimetric data of the curing process of all the formulations studied. The reaction enthalpy is mainly due to the opening of epoxy group because of the strained ring. For that reason, it can be seen that the enthalpy is decreased as the amount of HBP or its molecular weight is increased, since the proportion of DGEBA in the formulation is going down. As it is seen, the temperature of the maximum of the curing exotherm on adding HBP to the epoxy resin is maintained.

The T_gs of the materials are slightly higher when the proportion of HBP is limited to 10 wt.% and higher proportions of HBP reduce this parameter. The high functionality and the stiffness which is conferred by the cycloaliphatic units of the HBP structure lead to higher values than those determined for S1200 modified materials reported previously [20].

Table 2 Calorimetric data of DGEBA/MTHPA/BDMA mixtures with different percentages of H1500 or H30000

	DSC				DMTA		TGA	
Formulation (% HBP)	**Δh (J/g)**	**Δh[a] (kJ/ee)**	**T_{max}[b] (ºC)**	**T_g[c] (ºC)**	**$T_{\tan\delta}$[d] (ºC)**	**E'[e] (MPa)**	**$T_{2\%}$[f] (ºC)**	**T_{max} (ºC)**
DGEBA/MTHPA/0%	245	90	165	92	118	11.5	283	413
H1500								
DGEBA/MTHPA/5%	238	90	164	103	129	20.9	268	411
DGEBA/MTHPA/10%	232	95	162	103	130	14.1	252	415
DGEBA/MTHPA/15%	228	98	161	94	125	11.2	254	409
DGEBA/MTHPA/20%	204	89	160	90	127	8.3	259	413
H30000								
DGEBA/MTHPA/5%	230	93	165	100	128	13.8	265	412
DGEBA/MTHPA/10%	220	98	165	106	122	11.5	237	414

a. Enthalpies per equivalent of epoxy group.
b. Temperature of the maximum of the curing exotherm.
c. Glass transition temperature obtained by DSC. Second scan after dynamic curing.
d. Temperature of the maximum of the tan δ.
e. Storage modulus of material at the rubbery region at tan δ + 50 ºC.
f. Temperature of a 2 % of weigth loss calculated by thermogravimetry.

Study of the gelation and shrinkage during curing

The irreversible transformation of a viscous liquid to an elastic gel is called gel point. At this point, the formation of a crosslinked network begins and gelation defines the upper limit in which the material can be applied. In the curing process, the loss of mobility after the gelation leads to the appearance of internal stresses, which originate voids and cracks in the thermoset and therefore, it is desirable to advance the gelation until higher conversions.

Molecular gelation takes place at a defined conversion of the crosslinking reaction (α_{gel}) and it depends on the reactivity, stoichiometry and functionality of the reactants. The conversion at gelation can be calculated if the chemical process is well known. In the present case, the concurrence between several chemical reactions prevents the conversion at the gelation to be calculated.

To experimentally determine the gelation point we used TMA, in which the gelation is seen as a reduction in the oscillation amplitude because the gelified material is less deformable. This reduction is better observed in the signal derivative (**Figure 2**) where the effect of volume change is eliminated.

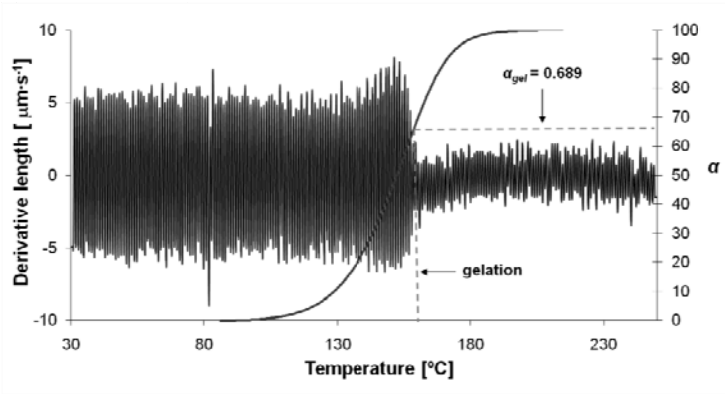

Figure 2 Gel point determination using combined TMA and DSC for the mixture DGEBA/MTHPA with 10 wt.% of H30000 and 0.5 wt.% of BDMA

When the material reaches sufficient mechanical stability (gelation) the TMA measuring probe deforms less the sample and the amplitude of the oscillations is reduced [23]. The gel conversion, α_{gel}, can be determined as the DSC conversion at the temperature gelled in TMA in a non-isothermal experiment. The figure shows the calculation method applied to the formulation containing a 10 wt.% of H30000, which lead to a α_{gel} = 0.69. In **Table 3** the conversion at the gelation is shown for all the formulations studied.

As can be seen, the addition of HBP produces a progressive slightly increase of this parameter. However, the gelation time does not show any regular tendency due to the combination of the kinetics of the curing and the variation of the conversion at the gelation. The conversions at the gelation are similar to those reported previously in formulations containing Boltorn® H30 [15], but the gelation time is a little longer for H1500 modified materials, which can be advantageous from the point of view of the application.

By isothermal TMA, the degree of shrinkage ($\alpha_{shrinkage}$) during curing at 120 ºC has been determined. Experimentally, one can detect the gelation point by using TMA starting at a region in which contraction is not observed between two contraction steps in the sample. In a previous study [24] we proved, by solubility test and DMTA essays, how this point can be associated to the gelation. **Figure 3** shows the plot of the shrinkage evolution during the curing at 120 ºC against time for the formulations containing different proportions of H1500.

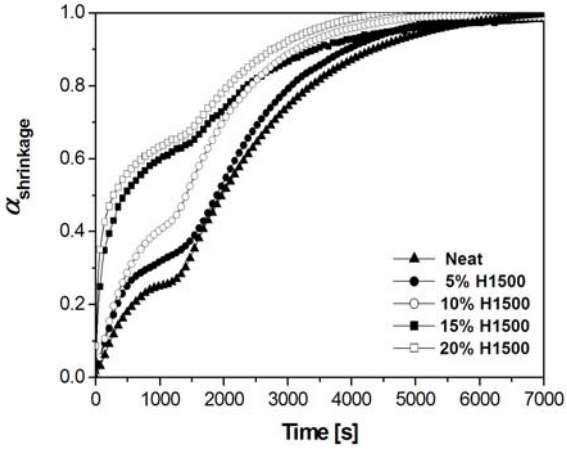

Figure 3 Degree of shrinkage, $\alpha_{shrinkage}$, versus time of the curing determined by TMA at 120 ºC of mixtures DGEBA/MTHPA and DGEBA/MTHPA/H1500 in different weight percentages

The first stage of contraction, before gelation, increases steadily with the percentage of HBP, and this is beneficial because at this stage the materials have enough mobility to withstand deformations. The increase in the shrinkage before gelation can be explained by the polycondensation mechanism (**Scheme 2** (**a**)), with a high shrinkage, which takes place between hydroxyl groups of the HBP and anhydrides. After gelation, the shrinkage decreases with increasing amount of HBP. This can be also related to the curing mechanism, which at the final stages takes mainly place by ring-opening (represented in **Scheme 2** (**b**)), which leads to less contraction.

Because TMA allows determining the relative contraction before and after gelation during the curing process, but not to quantify the global shrinkage, we evaluated it by determining the densities of all the formulations before and after curing by gas pycnometry. From the densities the shrinkage was calculated. These values are collected in **Table 3**, where we can observe that on increasing the proportion of HBP in the formulation the shrinkage is reduced. This is more pronounced when H30000 was used as a modifier. From the degree of shrinkage at the gelation and the global shrinkage we can estimate the contraction after gelation, which is notably reduced on increasing the proportion of HBP and values of ~ 0.5-0.6 % have been reached. From this point of view, the addition of high molecular weight HBP seems to be more beneficial, since a 10 wt.% of H30000 or 20 wt.% of H1500 lead to similar values for shrinkage.

Table 3 Gelation data, densities, shrinkage, CTEs and gravimetric water diffusion coefficients of the systems studied

Formulation (% HBP)	α_{gel} [a]	t_{gel} [b] (min)	α_{shrink} [c]	ρ_{mon} (g/cm^3)	ρ_{pol} (g/cm^3)	*Shrink.*[d] (%)	*Shrink.*[e] *after gel.* (%)	CTE_{glass} $\cdot 10^6$ (K^{-1})	CTE_{rubber} $\cdot 10^6$ (K^{-1})	$D \cdot 10^{8}$[f] (cm^2/s)
DGEBA/MTHPA/0%	0.64	21.5	0.27	1.182	1.214	2.64	1.93	64.3	201.5	4.3 (0.2)
H1500										
DGEBA/MTHPA/5%	0.65	24.0	0.37	1.181	1.209	2.38	1.50	62.1	193.8	3.4 (0.3)
DGEBA/MTHPA/10%	0.67	20.6	0.43	1.180	1.208	2.32	1.32	61.7	190.1	2.4 (0.2)
DGEBA/MTHPA/15%	0.70	23.7	0.64	1.180	1.205	2.08	0.75	58.6	188.3	1.2 (0.2)
DGEBA/MTHPA/20%	0.73	23.9	0.69	1.182	1.204	1.81	0.56	50.4	185.8	0.8 (0.0)
H30000										
DGEBA/MTHPA/5%	0.65	18.7	0.33	1.177	1.200	1.92	1.29	44.5	187.9	1.0 (0.0)
DGEBA/MTHPA/10%	0.69	22.1	0.46	1.184	1.198	1.10	0.59	28.0	178.4	0.9 (0.0)

a. Determined as the conversion at the gelation determined as the conversion reached by non-isothermal TMA and DSC tests at 10 ºC/min.
b. Gelation time determined by TMA at 120 ºC.
c. Degree of shrinkage before gelation determined by TMA at 120 ºC.
d. Global shrinkage on curing determined as $[(\rho_{polymer}-\rho_{monomer})/\rho_{polymer}]$.
e. Degree of shrinkage after gelation determined as $[\text{shrinkage}\cdot(1-\alpha_{shrink})]$.
f. Water diffusion coefficients with the standard deviations are shown in parentheses.

Study of the thermal degradability

To confirm that our modification procedure increases the reworkability of the thermosets, our materials were analyzed by TGA. **Figure 4** shows the DTG curves for the H1500 or H30000 modified materials and the main data for all the materials studied are collected in **Table 2**.

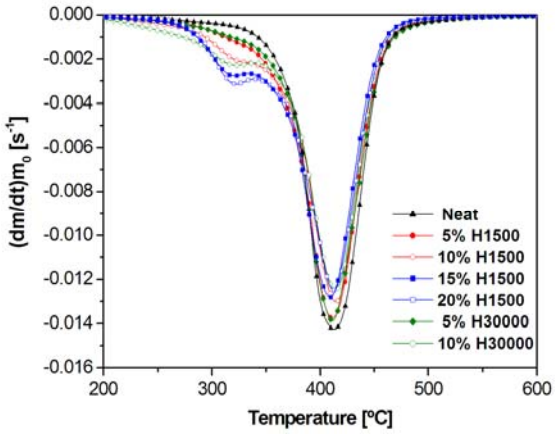

Figure 4 DTG curves at 10 ºC/min in N_2 atmosphere of thermosetting materials obtained from DGEBA/MTHPA containing different proportions of H1500 or H30000

DTG curves show that the addition of HBP leads to the appearance of a shoulder at 325 ºC, which increases with the proportion of HBP. This peak can be due to the rupture of the secondary ester bonds of the HBP, which leads to the formation of little fragments able to be volatilized. The main peak corresponds to the degradation of the crosslinked network and it remains similar for all materials.

A valuable TGA data is the $T_{2\%}$ because when the material losses a 2 % in weight the mechanical properties of the materials go down and the coatings can be removed from the substrate. From the values of the table, we can see that the addition of H1500 increases the reworkability, but a further addition does no increase it. On increasing the molecular weight of the modifier the $T_{2\%}$ is going down, because of the higher proportion of ester linkages in the material. It was reported [25], that the optimal temperatures for safe rework operations are in the range 230 - 250 ºC in N_2 atmosphere, and thus the materials containing proportions of 10 wt.% of HBP are able to be classified as reworkable thermosets.

On comparing the materials prepared from H1500 with those obtained from S1200, both with a comparable molecular weight, we can state that S1200 leads to higher improvements on the reworkability [20]. This fact can be rationalized by the less flexible structure of the cycloaliphatic HBPs which makes the formation of the six membered cycles, adopted in the transition state of the pyrolitic *β*-elimination process, difficult [26].

European Polymer Journal **2010**, 46, 1498 – 1509

Determination of thermal expansion coefficient

One of the most common causes of internal stresses in coatings is produced by the mismatch in the thermal expansion coefficients (*CTE*s) between the coating and the substrate. **Table 3** collects the *CTE* values determined by TMA in the glassy and rubbery states. It is worth to note that *CTE*s decrease on increasing the proportion of H1500. This decrease is more evident than the observed for S1200 modified materials [20] and it can be explained in the basis of the more rigid structure of the cycloaliphatic HBP and on the degree of crosslinking achieved. On increasing the molecular weight of the HBP there is also a decrease in the *CTE* values.

It was reported that by adding Boltorn® E1, to an epoxy system the *CTE* in the glassy state does not change, but it increases in the rubbery state from 185 to 260 K^{-1}. This observation was rationalized by the phase-separated particles, which appear in the thermoset. Thus, the *CTE* below T_g was dominated by the neat epoxy resin and above T_g by the HBP domains. In our case, *CTE* decreases in both regions which is due to the homogeneous character of the material.

Study of the thermomechanical properties

The mechanical relaxation spectra and the tan δ plot of all the materials prepared were registered. The tan δ curves were unimodal with a similar sharpness, which accounts for the homogeneity of these materials. The characteristic parameters associated to these spectra are shown in **Table 2**. As can be seen, the addition of HBPs increases the tan δ temperature, but it does not change appreciably on increasing the proportion added. Relaxed modulus increased on adding a 5 wt.% of H1500 or H30000 but further additions reduce this value. This could indicate that in our materials there is no a complete reaction of hydroxyl groups when a high proportion of HBP was added to the formulation. It has been reported that the increase in the molecular weight of a hydroxyl-ended HBP leads to a partial fold back into the HBP molecule, thus leaving less hydroxyl groups able to react with anhydrides [18].

Many authors observed that the incorporation of HBPs to epoxy resins leads to a decrease of the tan δ value, which was attributed to a higher free volume inside the network caused by the HBP [18,22]. Moreover, the modification with HBP reduces the relaxed modulus in systems in which hydroxyl terminal groups remained not-covalently linked to the matrix [18]. Thus, the covalent linkage of the HBP to the epoxy matrix is necessary to maintain the thermomechanical characteristics.

Mechanical characterization

Several authors [5-7,22] studied the effect of HBPs as toughners in epoxy resins and they could demonstrate their beneficial effect on this property, but the maximum effect was obtained in phase separated materials forming globular micro-particles in a continuous epoxy matrix. Fu *et al.* [27] observed a maximum improvement when they added a 5 - 15 wt.% of and aliphatic-aromatic hyperbranched polyester to the DGEBA matrix and in this way improvements of about 2 - 7 times in toughness were observed, although with a decrease in the T_g value, because of the flexibility of the HBP structure.

The effect of adding our poly(ester-amide) HBPs to the formulations in the impact strength is shown in **Figure 5**, since it is a useful measure for the evaluation of the toughness or brittleness. It can be seen that only the materials containing a 5 wt.% of H1500 and a 10 wt.% of H30000 have higher impact strength.

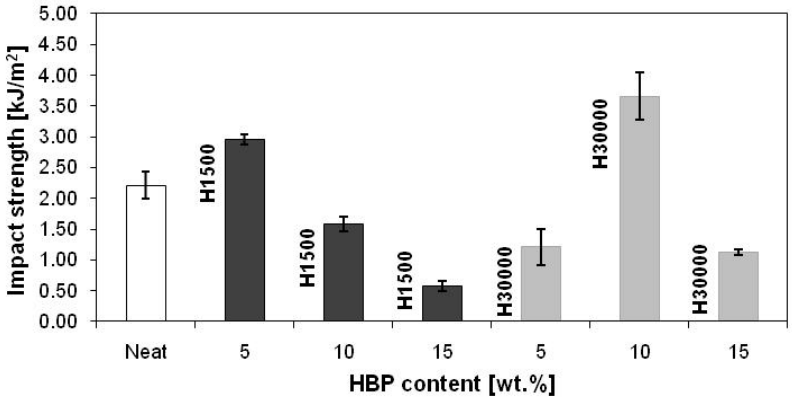

Figure 5 Dependence of impact strength of DGEBA/MTHPA thermosets containing different weight percentages of H1500 or H30000

The addition of a 10 wt.% of higher molecular weight HBP leads to the highest improvement in toughness. In our previous study [20], the addition of S1200 in percentages between 10 and 20 wt.% led to a slight improvement on impact strength, reaching the highest value for the thermoset containing 10 wt.% of HBP. The superior increase in toughness, obtained in the latter study, can be explained by the more flexible structure of S1200 introduced in the network. Flexural moduli of elasticity were determined for all the materials prepared in a three point bending assembly. The values are represented in **Figure 6**.

European Polymer Journal **2010**, 46, 1498 – 1509

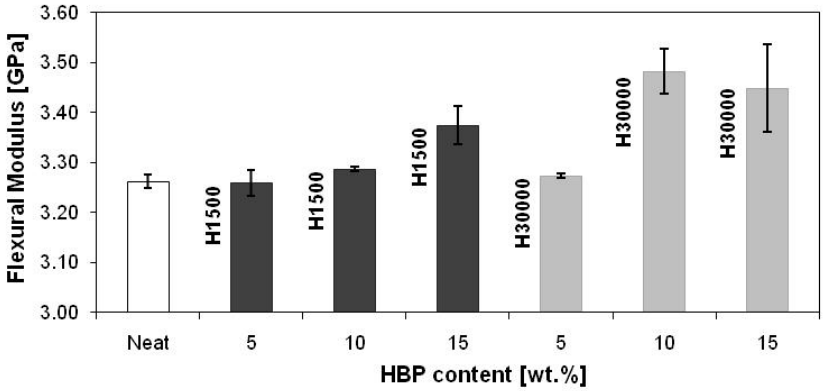

Figure 6 Dependence of flexural modulus of DGEBA/MTHPA thermosets containing different weight percentages of H1500 or H30000

In general, the addition of HBP increases the rigidity of the material, but the influence is higher when the molecular weight of the HBP increases. Although the addition of H1500 leads to a regular increase with the proportion, on adding H30000 there is not a clear tendency. The maximum modulus was reached for the material containing a 10 wt.% of H30000. An increase in the rigidity of the material on increasing the proportion of HBP was also observed on adding S1200 to a DGEBA/MTHPA formulation [20], but there was no relationship between this property and the proportion of HBP, since a 10 wt.% of HBP led to the maximum value. Other authors [8,22] described a loss of this modulus on adding HBP, but the structure of the HBP was much more flexible than that of the H1500 and H30000.

Microhardness is a measure of the resistance that one body offers against penetration by another. This technique is used in coatings industry to characterize the mechanical properties related to resistance and hardness of materials and it measures their capability to resist static loads or applied at low rates. As we can see in **Figure 7**, only the addition of H30000 increases the microhardness in reference to pure cured DGEBA.

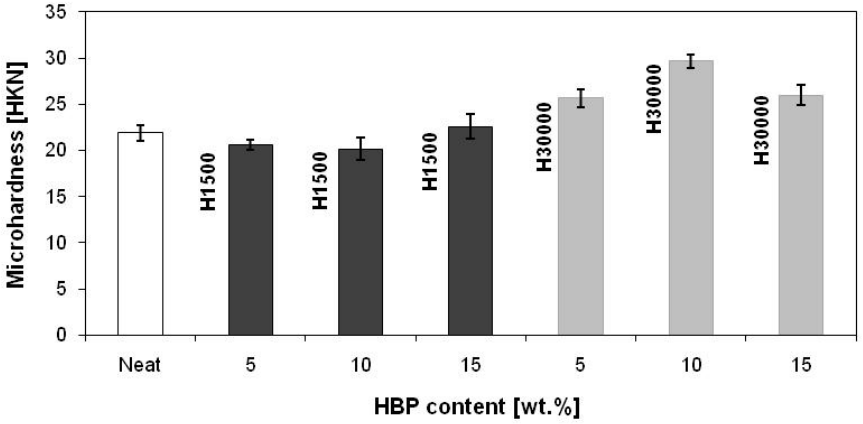

Figure 7 Dependence of microhardness of DGEBA/MTHPA thermosets containing different weight percentages of H1500 or H30000

From all the mechanical tests performed we can state that the more beneficial effect was reached when a 10 wt.% of H30000 was added to the formulation.

Morphology analysis of the fractures by ESEM

The toughness behaviour of DGEBA/MTHPA and the HBPs modified thermosets can be explained in terms of morphology observed by ESEM. The fracture surfaces after impact tests were investigated by this technique and the most representative micrographs are shown in **Figure 8**.

All the micrographs presented a homogeneous appearance without any phase separation, similarly to the observed in S1200 modified materials, in spite of their different hydrophilic/hydrophobic character [20]. This homogeneity can be attributed to the covalent bonding of the reactive groups of HBPs to anhydrides in the matrix. The smooth glassy fractured surface with little cracks in the unmodified material observed in **Figure 8** (**a**) accounts for its poor impact strength. In contrast, the fracture surface of the materials with a 5 wt.% of H1500 **Figure 8** (**b**) or with a 10 wt.% of H30000 **Figure 8** (**c**) are rougher than that of the unmodified, suggesting that the impact specimens break more yieldingly. The observations of the fractured surfaces agree with the impact strength values measured (**Figure 5**).

European Polymer Journal **2010**, 46, 1498 – 1509

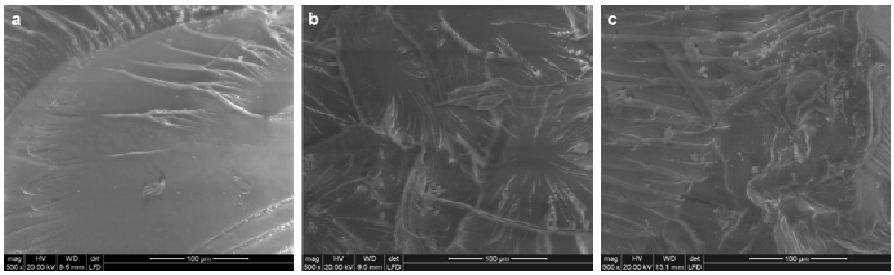

Figure 8 ESEM micrographs for fracture surfaces of the following materials cured at 150 ºC: (**a**) neat DGEBA/MTHPA; (**b**) 5 wt.% H1500/DGEBA/MTHPA; (**c**) 10 wt.% H30000/DGEBA/MTHPA

According tu Fu *et al.* [27] it seems that there is an optimum toughness value versus the generation number and content of HBP, which can be explained as synergism combination among the plastic deformation and "in situ" toughening mechanisms [27].

Water uptake behaviour

The water absorption curves against time for the thermosets obtained are shown in **Figure 9**.

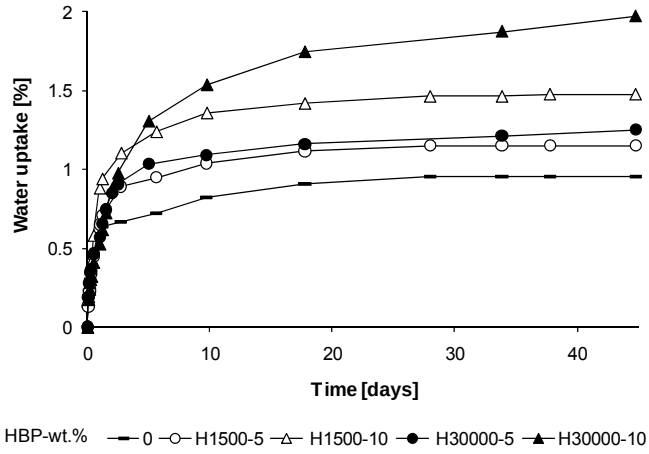

Figure 9 Water absorption curves against time at 50 ºC for DGEBA/MTHPA and DGEBA/MTHPA modified with different weight percentages of H1500 or H30000.

It is clear that HBP incorporation leads to an increase in the amount of absorbed water (M_{max}) due to the higher polarity of the thermosets containing the hydroxyl-ended cycloaliphatic poly(ester-amide), compared with neat DGEBA/MTHPA material. The water uptake increases with the proportion of HBP and reaches the highest values for H30000 modified thermosets. The equilibrium

water uptake (M_{max}) was taken as the maximum values reached of the water absorption curves and were used to calculate the corresponding diffusion coefficients, which are collected in **Table 3**. However the diffusion coefficient, calculated by the equations given in experimental part, decreases with the amount of HBP. This indicates that with the addition of HBPs, the rate of absorption initially decreases but the equilibrium saturation percentages increase.

The hydrophobic character of H1500 and H30000 in comparison to the more hydrophilic S1200 [20] leads to a lower water uptake for the materials prepared in the present study.

Conclusions

The addition of a hydroxyl terminated cycloaliphatic hyperbranched poly(ester-amide)s to epoxy/anhydride systems, in presence of a tertiary amine as catalyst, affects the mechanism of the curing process favoring the non-catalyzed mechanism. This implies the reaction of hydroxyl and epoxy groups with anhydrides by a polycondensation process, leading to the covalent incorporation of the HBP to the network from the very beginning of the curing process.

On increasing the proportion of HBP a progressive decrease of the global shrinkage is observed. This reduction is more pronounced for the HBP with high molecular weight. Moreover, the contraction after gelation is notably reduced and values of ~ 0.5 - 0.6 % have been reached.

The thermal reworkability of the thermosets increases on adding HBP due to an earlier start of the thermal degradation. Thus, materials containing 10 wt.% of HBP are able to be classified as reworkable thermosets.

By DMTA and ESEM the homogeneous character of the materials prepared has been demonstrated. The addition of HBPs increases the tan δ temperature and the relaxed modulus increases on adding a 5 wt.% of H1500 or H30000 because further HBP content reduces this parameter.

Thermal expansion coefficients in the glassy and rubbery states decrease on increasing the proportion of H1500. These coefficients are even more reduced when the modifier H30000 is used.

Mechanical properties (elastic modulus, impact strength and microhardness) show a maximum value when a 10 wt.% of H30000 was added to the formulation.

The presence of HBPs in the materials increases the water uptake, proportionally to the amount added, but decreases the diffusion coefficients. The water uptake is higher when H30000 is added in the formulation.

In summary, hyperbranched poly(ester-amide)s of Hybrane H1500 type are also very suitable for increasing the toughness and for reducing the shrinkage in epoxy thermosets. Significantly high molar mass samples of HBP (of 30,000 g/mol) and an addition of 10 wt.% seem to be the most favorable conditions for achieving optimized thermosets which can be reworked.

Acknowledgements

DSM is acknowledged for hyperbranched polymer Hybrane® H1500 and Hunstman Advanced Materials for the HY918 (MTHPA) supply. The authors from the Universitat Rovira i Virgili and from Universitat Politècnica de Catalunya would like to thank MICINN (Ministerio de Ciencia e Innovación) and FEDER (Fondo Europeo de Desarrollo Regional) (MAT2008-06284-C03-01 and MAT2008-06284-C03-02), Comissionat per a Universitats i Recerca del DIUE de la Generalitat de Catalunya (2009-SGR-1512) and the Germany-Spanish collaboration program (HA2007-0022, DAAD PPP D/07/13493) for their financial support. M.M. acknowledges the grant FI-DGR 2009 from the Catalonian Government.

References

[1] May CA, editor. *Epoxy resins. Chemistry and technology.* Marcel Dekker, New York, **1988**.
[2] Pascault, J.P., Williams, R.J.J. In: Paul DR, Bucknall CB, editors. *Polymer blends*, vol. 1., Wiley, New York, **2000**, 379-415.
[3] Thomas, R.; Durix, S.; Sinturel, C.; Omonov, T.; Goossens, S.; Groeninckx, G.; *et al*. Polymer **2007**, 48, 1695-1710.
[4] Day, R.J.; Lovell, P.A.; Wazzan, A.A. Compos. Sci. Technol. **2001**, 61, 41-56.
[5] Boogh, L.; Pettersson, B.; Månson, J.A.E. Polymer **1999**, 40, 2249-2261.
[6] Cicala, G., Recca, A. Polym. Eng. Sci. **2008**, 48, 2382-2388.
[7] Ratna, D.; Varley, R.; Simon, G.P. J. Appl. Polym. Sci. **2003**, 89, 2339-2345.
[8] Sangermano, M.; Malucelli, G.; Bongiovanni, R.; Priola, A.; Harden, A. Polym. Int. **2005**, 54, 917-922.
[9] Sadhir, R.K.; Luck, M.R. editors. *Expanding Monomers: Synthesis, Characterization and Applications.* CRC Press: Boca Raton, FL, **1992**.
[10 González, L.; Ramis, X.; Salla, J.M.; Mantecón, A.; Serra, A. J. Polym. Sci., Part A: Polym. Chem. **2008**, 46, 1229-1239.
[11] Canadell, J.; Mantecón, A.; Cádiz, V. J. Polym. Sci., Part A: Polym. Chem. **2007**, 45, 1980-1992.
[12] Klee, J.E.; Schneider, C.; Hölter, D.; Burgath, A.; Frey, H.; Mülhaupt, R. Polym. Adv. Technol. **2001**, 12, 346-354.
[13] Fernández-Francos, X.; Salla, J.M.; Cadenato, A.; Morancho, J.M.; Serra, A.; Mantecón, A.; Ramis, X. J. Appl. Polym. Sci. **2009**, 111, 2822-2829.
[14] Sangermano, M.; Priola, A.; Malucelli, G.; Bongiovanni, R.; Quaglia, A.; Amerio, E.; Voit, B.; Ziemer, A. Macromol. Mater. Eng. **2004**, 289, 442-446.
[15] Foix, D.; Yu, Y.; Serra, A.; Ramis, X.; Salla, J.M. Eur. Polym. J. **2009**, 45, 1454-1466.
[16] Eom, Y.; Boogh, L.; Michaud, V.; Månson, J.A.E. Polym. Compos. **2002**, 23, 1044-1056.
[17] Zhang, D.; Jia, D. J. Appl. Polym. Sci. **2006**, 101, 2504-2511.
[18] Cicala, G.; Recca, A.; Restuccia, C. Polym. Eng. Sci. **2005**, 45, 225-237.
[19] Chen, J.S.; Ober, C.K.; Poliks, M.D. Polymer **2002**, 43, 131-139.
[20] Morell, M.; Ramis, X.; Ferrando, F.; Yu, Y.; Serra, A. Polymer **2009**, 50, 5374-5383.
[21] Fang, K.J.; Xu, Z.G.; Jiang, X.; Zhang, X.; Fu, S.H. Polym. Bull. **2008**, 60, 533-543.
[22] Yang, J.P.; Chen, Z.K.; Yang, G.; Fu, A.Y.; Ye, L. Polymer **2008**, 49, 3168-3175.
[23] González, S.; Fernández-Francos, X.; Salla, J.M.; Serra, A.; Mantecón, A.; Ramis X. J. Appl. Polym. Sci. **2007**, 104, 3406-3416.
[24] Mas, C.; Ramis, X.; Salla, J.M.; Mantecón, A.; Serra, A. J. Polym. Sci., Part A: Polym. Chem. **2003**, 41, 2794-2808.
[25] Li, H.; Wong, C.P. I.E.E.E. Trans. Adv. Packaging **2004**, 27, 165-172.
[26] Sivasamy, P.; Palaniandavar, M.; Vijayakumar, C.T.; Ledered, K. Polym. Degrad. Stab. **1992**, 38, 15-21.

[27] Fu, J.F.; Shi, L.Y.; Yuan, S.; Zhong, Q.D.; Zhang, D.S.; Chen, Y.; Wu, J. Polym. Adv. Technol. **2008**, 19, 1597-1607.

III.4

SYNTHESIS OF A NEW HYPERBRANCHED POLYAMINOESTER AND ITS USE AS A REACTIVE MODIFIER IN ANIONIC CURING OF DGEBA THERMOSETS

Mireia Morell, Xavier Fernández-Francos, Xavier Ramis, Àngels Serra

Macromolecular Chemistry and Physics ***2010****, 211, 1879 – 1889*

UNIVERSITAT ROVIRA I VIRGILI
NOUS TERMOESTABLES EPOXÍDICS MODIFICATS AMB ESTRUCTURES DENDRÍTIQUES DE TIPUS HIPERRAMIFICAT I ESTRELLA
Mireia Morell Bel
DL:T. 155-2012

Macromolecular Chemistry and Physics **2010**, 211, 1879 – 1889

SYNTHESIS OF A NEW HYPERBRANCHED POLY(AMINOESTER) AND ITS USE AS A REACTIVE MODIFIER IN ANIONIC CURING OF DGEBA THERMOSETS

Mireia Morell,[1] Xavier Fernández-Francos,[2] Xavier Ramis,[2] Angels Serra[1]

[1] Department of Analytical and Organic Chemistry, University Rovira i Virgili, C/ Marcel·lí Domingo s/n, Tarragona 43007, Spain.
[2] Thermodynamics Laboratory, ETSEIB University Politècnica de Catalunya, C/ Av. Diagonal 647, Barcelona 08028, Spain.

Abstract

The synthesis and characterization of a new hyperbranched poly(aminoester) (PAE) with a flexible structure and hydroxyl groups as terminal chains has been performed. The influence of PAE in the anionic curing of DGEBA with 1-methylimidazole was studied. The curing reaction was investigated by DSC and FTIR. The covalent incorporation of the modifier in the matrix was proved. The addition of PAE to the formulation reduced the contraction on curing. The modified materials were more thermally degradable than neat DGEBA thermosets, which is advantageous from the point of view of the reworkability. Their T_gs were reduced by the flexibility introduced by the aliphatic structure of PAE. SEM microscopy on the fractured surface of cured samples revealed a homogeneous morphology and an effect of PAE as toughness enhancer.

Keywords: anionic polymerization; crosslinking; epoxy; hyperbranched; resins

Introduction

In several applications of epoxy resins, such as coatings or electronic encapsulations, properties such as toughness and low shrinkage are required [1,2]. During curing the epoxy resin usually shrinks which tends to originate loss of adhesion, cracks, voids and wrapping decreasing the protective capacity of the coating against corrosion. From a technological point of view, the reduction of shrinkage can be accomplished by adding inorganic fillers, but it leads to a loss of transparency among other disadvantages. As an alternative, we proposed the copolymerization of epoxy resins with lactones as for example Meldrum acid derivatives, which on reacting produce a decrease in the density of the materials [3]. However, this procedure leads to a reduction of the T_g of the thermosetting materials.

To fulfill the environmental requirements, degradability of the protective coating is also needed to allow the reworkability of the electronic devices. It is known that thermosetting materials cannot be recycled but they can be degraded under controlled conditions to remove them from the substrate, enabling the repairing or recycling of electronic devices assembled with such materials [4]. The improvement in reworkability can be achieved by the introduction of labile ester groups in the network. Aliphatic esters experience thermal degradation by a pyrolitic elimination process in which protons in the *γ*-position moves through a cyclic transition state to carbonylic oxygen to finally produce the scission of the polymeric

chain and the formation of vinyl and carboxylic groups [5]. According to this degradation mechanism, esters of secondary or tertiary alkyl groups are more easily degraded [6,7].

Toughness is also needed to prevent the loss of adhesion and the damage of electronic devices caused by brittle fractures. The impact resistance of glassy polymers may be increased by the addition of small quantities of rubbers. Rubbers promote crazing and shear yielding, which results in local absorption of energy [8]. Hyperbranched polymers (HBPs) can be also considered as a new class of reactive rubber, which can be used as modifiers for epoxy resins [9-11].

The main advantages over conventional toughening agents are: 1) their much lower prepolymer viscosity compared with the linear counterparts because their branched structure prevents chain entanglement and 2) their stronger adhesion with the matrix due to the high density of surface functional groups [12,13]. Furthermore, reactive end groups in the HBP allow its covalent attachment to the matrix. It was shown that a small percentage of such polymers is enough to significantly improve toughness without sacrificing stiffness and glass transition temperature [14] and therefore, their use has attracted great attention in last years in both academic and industrial research [15,16].

In previous papers we demonstrated that the addition of HBP to a curing system reduces the global shrinkage and that the presence of ester groups in the HBP structure increases the thermal degradability of the HBP-modified thermosets, which is valuable for reworkability purposes [17-19]. Thus, HBPs remain as the best candidates to simultaneously improve shrinkage, reworkability and toughness of epoxy thermosets.

The chemical incorporation of hydroxyl ended HBPs to the epoxy matrix has been accomplished by cationic curing by ring opening mechanism in photochemical [20] and thermal [17] conditions, but, until now, the modification of anionic ring-opening cured epoxy materials with hydroxyl terminated HBPs has not been reported. Ring opening mechanism is the most suitable from the point of view of the shrinkage because it does not eliminate small molecules and, for every bond that goes from a Van der Waals to a covalent distance, another bond goes from a covalent to a Van der Waals distance [21]. In previous studies, [22] we have evidenced the participation of hydroxyl groups in the polymerization of oligomeric DGEBA initiated by tertiary amines such as 1-methylimidazole (1MI) or 4-(N,N-dimethylamino)pyridine (DMAP). The presence of hydroxyl groups in the DGEBA oligomers increases the initiation rate and can overcome the effect of termination reactions, leading to higher conversion of epoxide groups.

In the present work, the one-pot polymerization of succinic anhydride (A* type monomer) and triisopropylalcoholamine (TIPA, B_3 monomer) in melt at 120 ºC has been carried out to obtain a novel hyperbranched poly(aminoester) (PAE). This new HBP has tertiary amines and secondary ester groups in the repeating unit and hydroxyl groups as the chain ends. This HBP has been used to modify DGEBA

Macromolecular Chemistry and Physics **2010**, 211, 1879 – 1889

using 1MI as anionic initiator. The crosslinking process has been monitored by Fourier-transform infrared (FT-IR) spectroscopy and DSC and the obtained materials have been characterized by thermal analysis, densitometry measurements and electronic microscopy.

Experimental

Materials

DGEBA (Epikote Resin 827) was provided by Shell Chemicals (epoxide equivalent weight (EEW) = 182.1 g/eq, *n* = 0.082). Triisopropanolamine (TIPA, 95 %, Aldrich), succinic anhydride (SA, 99 %, Fluka) and 1-methylimidazole (1MI, 99 %, Aldrich) were use without further purification.

Synthesis of hyperbranched poly(ester-amine) (PAE) (**Scheme 1**)

The synthesis of PAE was done in the melt as follows. TIPA (5.0 g, 0.026 mol) and SA (2.61 g, 0.026 mol) were introduced into a two necked flask equipped with a thermometer, a gas inlet to fill the flask with nitrogen and magnetic stirring. The reaction mixture was gradually heated in an oil bath to 120 °C and reacted for 2 hours under nitrogen at this temperature. Then, to drive the reaction to higher conversion, vacuum was applied for further 3 hours maintaining a vigorous stirring. After polymerization, the residual unreacted monomers were removed under reduced pressure at 60 ºC overnight. The conversion of the resulting polymer was 88 % (6.50 g).

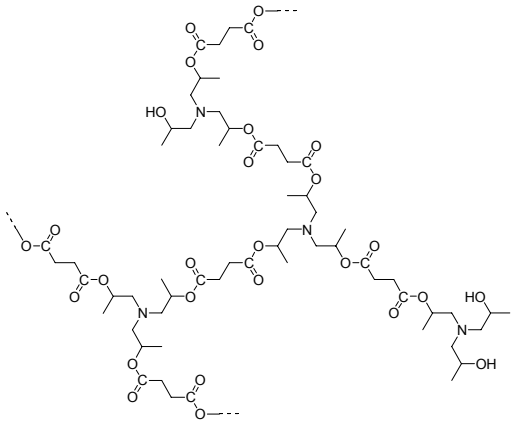

Scheme 1 Idealized chemical structure of the hyperbranched polyaminoester PAE studied

^{1}H NMR (acetone-d_6) δ *ppm*: 4.98 (complex m, C**H**), 3.90-4.64 (broad, O**H**), 3.72-3.90 (complex m, C**H**), 2.32-2.76 (complex m, C$\mathbf{H_2}$), 1.19-1.21 (complex m, C**H**), 1.05-1.15 (complex m, C$\mathbf{H_3}$); ^{13}C NMR (acetone-d_6) δ *ppm*: 16.8, 20.9, 28.7, 61.2, 63.2-66.7 (broad), 68.8, 172.6-174.6 (broad); FTIR (ATR) (cm^{-1}): 3410 (OH,

broad), 1729 (C=O); $\overline{M_w}$ = 3,200 g/mol, $\overline{M_n}$ = 1,200 g/mol and a polydispersity of 2.7; hydroxyl index: 120 mg KOH/g.

Preparation of curing mixtures

The mixtures were prepared by adding the required amount of PAE into the epoxy resin on heating until the HBP was dissolved and the solution became clear. Then, 1 phr (part per hundred parts of mixture) of 1-methylimidazole (1MI) was added and the resulting solution was stirred and cooled down to -10 ºC to prevent polymerization. Mixtures containing 5-10 wt.% (by weight) of PAE were prepared. The compositions of the formulations studied are detailed in **Table 1**.

Table 1 Compositions of the formulations with different weight percentatges of PAE using 5 phr of 1MI as initiator

PAE (wt.%)	$n_{HBP}:n_{epoxy}$ [a]	$eq_{epoxy}:eq_{init}$ [b]	$eq_{epoxy}:eq_{OH}$ [b]	$eq_{init}:eq_{OH}$ [b]
0	0.0000	9.0	24.4	2.7
5	0.0064	8.6	16.2	1.9
10	0.0126	8.1	11.8	1.4

a. Molar ratio (hyperbranched polymer/DGEBA)
b. Equivalent ratio (epoxy/initiator-epoxy/hydroxyl-initiator/hydroxyl).

Characterization techniques

^{1}H and ^{13}C NMR spectra were recorded on a Varian Gemini 400 spectrometer, operated at 400 MHz and 100.16 MHz, respectively. Acetone-d_6 was used as the solvent.

The molecular weight distribution was determined with a Waters gel permeation chromatograph (SEC) equipped with a Waters 510 differential RI detector (RID-6A from Shimadzu). SEC was operated using three Waters SHODEX Columns (K80M, Gel 5 μm MIXED-D, Gel 3 μm MIXED-E) at a nominal flow rate of 1 mL·min^{-1} and a sample concentration of 0.1 % in tetrahydrofuran (THF) as solvent. Monodispersed polystyrene standards were purchased from Polymer Laboratories for instrument calibration.

The amount of hydroxyl groups was determined according to ISO 2554-1974. An acetylating solution was prepared by dissolving 11.8 mL of acetic anhydride in 100 mL of pyridine. About 0.4 – 0.6 g of the polymer sample was dissolved in 5 mL of the acetylating solution. The mixture was stirred for 20 min at 130 ºC. Thereafter, at the same temperature, 8 mL of water was added in order to hydrolyze the excess acetic anhydride. Finally, the solution was titrated with 1 N ethanolic KOH solution to determine the equivalence point. An analogous “blank experiment” was performed without the polymer sample with exactly the same amount of the acetylating mixture. The hydroxyl number (N_{OH}) was calculated from the results of both titrations using the formula:

$$N_{OH} = \frac{(V_0 - V_1) \cdot C \cdot M_{KOH}}{m} + AN \quad (1)$$

where, V_0 and V_1 are the equivalence titration volume of KOH in mL from the blank experiment and from the sample titration, respectively; C is the concentration of KOH in eq/l; M_{KOH} is the molecular weight of KOH in g/mol; m is the mass of polymer sample in grams; and AN is the acid number, which has not been taken into account in this case because it is very low.

Calorimetric analyses were carried out on a Mettler DSC-821e thermal analyzer. Samples of approximately 5 mg in weight were cured in aluminum pans in a nitrogen atmosphere. The calorimeter was calibrated using an indium standard (heat flow calibration) and an indium-lead-zinc standard (temperature calibration). Non-isothermal experiments were performed from 20 to 250 ºC at heating rates of 2, 5, 10, and 15 ºC/min to determine the reaction heat and the kinetic parameters. In non-isothermal curing process the degree of conversion by DSC (α_{DSC}) was calculated as follows:

$$\alpha_{DSC} = \frac{\Delta H_T}{\Delta H_{dyn}} \quad (2)$$

where ΔH_T is the heat released up to a temperature T, obtained by integration of the calorimetric signal up to this temperature, and ΔH_{dyn} is the total reaction heat associated with the complete conversion of all reactive groups.

The glass transition temperatures (T_gs) of the complete cured materials were determined by means of a second scan at 20 ºC/min, as the temperature of the half-way point of the jump in the heat capacity when the material changed from glassy to the rubbery state under N_2 atmosphere and the error is estimated to be approximately ± 1 °C. The T_g of the HBPs were determined by a similar procedure.

The kinetic triplet [pre-exponential factor, activation energy and kinetic model] of the curing process was determined using integral isoconversional non-isothermal kinetic analysis, Kissinger-Akahira-Sunose equation, combined with the Coats-Redfern procedure. Details of the kinetic methodology are given in previous publications [23,24].

An FT-IR spectrophotometer FTIR-680PLUS from JASCO with a resolution of 4 cm^{-1} in the absorbance mode was used to monitor the isothermal curing process at 120 ºC. This device was equipped with an attenuated-total-reflection accessory with thermal control and a diamond crystal (Golden Gate heated single-reflection diamond ATR, Specac-Teknokroma). The disappearance of the absorbance peak at 913 cm^{-1} was used to monitor the epoxy equivalent conversion. The activation of 1MI was followed by the increasing peak at 1580 cm^{-1}. The peak at 1508 cm^{-1} of the phenyl group was chosen as an internal standard. Conversion of the epoxy and the activation of 1MI were determined by the Lambert-Beer law from the normalized changes of absorbance at 913 and 1580 cm^{-1}, respectively.

$$\alpha(t)_{epoxy} = 1 - \left(\frac{\overline{A}^{t}_{913}}{\overline{A}^{0}_{913}}\right),\ \alpha(t)_{1MI,activation} = \left(\frac{\overline{A}^{t}_{1580}}{\overline{A}^{0}_{1580}}\right) \quad (3)$$

where $\bar{A}^{0}$ and $\bar{A}^{t}$ are, respectively, the normalized absorbance of the reactive group before curing and after a reaction time *t*.

Thermomechanical analyses were carried out on a Mettler TMA40 thermomechanical analyzer. The samples were supported by two small circular ceramic plates and silanized glass fibers, which were impregnated with the samples. The conversion at the gel point was evaluated by means of non-isothermal experiments performed between 40 and 225 ºC at a heating rate of 5 ºC/min applying a periodic force that change (cycle time = 12s) from 0.0025 to 0.01 N. The gel point was taken in TMA as the temperature at which a sudden decrease in the amplitude of the oscillations was observed. The gel conversion, α_{gel}, was determined as the DSC conversion at the temperature gelled in TMA in a non-isothermal experiment. The overall shrinkage was calculated from the densities of the materials before and after curing, which were determined using a Micromeritics AccuPyc 1330 gas pycnometer thermostatted at 30 ºC.

Thermogravimetric analysis (TGA) was carried out in a Mettler TGA/SDTA 851e thermobalance. Cured samples with an approximate mass of 8 mg were degraded between 30 and 800ºC at a heating rate of 10 ºC/min in N_2 (100 cm^3/min measured in normal conditions).

Dynamic-mechanical/thermal analysis (DMTA) was carried out with a TA Instruments DMTA 2980 analyzer. The samples were cured isothermally in a mould at 120 ºC for 1.5 h and then post-cured for 1 h at 150 ºC. Single cantilever bending at 1 Hz was performed at 3 ºC/min, from -100 ºC to 250 ºC on prismatic rectangular samples (20 x 5 x 1.5 mm^3). Two dynamic scans were registered in order to make sure that a complete cure was achieved. The fracture area of the specimens was observed with scanning electron microscope (SEM). The samples were metalized with gold and observed with a Jeol JSM 6400 with a 3.5 nm resolution.

Macromolecular Chemistry and Physics **2010**, 211, 1879 – 1889

Results and discussion

Synthesis and characterization of PAE

The use of HBPs as reactive modifiers to improve epoxy thermosets has been mainly centered in commercial Boltorn® type polyesters with hydroxyl or epoxy groups as chain ends [9,25-28]. Tailoring of HBPs structure and their use as polymeric modifiers in epoxy formulations can improve the properties of the resulting thermosets. In this work, we have synthesized a new flexible hyperbranched PAE with hydroxyl groups as chain ends and secondary alkyl ester groups in the repetitive unit. Hydroxyl groups can react with the epoxy matrix, whereas the presence of ester groups can improve the reworkability of the HBP-modified thermosets.

Several HBPs of the family of hyperbranched PAEs have been studied in detail. Although the most classical way to access HBPs is the condensation reaction of AB_n monomers, the synthetic strategies follow predominantly a pseudo-one step process which involves the in situ formation of AB_2 monomer due to the selective reactivity of functionalities of the starting monomers [29-31]. This approach has some advantages because the desired AB_n monomers sometimes involve a great synthetic effort. This attempt is one of the ways to improve the A_2 + B_3 approach since it is well known that these systems can gel upon reaction [32].

One of the important aspects to avoid crosslinking and control the monomer conversion to high extent in the A_2 + B_3 approach is the selection of the monomer ratio of reactants [33,34]. Komber *et al.* [35], described the features of an A_2 + B_3 hyperbranched aromatic polyester synthesis by melt polycondensation. In that work, it was pointed out that by setting the molar ratio to 1:1, it is possible to reach 80 % of monomer conversion and a degree of branching of nearly 50 % without gel formation. Following these results, we prepared a hyperbranched PAE from TIPA (B_3) and SA (A_2 or A*) with a $\overline{M_W}$ of 3,000 g/mol, a polydispersity of 2.7, a hydroxyl index of 120 mg KOH/g and a T_g = -15 ºC. The idealized chemical structure of this HBP is shown in **Scheme 1**. The structure of the polymer was characterized by ^{1}H and ^{13}C NMR (see **Figure 1** for spectra and assignments).

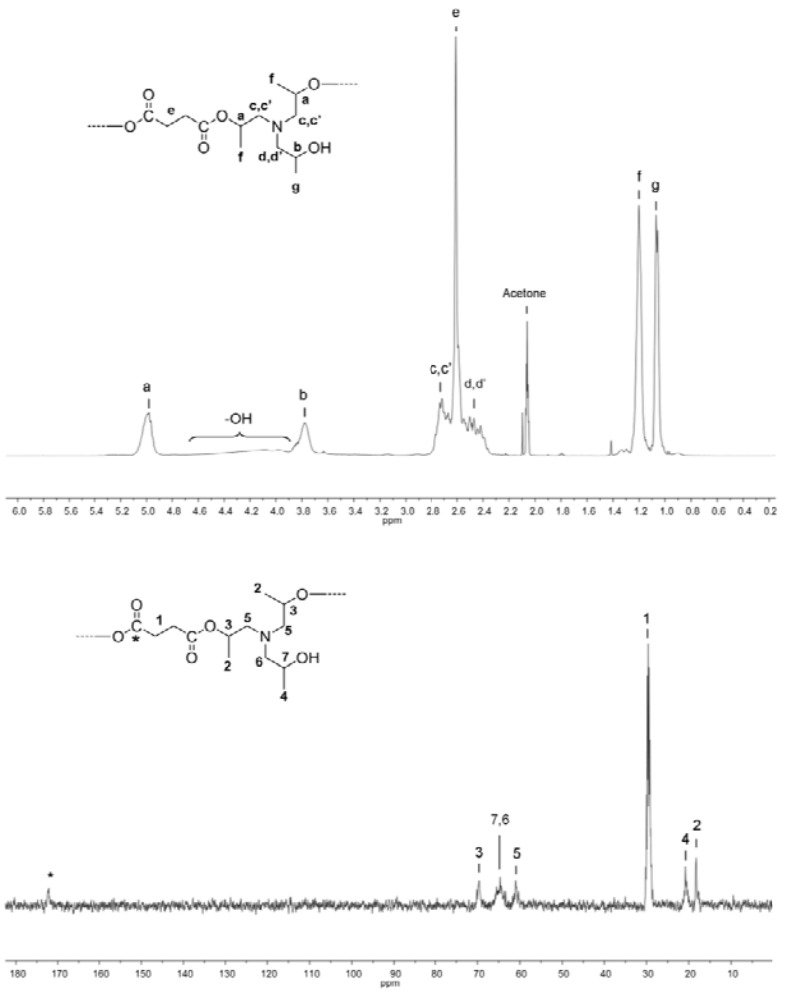

Figure 1 ^{1}H and ^{13}C NMR spectra of hyperbranched PAE obtained in acetone-d_6

Studies on the curing of DGEBA/PAE/1MI formulations

In the preparation of epoxy thermosets the selection of the curing agent is of a great importance, but especially when a HBP modifier is added to the formulation. Some authors used primary amines as curing agents, which did not chemically incorporate hydroxyl ended HBPs to the epoxy matrix and thus microphase separation occurred [26,36]. Other authors selected anhydrides as curing agents, which allowed the covalent incorporation of hydroxylic HBP to the epoxy matrix [18,25] obtaining homogeneous materials. In both cases, toughness enhancement was observed.

Among the polymerization mechanisms, ring opening is the most advantageous in the reduction of curing shrinkage. Cationic initiators have been

Macromolecular Chemistry and Physics **2010**, 211, 1879 – 1889

used to cure mixtures of epoxy resins and hydroxyl ended HBPs in both thermal and photochemical conditions [17,20]. In these systems, homogeneous materials have been usually obtained by the chemical incorporation of hydroxyl groups by the monomer activated mechanism [37]. However, in our case, the presence of amines in the PAE structure deactivates the ring-opening polymerization process when it is initiated by Lewis acids such as lanthanide triflates, which does not happen when these basic groups are not present [17].

The anionic curing of epoxy oligomers using HBPs as polymeric modifiers has not yet been described. Anionic curing of epoxy resins leads to the formation of alkoxides as propagating species by nucleophilic attack of the anionic initiator to the epoxy ring [38]. The role of hydroxyl groups in the curing of epoxy resins initiated by tertiary amines was reported in detail in a previous publication [22]. Hydroxyl groups can facilitate the attack of the tertiary amine on the oxirane group, enhancing the initiation rate. An acid-base equilibrium may also be established between hydroxyl groups of the HBP and the alkoxide formed by attack of the tertiary amine to epoxide, resulting in the formation of alkoxides as terminal groups in the HBP. In this way, hydroxyl groups from the HBP can actively participate as chain transfer agents, thus promoting covalent linkage of the HBP structure to the epoxy matrix. The reaction of hydroxyl groups with epoxides seems to greatly influence the reduction of the shrinkage on curing [17-19] and therefore their participation in the curing process is also important for that purpose.

First, we tested the self curing of PAE/DGEBA mixtures and a very small exotherm centered at 150 ºC could be observed in a DSC scan, which allowed us to conclude that amine groups of PAE were not nucleophilic enough to initiate an appreciable crosslinking. For this reason, we investigated the use of 1MI as initiator. A minimum amount of 5 phr of 1MI was necessary to reach the complete curing of these mixtures. **Figure 2** shows the calorimetric curves obtained for the three formulations.

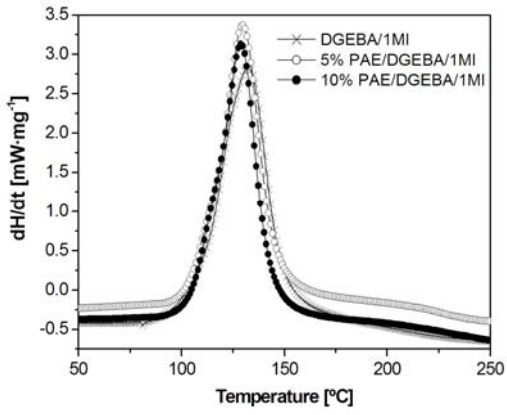

Figure 2 DSC scanning curves against temperature of the curing of DGEBA and DGEBA containing 5 and 10 wt.% of PAE at a heating rate of 10ºC/min

It can be observed that there is no much influence on the crosslinking exotherm on changing the composition of the formulation. Therefore, the overall curing process is essentially the same for all formulations. In **Table 2** we can see that the enthalpy released in J/g decreases when increasing the proportion of PAE in the formulation. However, the enthalpy per equivalent of epoxide does not change significantly and is very similar in all cases to those previously reported [39]. Thus, it can be deduced that complete curing is achieved. The flexible structure of PAE leads to a slight decrease of the T_g, but even when a 10 wt.% of HBP was in the material this value is higher than 120 ºC. This result indicates that the network structure retains a high degree of crosslinking when PAE is added.

Table 2 Calorimetric data, glass transition temperature estimated by Fox equation and kinetic parameters (apparent activation energy, pre-exponential factor and rate constant at a conversion of 0.5) of the systems studied

PAE (wt.%)	Δh (J/g)	Δh[a] (kJ/ee)	T_g (ºC)	T_g[b] (ºC)	T_{max}[c] (ºC)	E_a[d] (kJ/mol)	ln A[e] (s^{-1})	$k_{120ºC}$ x 10^3[f] (s^{-1})
0	638	116.1	146.0	146.0	132	60.1	12.89	4.07
5	602	115.3	133.0	133.3	130	62.9	13.87	5.15
10	552	111.6	122.0	121.4	129	63.0	13.96	5.47

a. Enthalpy per equivalent of epoxy group.
b. Glass transition temperature of the cured materials predicted by using the Fox equation: $1/T_g = w/T_{g,PAE} + (1\text{-}w)/T_{g,DGEBA}$ where $T_{g,PAE}$ is the calorimetric glass transition temperature of PAE (-15 ºC), $T_{g,DGEBA}$ is the calorimetric glass transition temperature of neat DGEBA (146 ºC) and w is the weight fraction of PAE in the formulations.
c. Temperature of the maximum of the curing exotherm.
d. Value of activation energies evaluated by isoconversional non-isothermal procedure.
e. Values of pre-exponential factor A_2 kinetic model with $g(\alpha) = [-\ln(1-\alpha)]^{1/2}$.
f. Values of rate constant at 120 ºC calculated using the Arrhenius equation.

To know the influence of PAE in the curing process, the kinetics of the mixtures was studied by means of DSC. **Figure 3** plots the evolution of the conversion degrees against temperature. As it can be seen, the presence of PAE slightly reduces the reactivity of the system at low conversions, but above a value of 0.2 the reactivity is enhanced by the presence of this modifier.

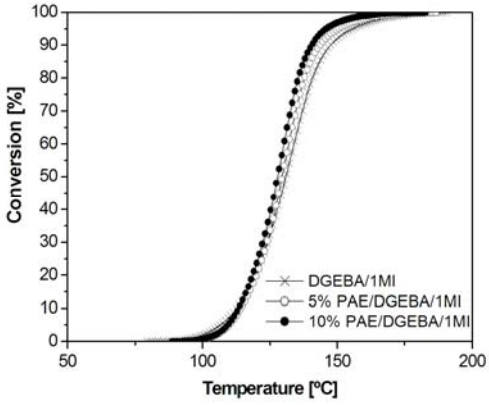

Figure 3 Conversion degree against temperature of the curing of DGEBA and DGEBA containing 5 and 10 wt.% of PAE at a heating rate of 10 ºC/min

Macromolecular Chemistry and Physics **2010**, 211, 1879 – 1889

A comparable behavior can be observed by monitoring the band at 915 cm^{-1}, corresponding to the epoxy groups, during the curing process at 120 ºC by ATR-FTIR spectroscopy, as represented in **Figure 4**.

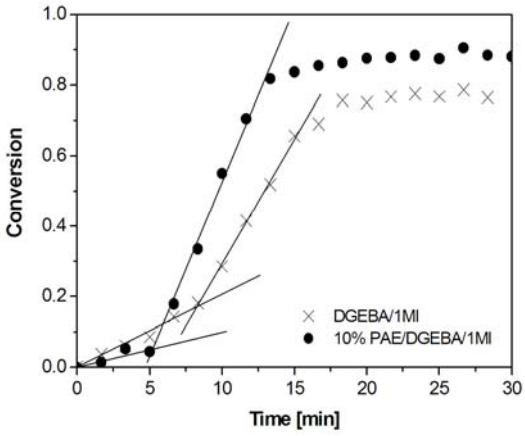

Figure 4 Conversion of epoxy groups by FT-IR (ATR) of formulation DGEBA with 5 phr of 1MI and the same formulation containing 10 wt.% of PAE during isothermal polymerization at 120 ºC

It can be seen that, in the first stages of the reaction, there is a slight delay in the conversion of epoxide groups observed in the PAE formulation, whereas at degrees of conversion higher than 0.5 a contrary effect appears. These results differ from the ones reported in a previous publication, in which the addition of hydroxyl groups to the reactive mixture not only increased the final epoxy conversion, but also accelerated the initial curing reaction [22]. According to Rozenberg [40], the initiation of epoxy polymerization by tertiary amines requires the presence of proton donors such as hydroxyl groups, which activate the epoxy by hydrogen bonding. Thus, it seems that the presence of PAE should activate the curing from the very beginning, which is not observed in our case. The possibility of intramolecular hydrogen bonding in the PAE structure can explain this behavior, since tertiary amines of the PAE structure can effectively act as proton acceptors. Thus, hydroxyls are not free to activate the epoxy groups in front of nucleophilic attack. Moreover, hydroxyl groups in the HBP can partially inactivate by hydrogen bonding 1MI molecules to produce the nucleophilic attack to the epoxide ring.

If we observe the shape of the curves in **Figure 4**, it seems that the curing takes place in two different stages with two very different reaction rates. It can be observed that the first step of the curing of neat DGEBA, which can be associated to the ring-opening of epoxide groups by nucleophilic attack of the 1MI, reaches up to ca 0.1, which agrees well with the initiator to epoxy equivalent ratio, as previously reported [22]. Conversion at the end of this first step for the PAE formulations is lower than that of neat DGEBA and it ends earlier in time. Therefore, it seems that the initiation step takes shorter with the addition of HBP but consumes a lower amount of epoxy groups, which makes us hypothesize the concurrence of the inactivation of 1MI and that an alternative initiation process is taking place, such as

the acid-base equilibrium between hydroxyl groups and alkoxides described above. This second process corresponds to the propagation step, in which alkoxides act as active chain ends, along with regeneration of the initiator and reinitiation. The addition of hydroxyl groups of PAE slightly increases the reaction rate during the propagation step. This can be explained by the occurrence of regeneration reactions, which release free tertiary amine that can reinitiate the curing process [22,41]. A ratio between active initiator and free tertiary amine throughout the curing process may be established. Because initiation by either mechanism is favored by the presence of hydroxyl groups, the ratio of active species with respect to free tertiary amine may be higher in the presence of hydroxyl groups, thus explaining the higher apparent propagation rate in the presence of PAE. **Figure 5** shows the evolution of the band at 1580 cm^{-1}, corresponding to the imidazolium cation in the curing of DGEBA and in a DGEBA/PAE formulation.

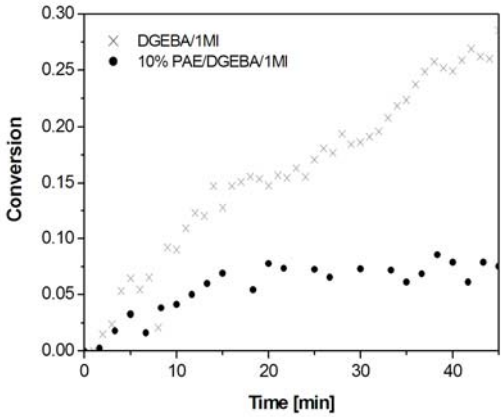

Figure 5 Evolution of the 1580 cm^{-1} imidazolium band during curing at 120 ºC for DGEBA and DGEBA formulations with 10 wt.% of PAE, both with 5 phr of 1MI

As we can see, the presence of PAE in the mixture leads to a lower proportion of imidazolium cation, which can be attributed to the higher regeneration ability or to the inactivation of the 1MI by means of hydroxyl bonding. In fact, the presence of PAE in the formulation requires a higher amount of 1MI (5 phr in front of 2 phr, used in a previous study [22]). The regeneration of 1MI leads to the formation of an enol ether band at 1678 cm^{-1}, as previously reported. This band was observed by FT-IR on curing, confirming the existence of this process.

A higher conversion of epoxide groups is reached when PAE is included in the formulation (see **Figure 4**), which might be caused by a delayed vitrification due to the formation of a less cross-linked network. The presence of the flexible structure of PAE in the formulation affects the T_g and consequently the vitrification process, allowing it to reach a higher epoxy conversion in the mixtures containing PAE when cured at 120 ºC.

To calculate the kinetic parameters of the curing process, we applied an isoconversional integral method at a conversion of 0.5. We calculated the apparent

Macromolecular Chemistry and Physics **2010**, 211, 1879 – 1889

activation energy and the pre-exponential factor for each formulation of the kinetic model selected, in this case A_2, following a previously described procedure [23]. From these values and using the Arrhenius equation the kinetic constant at 120 ºC was calculated. The results are collected in **Table 2**. At this temperature, the rate constant increases on increasing the proportion of PAE in the formulation according to the conversion-temperature curves in **Figures 3** and **4**.

Study of the gelation process and shrinkage of the formulations

The apparition of internal stresses in thermosets is mainly due to the shrinkage produced when the network structure loses its mobility. For this reason, both the advancement of the gelation up to higher conversions and the reduction of the global shrinkage are desirable to reduce them.

Experimentally, the gelation point can be determined by TMA, observing the point at which the material reaches sufficient mechanical stability (gelation) as it was previously described [41]. This procedure allowed us to determine the conversion at the gelation values collected in **Table 3**.

Table 3 Gel conversion, densities and shrinkage of the systems studied

PAE (wt.%)	α_{gel}[a] (%)	ρ_{mon} (g/cm^3)	ρ_{pol} (g/cm^3)	*Shrinkage*[b] (%)
0	30	1.157	1.176	1.62
5	26	1.167	1.180	1.10
10	27	1.167	1.173	0.51

a. Determined as the conversion reached by non-isothermal TMA and DSC tests at 5 ºC/min.
b. Shrinkage determined as $[(\rho_{polymer} - \rho_{monomer})/\rho_{polymer}]$.

As can be seen, from this point of view, there is no advantage in the addition of PAE to the formulation, since the values are similar and even slightly decrease. This result is similar to previously obtained in other DGEBA/HBP formulations [18,19] in which the presence of HBP did not influence the conversion at the gelation point.

From monomer and polymer densities we calculated the global shrinkage on curing, which are collected in the same table. As can be seen, the global shrinkage is steadily reduced on increasing the proportion of PAE in the formulation. This result fits well with our previous observation that the addition of hydroxylic HBPs to the epoxy matrix reduces the shrinkage, when the curing agent allows their covalent incorporation in the network structure. This can be explained if we take two facts in consideration: a) the introduction of a HBP in the formulation with a molecular weight higher than the epoxy resin reduces the amount of covalent linkages to be formed; b) the reaction of hydroxyl groups with epoxides reduce the intramolecular hydrogen bonding in the HBP, which leads to an expansion of the HBP structure. The expansion of hydroxyl ended HBP on reacting was reported previously by Lederer *et al.* [42]. The reduction of the shrinkage by adding PAE to the formulation accounts for a chemical incorporation of PAE in the network

structure. The bond formation is caused by an acid-base proton interchange, which leads to chain transfer processes. PAE incorporation in the network structure was also evidenced by the low soluble content (in chloroform) of the cured materials.

Study of the thermal degradability

In order to prepare reworkable thermosets, the introduction of ester groups has been extensively used as a strategy [4,6]. In the present work, we have designed and synthesized a new HBP having ester of secondary alkyl groups to be used as a modifier in epoxy thermosets. The covalent linkage of this modifier to the epoxy network introduces labile groups in the thermosetting structure that can be broken thermally. In this way, the thermoset applied as a coating or encapsulant can be eliminated by brushing or by the use of solvents.

To prove that our modification procedure leads to reworkable thermosets, our materials were analyzed by TGA. **Figure 6** shows the TGA curves for the cured materials.

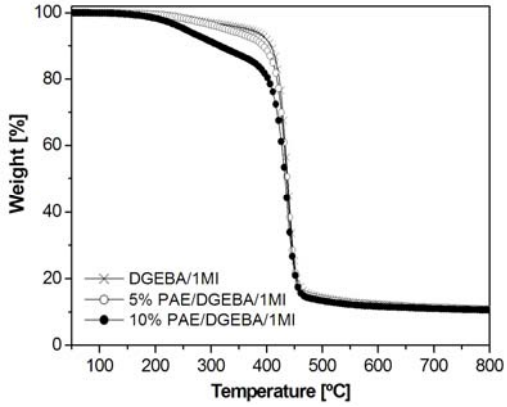

Figure 6 TG curves at 10 ºC/min in N_2 atmosphere of thermosetting materials obtained from DGEBA/1MI containing different proportions of PAE

In **Table 4**, the thermogravimetric parameters are collected. As can be seen in the **Figure 6**, the addition of PAE to the formulation leads to a big variation in the onset temperature, but it does not affect the main degradation process or the char remaining after degradation.

The values of the onset temperatures decrease approximately 100 ºC on adding a 10 wt.% of PAE to the formulation. This onset temperature is the same as that obtained in the modification of DGEBA with commercial S1200 Hybrane®, which also has secondary alkyl ester groups in the structure, but in that case we used methyltetrahydrophtalic anhydride as a curing agent, which introduces a high proportion of ester groups on reacting [18]. In the present work, we used a tertiary amine as initiator and therefore the network is mainly composed by polyether structures with a higher crosslinking density. The different chemical structure of the

Macromolecular Chemistry and Physics **2010**, 211, 1879 – 1889

network is reflected in the temperature of the maximum rate of degradation, which is much higher in the anionic cured materials than in the previous anhydride cured materials, because of the higher stability of ether bonds.

Table 4 TGA and DMTA data of thermosetting materials obtained from DGEBA/1MI thermosets containing different proportions of PAE

PAE (wt.%)	TGA		DMTA	
	T_{onset} [a] (ºC)	T_{max} [b] (ºC)	E' [c] (MPa)	$T_{\tan\delta}$ [d] (ºC)
0	358	439	58.9	175
5	329	441	50.1	160
10	254	439	40.0	147

a. Temperature of the onset decomposition on the TGA data at 10 ºC/min calculated for a 2 % of weight loss.
b. Temperature of the maximum decomposition rate based on the TGA data at 10 ºC/min.
c. Relaxed modulus determined at the $T_{\tan\delta}$ + 40 ºC.
d. Temperature of maximum of tan δ at 1 Hz.

Study of the thermomechanical properties

Figure 7 shows the dynamic mechanical spectra for the obtained thermosets and **Table 4** the values of relaxed modulus and tan δ measured from them.

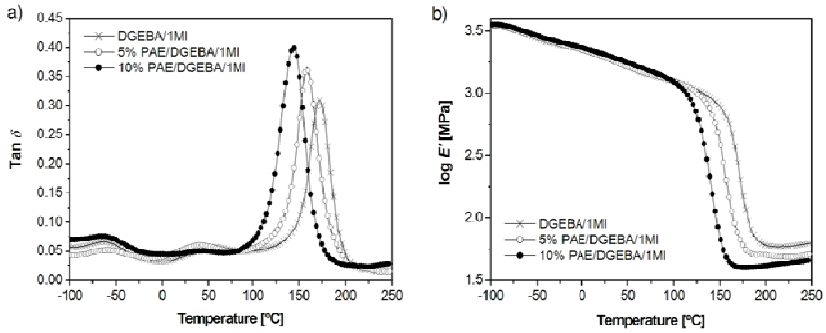

Figure 7 a) Tan δ against temperature at 1 Hz for the materials obtained; **b**) Logarithm of the storage modulus (E') against temperature at 1 Hz of the materials obtained

The tan δ versus temperature curve (**a**) displays a well-defined relaxation peak, attributed to the glass transition that slightly shifts to lower temperatures on increasing the proportion of PAE in the material. This behavior, in addition to the low soluble material content (in chloroform) in cured systems, indicates the incorporation of PAE structure in the epoxy matrix. There are also other weak transitions at lower temperatures that also appear in neat DGEBA and their area is not proportional to the amount of PAE in the material, therefore, they cannot be assigned to the presence of PAE rich phases. Both facts reflect the chemical incorporation of PAE into the material to produce homogeneous materials due to the full miscibility of PAE into the epoxy network.

Tan *δ* is related to properties such as damping of free vibrations and it has been described that there is a relationship between the area under tan *δ* curve and the damping characteristics. Also the height and the width at half height can be associated to this property [43,44]. The value of the area indicates the ability to convert mechanical energy into heat through molecular motion. Therefore, the materials with a higher value of area have high damping properties in those selected temperatures and frequency range. As can be seen, the area increases with the proportion of PAE, which indicates an increase in the damping ability. This behavior was also observed by Cicala *et al.* [44], in Boltorn® containing materials and damping properties were much better that in materials modified with linear polymers. They explain this improvement in terms of the structure of the HBP, as a globular shape with many free flexible branches.

In **Figure 7** (**b**) the evolution of the storage modulus with the temperature for the materials prepared is plotted. The curves clearly show that elastic modulus decreases in the rubbery region on increasing the proportion of PAE, due to the flexibility introduced by its structure and also to a lower crosslinking density.

Morphology analysis by SEM

The toughness behavior of PAE modified thermosets can be explained in terms of the morphology observed by SEM. The cryogenic fracture surfaces were investigated by this technique and a micrograph for each material is shown in **Figure 8**.

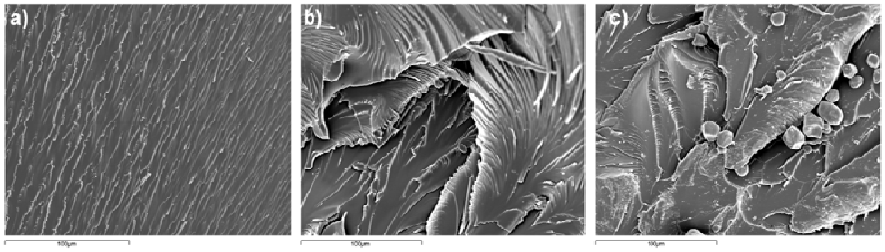

Figure 8 SEM micrographs for fracture surfaces of the following materials cured for 1.5 h at 120 ºC and post-cured for 1 h at 150 ºC: **a**) DGEBA/1MI; **b**) 5 wt.% PAE/DGEBA/1MI; **c**) 10 wt.% PAE/DGEBA/1MI

First of all, it can be appreciated that all the micrographs present a homogeneous appearance without any phase separation, although PAE is a hydrophilic polymer and the epoxy matrix is hydrophobic. This result is consistent with the fact that experimental T_gs (**Table 2**) fit quite well with T_gs calculated by the Fox equation [45]. The smooth glassy surface of neat epoxy thermoset (**Figure 8** (**a**)) is a substantial evidence of its brittle failure, since the regularly oriented cracks are developed freely. In contrast, the rougher fracture surface of materials with a 5 or 10 wt.% of PAE in **Figure 8** (**b**) seems to suggest a significant increase in matrix yielding and a subsequent toughness enhancement, the improvement being noticeable with just 5 wt.% of PAE.

Macromolecular Chemistry and Physics **2010**, 211, 1879 – 1889

Conclusions

Following an A_2 + B_3 approach, a new hydroxyl ended hyperbranched polyaminoester was obtained from triisopropanolamine and succinic anhydride. The polymer was characterized by standard procedures.

The addition of a hydroxyl ended PAE modifier to DGEBA allowed its covalent incorporation when 1-methylimidazole was used as an anionic initiator, through an acid-base equilibrium between the alkoxide groups formed in the opening of epoxides and hydroxyl groups of the HBP and its participation in the initiation step. In this way, completely homogeneous materials were obtained due to complete miscibility of PAE into DGEBA.

The addition of PAE to the formulation retarded the conversion of epoxy groups at the beginning of the curing process, but later on the curing was accelerated.

The global shrinkage on curing was notably reduced on adding PAE to the formulation.

The thermal reworkability of the thermosets was improved on adding a higher proportion of PAE by the presence of secondary alkyl esters in the structure that can be broken by *β*-elimination processes.

The tan *δ* temperatures were reduced on increasing the proportion of PAE in the material because of the compatibility of PAE in the epoxy matrix. However, the area under the curves was increased, which accounts for an improved damping ability. The addition of PAE to the formulation increased the flexibility of the material and seems to improve the toughness of the thermosets obtained.

Acknowledgements

The authors would like to thank MICINN (Ministerio de Ciencia e Innovación) and FEDER (Fondo Europeo de Desarrollo Regional) (MAT2008-06284-C03-01 and MAT2008-06284-C03-02) and the Comissionat per a Universitat i Recerca del DIUE de la Generalitat de Catalunya (2009-SGR-1512) for their financial support. M.M. acknowledges the grant FI-DGR 2009 from the Catalonian Government.

References

[1] May CA, editor. *Epoxy resins. Chemistry and technology.* Marcel Dekker, New York, **1988**.
[2] Petrie, E.M. *Epoxy adhesive formulations.* McGraw-Hill, New York, **2006**.
[3] González, L.; Ramis, X.; Salla, J.M.; Serra, A.; Mantecón, A. Eur. Polym. J. **2008**, 44, 1537-1547.
[4] Chen, J.S.; Ober, C.K.; Poliks, M.D. Polymer **2002**, 43, 131-139.
[5] March, J. *Advanced Organic Chemistry: Reactions, Mechanism, and Structure.* 2on ed, McGraw-Hill, Tokyo, **1977**, p. 917.
[6] Wang, L.; Li, H.; Wong, C.P. J. Polym. Sci., Part A: Polym. Chem. **2000**, 38, 3771-3782.
[7] Arasa, M.; Ramis, X.; Salla, J.M.; Mantecón, A.; Serra, A. Polym. Degrad. Stab. **2007**, 92, 2214-2222.

[8] Sperling, L.H. *Introduction to Physical Polymer Science.* 4th ed, Wiley Interscience, Hoboken, New Jersey, **2006**, p. 573.
[9] Boogh, L.; Pettersson, B.; Månson, J.A.E. Polymer **1999**, 40, 2249-2261.
[10] Ratna, D.; Varley, R.; Simon, G.P. J. Appl. Polym. Sci. **2003**, 89, 2339-2345.
[11] Schroder, N.L.; Konczol, W.; Doll, M.R. J. Appl. Polym. Sci. **1998**, 70, 785-796.
[12] Voit, B., Bruchmann, B. *Hyperbranched Polymers: Synthesis, Properties and Applications.* Wiley & Sons, New York, **2007**, chapter 19.
[13] Zhang, D.; Jia, D. J. Appl. Polym. Sci. **2006**, 101, 2504-2511.
[14] Ratna, D.; Varley, R.; Singh, R.J.; Simon, G.P. J. Mater. Sci. **2003**, 38, 147-154.
[15] Mulkern, T.J. Polymer **2000**, 41, 3193-3203.
[16] Basheer, R.A.; Wokman, D.B.; Chaudhuri, A.K.; Bouguettaya, M. USA Patent US **2006**/0252892 A1.
[17] Fernández-Francos, X.; Salla, J.M.; Cadenato, A.; Morancho, J.M.; Serra, A.; Mantecón, A.; Ramis, X. J. Appl. Polym. Sci. **2009**, 111, 2822-2829.
[18] Morell, M.; Ramis, X.; Ferrando, F.; Yu, Y.; Serra, A. Polymer **2009**, 50, 5374-5383.
[19] Morell, M.; Erber, M.; Ramis, X.; Ferrando, F.; Voit, B.; Serra, A. Eur. Polym. J. **2010**, 46, 1498-1509.
[20] Sangermano, M.; Amerio, E.; Di Gianni, A.; Priola, A.; Pospiech, D.; Voit, B. Macromol. Symp. **2007**, 254, 9-15.
[21] Sadhir, R.K.; Luck, M.R. editors. *Expanding Monomers: Synthesis, Characterization and Applications.* CRC Press: Boca Raton, FL, **1992**.
[22] Fernández-Francos, X.; Cook, W.D.; Serra, A.; Ramis, X.; Liang, G.G.; Salla, J.M. Polymer **2010**, 51, 26-34.
[23] Ramis, X.; Salla, J.M.; Mas, C.; Mantecón, A.; Serra, A. J. Appl. Polym. Sci. **2004**, 92, 381-393.
[24] Ramis, X.; Salla, J.M.; Cadenato, A.; Morancho, J.M. J. Thermal. Anal. Calorim. **2003**, 72, 707-718.
[25] Yang, J.P.; Chen, Z.K.; Yang, G.; Fu, A.Y.; Ye, L. Polymer **2008**, 49, 3168-3175.
[26] Cicala, G.; Recca, A.; Restuccia, C. Polym. Eng. Sci. **2005**, 45, 225-237.
[27] Varley, R.J.; Tian, W. Polym. Int. **2004**, 53, 69-77.
[28] Cicala, G.; Recca, G. J. Appl. Polym. Sci. **2010**, 115, 1395-1406.
[29] Zhang, H.; Zheng, Y.; Yu, P.; Mo, S.; Wang, R. Polymer **2009**, 50, 2953-2957.
[30] Gao, C.; Tang, W.; Yan, D. J. Polym. Sci., Part A: Polym. Chem. **2002**, 40, 2340-2349.
[31] Lim, Y.B.; Kim, S.M.; Lee, Y.; Lee, W.K.; Yang, T.G.; Lee, M.J.; Suh, H.; Park, J.S. J. Am. Chem. Soc. **2001**, 123, 2460-2461.
[32] Flory, P.J. J. Am. Chem. Soc. **1941**, 63, 3083-3090.
[33] Emrick, T.; Chang, H.T.; Fréchet, J.M.J. Macromolecules **1999**, 32, 6380-6382.
[34] Voit, B.; Lederer, A. Chem. Rev. **2009**, 109, 5924-5973.
[35] Reisch, A.; Komber, H.; Voit, B. Macromolecules **2007**, 40, 6846-6858.
[36] Xu, G.; Shi, W.; Gong, M.; Yu, F.; Feng, J. Polym. Adv. Technol. **2004**, 15, 639-644.
[37] Kubisa, P.; Penczek, S. Prog. Polym. Sci. **1999**, 24, 1409-1437.
[38] Dell'Erba, J.; Williams, R.J.J. Polym. Eng. Sci. **2006**, 46, 351-359.
[39] Brandrup, J., Immergut, E.H. editors. *Polymer Handbook.* Wiley, New York, **1975**.
[40] Rozenberg, B.A. Adv. Polym. Sci. **1986**, 75, 113-165.
[41] González, S.; Fernández-Francos, X.; Salla, J.M.; Serra, A.; Mantecón, A.; Ramis X. J. Appl. Polym. Sci. **2007**, 104, 3406-3416.
[42] Lederer, A.; Elrehim, M.A.; Schallausky, F.; Voigt, D.; Voit, B. e-Polymers, **2006**, 039, 1-14.
[43] Chern, Y.C.; Tseng, S.M.; Hsieh, K.H. J. Appl. Polym. Sci. **1999**, 74, 328-335.
[44] Cicala, G., Recca, A. Polym. Eng. Sci. **2008**, 48, 2382-2388.
[45] Mezzenga, R.; Månson, J.A.E. J. Mater. Sci. **2001**, 36, 4883-4891.

CAPÍTOL IV

Síntesi de polímers estrella mitjançant ROP i el seu ús com a modificants del DGEBA

UNIVERSITAT ROVIRA I VIRGILI
NOUS TERMOESTABLES EPOXÍDICS MODIFICATS AMB ESTRUCTURES DENDRÍTIQUES DE TIPUS HIPERRAMIFICAT I ESTRELLA
Mireia Morell Bel
DL:T. 155-2012

IV.1 INTRODUCCIÓ

Com s'ha comentat al capítol I (apartat **I.1.5**) els polímers estrella poden ser obtinguts tan per la via del *core-first* com per la via de *l'arm-first*. Actualment la via del *core-firs*t ha resultat ser una de les àrees d'especial interès ja que permet obtenir estructures més ben definides que la via *arm-first*. La majoria de polimeritzacions, radicalàries controlades, per obertura d'anell, aniònica o catiònica, es poden aplicar emprant un HBP com a macroiniciador. Entre els nuclis hiperramificats més utilitzats en l'obtenció de polímers estrella destaquen els polièsters [1], els polièters (per exemple: el poliglicidol) [2] o la polietilenimina [3].

En el present capítol, es descriu l'obtenció de polímers estrella amb braços de poli(*ε*-caprolactona) mitjançat la via *core-first,* emprant dos nuclis hiperramificats diferents: el poliglicidol hiperramificat, sintetitzat per obertura d'anell del glicidol (monòmer de tipus AB_2) i el poli(*p*-clorometilestirè) hiperramificat, obtingut per autopolicondensació vinílica del *p*-clorometilestirè (monòmer del tipus AB*).

IV.1.1 Poli(glicidol) hiperramificat obtingut per polimerització per obertura d'anell aniònica (ROMBP)

Els monòmers AB_2 contenint grups oxirà i hidroxil a la seva estructura poden ser polimeritzats per obertura d'anell ramificada (ROMBP, *Ring-Opening Multibranching Polymerization*) tan per via catiònica com aniònica.

Per via catiònica s'empren iniciadors catiònics com àcids de Lewis, per exemple l'àcid trifluorometansulfònic (TfOH) o bé el trifluorur de bor eterat ($BF_3{\cdot}OEt_2$). Dworak *i col.* i Penczek *i col.,* [4] van ser els primers en estudiar la coexistència entre el mecanisme de terminació de cadena activa (ACE) i de monòmer activat (AM) en la polimerització del glicidol. Van poder concloure que certs iniciadors afavoreixen el mecanisme AM que és l'únic responsable de la ramificació del polímer ja que el mecanisme ACE només permet el creixement

[1] a) Xia, W.; Jiang, G.; Chen, W. *Synthesis and drug-release properties of hyperbranched polyesters grafted with biocompatible poly(ε-caprolactone)* J. Appl. Polym. Sci. **2008**, 109, 2089-2094. b) Xia, C.; Ding, X.; Sun, Y.; Liu, H.; Li, Y. *Hyperbranched-upon-dendritic macromolecules as unimolecular hosts for controlled release* J. Polym. Sci. Part A: Polym. Chem. **2010**, 48, 4013-4019.
[2] Zhang, X.; Cheng, J.; Wang, Q.; Zhong, Z.; Zhuo, R. *Miktoarm copolymers bearing one poly(ethylene glycol) chain and several poly(ε-caprolactone) chains on a hyperbranched polyglycerol core* Macromolecules **2010**, 43, 6671-6677.
[3] Adeli, M.; Haag, R. *Multiarm star nanocarriers containing a poly(ethylene imine) core and polylactide arms* J. Polym. Sci. Part A: Polym. Chem. **2006**, 44, 5740-5749.
[4] a) Tokar, R.; Kubisa, P.; Penczek, S.; Dworak, A. *Cationic polymerization of glycidol: coexistence of the activated monomer and active chain end mechanism* Macromolecules **1994**, 27, 320. b) Dworak, A.; Walach, W.; Trzebicka, B. Cationic polymerization of glycidol. *Polymer structure and polymerization mechanism* Macromol. Chem. Phys. **1995**, 196, 1963-1970.

lineal. Altres autors [5], van poder concloure que el mecanisme AM es donava principalment a conversions elevades mentre que a conversions baixes predominaven unitats lineals. Per tant necessitaven temps de reacció molt llargs per obtenir un grau de ramificació relativament elevat però, en cap cas, pròxim al teòric en polimeritzacions de monòmers AB_2.

Així doncs, la via catiònica presenta una sèrie d'inconvenients com ara la dificultat de seguir el procés de polimerització, la impossibilitat d'assolir valors de *DB* pròxim al teòric i la limitada disponibilitat de monòmers.

A través de la via aniònica la reacció procedeix de manera "*living*", és a dir, en absència de reaccions de terminació la reacció procedeix si el sistema es alimentat amb més monòmer. La polimerització s'inicia per l'addició d'una base com ara alcòxids, hidròxids, o compostos organometàl·lics com ara fosfines o *n*-butil liti (*n*-BuLi). Frey *i col.* [6], van ser els principals investigadors de la síntesi i la caracterització estructural per mitjà de RMN de ^{13}C del poliglicidol hiperramificat a través d'aquesta via. En els seus treballs, van descriure l'obtenció d'aquest polímer emprant l'iniciador trifuncional tris(hidroximetil)propà (TMP). Per tal de reduir la polidispersitat del polímer controlaven la concentració d'espècies mitjançant la desprotonació parcial, normalment del 10 %, del TMP a través de bases fortes com ara el metilat de potassi (MeOK) juntament amb la posterior eliminació del metanol format. A més a més, vàren establir que l'addició lenta del monòmer era imprescindible per prevenir la homopolimerització del glicidol iniciat per monòmer desprotonat així com la formació d'espècies cícliques. D'aquesta manera s'obtenen valors de polidispersitat molt baixos, al voltant de 1.3 - 1.5, i un bon control del pes molecular regulable en funció de la relació monòmer:iniciador.

La reacció de polimerització presenta un mecanisme de terminació reversible. En primer lloc, l'atac nucleòfil de l'alcòxid té lloc al carboni no substituït del grup oxirà donant lloc a un alcòxid secundari. Part d'aquests alcòxids secundaris formats poden evolucionar cap a alcòxids primaris més estables i més reactius a través d'un equilibri de transferència de protó. Ambdós alcòxids segueixen reaccionant a través del mecanisme ACE. A l'**Esquema IV-1** es mostra el mecanisme descrit així com les diferents subunitats presents en l'estructura polimèrica.

[5] a) Yan, D.; Hou, X.; Zhu, J.; Kosman, J. J.; Wu, H.-S. *A new approach to control crystallinity of resulting polymers: Self-condensing ring opening polymerization* Macromol. Rapid Commun. **2000**, 21, 557-561. b) Magnusson, H.; Malmström, E.; Hult, A. *Influence of reaction conditions on degree of branching in hyperbranched aliphatic polyethers from 3-ethyl-3-(hydroxymethyl)oxetane* Macromolecules **2001**, 34, 5786-5791.
[6] a) Sunder, A.; Hanselmann, R.; Frey, H.; Mülhaupt, R. Controlled synthesis of hyperbranched polyglycerols by ring-opening multibranching polymerization Macromolecules **1999**, 32, 4240-4246. b) Sunder, A.; Frey, H.; Mülhaupt, R. *Hyperbranched polyglycerols by ring-opening multibranching polymerization* Macromol. Symp. **2000**, 153, 187-196. c) Sunder, A.; Frey, H.; Mülhaupt, R. *Hyperbranched polyether polyols: a modular approach to complex polymer architectures* Adv. Mater. **2000**, 12, 235-239.

Si és un alcòxid secundari el que es propaga, la cadena polimèrica està unida a una unitat glicerol i es genera una unitat lineal 1,3 ($L_{1,3}$). La unitat L_{14} es forma quan un alcòxid primari es propaga. La reacció de dos alcòxids d'una mateixa unitat monomèrica, el primari i el secundari, genera una unitat dendrítica (*D*) i per tant es forma un punt de ramificació. Finalment, si una unitat de monòmer es desactiva per transferència de protó es forma una unitat terminal (*T*) amb dos grups hidroxil finals.

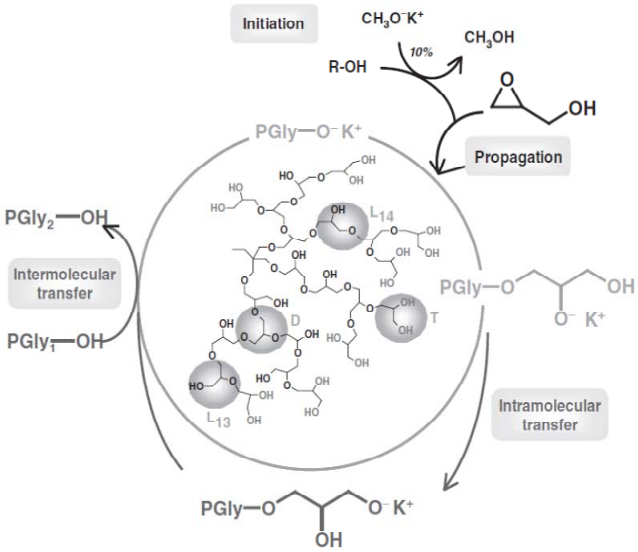

Esquema IV-1 Mecanisme de la polimerització ROMBP del glicidol i estructura esquemàtica del poliglicidol hiperramificat format

El poliglicidol hiperramificat presenta una sèrie de propietats que el fan ser bon candidat per múltiples aplicacions tan en el camp tecnològic com en el biomèdic. Concretament, presenta una estructura ben definida, una elevada solubilitat en medis polars així com una elevada flexibilitat estructural i un gran nombre de grups reactius terminals [7].

IV.1.2 Poli(*p*-clorometilestirè) hiperramificat obtingut per autopolicondensació vinílica (SCVP)

Els monòmers vinílics no poden ser polimeritzats via policondensació de monòmers AB_x. En aquest cas, els monòmers emprats han de ser monòmers i iniciadors al mateix temps. Per això, s'anomenen *inímers* (INIciador + monòMER) i polimeritzen a través d'autopolicondensació vinílica (SCVP, *self-condensing vinyl*

[7] Wilms, D.; Stiriba, S.E.; Frey, H. *Hyperbranched polyglycerols: from the controlled synthesis of biocompatible polyether polyols to multipurpose applications* Acc. Chem. Res. **2010**, 43, 129-141.

polymerization). Aquesta aproximació es basa en l'homopolimerització de monòmers de tipus AB* on B* és un grup capaç d'iniciar la polimerització de grups vinil, A.

A l'**Esquema IV-2** es mostren alguns dels inímers de tipus acrilat [8], metacrilat [9] o estirènic [10] més emprats polimeritzats per SCVP.

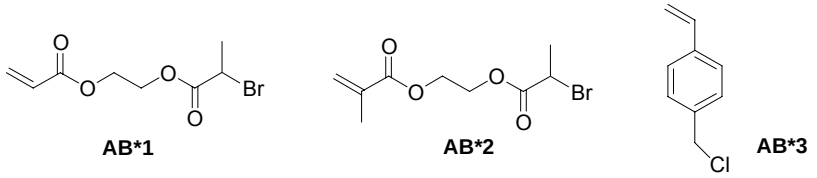

Esquema IV-2 Inímers (AB*) més emprats en SCVP. **AB*1** 2-(2-bromopropionil) etil acrilat, **AB*2** 2-(2-bromopropionil) etil metacrilat i **AB*3** *p*-clorometilestirè

Per tal d'iniciar la polimerització, en primer lloc, es duu a terme l'activació del grup B*. A l'**Esquema IV-3** es mostra l'activació d'un inímer, el *p*-clorometilestirè, per mitjà d'un catalitzador com ara el clorur de Cu (I) (CuCl) o un àcid de Lewis. Aquest transforma l'espècie inactiva en una espècie activa radicalària o catiònica la qual pot atacar a un altre grup vinil d'un altre inímer.

Esquema IV-3 Procés d'activació del *p*-clorometilestirè a través de SCVP

En el procés anteriorment descrit es mostra la formació d'un centre actiu (A*) el qual és capaç de propagar i un centre (b) que indica una posició inactiva i que per tant no pot seguir polimeritzant.

En termes estructurals, a l'**Esquema IV-4** es mostra un hexàmer del *p*-clorometilestirè el qual conté 5 unitats estructurals diferents. La unitat terminal *T* es basa en dos centres actius (A* i B*). La unitat T_v consisteix en un grup vinil (A) i

[8] Matyjaszewski, K.; Gaynor, S.G.; Kulfan, A.; Podwika, M. *Preparation of hyperbranched polyacrylates by atom transfer radical polymerization. 1. Acrylic AB* monomers in "living" radical polymerizations* Macromolecules **1997**, 30, 5192-5194.
[9] Matyjaszewski, K.; Pyun, J.; Gaynor, S.G. *Preparation of hyperbranched polyacrylates by atom transfer radical polymerization, 4. The use of zero-valent copper* Macromol. Rapid Commun, **1998**, 19, 665-670.
[10] Weimer, M.W.; Fréchet, J.M.J.; Gitsov, I. *Importance of active-site reactivity and reaction conditions in the preparation of hyperbranched polymers by self-condensing vinyl polymerization: Highly branched vs. linear poly[4-(chloromethyl)styrene] by metal-catalyzed "living" radical polymerization* J. Polym. Sci., Part A: Polym. Chem. **1998**, 36, 955-970.

centre inactiu (b). La unitat dendrítica *D*, està composta per dos centres inactius (a i b). A més a més, existeixen dos tipus d'unitats lineals (L_v i L_c). L_v, es forma per reacció entre un grup B* i un vinílic (A) per poliaddició. En canvi L_c, es forma per reacció entre un grup B* i un vinílic (A).

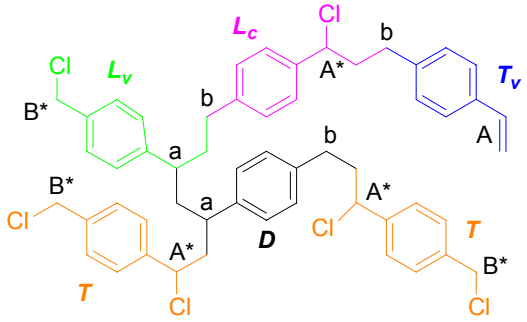

Esquema IV-4 Estructura d'un possible hexàmer del *p*-clorometilestirè obtingut per SCVP

Per tal de preparar aquest tipus de polímers normalment es fa ús de sistemes de polimerització controlada per tal d'evitar processos de gelificació o entrecreuament causats per reaccions de transferència de cadena o recombinació. Entre aquests, la polimerització radicalària controlada la qual engloba diferents tipus de processos com ara, ATRP (*atom transfer radical polymerizatio*n), NMRP (*nitroxide-mediated radical polymerization*) i RAFT (*reversible addition-fragmentation chain transfer*), és el sistema més utilitzat. Aquests processos es basen en establir un equilibri dinàmic ràpid entre les cadenes creixents radicalàries i la gran majoria d'espècies latents.

Un dels principals inconvenients del poli(*p*-clorometilestirè) hiperramificat així com d'altres polímers obtinguts per SCVP, és la presència d'àtoms halògens, com ara Br o Cl, com a grups terminals. Aquests grups són tèrmicament poc estables i molt reactius en presència de llum UV fent que el polímer esdevingui insoluble amb el pas del temps. Per tant, la seva modificació permet evitar els punts anteriorment descrits així com obtenir nous polímers funcionals (**Esquema IV-5**). Weimer *i col.* [11], varen descriure vàries reaccions de modificació per tal d'incorporar grups acetat (**1a**), ftalimida (**1b**), nitril (**1c**) i etil tioèter (**1d**). Georgi *i col.* recentment [12], han dut a terme satisfactòriament altres reaccions de modificació com ara la hidrogenació amb diferents agents reductors (**2a**) així com la introducció d'altres grups funcionals com ara, acetat (**1a**), fenil èter (**2b**), benzoat (**2c**), poliestirè-carboxilat (**2d**), azida (**2e**) i hidroxil (**2f**).

[11] Weimer, M.W.; Fréchet, J.M.J.; Gitsov, I. *Importance of active-site reactivity and reaction conditions in the preparation of hyperbranched polymers by self-condensing vinyl polymerization: Highly branched vs. linear poly[4-(chloromethyl)styrene] by metal-catalyzed "living" radical polymerization* J. Polym. Sci., Part A: Polym. Chem. **1998**, 36, 955-970.
[12] Georgi, U.; Erber, M.; Stadermann, J.; Abulikemu, M.; Komber, H.; Lederer, A.; Voit, B. *New approaches to hypebranched poly(4-chloromethylstyrene) and introduction of various functional end groups by polymer-analogous reactions* J. Polym. Sci., Part A: Polym. Chem. **2010**, 48, 2224-2235.

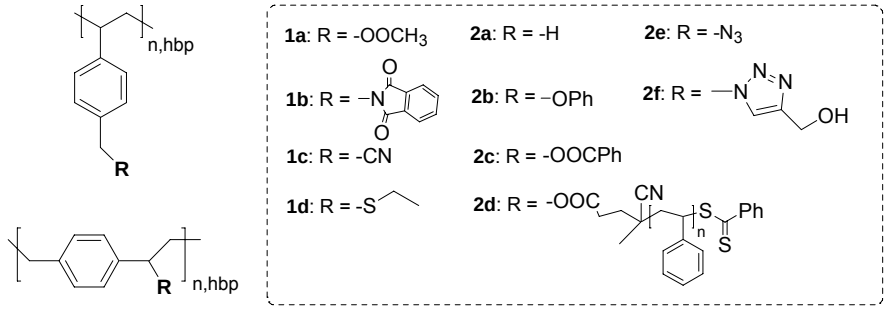

Esquema IV-5 Transformació dels grups clorometil i clorometilè del poli(*p*-clorometilestirè) en diferents funcionalitats descrites fins ara a la bibliografia

IV.1.3 Polímers estrella amb nucli hiperramificat obtinguts per polimerització per obertura d'anell (ROP) a través del mètode "*core-first*"

És conegut que els esters cíclics, com ara la *ε*-caprolactona (*ε*-CL) o la lactida (D-LA, L-LA o meso-LA), poden ser polimeritzats de manera controlada emprant catalitzadors d'estany, com per exemple el 2-etilhexanoat d'estany ($Sn(Oct)_2$), en combinació amb iniciadors com ara grups hidroxil (R-OH), o amines primàries [13]. Concretament, la polimerització en presència de grups hidroxil comença amb la formació de les espècies actives de tipus alcòxid RO-Sn-Oct o bé RO-Sn-OR segons els equilibris establerts següents:

$$Sn(Oct)_2 + R\text{-}OH \rightleftharpoons RO\text{-}Sn\text{-}Oct + Oct\text{-}H$$

$$RO\text{-}Sn\text{-}Oct + R\text{-}OH \rightleftharpoons RO\text{-}Sn\text{-}OR + Oct\text{-}H$$

Esquema IV-6 Formació de les espècies actives RO-Sn-Oct i RO-Sn-OR per mitjà de reaccions de transferència entre el $Sn(Oct)_2$ i grups OH. (Oct = $C_4H_9CH(C_2H_5)C(O)O^-$)

Seguidament, es produeix la inserció del monòmer entre l'enllaç ···-Sn**-**OR per formar espècies de tipus ···-Sn-O-$(CH_2)_5$-C(O)-OR les quals poden propagar la reacció de polimerització incorporant més monòmer. Finalment, es produeix novament una reacció de transferència a través de l'àcid Oct-H present al medi protonant l'alcòxid de la cadena activa i regenerant el catalitzador (**Esquema IV-7**).

13 a) Kowalski, A.; Duda, A.; Penczek, S. *Kinetics and mechanism of cyclic esters polymerization initiated with tin(II) octoate, 1. Polymerization of ε-caprolactone* Macromol. Rapid Commun. **1998**, 19, 567-572. b) Kowalski, A.; Libiszowski, J.; Biela, T.; Cypryk, M.; Duda, A.; Penczek, S. *Kinetics and mechanism of cyclic esters polymerization initiated with tin(II) octoate. polymerization of ε-caprolactone and l,l-lactide co-initiated with primary amines* Macromolecules **2005**, 38, 8170-8176.

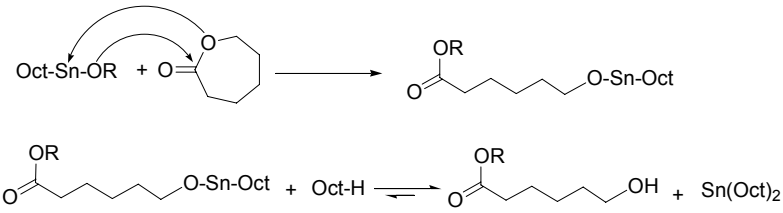

Esquema IV-7 Etapes d' inserció del monòmer i de terminació en la polimerització per obertura d'anell de la ε-caprolactona (ε-CL) catalitzada per $Sn(Oct)_2$

Aprofitant que certs grups, com s'ha descrit anteriorment, poden actuar de co-iniciadors, alguns autors han descrit la obtenció de polímers estrella emprant un nucli polifuncional com ara un polímer hiperramificat amb grups hidroxil o amina terminals.

Uns dels primers en dur-ho a terme van ser Hedrick *i col.* [14], els quals van emprar poliesters hiperramificats i dendrímers per obtenir polímers estrella amb braços de poli(ε-caprolactona). Frey *i col.* també van aconseguir sintetitzar polímers estrella contenint un promig de 55 braços de poli(ε-caprolactona) però en aquest cas, emprant un poliglicidol hiperramificat i modificat amb braços de poliòxid d'etilè [15]. En un altre treball realitzat pel mateix autor, es va polimeritzar glicolida a partir de varis poliglicidols hiperramificats de diferent pes molecular obtenint polímer estrella amb una dispersitat relativament baixa, entre 1.3 i 2.0 [16].

En canvi Lin *i col.* així com Cao *i col.*, van obtenir satisfactòriament el mateix tipus d'estructura a partir d'una poli(ester-amida) o polietilenimina com a nucli hiperramificat multifuncional, respectivament [17]. En ambdós treballs, es va estudiar l'efecte de la longitud dels braços de poli(ε-caprolactona) amb la capacitat d'encapsular colorant.

L'obtenció de polímers estrella obtingudes per polimerització per obertura d'anell (ROP) encara és un camp poc explorat ja existeixen relativament pocs nuclis hiperramificats aptes per ser utilitzats en aquest tipus de polimerització. Per exemple, l'ús de polímers hiperramificats estirènics com a macroiniciadors de lactones no ha sigut descrit.

[14] Trollsås, M.; Hawker, C.J.; Remenar, J.F.; Hedrick, J.L.; Johansson, H.; Ihre, H.; Hult, A. *Highly branched radial block copolymers via dendritic initiation of aliphatic polyesters* J. Polym. Sci., Part A: Polym. Chem. **1998**, 36, 2793-2798.
[15] Burgath, A.; Sunder, A.; Neuner, I.; Mülhaupt, R.; Frey, H. *Multi-arm star block copolymers based on ε-caprolactone with hyperbranched polyglycerol core* Macromol. Chem. Phys. **2000**, 201, 792-797.
[16] Wolf, F.K.; Fischer, A.M.; Frey, H. *Poly(glycolide) multi-arm star polymers: Improved solubility via limited arm length* Beilstein J. Org. Chem. **2010**, 6, No. 67.
[17] a) Lin, Y.; Liu, X.; Dong, Z.; Li, B.; Chen, X.; Li, Y.S. *Amphiphilic core-shell nanocarriers based on hyperbranched poly(ester-amide)-star-PCL: Synthesis, characterization, and potential as efficient phase transfer agent* Biomacromolecules **2008**, 9, 2629-2636. b) Cao, P.F.; Xiang, R.; Liu, X.Y.; Zhang, C.X.; Cheng, F.; Chen, Y. *Modulating the guest encapsulation and release properties of multi-arm star polyethylenimine-block-poly(ε-caprolactone)* J. Polym. Sci., Part A: Polym. Chem. **2009**, 47, 5184-5193.

UNIVERSITAT ROVIRA I VIRGILI
NOUS TERMOESTABLES EPOXÍDICS MODIFICATS AMB ESTRUCTURES DENDRÍTIQUES DE TIPUS HIPERRAMIFICAT I ESTRELLA
Mireia Morell Bel
DL:T. 155-2012

IV.2

MULTIARM STAR POLY(GLYCIDOL)-*block*-POLY(ε-CAPROLACTONE) OF DIFFERENT ARM LENGTHS AND THEIR USE AS MODIFIERS OF DIGLYCIDYLETHER OF BISPHENOL A THERMOSETS

Mireia Morell, Albena Lederer, Xavier Ramis, Brigitte Voit, Àngels Serra

Journal of Polymer Science, Part A: Polymer Chemistry ***2011****, 49, 2395 – 2406*

UNIVERSITAT ROVIRA I VIRGILI
NOUS TERMOESTABLES EPOXÍDICS MODIFICATS AMB ESTRUCTURES DENDRÍTIQUES DE TIPUS HIPERRAMIFICAT I ESTRELLA
Mireia Morell Bel
DL:T. 155-2012

Journal of Polymer Science, Part A: Polymer Chemistry **2011**, 49, 2395 – 2406

MULTIARM STAR POLY(GLYCIDOL)-*block*-POLY(*ε*-CAPROLACTONE) OF DIFFERENT ARM LENGTHS AND THEIR USE AS MODIFIERS OF DIGLYCIDYLETHER OF BISPHENOL A THERMOSETS

Mireia Morell,[1] Albena Lederer,[2] Xavier Ramis,[3] Brigitte Voit,[2] Àngels Serra[1]

[1] Department of Analytical and Organic Chemistry, Universitat Rovira i Virgili, C/ Marcel·lí Domingo s/n, Tarragona 43007, Spain.
[2] Leibniz-Institut für Polymerforschung Dresden e.V., Hohe Strasse 6, Dresden 01069, Germany.
[3] Thermodynamics Laboratory, ETSEIB Universitat Politècnica de Catalunya, Av. Diagonal 647, Barcelona 08028, Spain.

Abstract

Well-defined multiarm star copolymers, hyperbranched poly(glycidol)-*b*-poly(*ε*-caprolactone), with an average of about 100-110 arms per molecule and a molecular weight of arms of 3,000 g/mol (PGOH-*b*-PCL_{30}) and 1,000 g/mol (PGOH-*b*-PCL_{10}) were synthesized by cationic ring-opening polymerization of *ε*-caprolactone from a poly(glycidol) core and used to modify diglycidylether of bisphenol A formulations. The curing process, studied by dynamic scanning calorimetry, was only slightly retarded when PGOH-*b*-PCL_x were added to the formulation. By rheometry, the effect of this new topology and the arm length on the complex viscosity (η^*) and gelation of the reactive mixture was analyzed in detail. The addition of these new reactive modifiers decreases the global shrinkage and increases the conversion at gelation. In addition, the modified thermosets have an improved reworkability. The homogeneity of pure DGEBA and modified thermosets was proved by dynamic thermomechanical analysis and electronic microscopy (ESEM). Addition of star-like structures led to a more toughened fracture of the thermoset in comparison to pure DGEBA.

Keywords: anionic polymerization; epoxy resin; hyperbranched; star polymers; thermosets

Introduction

Epoxy resins are one of the most important classes of thermosetting materials, being widely used as coatings, electrical and electronic materials, adhesives, and in structural applications because of their attractive properties such as thermal stability and good electrical properties [1,2]. The main objectives of our research on epoxy-based materials are to face some of the limitations of these kinds of materials, for instance, by the control of shrinkage and the enhancement of toughness.

It has been proved that the substitution of linear thermoplastic precursor polymers by hyperbranched polymers (HBPs) as reactive modifiers leads to a significant improvement of these properties without affecting the thermomechanical characteristics [3-6].

Another advantage over linear conventional toughening agents is that dendritic polymers offer a lower precursor polymer viscosity because of their structure and the lack of chain entanglement [7]. In fact, a viscosity not exceeding 0.5 Pa·s is necessary to allow flowing through the mould in some industrial processes, such as the resin transfer molding [8,9]. Therefore, the use of polymeric

materials in any industrial process requires accurate information of their rheological behavior.

In addition to HBPs, multiarm star copolymers can also be considered as a new class of reactive modifiers for epoxy resins [10]. Two major strategies have been used for their preparation: the "core-first" approach which involves the living polymerization from a multifunctional core [11-14], and the "arm-first" approach, which consists in linking reactive polymer chains to a functionalized core or to a small amount of bifunctional vinyl compounds capable to crosslink [15-16]. Among them, the "core-first" strategy established itself as the most effective for the preparation of this polymer topology.

For the preparation of larger amounts of well-defined star polymers with a large number of arms, dendrimers as cores are not suitable due to their rather complicated and expensive synthesis. For that reason, HBPs can be considered as good candidates to be used as multifunctional core structures. Among them, hyperbranched poly(glycidol) (PGOH) with low molar-mass dispersity, obtained via ring-opening anionic polymerization is one of the most used macroinitiators because it possesses a flexible polyether backbone, multiple hydroxyl groups and a hydrophilic character [11,17-19].

In a recent study, hyperbranched poly(glycidol) was used as chemical modifier of DGEBA (diglycidylether of bisphenol A). Despite of the good properties, hb poly(glycidol) resulted to be partially immiscible with the epoxy resin due to hydrogen bonding caused by the high number of hydroxyl groups [20]. Therefore, its use as core structure to obtain star copolymers can derive in a totally different behavior. The arms can reduce the intramolecular bonding, which derives in the increase of the solubility and the free volume of the macromolecule in the epoxy matrix.

A large set of monomers can be polymerized by controlled polymerization methods. For example, multiarm poly(ε-caprolactone) (PCL) star copolymers have been synthesized by ring-opening polymerization of ε-caprolactone using poly(glycidol)-*b*-poly(ethylene oxide) and linear poly(glycidol) as multifunctional initiators using $Sn(Oct)_2$ as catalyst [21,22]. Tailoring the ratio of active sites to the amount of monomer is possible to control the arm length.

PCL is a hydrophobic, semi-crystalline polyester with a high chain flexibility, which is miscible in the most epoxy systems [23-25]. The use of this block to modify epoxy resins appears as a good choice as aliphatic esters can experiment thermal degradation by a pyrolytic elimination process and therefore this polymer fulfills the environmental requirements, which involve the degradability of the protective coating to allow the reworkability of the electronic devices [26]. Moreover, its flexible structure is capable to promote crazing and shear yielding and to absorb the energy locally. Therefore, it can improve the toughness also needed to prevent the loss of adhesion and the damage of the electronic devices caused by brittle fractures [27].

The chemical incorporation of hydroxyl-terminated HBPs to the epoxy matrix has been accomplished by anionic curing by ring-opening mechanism in thermal conditions. Concretely in previous studies [28,29], it was proved that hydroxyl groups are able to react when the polymerization of DGEBA was initiated by tertiary amines such as 1-methylimidazole (1MI) or 4-(*N*,*N*-dimethylamino)pyridine (DMAP).

Until now, the chemical incorporation of hydroxyl-terminated star copolymers during the anionic curing of DGEBA has not been reported. Therefore in this work, we propose the use of well-defined multiarm star copolymers based on poly(glycidol)-*b*-poly(*ε*-caprolactone) (PGOH-*b*-PCL_x) of different arm lengths as chemical modifiers of DGEBA. Our aim is to investigate the influence of this new polymer topology and the arm length variation on the rheological behavior, curing and gelation processes and on the final properties of the resulting PGOH-*b*-PCL_x/DGEBA thermosets.

Experimental

Materials

Glycidol (96 %) was distilled under reduced pressure and stored over molecular sieves at 2-5 ºC, dioxane was dried over calcium hydride and subsequently distilled and *ε*-caprolactone (*ε*-CL, 97 %) was dried over calcium hydride and subsequently distilled under vacuum. Trimethylolpropane (TMP, 97 %), potassium methylate solution (25 % v/v in methanol), tin (II) 2-ethylhexanoate ($Sn(Oct)_2$, 98 %) and 1-methylimidazole (1MI, 99 %) were used without further purification. All these chemicals were purchased from Sigma-Aldrich. Solvents were purchased from Scharlab.

Diglycidylether of bisphenol A (DGEBA) Epikote Resin 827 was provided by Shell Chemicals (epoxide equivalent weight (EEW) = 182.1 g/eq, n = 0.082).

Synthesis of PGOH-b-PCL_x multiarm star copolymers

Hyperbranched poly(glycidol), PGOH, $\overline{M_n}$ (by ^{1}H NMR) 7,900 g/mol with an average of 100-110 hydroxyl group per molecule was prepared according to already published procedures [30,31] and dried under vacuum for 2 days at 50 ºC.

^{1}H NMR (400 MHz, DMSO-d_6) δ *ppm*: 4.8-4.3 (O**H**), 3.8-3.2 (C**H**O/C**H**OH/C$\mathbf{H_2}$O/C$\mathbf{H_2}$OH, poly(glycidol) backbone), 1.28 (C$\mathbf{H_2}$, TMP in the PGOH) and 0.81 (C$\mathbf{H_3}$, TMP in the PGOH); ^{13}C NMR (100.6 MHz, DMSO-d_6) δ *ppm*: 80.9-80.0 (**C**H linear unit), 79.0-78.0 (**C**H dendritic unit), 74.0-72.8 (**C**H_2 linear unit), 72.5-70.6 (**C**H_2/**C**H terminal and dendritic unit), 69.6-68.4 (**C**H linear unit), 63.9-63.1 (**C**H_2 terminal unit) and 61.5-61.0 (**C**H_2 linear unit); FTIR (ATR) (cm^{-1}): 3370 (OH), 1170-980 (C-O-C st asym/sym); $\overline{M_n}$ (SEC-LS) = 10,500 g/mol, $\overline{M_w} / \overline{M_n}$ = 1.48.

The signal assignment and the degree of branching (*DB*) of PGOH, according to the Frey's definition, were determined according to [30]. *DB* was 0.49, calculated from ^{13}C NMR signal intensities obtained under quantitative conditions.

PGOH-b-PCL$_x$

The synthesis is exemplified for PGOH-*b*-PCL$_{10}$. PGOH (0.5 g, 0.048 mmol) and 7.74 g of ε-CL (68 mmol) were placed at room temperature in a two-necked flask equipped with a magnetic stirrer and a gas inlet to fill the flask with argon. Then, 0.12 g of Sn(Oct)$_2$ (0.3 mmol) was added to the solution mixture and the flask was immersed in an oil bath thermostated at 130 ºC during 24 hours. After that, the crude product was dissolved in chloroform and the polymer was isolated by precipitation in 10-fold cold diethyl ether and then filtered and dried at 45 ºC under vacuum for 2 days.

^1H NMR (400 MHz, $CDCl_3$) *δ ppm* (**Figure 1**): 5.20-4.92 (C**H**-OCO-, PGOH core), 4.35-3.80 (C**H$_2$**-OCO-, PGOH core), 4.07 (-C**H$_2$**-OCO-, **6**), 3.80-3.40 (PGOH core), 3.65 (-C**H$_2$**-OH, **6'**), 2.30 (-C**H$_2$**-COO-, **2** and **2'**), 1.70-1.50 (-C**H$_2$**-, **4, 4'** and **5, 5'**), 1.40 (-C**H$_2$**-, **3** and **3'**) and 0.88 (C**H$_3$**, TMP, PGOH core); ^{13}C NMR (100.6 MHz, $CDCl_3$) *δ ppm*: 173.6 (C=O, **1'**), 173.4 (C=O, **1**), 79.0-62.0 (PGOH core), 64.0 (-**C**H$_2$-OCO-, **6**), 62.4 (-**C**H$_2$-OCO-, **6'**), 34.1 (-**C**H$_2$-COO-, **2'**), 33.9 (-**C**H$_2$-COO-, **2**), 32.2 (-**C**H$_2$-, **5'**), 28.2 (-**C**H$_2$-, **5**), 25.4 (-**C**H$_2$-, **4**), 25.2 (-**C**H$_2$-, **4'**), 24.6 (-**C**H$_2$-, **3'**) and 24.4 (-**C**H$_2$-, **3**); FTIR (ATR) (cm^{-1}): 3480 (OH), 1720 (C=O), 1200-1120 (C-O-C st as/s).

Average molecular weights and thermal data of all the stars obtained are given in **Table 1.**

Table 1 Data of the PGOH core and multiarm star copolymers PGOH-*b*-PCL$_x$ used in this study

Entry	[εCL:OH]	*Conv.*[a] [%]	$\overline{M}_{n,calc}$[b] (g/mol)	$\overline{M}_{n,exp}$[c] (g/mol)	D[c]	$\overline{DP}_{arm}$[d]	Δh_m[e] (J/g)	T_m[e] (ºC)	$T_{2\%}$[f] (ºC)
PGOH	-	-	-	10,500	1.48	-	-	-	373
PGOH-*b*-PCL$_{10}$	10:1	80	99,400-108,600	89,100	1.69	8	65.4	45.3	278
PGOH-*b*-PCL$_{30}$	30:1	75	265,300-291,000	225,700	2.05	27	84.4	59.2	268

a. Conversion determined gravimetrically.

b. Theoretical $\overline{M}_{n,calc}$ = ([ε-CL]/[OH]) x $M_{\varepsilon-CL}$ x conversion x N_{OH} + $\overline{M}_n$ (macroinitiator), being N_{OH} 100-110.

c. $\overline{M}_n$ and $\overline{M}_w / \overline{M}_n$ (D) were determined by SEC-MALLS with DMAc as solvent.

d. Degree of polymerization ($\overline{DP}_{arm}$) was determined by ^{13}C NMR in quantitative conditions as: Int (5) / Int (5') + 1 (end group).

e. Data obtained from the second DSC scan at 10 ºC/min.

f. Temperature of the onset of degradation under N_2 at 10 ºC/min.

Journal of Polymer Science, Part A: Polymer Chemistry **2011**, 49, 2395 – 2406

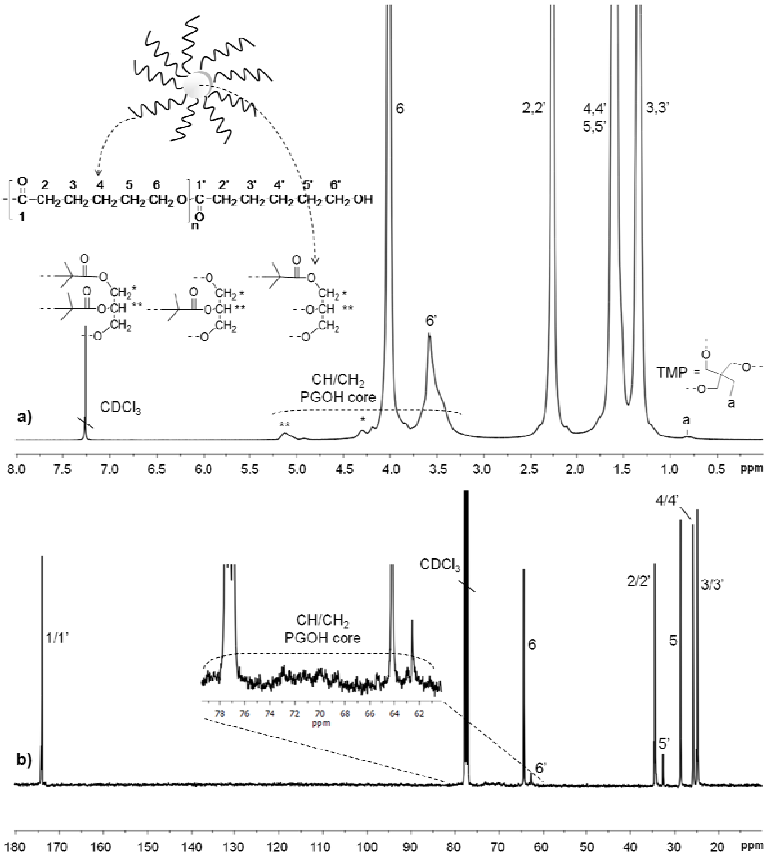

Figure 1 ^{1}H (**a**) and ^{13}C NMR (**b**) spectra of multiarm star copolymer PGOH-*b*-PCL_{10} in $CDCl_3$

Preparation of epoxy thermosets

The mixtures were prepared by adding the required amount of PGOH-*b*-PCL_x into the epoxy resin and gently heating until it was dissolved and the solution became clear. Then, 5 phr (part per hundred parts of mixture) of 1MI was added, and the resulting solution was stirred and cooled down to - 10 ºC to prevent polymerization. Mixtures containing 5 – 10 wt.% (by weight) of PGOH-*b*-PCL_x were prepared. The compositions of the formulations studied are detailed in **Table 2.**

Characterization

^{1}H NMR and ^{13}C NMR measurements were carried out at 400 MHz and 100.6 MHz, respectively, in a Varian Gemini 400 spectrometer. $CDCl_3$ and DMSO-d_6 were used as solvents for NMR measurements. For internal calibration the solvent signals were used: δ (^{13}C) = 77.16 ppm, δ (^{1}H) = 7.26 ppm for $CDCl_3$ and δ (^{13}C) = 39.52 ppm, δ (^{1}H) = 2.50 ppm for DMSO-d_6. Quantitative ^{13}C NMR experiments were recorded using a delay time between sampling pulses equal to 8 seconds and the sequence inverse gated decoupling.

The FTIR spectra were collected in a spectrophotometer FTIR-680PLUS from JASCO with a resolution of 4 cm^{-1}. This device was equipped with an attenuated-total-reflection accessory with a diamond crystal (Golden Gate heated single-reflection diamond ATR, Specac-Teknokroma).

The determination of molecular weights and molecular weight distributions were carried out on a modular build SEC-system using an Agilent 1200 series pump coupled with a multiangle laser light scattering (MALLS) detector Tristar MiniDawn (Wyatt Technology) and Knauer RI detector in combination with a PolarGel-M-column (Polymer Laboratories) in DMAc mixed with 3 $g \cdot L^{-1}$ LiCl. The evaluations of the molecular weights were made using software ASTRA 4.9 (Wyatt Technology).

Calorimetric analyses were carried out on a Mettler (DSC)-822e thermal analyzer. Samples of ~ 5 mg in weight were placed in aluminum pans under nitrogen atmosphere. The calorimeter was calibrated using an indium standard (heat flow calibration) and an indium-lead-zinc standard (temperature calibration).

Multiarm star polymers (PGOH-*b*-PCL_x) were heated from – 50 to 150 ºC with a heating rate of 10 ºC/min, cooled down to – 100 ºC with a cooling rate of – 10 ºC/min and then heated again to 150 ºC at the same heating rate. Δh_m and T_m values were obtained from the second heating curves. Thermal data are collected in **Table 1**.

Nonisothermal curing experiments were performed from 20 to 250 ºC at heating rates of 2, 5, 10, and 15 ºC/min to determine the reaction heat and the kinetic parameters. In nonisothermal curing process, the degree of conversion by DSC (α_{DSC}) was calculated as follows:

$$\alpha_{DSC} = \frac{\Delta H_T}{\Delta H_{dyn}} \quad (1)$$

where ΔH_T is the heat released up to a temperature T, obtained by integration of the calorimetric signal up to this temperature, and ΔH_{dyn} is the total reaction heat associated with the complete conversion of all reactive groups.

The glass transition temperatures (T_gs) of the completed cured materials were determined, by means of a second scan at 20 ºC/min, as the temperature of the half-way point of the jump in the heat capacity when the material changed from glassy to the rubbery state under N_2 atmosphere and the error is estimated to be ~ ± 1 °C.

The kinetic triplet [pre-exponential factor, activation energy and kinetic model] of the curing process was determined using integral isoconversional nonisothermal kinetic analysis, Kissinger-Akahira-Sunose equation, combined with the Coats-

Journal of Polymer Science, Part A: Polymer Chemistry **2011**, 49, 2395 – 2406

Redfern procedure. Details of the kinetic methodology are given in previous publications [32,33].

Thermogravimetric analyses were carried out in a Mettler TGA/SDTA851e/LF/1100 thermobalance. Samples with an approximate mass of 8 mg were degraded between 30 and 800 ºC at a heating rate of 10 ºC/min in N_2 (100 cm^3/min measured in normal conditions).

Dynamic mechanical analyses were carried out with a TA Instruments DMA Q800. The samples were cured isothermally in a mould at 120 ºC for 1.5 h and then postcured for 1 h at 150 ºC. Single cantilever bending at 1 Hz and amplitude of deformation of 30 mm was performed at 3 ºC/min, from 40 ºC to 250 ºC on prismatic rectangular samples (20 x 5 x 1.5 mm^3).

The overall shrinkage was calculated from the densities of the materials before and after curing, which were determined using a Micromeritics AccuPyc 1330 Gas Pycnometer thermostated at 30 ºC.

Rheological measurements were carried out in the parallel plates (geometry of 25 mm) mode with an ARG2 rheometer (TA Instruments, UK, equipped with a Peltier system).

The gelation time was determined by setting the device in time sweep and multiwave oscillation mode. Experiments were performed isothermally at 80 ºC. Because the viscosity of the system changes significantly during the curing process, a control program was used in which the oscillation amplitude diminishes with an increase in the applied stress. By doing so, the curing process can be characterized in the whole range of conversion. Gel time was taken as the point where tan δ is independent of frequency [34]. The conversion at gelation (α_{gel}) and the T_g of the gelled material ($T_{g,gel}$) were determined by stopping the rheology experiment at gelation and performing a subsequent dynamic DSC scan of the gelled sample.

Complex viscosity (η^*) of the pre-cured mixtures were recorded as function of angular frequency (0.1 – 15 rad/s) stating a constant deformation of 50 % at 80 ºC.

The cryofracture area of the specimens was observed with an environmental scanning electron microscope (ESEM) model FEI Quanta 600.

Results and discussion

Hyperbranched poly(glycidol) (PGOH) was prepared according to previously published procedures by anionic polymerization of glycidol employing as initiator the potassium salt of trimethylolpropane (TMP) [30,31]. Subsequently, the obtained PGOH was used as the macroinitiator core to grow PCL arms by cationic ring-opening polymerization catalyzed by $Sn(Oct)_2$. The “core first” synthetic pathway is depicted in **Scheme 1**.

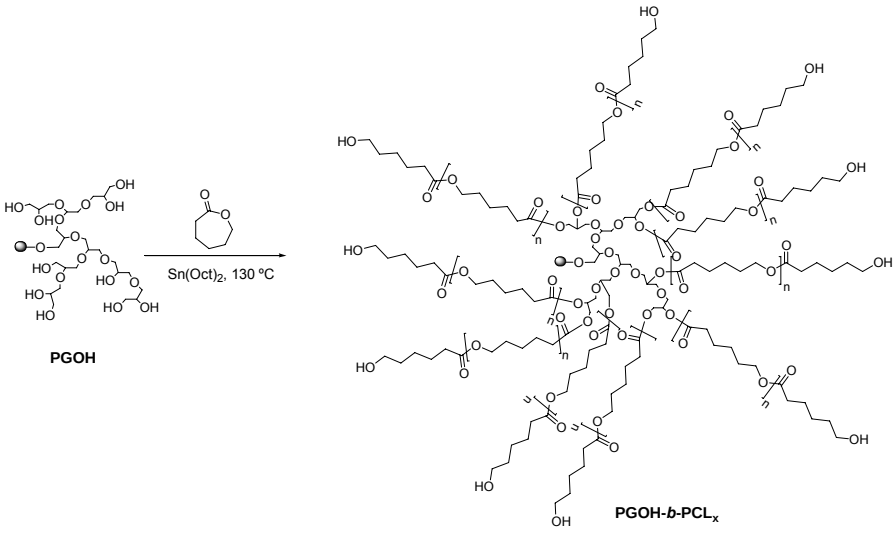

Scheme 1 Synthetic route to multiarm star copolymers PGOH-*b*-PCL_x

Synthesis and characterization of multiarm star poly(glycidol)-block-poly(ε-caprolactone)

To synthesize well-defined multiarm star poly(glycidol)-*block*-poly(ε-caprolactone), we selected the cationic ring-opening polymerization of ε-caprolactone taking a hyperbranched poly(glycidol) (PGOH) as macroinitiator. This reaction is catalyzed by tin (II) octoate. The number of hydroxyl groups per molecule (N_{OH}) of the PGOH was determined from the ^{1}H NMR molecular weight ($\overline{M_n}$ by ^{1}H NMR = 7,900 g/mol), assuming one hydroxyl group per repeating unit and it resulted to be on average 100-110.

The ratio of ε-caprolactone (ε-CL) to initiating hydroxyl groups in the feed was 30 or 10 to obtain different arms lengths. The reaction was performed in bulk at 130 ºC for 24 h. After precipitation in cold diethyl ether and drying in vacuum, the polymers were obtained as white waxy or fibrous solids depending on the molecular weight. The synthetic procedure used was similar to the one described by Burgath *et al.* where ε-CL was polymerized from poly(ethylene oxide) arms connected to a hyperbranched polyglycidol core [21]. Lin *et al*. used the same methodology but using a hyperbranched poly(ester amide) as a core [35].

The chemical structure of the purified PGOH-*b*-PCL_x could be confirmed by quantitative ^{1}H and ^{13}C NMR analysis (**Figure 1**). In **Figure 1** (**a**), the signal assignment of the proton spectrum of PGOH-*b*-PCL_{10} is observed. All the methylene protons of the PCL arms overlap with those of the terminal unit with the exception of methylene protons (**6** and **6')** linked to ester and hydroxyl groups. Moreover, the small broad signals in the region from 5.20-3.40 ppm could be assigned to PGOH core.

Journal of Polymer Science, Part A: Polymer Chemistry **2011**, 49, 2395 – 2406

As the PCL signals resulted partially overlapped by core proton signals, the determination of the degree of polymerization of PCL arms ($\overline{DP}_{arm}$) was calculated from the ^{13}C NMR, registered under quantitative conditions, (see **Figure 1** (**b**)) by dividing the integration values of peak **5** by peak **5'** and adding a terminal unit:

$$\overline{DP}_{arm} = \frac{I_5}{I_5'} + 1 \qquad (2)$$

The use of the signals of carbons **5** and **5'** for *DP* evaluation of the arms is possible due to the absence of PCL homopolymer, which was confirmed by SEC data, as will be discussed below. The characterization data listed in **Table 1** show that the experimental values $\overline{DP}_{arm}$ were only consistently slightly lower than the theoretical ones. This fact can be rationalized because of the incomplete monomer conversion due to the increased viscosity during the reaction in bulk.

By using linear standards, the molecular weights of star polymers are usually underestimated by SEC. Therefore, SEC equipped with multiangle laser light scattering detector was used to yield absolute molecular weights. **Figure 2** shows the plot of molar mass distribution according to MALLS signals of PGOH, PGOH-*b*-PCL_{10}, and PGOH-*b*-PCL_{30}.

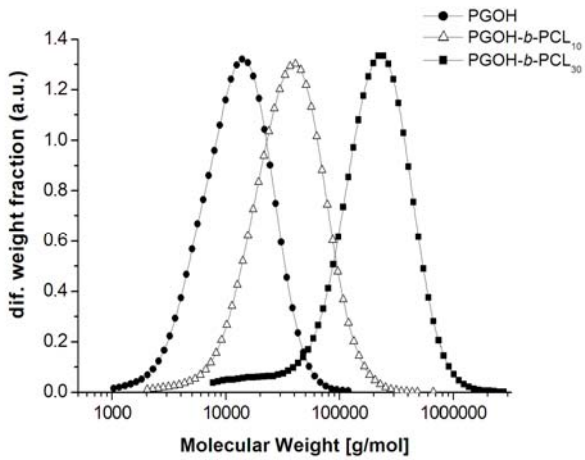

Figure 2 Molar mass distribution of PGOH and the corresponding star copolymers (PGOH-*b*-PCL_x) determined by SEC-LS in DMAc

All polymers presented symmetrical and unimodal peaks as well as the absence of signals at lower molecular weight, meaning no detectable PCL homopolymer formed during the ring-opening polymerization. As collected in **Table 1**, the molar-mass dispersity is quite narrow, which indicates that polymers were synthesized in a controlled manner. Furthermore, the increase of the molecular weight with increasing the ratio ε-CL/OH is evident according to SEC results. The molecular weights estimated by light scattering measurements ($\overline{M}_{n,exp}$ in **Table 1**)

are slightly lower than the theoretical molecular weights ($\overline{M}_{n,cal}$), due to the incomplete conversion of CL. The results verify the good control of the star topologies.

From thermal data it was observed that the melting temperature (T_m) and the heat of fusion (Δh_m) increased with increasing the molecular weight of the star polymer. This had been expected due to the effect of molecular weight on the thermal transitions of semicrystalline polymers. Concerning thermal stability, the obtained PGOH-*b*-PCL$_x$ showed to be thermally stable up to 270 - 280 ºC.

Curing of DGEBA with different proportions of PGOH-b-PCL$_x$

In a previous work, it was confirmed that 5 phr of 1-methylimidazole (1MI) (0.61 mmol of initiator per gram of mixture) were necessary to assure the complete cure of DGEBA [36]. Therefore, this amount of anionic initiator was selected to prepare the formulations studied, which are collected in **Table 2**.

Figure 3 shows the DSC exotherms (**a**) and the plots of degrees of conversion against temperature (**b**) recorded at 10 ºC/min of neat DGEBA/1MI and DGEBA/1MI/PGOH-*b*-PCL$_x$ formulations.

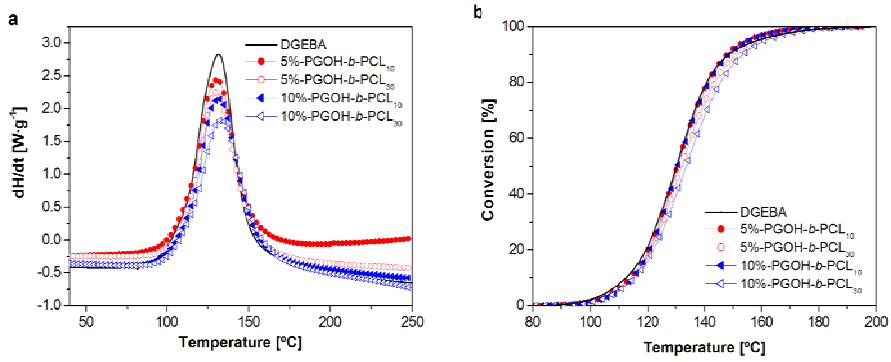

Figure 3 DSC scanning curves (**a**) and conversion degree (**b**) against temperature of the curing of DGEBA and DGEBA containing 5 or 10 wt.% of PGOH-*b*-PCL$_x$ at a heating rate of 10 ºC/min

It can be observed, that there is not much influence on the temperature or shape of the curing exotherm neither changing the proportion of PGOH-*b*-PCL$_x$ star nor the arm length of the star in the reactive mixture, but a slight deceleration is observed in the conversion curves on increasing the proportion of the star in the formulation. The retarding effect is more pronounced when the arms of the star are longer, which could be attributed to the effect of the increased viscosity of the mixture.

It was reported that the increase of the concentration of hydroxyl groups in the anionic ring-opening polymerization of DGEBA led to an increase in the curing rate

in the initiation step because of more activating species were formed [28,29] and in some cases even the propagation proceeded faster. Thus, one may expect that the addition of hydroxyl-terminated star polymers to the formulation should increase the curing rate. However, it should be considered that on adding this modifier the concentration of epoxy groups decreases (see **Table 2**) and this fact can explain the observed deceleration.

Table 2 Composition and calorimetric data of DGEBA/1MI mixtures with different percentages of PGOH-*b*-PCL_{10} or PGOH-*b*-PCL_{30}

Formulation[a] (wt.%)	meq_{epoxy} /mL[b]	meq_{OH} /mL[b]	E_a[c] (kJ/mol)	ln A[d] (s^{-1})	$k_{120\,°C}$ x 10^{3}[e] (s^{-1})	Δh (J/g)	Δh[f] (kJ/ee)	T_g[g] (ºC)
0	6.4	0.27	60.1	12.89	4.07	638	116.1	146
PGOH-*b*-PCL_{10}								
5	6.0	0.32 - 0.33	47.2	8.90	3.92	467	89.5	131
10	5.7	0.37 - 0.38	47.7	9.03	3.87	448	90.6	113
PGOH-*b*-PCL_{30}								
5	6.0	0.28 - 0.29	54.4	11.09	3.86	492	94.3	131
10	5.7	0.29 - 0.30	50.8	9.88	3.42	458	92.6	114

a. % by weight of multiarm star copolymer.
b. Epoxy and hydroxyl concentration of the formulations. Hydroxyl content was determined taking into account an average N_{OH} from 100 to 110. Volume was determined using the monomer density values collected in Table 4.
c. Values of activation energies at 50 % of conversion were evaluated by isoconversional nonisothermal procedure.
d. Values of pre-exponential factor for A_2 kinetic model with $g(\alpha) = [-ln(1-\alpha)]^{1/2}$.
e. Values of rate constant at 120 ºC calculated using the Arrhenius equation.
f. Enthalpy value per equivalent of epoxy group.
g. Glass transition temperature obtained by DSC. Second scan after dynamic curing at 20 ºC/min.

Another factor that can contribute to explain this behavior is that the hydroxyl groups coming from star polymers can be associated internally with the carbonyl groups of PCL arms, and therefore their activity can be reduced. On increasing the length of the arms, the concentration of epoxy remains unchanged but the hydroxyl proportion diminishes.

The kinetic parameters of the curing process were calculated and the values are collected in **Table 2**. Although activation energies and pre-exponential factors do not vary in an expected way, the constant rates calculated at 120 ºC are reduced on increasing the proportion of modifier and the length of the arms of the stars.

Calorimetric data of the curing process of the formulations studied are collected in the same table. The heat released is mainly due to the opening of epoxy groups because of the ring strain. For that reason, it is shown that the enthalpy per gram mixture decreases on increasing the proportion of PGOH-*b*-PCL_x, since the proportion of DGEBA in the formulation is reduced. If we take the enthalpy per epoxy equivalent into account, all formulations exhibit a value close to 100 kJ/ee, which is an acknowledged value for epoxy resin curing [37]. By FTIR-ATR spectroscopy, we could prove the complete curing of the formulations, since all the epoxy groups were reacted as shown by the disappearance of the absorption at 913 cm^{-1}.

On increasing the proportion of PGOH-*b*-PCL_x star in the material the T_g of the resin decreases, but the decrease was not further affected by the length of the arms. This fact could be attributed to the special topology of the star-shaped

polymer. The miscibility before curing was evidenced by optical microscopy and after curing it was confirmed by ESEM, as will be commented afterwards.

Poly(ε-caprolactone) is a semicrystalline polymer and the FTIR spectrum of the pure PGOH-*b*-PCL_{30} presents a main sharp absorption band at 1720 cm^{-1} attributed to the stretching vibration of carbonylic groups in crystalline domains [38] such as it is represented in **Figure 4** (**a**). In the same figure, we can see that in the spectrum of the thermoset obtained from a DGEBA/1MI 10 wt.% of PGOH-*b*-PCL_{30} (**b**) the main peak is shifted to 1732 cm^{-1}. This fact indicates that PCL arms are in the amorphous state in the thermoset, according to the assignments made by Coleman and Painter [38]. In addition, a new shoulder at lower frequency (1709 cm^{-1}) appears which can be assigned to the stretching vibration of hydrogen-bonded carbonyl groups. This fact supports that intermolecular interactions between PCL chains and the epoxy network exist in the thermoset.

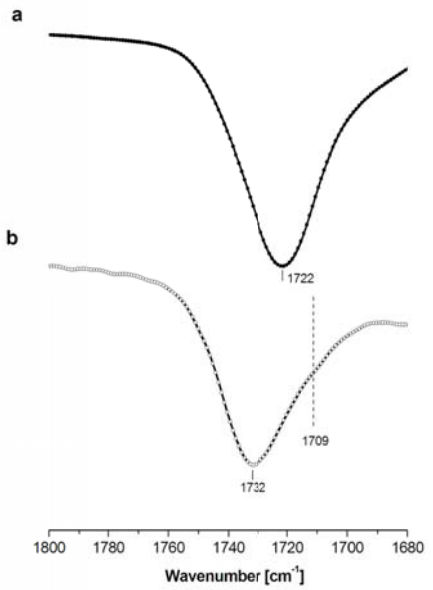

Figure 4 FTIR-ATR spectra of PGOH-*b*-PCL_{30} (**a**) and DGEBA thermoset with a 10 wt.% of PGOH-*b*-PCL_{30} (**b**) in the range of 1680-1800 cm^{-1}

Journal of Polymer Science, Part A: Polymer Chemistry **2011**, 49, 2395 – 2406

Rheological and shrinkage properties of the formulations

Figure 5 shows the evolution of tan δ during cure of neat DGEBA and the formulations with 5 or 10 wt.% of PGOH-*b*-PCL_x. As it can be seen, the addition of star polymers leads to retardation of the gelation.

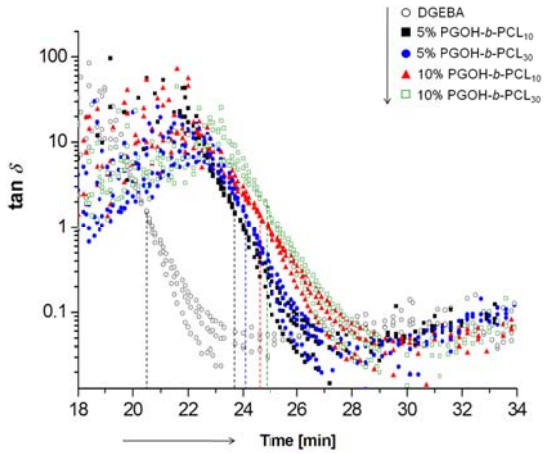

Figure 5 Evolution of tan δ during curing at 80 ºC of the formulations DGEBA/1MI and DGEBA/1MI containing 5 and 10 wt.% of PGOH-*b*-PCL_x in the range from 18 to 34 minutes

Gel times were calculated from the point where tan δ is independent of frequency [34]. The results obtained for all the formulations studied at 80 ºC are collected in **Table 3**. In the same table, the conversion and T_g at the gel point are also given. The gelation time slightly increases with the proportion of PGOH-*b*-PCL_x and with the the length of the arms. This result is significant from the point of view of the application, as it indicates a longer pot-life of these modified formulations.

Table 3 Gel conversion, densities, shrinkage of the systems studied

Formulation[a] (wt.%)	t_{gel} (min)	α_{gel}[b] (%)	$T_{g,gel}$ (ºC)	ρ_{mon} (g/cm^3)	ρ_{pol} (g/cm^3)	Shrinkage[c] (%)
0	20.5	52	3.1	1.157	1.176	1.62
PGOH-*b*-PCL_{10}						
5	23.5	58	-0.9	1.157	1.174	1.45
10	24.7	65	-8.3	1.154	1.170	1.37
PGOH-*b*-PCL_{30}						
5	24.1	60	-0.4	1.156	1.174	1.53
10	25.2	63	-7.5	1.155	1.168	0.77

a. % by weight of multiarm star copolymer.
b. Determined as the conversion reached by rheometry and DSC tests at 10 ºC/min.
c. Shrinkage determined as $[(\rho_{polymer} - \rho_{monomer})/\rho_{polymer}]$.

Conversion at the gel point (α_{gel}) increases with the proportion of modifiers. This result is beneficial to reduce the formation of internal stress on curing. After the gel point, the material loses its mobility and the shrinkage produced after gelation

leads to the stress appearance and to the formation of microcracks and microdeformations. Also, the reduction of internal stresses can affect positively the toughness characteristics of the materials.

It is known that the anionic homopolymerization as a chain-growth process shows a lower conversion at gelation than a step-growth process, such as in epoxy-anhydride system. The conversion at gelation is defined by the kinetic chain length (KCL) [39,40]. Two main factors can increase the conversion at gelation reducing the KCL: hydroxyl group and initiator concentration [28,41]. In reference to the first one, on increasing the proportion of the star in the formulation the hydroxyl proportion increases (**Table 2**). In reference to the initiator concentration, on adding a greater proportion of modifier the proportion of epoxide in the formulation diminishes, and therefore the relation of initiator to epoxide is higher. In this way, the number of growing chains becomes higher and accounts for a reduction of KCL, which leads to the subsequent higher conversion at the gel point.

The global shrinkage on curing was calculated from the densities before and after curing by pycnometry. As we can see in **Table 3**, the addition of the star polymers reduces the global shrinkage and a value of less than 1 % is reached on adding 10 wt.% of PGOH-*b*-PCL_{30}. This fact, together with the higher conversion at gelation, may contribute to inhibit the formation of internal stresses.

By rheological experiments, the complex viscosity of the mixtures at 80 ºC was determined on varying the angular frequency, as it is shown in **Figure 6**. All formulations show a Newtonian behavior and little differences among them. It has been reported by several authors that the addition of HBPs increases the prepolymer viscosity in comparison to the neat formulation [8,42,43]. In our case, viscosities are relatively unaffected and even decreases when a 5 wt.% of PGOH-*b*-PCL_{10} was added.

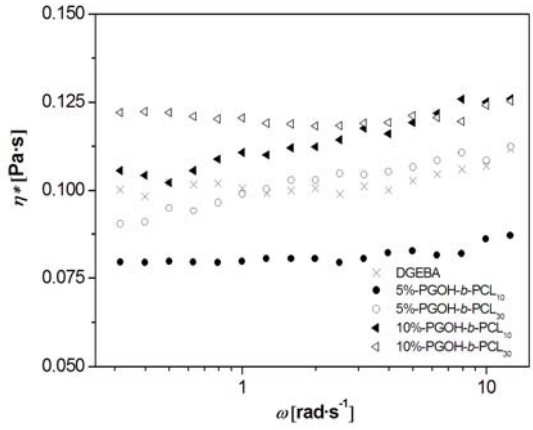

Figure 6 Complex viscosity (η^*) against angular frequency (ω) at 80 ºC for neat DGEBA/1MI and DGEBA/1MI containing 5 and 10 wt.% of PGOH-*b*-PCL_x

Journal of Polymer Science, Part A: Polymer Chemistry **2011**, 49, 2395 – 2406

All these facts evidence that the utilization of PGOH-*b*-PCL_x star copolymers as epoxy modifiers does not worsen the processability of the resin.

Thermal and thermomechanical properties of the thermosets obtained

The materials obtained were characterized by dynamic thermomechanical analysis. The tan *δ* plot against temperature for all the materials are represented in **Figure 7** and **Table 4** collects the thermomechanical data.

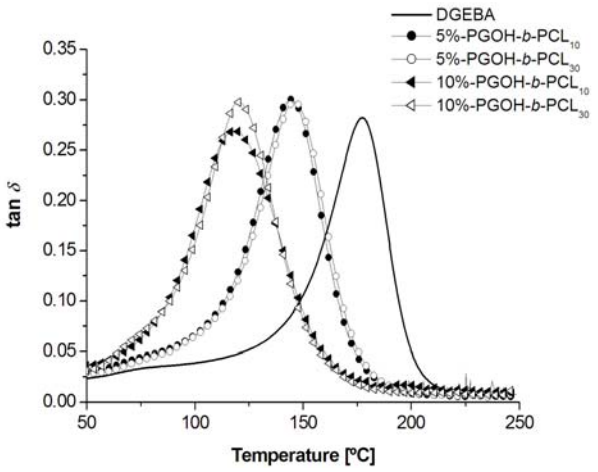

Figure 7 Tan *δ* against temperature at 1 Hz for the thermosets obtained

As we can see, the curves are unimodal and quite narrow. No relaxations were observed at low temperature, which evidences the homogeneous character of the modified materials. On increasing the proportion of the modifier, tan *δ* value decreases but there is no effect given by the length of the arms, similarly to the behavior observed by DSC. The width of the curve increases slightly on increasing the proportion of modifier, but again the length of the arms does not affect these characteristics. The broadness increment of the curve indicates a higher damping ability that can positively affect the toughness.

In **Table 4**, the decrease of the modulus after relaxation on adding the modifier can be appreciated. This parameter is affected by the length of the arm, because it is related with the degree of crosslinking and rigidity of the thermoset, which is lower when the arms length of the star additives increases. It seems that the special topology of the stars has a strong effect on the thermomechanical characteristics in the rubbery state, due to a higher contribution of the linear-like behavior caused by the arms.

Table 4 TGA and DMTA data obtained from DGEBA/1MI thermosets containing different proportions of multiarm star copolymers PGOH-*b*-PCL_{10} or PGOH-*b*-PCL_{30}

Formulation[a] (wt.%)	DMTA		TGA	
	$T_{\tan\delta}$[b] (ºC)	E'[c] (MPa)	T_{onset}[d] (ºC)	T_{max}[e] (ºC)
0	178	96.3	358	439
PGOH-*b*-PCL_{10}				
5	144	91.1	248	452
10	118	78.9	245	448
PGOH-*b*-PCL_{30}				
5	146	84.3	264	452
10	120	60.4	255	452

a. % by weight of multiarm star copolymer.
b. Temperature of maximum of the tan δ at 1 Hz.
c. Relaxed modulus determined at the $T_{\tan\delta}$ + 40 ºC.
d. Temperature of the onset decomposition on the TGA data at 10 ºC/min calculated for a 2 % of weight loss.
e. Temperature of the maximum decomposition rate based on the TGA data at 10 ºC/min.

The thermal stability of the materials obtained was investigated by thermogravimetry. **Figure 8** represents the loss of weight against temperature, and the data are collected in **Table 4**. The initial decomposition temperature of the modified thermosets decreases practically 100 ºC, and it falls in the range of temperatures reported for reworkable thermosets [26]. The loss of thermal stability is due to the presence of ester groups in the PCL blocks, which can suffer a *β*-elimination process leading to the breakage of the polymeric network and to the formation of little fragments that can evolve at high temperature.

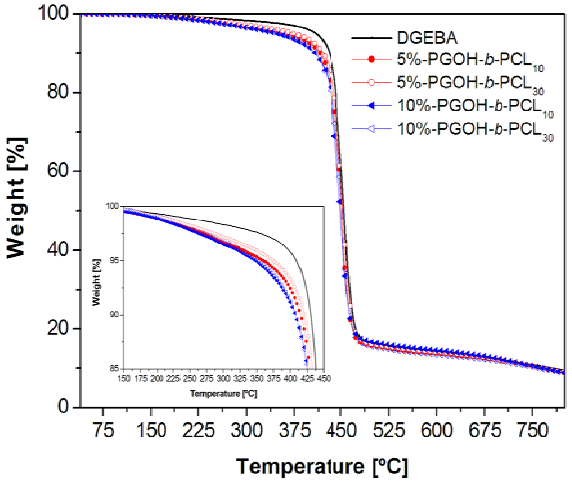

Figure 8 Thermogravimetric curves at 10 ºC/min in N_2 atmosphere of thermosetting materials obtained from DGEBA/1MI and DGEBA/1MI containing different proportions of PGOH-*b*-PCL_x

Journal of Polymer Science, Part A: Polymer Chemistry **2011**, 49, 2395 – 2406

Morphology characterization by ESEM

The toughness behavior of neat DGEBA and DGEBA/PGOH-*b*-PCL_x modified thermosets has been investigated looking at the morphology of the cryofracture observed by ESEM. **Figure 9** shows the micrographs of the morphologies of all the fractured materials.

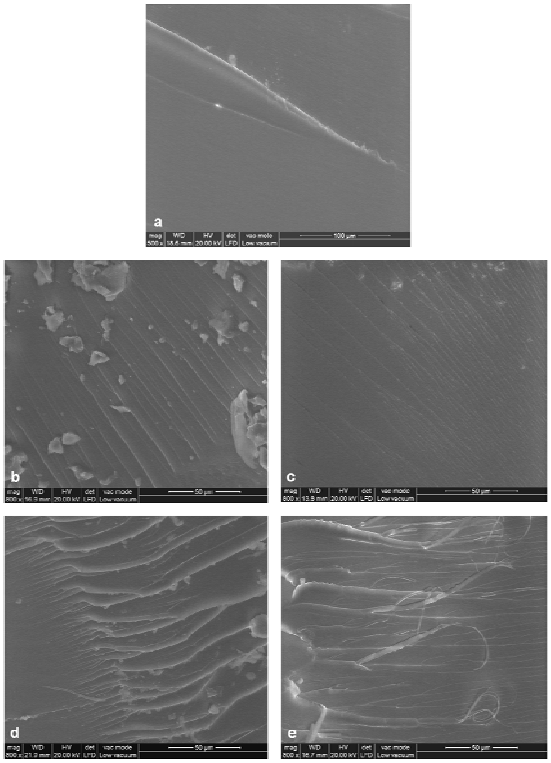

Figure 9 ESEM micrographs for cryofractured surfaces of the following materials cured 1.5 h at 120 ºC and post-cured 1 h at 150 ºC: **a**) DGEBA/1MI; **b**) 5 wt.% PGOH-*b*-PCL_{10}/DGEBA/1MI; **c**) 10 wt.% PGOH-*b*-PCL_{10}/DGEBA/1MI; **d**) 5 wt.% PGOH-*b*-PCL_{30}/DGEBA/1MI and **e**) 10 wt.% PGOH-*b*-PCL_{30}/DGEBA/1MI

First of all, it can be appreciated that the materials are homogeneous without any sign of micro- or nanophase separation, due to the good compatibility between PCL and the DGEBA network. Moreover, the fracture of the neat epoxy material (**a**) appears as a smooth glassy surface with an only deformation, which accounts for its poor impact strength. When the material contains 5 or 10 wt.% of PGOH-*b*-PCL_{10} some cracks appear without appreciable influence of the star proportion (**b** and **c**). When 5 or 10 wt.% of PGOH-*b*-PCL_{30} were added (**d** and **e**), the morphology changes and the micrographs present some fibrillation which is an indication of the transition from brittle to ductile stage. The presence of fibrils originated by plastic deformation could be due to the flexibility of the PCL arms as the extent of these fibrils increases on increasing the proportion of the star in the

thermoset. Thus, we can conclude that a more tough and ductile material is obtained with stars with longer PCL arms and toughness increases on increasing the star proportion in the formulation.

Conclusions

Following a "core-first" strategy, multiarm star copolymers based on hyperbranched poly(glycidol) core and poly(ε-caprolactone) arms of different arm lengths were obtained by a cationic ring-opening polymerization procedure. The stars obtained were characterized and their well defined architecture was demonstrated.

These star polymers were used as modifiers in the curing of DGEBA by 1-methylimidazole as anionic initiator. The addition of these modifiers to the reactive mixture slightly retarded the curing and increased the gelation time and the conversion at the gel point. In addition, the star modifiers reduced the global shrinkage on curing. It is expected that all these facts allow reducing the formation of internal stresses on curing. These effects were more pronounced when the arm length of the star was longer.

From the point of view of the processability, the addition of the synthesized stars to DGEBA formulations did not significantly increase much the viscosity and the addition of 5 wt.% of PGOH-*b*-PCL_{10} led even to a reduction of the viscosity in comparison to the neat formulation.

T_gs of the materials prepared were lower than that of the neat DGEBA but the special topology of the stars did not affect negatively this parameter on increasing the length of the arms. In contrast, the modulus in the rubbery state decreased on both, increasing the proportion of the star in the formulation or the length of the arms.

Because of the presence of the PCL blocks, the modified thermosets showed a reduction on thermal stability by 100 ºC compared with the neat epoxy thermoset. The materials obtained from PGOH-*b*-PCL_{10} could be considered as thermally reworkable thermosets.

The addition of PGOH-*b*-PCL_x modifiers to the formulation allowed to maintain the homogeneous appearance of the materials but changed the fracture surface from brittle to ductile, especially when the PGOH-*b*-PCL_{30} was added in a 10 wt.%.

Thus, one can conclude that PGOH-*b*-PCL_x star-like structures are suitable modifiers for epoxy resins enhancing toughness, reducing shrinkage and providing reworkability without affecting negatively the curing process and processability.

Acknowledgements

The authors from the Universitat Rovira i Virgili and Universitat Politècnica de Catalunya would like to thank MICINN (Ministerio de Ciencia e Innovación) and FEDER (Fondo Europeo de Desarrollo Regional) (MAT2008-06284-C03-01 and MAT2008-06284-C03-02) and to the Comissionat per a Universitat i Recerca de la Generalitat de Catalunya (2009-SGR-1512). All the authors thank to the Germany-Spanish collaboration program (HA2007-0022, DAAD PPP

Journal of Polymer Science, Part A: Polymer Chemistry **2011**, 49, 2395 – 2406

D/07/13493) for their financial support. M.M. acknowledges the grant FI-DGR 2009 from the Catalonian Government and the mobility fellowship from MICINN.

References

[1] May CA, editor. *Epoxy resins. Chemistry and technology.* Marcel Dekker, New York, **1988**.
[2] Petrie, E.M. *Epoxy adhesive formulations.* McGraw-Hill, New York, **2006**.
[3] Morell, M.; Erber, M.; Ramis, X.; Ferrando, F.; Voit, B.; Serra, A. Eur. Polym. J. **2010**, 46, 1498-1509.
[4] Yang, J.P.; Chen, Z.K.; Yang, G.; Fu, A.Y.; Ye, L. Polymer **2008**, 49, 3168-3175.
[5] Morell, M.; Ramis, X.; Ferrando, F.; Yu, Y.; Serra, A. Polymer **2009**, 50, 5374-5383.
[6] Zhang, J.; Guo, Q.; Fox, B. J. Polym. Sci., Part B: Polym. Phys. **2010**, 48, 417-424.
[7] Voit, B.; Lederer, A. Chem. Rev. **2009**, 109, 5924-5973.
[8] Corcione, C.E.; Frigione, M. Polym. Test. **2009**, 28, 830-835.
[9] Cicala, G., Recca, A. Polym. Eng. Sci. **2008**, 48, 2382-2388.
[10] Meng, Y.; Zhang, X.H.; Du, B.Y.; Zhou, B.X.; Zhou, X.; Qi, G.R. Polymer **2011**, 52, 391-399.
[11] Maier, S.; Sunder, A.; Frey, H.; Mülhaupt, R. Macromol. Rapid Commun. **2000**, 21, 226-230.
[12] Liu, C.; Zhang, Y.; Huang, J. Macromolecules **2008**, 41, 325-331.
[13] Gao, H.; Matyjaszewski, K. Macromolecules **2008**, 41, 1118-1125.
[14] Mendrek, M.; Trzebicka, B.; Walach, W.; Dworak, A. Eur. Pol. J. **2010**, 46, 2341-2351.
[15] Kanaoka, S.; Sawamoto, M.; Higashimua, T. Macromolecules **1991**, 24, 2309-2313.
[16] Xia, J.; Zhang, X.; Matyjaszewski, K. Macromolecules **1999**, 32, 4482-4484.
[17] Kautz, H.; Sunder, A.; Frey, H. Macromol. Symp. **2001**, 163, 67-73.
[18] Kainthan, R.K.; Muliawan, E.B.; Hatzikiriakos, S.G.; Brooks, D.E. Macromolecules **2006**, 39, 7708-7717.
[19] Chen, Y.; Shen, Z.; Barriau, E.; Krautz, H.; Frey, H. Biomacromolecules **2006**, 7, 919-926.
[20] Santiago, D.; Morell, M.; Fernández-Francos, X.; Serra, A.; Salla, J.M.; Ramis, X. React. Funct. Polym. **2011**, 71, 380-389.
[21] Burgath, A.; Sunder, A.; Neuner, I.; Mülhaupt, R.; Frey, H. Macromol. Chem. Phys. **2000**, 201, 792–797.
[22] Hans, M.; Mourran, A.; Henke, A.; Keul, H.; Moeller, M. Macromolecules **2009**, 42, 1031-1036.
[23] Guo, Q.; Groeninckx, G. Polymer **2001**, 42, 8647-8655.
[24] Fan, W.; Wang, L.; Zheng, S. Macromolecules **2009**, 42, 327-336.
[25] Hameed, N.; Guo, Q.; Hanley, T.; Mai, Y.W. J. Polym. Sci., Part B: Polym. Phys. **2010**, 48, 790-800.
[26] Chen, J.S.; Ober, C.K.; Poliks, M.D. Polymer **2002**, 43, 131-139.
[27] Sperling, L.H. *Introduction to Physical Polymer Science*. 4th ed, Wiley Interscience, Hoboken, New Jersey, **2006**, p. 573.
[28] Fernández-Francos, X.; Cook, W.D.; Serra, A.; Ramis, X.; Liang, G.G.; Salla, J.M. Polymer **2010**, 51, 26-34.
[29] Morell, M.; Fernández-Francos, X.; Ramis, X., Serra, A. Macromol. Chem. Phys. **2010**, 211, 1879-1889.
[30] Sunder, A.; Hanselmann, R.; Frey, H.; Mülhaupt, R. Macromolecules **1999**, 32, 4240-4246.
[31] Sunder, A.; Mülhaupt, R.; Frey, H. Macromolecules **2000**, 33, 309-314.
[32] Ramis, X.; Salla, J.M.; Mas, C.; Mantecón, A.; Serra, A. J. Appl. Polym. Sci. **2004**, 92, 381–393.

[33] Ramis, X.; Salla, J.M.; Cadenato, A.; Morancho, J.M. J. Thermal. Anal. Calorim. **2003**, 72, 707-718.
[34] Pascault, J.P., Sautereau, H., Verdu, J., Williams, R.J.J. *Thermosetting Polymers*, Marcel Dekker, New York, **2002**.
[35] Lin, Y.; Liu, X.; Dong, Z.; Li, B.; Chen, X.; Li, Y.S. Biomacromolecules **2008**, 9, 2629-2636.
[36] Fernández-Francos, X.; Salla, J.M.; Mantecón, A.; Serra, A.; Ramis, X. J. Appl. Polym. Sci. **2008**, 109, 2304-2315.
[37] Brandrup, J., Immergut, E.H. editors. *Polymer Handbook*. Wiley, New York, **1975**.
[38] Coleman, M.M.; Painter, P.C. Prog. Polym. Sci. **1995**, 20, 1-9.
[39] Dusek, K.; Lunak, S.; Matejka, L. Polym. Bull. **1982**, 7, 145-152.
[40] Miller, D.R.; Valles, E.M.; Macosko, C.W. Polym. Eng. Sci. **1979**, 19, 272-283.
[41] (a) Dell'Erba, I.E.; Williams, R.J.J. Polym. Eng. Sci. **2006**, 46, 351-359; (b) Ooi, S.K.; Cook, W.D.; Simon, G.P.; Such, C.H. Polymer **2000**, 41, 3639-3649; (c) Ricciardi, F.; Romanchick, W.A.; Joullie, M.M. J. Polym. Sci., Polym. Chem. Ed. **1983**, 21, 1475-1490; (d) Rozenberg, B.A. Adv. Polym. Sci. **1986**, 75, 113-165.
[42] Cicala, G.; Recca, A.; Restuccia, C. Polym. Eng. Sci. **2005**, 45, 225-237.
[43] Varley, R.J.; Tian, W. Polym. Int. **2004**, 53, 69-77.

IV.3

EFFECT OF POLYMER TOPOLOGY ON THE CURING PROCESS AND MECHANICAL CHARACTERISTICS OF EPOXY THERMOSETS MODIFIED WITH LINEAR OR MULTIARM STAR POLY(ε-CAPROLACTONE)

Mireia Morell, Xavier Ramis, Francesc Ferrando, Àngels Serra

Polymer ***2011****, 52, 4694 – 4702*

UNIVERSITAT ROVIRA I VIRGILI
NOUS TERMOESTABLES EPOXÍDICS MODIFICATS AMB ESTRUCTURES DENDRÍTIQUES DE TIPUS HIPERRAMIFICAT I ESTRELLA
Mireia Morell Bel
DL:T. 155-2012

Polymer **2011**, 52, 4694 – 4702

EFFECT OF POLYMER TOPOLOGY ON THE CURING PROCESS AND MECHANICAL CHARACTERISTICS OF EPOXY THERMOSETS MODIFIED WITH LINEAR OR MULTIARM STAR POLY(*ε*-CAPROLACTONE)

Mireia Morell,[1] Xavier Ramis,[2] Francesc Ferrando,[3] Àngels Serra[1]

[1] Department of Analytical and Organic Chemistry, Universitat Rovira i Virgili, C/ Marcel·lí Domingo s/n, Tarragona 43007, Spain.
[2] Thermodynamics Laboratory, ETSEIB Universitat Politècnica de Catalunya, Av. Diagonal 647, Barcelona 08028, Spain.
[3] Department of Mechanical Engineering, Universitat Rovira i Virgili, C/ Països Catalans, 26, Tarragona 43007, Spain.

Abstract

A well-defined multiarm star copolymer, hyperbranched poly(glycidol)-*b*-poly(*ε*-caprolactone), with an average of 100-110 arms per molecule and a molecular weight of arms of 1,000 g/mol (s-PCL) and a linear PCL analog (l-PCL) were used as modifiers in the curing of diglycidylether of bisphenol A (DGEBA) using ytterbium triflate as cationic initiator. The effect of the polymer topology on the curing and gelation was studied by dynamic scanning calorimetry (DSC) and rheometry. The addition of s-PCL to the resin left the complex viscosity (η^*) practically unaltered. In contrast the addition of l-PCL incremented substantially the viscosity. The addition of star-shaped modifiers decreased the shrinkage after gelation in a higher extent than the linear analog. The homogeneity of pure DGEBA and modified thermosets was proved by dynamic thermomechanical analysis (DMTA) and electronic microscopy (SEM). The addition of star-like structures led to a higher impact energy fracture in comparison to pure DGEBA and l-PCL modified thermosets and to a lower effect on the microhardness than the linear analog.

Keywords: star polymers; hyperbranched; epoxy resin

Introduction

Epoxy resins are widely used as coatings, electrical and electronic materials, adhesives and in structural applications because of their attractive properties such as thermal stability and good electrical characteristics [1-3]. However, their high crosslink density leads to a low impact resistance, which places a limitation on their potential range of applications. In addition to their brittleness, when epoxy resins are used as coatings, the shrinkage on curing can originate serious problems resulting from the generation of microvoids and microcracks, the loss of adhesion and deformation due to warping, all of which are promoted by the generation of internal stresses. These drawbacks reduce the protection capability and durability of the coating and allow corrosion of the substrate as a result of the penetration of moisture. On the other hand, at the end of the service life of the coated devices, it is difficult to recycle or to repair them because the epoxy coating cannot be easily removed by solvents or thermal treatment; only pyrolysis can be used, which involves a significant waste of energy in addition to some other problems.

An efficient route which has proved to improve toughening of thermosets is the use of flexible linear thermoplastic polymers. However, its substitution for dendritic

type polymers to modify epoxy thermosets is a current approach used to avoid some of the troubles that these kinds of modifiers present [4-6]. Some of the main negative aspects are the reduced solubility in the epoxy oligomer, especially when the molecular weight of the modifier is higher than 10^4 g/mol, which difficult the manipulation of the mixtures and the good dispersion of the catalyst. Moreover, the linear topology leads to a higher solution and melt polymer viscosities caused by the extensive chain entanglement taking place [7,8].

In previous studies we have explored the use of hyperbranched polymers (HBPs) to improve mechanical properties, reduce shrinkage on curing and increase the reworkability of epoxy thermosets. By this methodology all of these objectives were partially accomplished but we would like to go further on it [9-11].

Additionally to hyperbranched polymers, multiarm star copolymers can also be considered as a new class of reactive modifiers for epoxy resins [12]. We have recently studied the use of multiarm star-shaped block copolymers as reactive modifiers for epoxy thermosets. To do that, we synthesized well-defined multiarm star copolymers based on poly(glycidol)-*b*-poly(ε-caprolactone) of different arm length using the "core-first" strategy [13]. Formulations of these copolymers with DGEBA using 1-methylimidazole as anionic initiator were cured and the characteristics of the materials were determined [14]. The results obtained were very promising in reference to the reduction of the shrinkage, processability and also reworkability. The materials obtained showed a ductile fracture in comparison with the neat epoxy thermoset, but no mechanical properties were evaluated. In this study, we could conclude that the special star architecture led to a good processability of the uncured formulation, especially for stars with shorter arms.

Until now the chemical incorporation of hydroxyl terminated star copolymer during the cationic curing of DGEBA has not been reported. Therefore in the present work, we propose the use of a well-defined multiarm star copolymer, poly(glycidol)-*b*-poly(ε-caprolactone) (s-PCL), as chemical modifier of DGEBA so as to enhance the mechanical, physical and thermal characteristics of the thermosets by the introduction of flexible multi-arm branched structures into the network which will result in an improvement of toughness without negatively affecting the glass transition temperature (T_g) of the final materials, following related studies [15,16]. In order to establish the topology effects, we have compared the properties of epoxy thermosets modified with multiarm star copolymer or linear PCL of similar molecular weight.

Polymer **2011**, 52, 4694 – 4702

Experimental section

Materials

Glycidol (96 %) was distilled under reduced pressure and stored over molecular sieves at 2 - 5 ºC. Dioxane was dried over calcium hydride and subsequently distilled. *ε*-Caprolactone (*ε*-CL, 97 %) was dried over calcium hydride and subsequently distilled under vacuum. Trimethylolpropane (TMP, 97 %), linear poly(*ε*-caprolactone), potassium methylate solution (25 % v/v in methanol), ytterbium triflate ($Yb(OTf)_3$, 99 %) and tin (II) 2-ethylhexanoate ($Sn(Oct)_2$, 98 %) were used without further purification. All these products were purchased from Sigma-Aldrich. Solvents were purchased from Scharlab.

Diglycidylether of bisphenol A (DGEBA) Epikote Resin 827 was provided by Shell Chemicals (epoxide equivalent weight (EEW) = 182.1 g/eq, n = 0.082).

Preparation of multiarm star poly(glycidol)-b-poly(ε-caprolactone) (**Scheme 1**)

A well-defined multiarm star copolymer based on poly(glycidol)-*b*-poly(*ε*-caprolactone) (s-PCL) was synthesized employing as macroinitiator a hyperbranched poly(glycidol) obtained by anionic ring-opening polymerization of glycidol [17], with an average number of hydroxyl initiating sites of 100 - 110 per molecule.

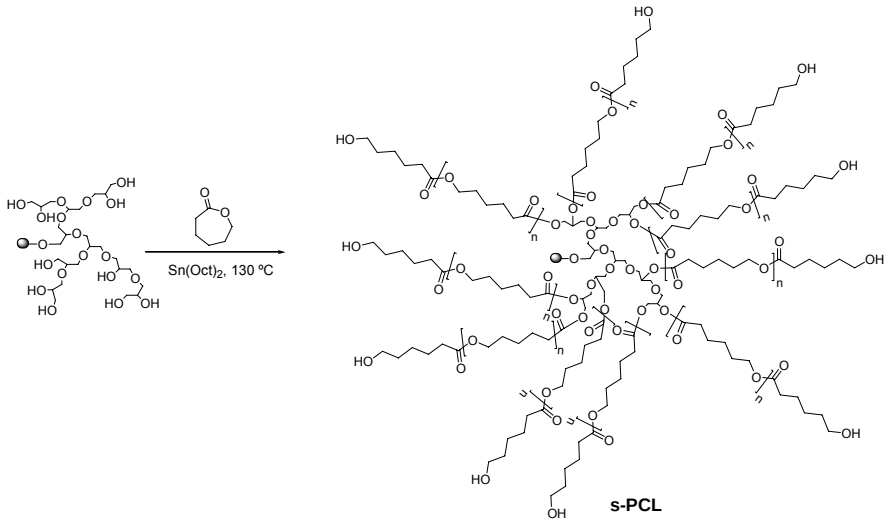

Scheme 1 Synthetic route to multiarm star copolymer s-PCL

The PCL arms were grown from the initiating sites of hyperbranched poly(glycidol) by cationic ring-opening polymerization of *ε*-caprolactone (*ε*-CL) using stannous (II) octoate ($Sn(Oct)_2$) as catalyst. The detailed synthetic procedure and the characterization of this multiarm star copolymer are described in a previous

publication [14]. In **Table 1** the characterization data obtained for l-PCL and s-PCL is specified.

Table 1 Data of the polymers used in this study

Entry	$\overline{M}_n$ (g/mol)	$\overline{M}_w / \overline{M}_n$	$\overline{DP}_{arm}$ [b]	N_{OH}	T_g [c] (ºC)	Δh_m [c] (J/g)	T_m [c] (ºC)	$T_{2\%}$ [d] (ºC)
s-PCL[a]	89.100	1.69	8	100-110	-	65.4	45.3	278
l-PCL	80.000	< 2.00	-	1	- 63	68.0	58.8	364

a. $\overline{M}_n$ and PDI were determined by SEC-MALLS with DMAc as solvent.
b. Degree of polymerization ($\overline{DP}_{arm}$) was determined by ^{13}C NMR in quantitative conditions.
c. Data obtained from the second DSC scan at 10 ºC/min.
d. Temperature of the 2 % of weight loss under N_2 at 10 ºC/min.

Preparation of epoxy thermosets

The mixtures were prepared by adding the required amount of s-PCL or l-PCL into the epoxy resin and gently heating (150 ºC) until it was dissolved and the solution became clear. Then, 1 phr (part per hundred parts of mixture) of ytterbium triflate was added and the resulting solution was stirred and cooled down to - 10 ºC to prevent polymerization. Mixtures containing 5 – 10 wt.% (by weight) of s-PCL or l-PCL were prepared. A neat formulation with DGEBA and 1 phr of ytterbium triflate was prepared to compare with the modified formulations. The compositions of the formulations studied are detailed in **Table 2.**

Characterization

The FTIR spectra were collected in a spectrophotometer FTIR-680PLUS from JASCO with a resolution of 4 cm^{-1}. This device was equipped with an attenuated-total-reflection accessory with a diamond crystal (Golden Gate heated single-reflection diamond ATR, Specac-Teknokroma).

Calorimetric analyses were carried out on a Mettler DSC-822e thermal analyzer. Samples of ~ 5 mg in weight were placed in aluminum pans under nitrogen atmosphere. The calorimeter was calibrated using an indium standard (heat flow calibration) and an indium-lead-zinc standard (temperature calibration).

Star-PCL and linear PCL were heated from – 50 to 150 ºC with a heating rate of 10 ºC/min, cooled down to – 100 ºC with a cooling rate of – 10 ºC/min and then heated again to 150 ºC at the same heating rate. T_g, Δh_m and T_m values were obtained from the second heating curves. Thermal data are collected in **Table 1**.

Non-isothermal curing experiments were performed from 30 to 250 ºC at heating rates of 2, 5, 10, and 15 ºC/min to determine the reaction heat and the kinetic parameters. In non-isothermal curing process the degree of conversion by DSC (α_{DSC}) was calculated as follows:

$$\alpha_{DSC} = \frac{\Delta H_T}{\Delta H_{dyn}} \quad (1)$$

Polymer **2011**, 52, 4694 – 4702

where ΔH_T is the heat released up to a temperature T, obtained by integration of the calorimetric signal up to this temperature, and ΔH_{dyn} is the total reaction heat associated with the complete conversion of all reactive groups obtained dynamically.

The glass transition temperatures (T_gs) of the completed cured materials were determined, by means of a second scan at 20 ºC/min, as the temperature of the half-way point of the jump in the heat capacity when the material changed from glassy to the rubbery state under N_2 atmosphere and the error is estimated to be approximately ± 1 ºC.

The kinetic triplet [pre-exponential factor, activation energy and kinetic model] of the curing process was determined using integral isoconversional non-isothermal kinetic analysis, Kissinger-Akahira-Sunose equation, combined with the Coats-Redfern procedure. Details of the kinetic methodology are given in previous publications [18,19].

The miscibility of the mixtures on increasing the temperature were investigated with an optical microscope Axiolab Zeiss equipped with a Linkam THMS 600 hot-stage connected to a TP-92 temperature control unit.

Thermogravimetric analyses were carried out in a Mettler TGA/SDTA851e/LF/1100 thermobalance. Samples with an approximate mass of 8 mg were degraded between 30 and 800 ºC at a heating rate of 10 ºC/min in N_2 (100 cm^3/min measured in normal conditions).

Dynamic mechanical analyses were carried out with a TA Instruments DMA Q800. The samples were cured isothermally in a mould at 150 ºC for 5 h and then post-cured for 4 h at 180 ºC. Single cantilever bending at 1 Hz was performed at 3 ºC/min, from 40 ºC to 250 ºC on prismatic rectangular samples (20 x 5 x 1.5 mm^3).

Rheological measurements were carried out in the parallel plates (geometry of 25 mm) mode with an ARG2 rheometer (TA Instruments, UK, equipped with a Peltier system). The gelation time was determined by setting the device in time sweep and multiwave oscillation mode. Experiments were performed isothermally at 110 ºC. Because the viscosity of the system changes significantly during the curing process, a control program was used in which the oscillation amplitude diminishes with an increase in the applied stress. By doing so, the curing process can be characterized in the whole range of conversion. Gel time was taken as the point where tan δ is independent of frequency [20]. The conversion at gelation (α_{gel}) was determined by stopping the rheology experiment at gelation and performing a subsequent dynamic DSC scan of the gelled sample.

The contraction after gelation (S_{gel}) was registered isothermally at 150 ºC by setting the normal force to zero and controlling the decrease of the gap as function of time. The initial gap point (h_0) was taken at the gel point and the actual gap point

(*h*) when the gap befell constant. The equation, derived by Shah et al. [21], to find out S_{gel} is described as follows:

$$S_{gel} = \left[\left(1+\frac{1}{3}\left(\frac{h-h_0}{h_0}\right)\right)^3 - 1\right] x100 \quad (2)$$

Two assumptions have to be taken into account: the first is that resin sample in plane strains are zero and the second that resin is incompressible.

Complex viscosity (η^*) of the pre-cured mixtures was recorded as function of angular frequency (0.1 – 100 rad/s) stating a constant deformation of 50 % at 110 ºC.

Microhardness was measured with a Wilson Wolpert (Micro- Knoop 401MAV) device following the ASTM D1474-98 (2002) standard procedure. For each material 10 determinations were made with a confidence level of 95 %. The Knoop microhardness (HKN) was calculated from the following equation:

$$HKN = L / A_p = L / l^2 \cdot C_p \quad (3)$$

where, L is the load applied to the indenter (0.025 Kg), A_p is the projected area of indentation in mm^2, l is the measured length of long diagonal of indentation in mm, C_p is the indenter constant (7.028×10^{-2}) relating l^2 to A_p. The values were obtained from 10 determinations with the calculated precision (95 % of confidence level).

The impact test was performed at room temperature by means of an Izod 5110 impact tester, according to ASTM D 4508-05 (2008) using rectangular samples (25 x 12 x 2 mm^3). The pendulum employed had a kinetic energy of 1 J.

The fracture area of the specimens after impact tests metalized with gold was observed with a Jeol JSM 6400 with a resolution of 3.5 nm.

Polymer **2011**, 52, 4694 – 4702

Results and discussion

Curing of DGEBA with different proportions of s-PCL or l-PCL

In a previous work it was confirmed that 1 phr of $Yb(OTf)_3$ was enough to assure the complete cure of DGEBA [22]. Therefore, this amount of initiator was selected to prepare the formulations studied, which are collected in **Table 2**.

Table 2 Composition and calorimetric data of DGEBA/$Yb(OTf)_3$ mixtures with different percentages of star-PCL or linear-PCL

Formulation[a] (wt.%)	initiator: epoxy	OH: epoxy	E_a[b] (kJ/mol)	ln A[c] (s^{-1})	$k_{180\,°C}$ x 10^3 (s^{-1})	Δh (J/g)	Δh[e] (kJ/ee)	T_{max} (ºC)	T_g[f] (ºC)
0	0.0029	0.041	79	16.08	6.48	512	93.2	175	132
s-PCL									
5	0.0031	0.055	72	12.84	5.76	507	97.1	188	114
10	0.0032	0.067	77	13.84	5.22	488	98.7	192	106
l-PCL									
5	0.0031	0.042	81	15.93	3.57	478	91.6	199	129
10	0.0032	0.043	98	20.62	4.93	448	90.6	194	110

a. % by weight of polymeric modifier.
b. Values of activation energies at 50 % of conversion were evaluated by isoconversional non-isothermal procedure.
c. Values of pre-exponential factor for R_3 kinetic model with $g(\alpha) = 1-(1-\alpha)^{1/3}$.
d. Values of rate constant at 180 ºC calculated using the Arrhenius equation.
e. Enthalpy value per equivalent of epoxy group.
f. Glass transition temperature obtained by DSC. Second scan after isothermal curing 5 h at 150 ºC and post-curing 4 h at 180 ºC.

Figure 1 shows the DSC exotherms (**a**) and the plot of the degree of conversion against temperature (**b**) recorded at 5 ºC/min of neat DGEBA and s-PCL/DGEBA or l-PCL/DGEBA formulations initiated by $Yb(OTf)_3$.

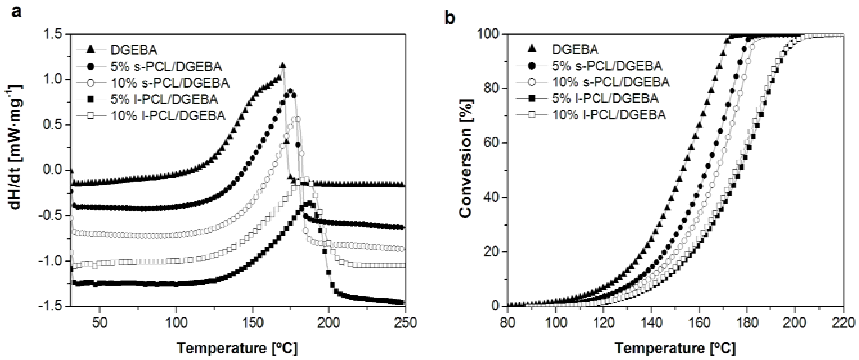

Figure 1 DSC scanning curves (**a**) and conversion degree (**b**) against temperature of the curing of DGEBA and DGEBA containing 5 and 10 wt.% of s-PCL or l-PCL at a heating rate of 10 ºC/min

At temperatures below 50 ºC the mixtures containing l-PCL show a very little endotherm that can be attributed to the presence of a small proportion of crystallites of PCL in the mixture. In contrast, the curves of mixtures containing s-PCL do not show any melting endotherm. In **Table 1** we can see that both PCL structures are semicrystalline, since melting temperatures could be measured. The fact that only l-

PCL curves present endotherms indicates that the solubility of the star polymer is higher than the linear analog. Moreover, the crystallization rate should be lower in the case of s-PCL, because of its topology. Actually, mixtures containing l-PCL had a milky appearance at room temperature in comparison with the s-PCL ones which were completely transparent. By optical microscopy it was possible to observe that l-PCL reached a total solubility in the epoxy resin on increasing the temperature.

The cure exotherms for all the formulations studied show similar shapes, but broader for the ones containing linear PCL. All the modified formulations show a deceleration in the conversion curves in reference to the neat resin. It can be seen, that on increasing the proportion of s-PCL the curing process slows down and the delay is even more pronounced on adding l-PCL to the formulation. Unexpectedly, there is not much influence of the proportion of this modifier in the curing evolution. The difference in the curing evolution between mixtures containing linear or star topologies could be attributed to different factors. The first one is the viscosity of the reactive mixture, higher for the linear modified formulations, as it will be further demonstrated. In addition, it should not be discarded the effect of the miscibility of the mixture, which is poorer for the linear analog. The second factor is related to the presence of a higher proportion of hydroxyl groups in the reactive mixture. Cationic epoxy polymerizations can take place by two different mechanisms: active chain end (ACE) and monomer activated (AM). Hydroxyl groups favor the second and increase the curing rate [23]. Mixtures containing s-PCL have a higher proportion of hydroxyl groups than the ones containing the linear polymer. Both factors accounts for a higher reactivity of the star modified formulations.

The kinetic parameters of the curing process were calculated and the values are collected in **Table 2**. Activation energies and pre-exponential factors are of the same order of magnitude and consistent with a cationic polymerization. From these parameters, by the Arrhenius equation, the constant rates at 180 ºC were calculated which fits with the order of reactivity observed in **Figure 1**(**b**).

Calorimetric data of the curing process of the formulations studied are collected in the same table. The heat released is mainly due to the opening of epoxy groups because of the ring strain. It is shown that the enthalpy per gram of mixture decreases on increasing the proportion of modifier. However, the enthalpy per epoxy equivalent for all the formulations exhibits a value of 90-100 kJ/ee which is accepted for epoxy resin curing [24]. The formulations containing star topologies show a higher heat release possibly due to the effect of the hydroxyl groups.

On increasing the proportion of modifier in the thermoset the T_g decreases, and this decrease is greater for the s-PCL modified formulations. This fact can be related to the presence of hydroxyl groups as chain ends, leading to more contribution of the AM mechanism and therefore to chain transfer processes that finally reduces the crosslinking density. Also, the interpenetration of the arms of the star in the epoxy network increases the plasticization of the material.

Polymer **2011**, 52, 4694 – 4702

By FTIR-ATR spectroscopy we could prove the complete curing of the formulations, since all the epoxy groups were reacted as shown by the disappearance of the absorption at 913 cm^{-1}.

The FTIR spectra of the pure s-PCL and l-PCL at 20 ºC present a main sharp absorption band at 1720 cm^{-1} attributed to the stretching vibration of carbonylic groups in crystalline domains [25]. After curing we observed that in the spectra of the thermosets containing a 10 wt.% of the star or linear polymers the main peak is shifted to 1732 cm^{-1}. This fact indicates that PCL arms are in the amorphous state in the thermoset. Thus, it can be deduced that a good compatibility exists between the modifiers and the epoxy matrix.

Rheological and shrinkage properties of the formulations

Multiarm star-branched polymers are known to behave like monomeric rigid spheres, in contrast to other branched polymers. The hydrodynamic volumes of such polymers are highly restricted due to their topologically branched structures. Compared to linear analogs with the same molecular weights, stars present less entanglement which is the main responsible for lower viscosity [26]. Therefore, these topologies are of interest when a low viscosity is desired as is the case of the coating technology.

By rheological experiments the complex viscosity of the mixtures at 110 ºC was determined on varying the angular frequency, as it is shown in **Figure 2**.

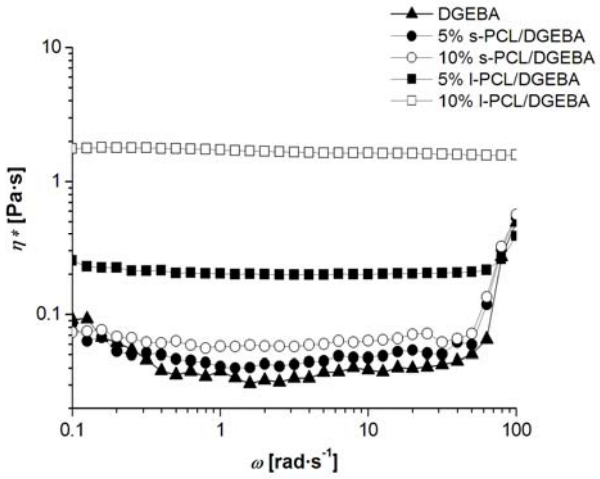

Figure 2 Complex viscosity (η^*) against angular frequency (ω) at 110 ºC for neat DGEBA and DGEBA containing 5 and 10 wt.% of s-PCL or l-PCL

All formulations show a Newtonian behavior in this range of frequencies. It should be noted that when the angular frequency is higher than 40 rad/s the neat formulation and the reactive mixtures containing s-PCL show an increased complex

viscosity which can be explained by the initiation of the curing that takes place for these systems at this temperature.

From the viscosity values, we can see that the addition of the star polymer in the reactive mixture does not increase much the viscosity which is quite different from the behavior observed on adding l-PCL. This fact evidences the advantages in the use of star-shaped polymers in epoxy systems in comparison to the use of their linear analogues as toughening agents.

Gelation process is an important phenomenological issue because after gelation the material losses its mobility and the internal stresses can appear if contraction occurs. Moreover, gelation times are important since they are related to the pot-life of the reactive mixture and therefore, to study the gelation characteristics is pretty important for the potential applicability of the coating.

In **Table 3** the gelation times and the conversion at the gel point (α_{gel}) are collected. As we can see, the gel time increases with the proportion of modifiers being slightly longer than that of the neat formulation. There are not big differences in the conversion at the gelation for all the formulations studied but it seems that the multifunctionality of the star topology reduces slightly this value. The linear topology does not influence the conversion values because it does not play any role in the curing reaction.

Table 3 Rheological, thermomechanical and thermogravimetrical data of the systems studied

Formulation[a] (wt.%)	t_{gel} (min)	α_{gel}[b] (%)	$T_{\tan\delta}$[c] (ºC)	E'[d] (MPa)	T_{onset}[e] (ºC)	T_{max}[f] (ºC)
0	12.5	31	150	34.0	298	362
s-PCL						
5	14.7	26	125	22.9	277	334
10	17.0	25	109	13.9	273	335
l-PCL						
5	16.4	28	135	24.8	280	334
10	20.5	32	121	18.6	284	331

a. % by weight of polymeric modifier.
b. Determined as the conversion reached by rheometry and DSC tests at 10 ºC/min.
c. Temperature of maximum of the tan δ at 1 Hz.
d. Relaxed modulus determined at the $T_{\tan\delta}$ + 50 ºC.
e. Temperature of the onset decomposition on the TGA data at 10 ºC/min calculated for a 2 % of weight loss.
f. Temperature of the maximum decomposition rate based on the TGA data at 10 ºC/min.

In addition to study the rheological behavior a rheometer can be also configured to measure the linear shrinkage. Torque or strain-controlled tests can be performed to monitor dimensional changes of the resin as it cures [27,28]. The low viscosity of the reactive mixtures before gelation makes difficult the correct measurement of the gap increment between plates. In contrast, the post-gelation shrinkage can be accurately registered. In fact, the shrinkage after gelation is the responsible of the appearance of internal stresses and defects in the thermoset.

Polymer **2011**, 52, 4694 – 4702

Therefore, its reduction is one of the main goals to improve the durability of the coatings.

As we can see in **Figure 3**, there is a notable reduction on the shrinkage on adding the star-shaped modifier in comparison to what happens on adding the linear analog. Probably, the s-PCL incorporated into the network increases the free volume and consequently reduces the shrinkage. Thus, from the point of view of the shrinkage evolution, again the selection of star topologies as modifiers is advantageous because it contributes to reduce in a higher extent the generation of internal stresses.

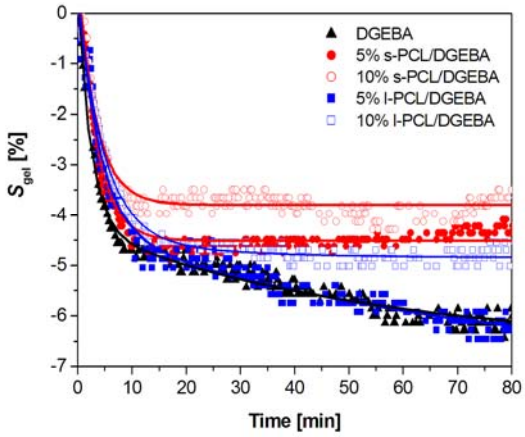

Figure 3 Shrinkage after gelation (S_{gel}) against time at 150 ºC for neat DGEBA and DGEBA containing 5 and 10 wt.% of s-PCL or l-PCL

Thermal and thermomechanical properties of the thermosets obtained

The materials obtained were characterized by DMTA. The tan δ plot against temperature for all the materials are represented in **Figure 4** and the thermomechanical data collected in **Table 3**.

As we can see, the tan δ curves are unimodal and no relaxations were appreciated at low temperature. Both facts evidence the homogeneous character of the modified materials. On increasing the proportion of star or linear modifier, tan δ value decreases and this decrease is more evident for the star modified thermosets. The size of the relaxation curves for star modified materials is greater than for the materials containing the linear analog which indicates better damping characteristics of the formers.

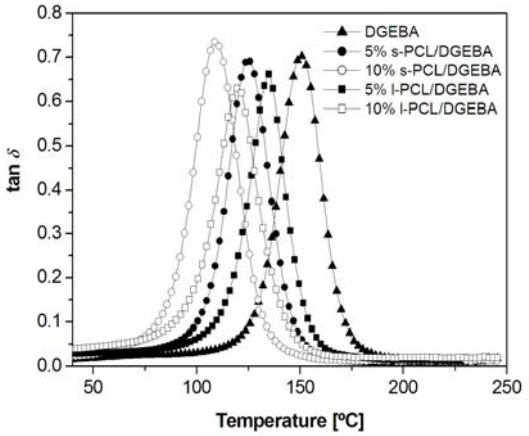

Figure 4 Tan *δ* against temperature at 1 Hz for the thermosets obtained

In **Table 3** the decrease of the modulus after relaxation on adding the modifier can be appreciated. This parameter is affected by the plasticizing effect caused by both linear and star topologies because it is related with the degree of crosslinking and the rigidity of the thermoset. Comparing both topologies it is possible to state that star modified thermosets present a lower modulus than the linear ones caused by a higher interpenetrating degree of the star arms into the epoxy matrix which increases the plasticizing effect and also by the chain transfer reactions originated by AM polymerization mechanism. The linear analog cannot be easily unentangled, due to its topology and the worse solubility in the epoxy resin. This could be an explanation of the higher tan *δ* values and the higher storage modulus at the rubbery state observed in comparison with the s-PCL modified thermosets.

The thermal stability of the materials obtained was investigated by thermogravimetry and the data are collected in **Table 3**. The modified thermosets show a slightly lower thermal stability than the unmodified thermoset, which can be attributed to the breakage of polyester chains through a *β*-elimination process. None of the modified thermosets can be considered as a reworkable [29]. The obtained results differ from the ones obtained when s-PCL was used as modifier in the anionic curing of DGEBA. In that case, the initial degradation temperature was below 250 ºC and the materials could be considered as reworkable [14].

Mechanical properties of the s-PCL and l-PCL modified thermosets

Several authors [5,6,15,30] studied the effect of hyperbranched polymers (HBPs) as toughners in epoxy resins and they could demonstrate their beneficial effect on this property. The maximum effect was obtained in phase separated materials forming globular micro or nanoparticles in a continuous epoxy matrix but high improvements were also observed in homogeneous modified materials because of the plasticization of the matrix that increases the ductility. Until now there are no reported data on the effect of multiarm star polymers as modifiers in epoxy resin on the impact strength.

Polymer **2011**, 52, 4694 – 4702

The effect of adding s-PCL or l-PCL to the formulations in the impact strength is shown in **Figure 5** (**a**).

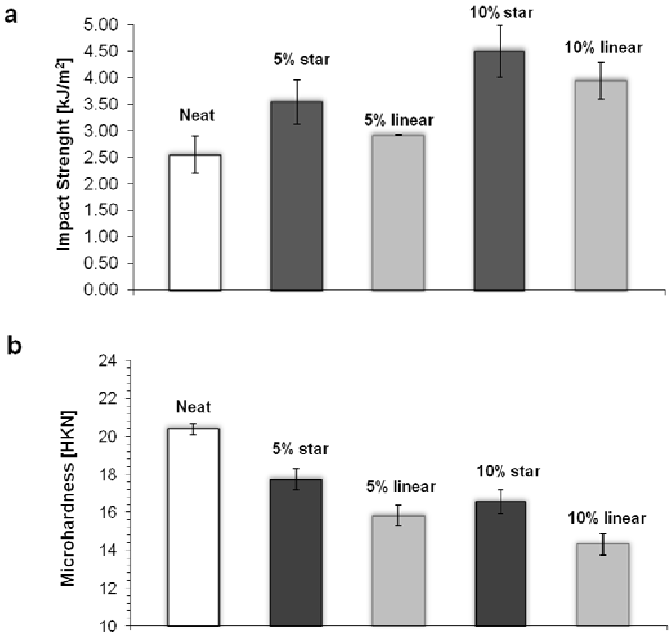

Figure 5 Impact strength (**a**) and microhardness (**b**) for the thermosets obtained

The values correspond to the energy consumption of the material in preventing crack propagation. It is possible to observe that the modification of DGEBA with star or linear PCL topologies improves this value in comparison with the neat material. Comparing both polymer architectures, the addition of s-PCL leads to higher improvements. A 75 % increase in the impact resistance, in reference to the neat material, was obtained for the modified thermoset containing a 10 wt.% of s-PCL. On the other hand, 10 wt.% l-PCL modified thermoset showed a lower improvement (55 %). The superior increase in toughness of multiarm star-modified thermosets obtained in the present study can be explained by the higher capacity of the arms of the star to interpenetrate into the epoxy network which increases the number of flexible points capable to be plastically deformed, increasing the ductility, which can be related to the reduction in the T_g value.

Indentation hardness measurements have proven to be useful in rating coatings on rigid substrates for their resistance to mechanical abuse, such as that produced by blows, gouging and scratching. As we can see in **Figure 5** (**b**), all the modified materials have a lower hardness value because of the plasticization caused by the addition of star and linear PCL modifiers. However, this decrease is slightly lower for the s-PCL, which is an advantage from the point of view of the applicability of these materials as coatings. This fact could be justified because of the presence of hydroxyl groups as chain ends in the star that can become covalently linked to the epoxy matrix.

Fractography by SEM

The toughness behaviour of DGEBA and the star and linear modified thermosets can be explained in terms of the morphologies observed by SEM. The fracture surfaces after impact tests were investigated by this technique and the most representative micrographs are shown in **Figure 6**.

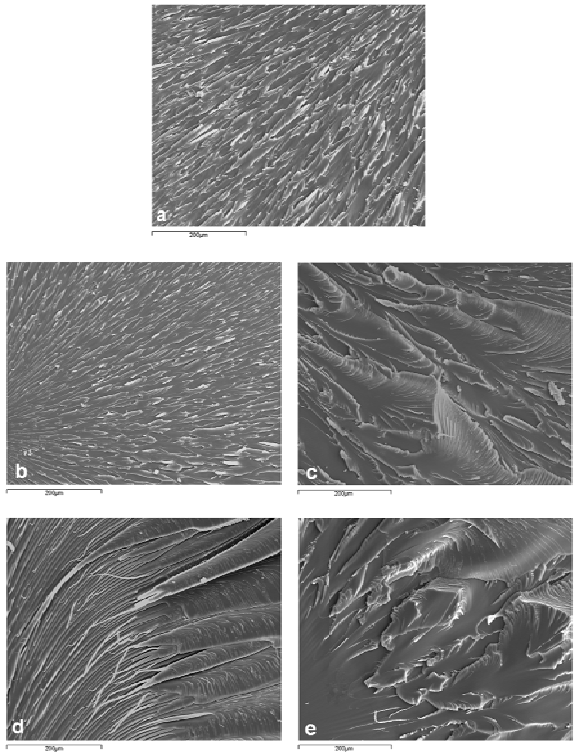

Figure 6 SEM micrographs for fractured surfaces of the following materials cured 5 h at 150 ºC and post-cured 4 h at 180 ºC: **a**) DGEBA; **b**) 5 wt.% l-PCL/DGEBA; **c**) 5 wt.% s-PCL/DGEBA; **d**) 10 wt.% l-PCL/DGEBA and **e**) 10 wt.% s-PCL/DGEBA

As it can be seen, all the micrographs presented a homogeneous appearance without any sign of phase separation due to the good compatibility of poly(*ε*-caprolactone) and DGEBA. The smooth glassy fractured surface, with little cracks, of the unmodified material **Figure 6** (**a**) accounts for its low impact strength. In contrast, the fracture surface of the materials with a 5-10 wt.% of l-PCL **Figure 6** (**b** and **d**) or with a 5-10 wt.% of s-PCL **Figure 6** (**c** and **e**) are rougher than that of the unmodified thermoset, suggesting that the impact specimens break more yieldingly. A higher amount of plastic deformation bands appear in the surfaces of these materials, which helps dissipating the fracture energy. This toughness improvement can be explained in terms of *in situ* reinforcing and toughening mechanism. The fibrils that appear in **Figure 6** (**d**) may arise from the l-PCL being pulled, since this polymer cannot react with epoxy matrix. Lower proportion of l-PCL does not lead to

the formation of fibrils, which is in accordance with the lower impact resistance measured. In contrast, the addition of different proportions of s-PCL to the formulation does not influence much the fracture morphology, although differences in the impact resistance were determined.

Conclusions

Following a "core-first" strategy, multiarm star copolymer was obtained by a cationic ring-opening polymerization of *ε*-caprolactone from hyperbranched poly(glycidol). The star obtained was used as modifier in the curing of DGEBA using $Yb(OTf)_3$ as cationic initiator. Linear poly(*ε*-caprolactone) of the same average molecular weight was also tested as modifier in order to compare the effect of both topologies. The addition of these modifiers to the reactive mixture slightly retarded the curing and increased the gelation time, especially for the linear modifier.

The addition of the star-shaped modifier reduced the shrinkage after gelation in a higher extent than the linear polymer. The linear topology increased the viscosity of the DGEBA formulations due to the entanglement, in contrast to that observed on adding the star-like PCL. Therefore, it is worth to state that the star topology does not worsen the processability of the neat formulation.

The T_gs of the modified materials were lower than that of the neat DGEBA but higher than 100 ºC, being higher for the materials modified with linear PCL.

Impact strength was improved on adding both s-PCL and l-PCL, but the highest value was obtained when a 10 wt.% of s-PCL was added to the formulation. Microhardness was slightly reduced by adding both modifiers, but a lower reduction was observed for the s-PCL modified thermosets, probably due to its covalent incorporation to the matrix.

The addition of s-PCL and l-PCL modifiers to the formulation allowed maintaining the homogeneous appearance of the materials but changed the fracture surface from brittle to ductile, especially when both modifiers were added in a 10 wt.%.

As a general conclusion star-like structures, in comparison to their linear analogs, are suitable epoxy resins modifiers due to their potential as toughening agents together with the capacity of reduce the curing shrinkage, without harmfully affecting the curing process and processability.

Acknowledgements

The authors from the Universitat Rovira i Virgili and Universitat Politècnica de Catalunya would like to thank MICINN (Ministerio de Ciencia e Innovación) and FEDER (Fondo Europeo de Desarrollo Regional) (MAT2008-06284-C03-01 and MAT2008-06284-C03-02) and to the Comissionat per a Universitat i Recerca de la Generalitat de Catalunya (2009-SGR-1512). M.M. acknowledges the grant FI-DGR 2009 from the Catalonian Government.

References

[1] May CA, editor. *Epoxy resins. Chemistry and technology*. Marcel Dekker, New York, **1988**, Chapter 1.
[2] Petrie, E.M. *Epoxy adhesive formulations.* McGraw-Hill, New York, **2006**.
[3] Pascault, J.P., Sautereau, H., Verdu, J., Williams, R.J.J., *Epoxy Polymers*, Wiley-VCH, Weinheim, **2010**.
[4] Cicala, G.; Recca, A.; Restuccia, C. Polym. Eng. Sci. **2005**, 45, 225-237.
[5] Yang, J.P.; Chen, Z.K.; Yang, G.; Fu, A.Y.; Ye, L. Polymer **2008**, 49, 3168-3175.
[6] Zhang, J.; Guo, Q.; Fox, B. J. Polym. Sci., Part B: Polym. Phys. **2010**, 48, 417-424.
[7] Corcione, C.E.; Frigione, M. Polym. Test. **2009**, 28, 830-835.
[8] Cicala, G., Recca, A. Polym. Eng. Sci. **2008**, 48, 2382-2388.
[9] Morell, M.; Erber, M.; Ramis, X.; Ferrando, F.; Voit, B.; Serra, A. Eur. Polym. J. **2010**, 46, 1498-1509.
[10] Morell, M.; Ramis, X.; Ferrando, F.; Yu, Y.; Serra, A. Polymer **2009**, 50, 5374-5383.
[11] Morell, M.; Fernández-Francos, X.; Ramis, X., Serra, A. Macromol. Chem. Phys. **2010**, 211, 1879-1889.
[12] Meng, Y.; Zhang, X.H.; Du, B.Y.; Zhou, B.X.; Zhou, X.; Qi, G.R. Polymer **2011**, 52, 391-399.
[13] Burgath, A.; Sunder, A.; Neuner, I.; Mülhaupt, R.; Frey, H. Macromol. Chem. Phys. **2000**, 201, 792-797.
[14] Morell, M.; Lederer, A.; Ramis, X.; Voit, B.; Serra, A. J. Polym. Sci., Part A: Polym. Chem. **2011**, 49, 2395-2406.
[15] Fu, J.F.; Shi, L.Y.; Yuan, S.; Zhong, Q.D.; Zhang, D.S.; Chen, Y.; Wu. J. Polym. Adv. Technol. **2008**, 19, 1597-1607.
[16] Karger-Kocsis, J.; Fröhlich, J.; Gryshchuk, O.; Kautz, H.; Frey, H.; Mülhaupt, R. Polymer **2004**, 45, 1185-1195.
[17] Sunder, A.; Hanselmann, R.; Frey, H.; Mülhaupt, R. Macromolecules **1999**, 32, 4240-4246.
[18] Ramis, X.; Salla, J.M.; Mas, C.; Mantecón, A.; Serra, A. J. Appl. Polym. Sci. **2004**, 92, 381–393.
[19] Ramis, X.; Salla, J.M.; Cadenato, A.; Morancho, J.M. J. Thermal. Anal. Calorim. **2003**, 72, 707-718.
[20] Pascault, J.P., Sautereau, H., Verdu, J., Williams, R.J.J., *Thermosetting Polymers*, Marcel Dekker, New York, **2002**, p. 188.
[21] Shah, D.U.; Schubel, P.J. Polym. Test. **2010**, 29, 629-639.
[22] Castell, P.; Galià, M.; Serra, A.; Salla, J. M.; Ramis, X. Polymer **2000**, 41, 8465-8474.
[23] Salla, J.M.; Fernández-Francos, X.; Ramis, X.; Mas, C.; Mantecón, A.; Serra, A. J. Therm. Anal. Calorim. **2008**, 91, 385-393.
[24] Brandrup, J., Immergut, E.H. editors. *Polymer Handbook.* Wiley, New York, **1975**.
[25] Coleman, M.M.; Painter, P.C. Prog. Polym. Sci. **1995**, 20, 1-9.
[26] Higashihara, T.; Hayashi, M.; Hirao, A. Prog. Polym. Sci. **2011**, 36, 323-375.
[27] Haider, M.; Hubert, P.; Lessard, L. Composites: Part A **2007**, 38, 994-1009.
[28] Li, Q.; Hutcheson, S.A.; McKenna, G.B.; Simon, S.L. J. Appl. Polym. Sci. **2008**, 24, 2719-2732.
[29] Chen, J.S.; Ober, C.K.; Poliks, M.D. Polymer **2002**, 43, 131-139.
[30] Fröhlich, J.; Kautz, H.; Thomann, R.; Frey, H.; Mülhaupt, R. Polymer **2004**, 45, 2155-2164.

IV.4

SYNTHESIS OF A NEW MULTIARM STAR POLYMER BASED ON HYPERBRACHED POLY(STYRENE) CORE AND POLY(ε-CAPROLACTONE) ARMS AND ITS USE AS REACTIVE MODIFIER OF EPOXY THERMOSETS

Mireia Morell, David Foix, Albena Lederer, Xavier Ramis, Brigitte Voit, Àngels Serra

Journa of Polymer Science, Part A: Polymer Chemistry ***2011****, 49, 4639 – 4649*

UNIVERSITAT ROVIRA I VIRGILI
NOUS TERMOESTABLES EPOXÍDICS MODIFICATS AMB ESTRUCTURES DENDRÍTIQUES DE TIPUS HIPERRAMIFICAT I ESTRELLA
Mireia Morell Bel
DL:T. 155-2012

Journal of Polymer Science, Part A: Polymer Chemistry **2011**, 49, 4639 – 4649

SYNTHESIS OF A NEW MULTIARM STAR POLYMER BASED ON HYPERBRANCHED POLY(STYRENE) CORE AND POLY(ε-CAPROLACTONE) ARMS AND ITS USE AS REACTIVE MODIFIER OF EPOXY THERMOSETS

Mireia Morell,[1] David Foix,[1] Albena Lederer,[2] Xavier Ramis,[3] Brigitte Voit,[2] Angels Serra[1]

[1] Department of Analytical and Organic Chemistry, University Rovira i Virgili, C/ Marcel·lí Domingo s/n, Tarragona 43007, Spain.
[2] Leibniz-Institut für Polymerforschung Dresden, Hohe Strasse 6, Dresden 01069, Germany.
[3] Thermodynamics Laboratory, ETSEIB University Politècnica de Catalunya, C/ Av. Diagonal 647, Barcelona 08028, Spain.

Abstract

A well-defined multiarm star copolymer poly(styrene)-*b*-poly(ε-caprolactone) (PSOH-*b*-PCL) with an average number of PCL arms per molecule of 60 has been prepared. 4-Chloromethyl styrene (4-CMS) was polymerized by means of atom transfer radical polymerization (ATRP) to obtain a hyperbranched poly(styrene) with chlorines as terminal groups. Subsequently, chlorines were substituted by reaction with diisopropanolamine (DIPA) to give the hydroxyl-ended derivative. Finally, the hydroxyl ended hyperbranched poly(styrene) has been used as a macroinitiator core to polymerize ε-caprolactone by means of cationic ring-opening polymerization so as to obtain the star copolymer. In a second step, PSOH-*b*-PCL was used as reactive modifier of diglycidylether of bisphenol A (DGEBA) formulations cured by 1-methyl imidazole (1MI) obtaining nanostructured thermosets. The curing process was studied by dynamic scanning calorimetry and infrared spectroscopy (FTIR). By rheometry the effect of this new polymer topology on the complex viscosity (η^*) of the reactive mixture and on the gelation process was also analyzed. The thermomechanical characteristics of the modified materials were determined.

Keywords: anionic polymerization; epoxy resin; hyperbranched; star polymers; thermosets

Introduction

Epoxy resins are known to be commonly used as thermosetting materials due to their excellent thermal and mechanical properties [1,2]. However, their inherent fragility can lead to the appearance of fractures which render the coating useless.

In terms of toughness improvement, different strategies have been developed for epoxy thermosets. The main one involves the use of flexible linear or dendritic polymers capable to plasticize the epoxy matrix increasing the ductility. This fact, despite of improving this property, usually worsen the thermomechanical characteristics of the modified materials [3-5].

In contrast, it has been observed that the formation of microstructures or nanostructures improves the overall properties without dropping down the crosslinking degree of the epoxy matrix. One of the possibilities employed to generate self-assembled structures is to start using a block copolymer completely miscible in the reactive mixture. In this case, phase separation of one of the blocks is achieved during the crosslinking polymerization while the other one remains

miscible at high degree of conversion. This methodology has been commonly applied employing diblock, triblock or tetrablock linear copolymers [6].

Additionally to linear block copolymers, multiarm stars can also be considered as a new class of modifiers for epoxy resins capable of generating self-assembled matrices [7]. Using this strategy, Meng *et al.* obtained nanostructured diglycidylether of bisphenol A (DGEBA) thermosets using core-crosslinked stars (CCS) based on poly(styrene) core with poly(ethylene oxide) or poly(styrene)-*b*-poly(ethylene oxide) arms both synthesized by the "arm-first" approach [8-9].

In addition to the "arm-first" method, another strategy established to obtain well-defined multiarm star copolymers is the "core-first" approach where the arms are grown from a multifunctional core. As dendrimers are not suitable due to their rather complicated and expensive synthesis, hyperbranched polymers (HBPs) are recommended to act as core molecules [10-12].

Hyperbranched poly(4-chloromethyl styrene) (PS), obtained via self-condensing vinyl polymerization (SCVP) using controlled atom transfer radical polymerization (ATRP) has been the object of several previous studies [13,14]. The benzyl position of chlorines in this HBP allows the nucleophilic substitution by several agents. Voit and coworkers [15] have substituted the final chlorine groups to obtain modified hyperbranched poly(styrene) with different polarities. However, the introduction of hydroxyl groups in this HBP has not been reported until now, but it is interesting with regard to further increase the complexity of the structures by getting new architectures, such as multiarm stars.

Multiarm poly(ε-caprolactone) (PCL) star copolymers have been synthesized by ring-opening polymerization of ε-caprolactone using poly(glycidol) as macroinitiator and $Sn(Oct)_2$ as catalyst [16,17]. PCL is a hydrophobic, semicrystalline polyester with a high chain flexibility which is miscible in the most epoxy systems [18-20].

In this article, we synthesize a new multiarm star block copolymer, poly(styrene)-*b*-poly(ε-caprolactone) (PSOH-*b*-PCL), using the hydroxyl terminated hyperbranched (PSOH) as core. As the PCL arms can act as the miscible block, we could expect the formation of nanoparticles in the epoxy matrix by the segregation of polystyrene block because of its insolubility in DGEBA. Moreover, the final hydroxyl groups of the PCL arms can get the star covalently linked to the epoxy matrix when using 1-methyl imidazole (1MI) as anionic curing initiator. In this way, thermomechanical characteristics of the epoxy resins should not be much influenced by addition of the star polymer.

Star polymer topology has proved to show some advantages over other toughening agents such as linear or HBPs. They offer a lower precursor polymer viscosity than the other agents because of their structure and the lack of chain entanglement [21]. Therefore, in the present work, we propose the use of the new synthesized multiarm star copolymer, PSOH-*b*-PCL as chemical modifier of

Journal of Polymer Science, Part A: Polymer Chemistry **2011**, 49, 4639 – 4649

DGEBA. Our aim is to investigate its influence in the curing and gelation processes and the possible formation of nanostructured thermosets.

Experimental

Materials

4-Chloromethylstyrene (4-CMS) from Sigma-Aldrich was purified by distillation under reduced pressure, subsequent passing over basic alumina and stored over molecular sieve at -20 ºC. $CuCl_2$ (98 %), 2,2′-bipyridine (Bpy, 99 %), tin(II) octoate ($Sn(Oct)_2$, 95 %), bis(2-hydroxypropyl)amine (DIPA, 98 %), and 1MI (99 %) were used without further purification. All these chemicals and analytical grade solvents (DMF, chlorobenzene) were purchased from Sigma-Aldrich. Other reagents and solvents were purchased from Scharlab.

DGEBA Epikote Resin 827 was provided by Shell Chemicals (epoxide equivalent weight (EEW) = 182.1 g/eq, n = 0.082).

AGET ATRP polymerization of 4-chloromethyl styrene (PS)

4-CMS (13.9 g, 106 mmol,), $CuCl_2$ (718 mg, 5.4 mmol), bipyridine (bpy, 1.67 g, 10.7 mmol) and chlorobenzene (40 mL) were added to a 100 mL three-necked round-bottomed flask equipped with a rubber septum and a magnetic stir bar. The solution was degassed by purging with argon for 20 min. Afterwards, 0.77 mL of $Sn(Oct)_2$ (2.4 mmol) were added via a syringe, and the solution was stirred until a homogenous and dark brown solution was observed. The reaction was carried out under argon and started at 115 ºC in a pre-heated oil bath. After 6 hours, the mixture was cooled down with liquid nitrogen, dissolved in 20 mL of THF and stirred until the dark brown Cu(I)-activator complex was oxidized to the inactive blue Cu(II) species. The reaction mixture was passed over neutral alumina to remove the copper compounds. The polymer was precipitated in cold methanol twice to remove residual monomer and the reducing agent, filtered and dried at 45 ºC under vacuum for 2 days.

The signal assignments were in accordance to those described in a previous article [13] and the degree of branching (*DB*) according to Frey's definition [22] of poly(4-CMS) (PS) was determined from the ^{1}H NMR signal integrations of the different polymer subunits and it was found to be 0.36.

In **Table 1**, the yield, average molecular weight and thermal data of the polymer obtained are collected.

Modification of poly(4-CMS) with bis(2-hydroxypropyl)amine DIPA (PSOH)

In a two-necked round-bottomed flask equipped with a septum rubber, a dropping funnel and a magnetic stir bar, 1.5 g of PS (3 mmol, 9.7 mmol of chlorine atoms) and 30 mL of anhydrous *N*,*N*-dimethylformamide (DMF) were added. The

solution was degassed by purging with argon until the polymer was dissolved. Afterwards, 13 g of DIPA (97 mmol) were dissolved in 10 mL of anhydrous DMF and the resulting solution was put in the dropping funnel. The purged system was heated at 45 ºC. Subsequently, the slow addition of DIPA/DMF solution was started. The reaction mixture was sealed and stirred for 4 days. The polymer was precipitated twice from DMF to distilled water (200 mL), filtered and dried under vacuum at 45 ºC for 5 days. By ^{1}H NMR, the degree of substitution of chlorine groups was estimated to be 90 %.

In **Table 1**, yield, average molecular weight and thermal data of the polymer obtained are collected.

^{1}H NMR (400 MHz, DMSO-d_6) δ *ppm* (**Figure 1**): 7.4-6.5 (**H$_{ar}$**), 6.7 (ArC**H**=CH$_2$, focal group), 5.72 and 5.18 (ArCH=C**H$_2$**, focal group), 4.5 (O**H**), 3.9-3.1 (C**H**/C**H$_2$** in styrene modified units **d**, **e** and C**H**, **c**), 2.8-1.5 (C**H**/C**H$_2$** in PS backbone units and C**H$_2$**, **b**) and 0.98 (-C**H$_3$**, **a**); ^{13}C NMR (100.6 MHz, DMSO-d_6) δ *ppm*: 143-135 (**C$_{ar}$**), 64.4-62.3 (**CH/C**H$_2$ **c**, **b**), 60.4-59.4 (**CH/C**H$_2$ in styrene modified units **d**, **e**), 34.5-27.1 (**C**H$_2$/**C**H in PS backbone units) and 20.7 (-**C**H$_3$, **a**); FTIR (ATR) (cm^{-1}): 3600-3100 (OH st), 3050 (arC-H st), 2930-2890 (C-H st), 1220-1080 (C-O-C, st as).

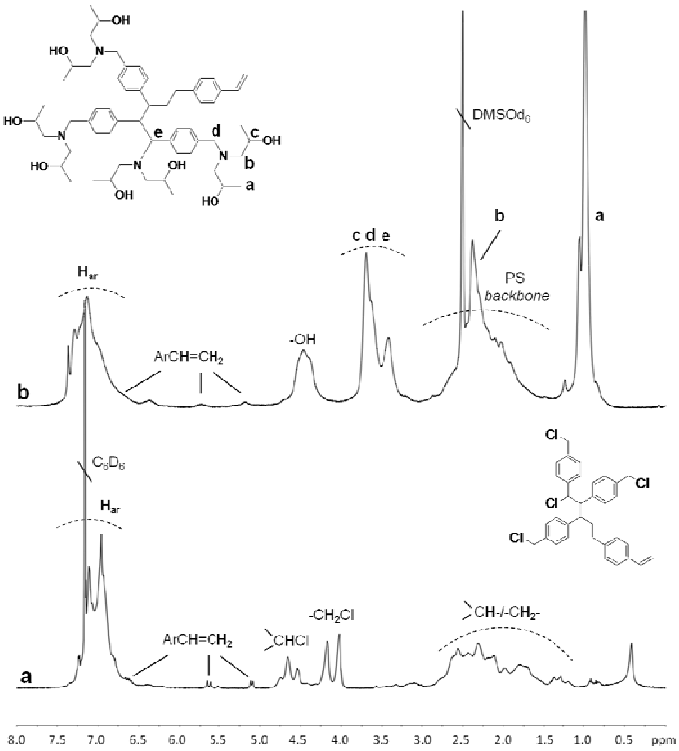

Figure 1 ^{1}H NMR spectra of (**a**) PS and (**b**) PSOH in C_6D_6 and DMSO-d_6, respectively

Journal of Polymer Science, Part A: Polymer Chemistry **2011**, 49, 4639 – 4649

Ring-opening polymerization of ε-caprolactone (ε-CL) from PSOH (PSOH-b-PCL)

PSOH (0.25 g, 0.03 mmol, 1.9 mmol of hydroxyl groups) and 2.17 g of ε-CL (19 mmol) were placed at room temperature in a two-necked flask equipped with a magnetic stirrer and a gas inlet to fill the flask with argon. Then, two drops of $Sn(Oct)_2$ were added to the solution mixture and the flask was immersed in an oil bath thermostated at 130 ºC during 3 hours. After that, the crude product was dissolved in chloroform and the polymer was isolated by precipitation in 10-fold cold diethyl ether and then filtered and dried at 45 ºC under vacuum for 2 days.

^{1}H NMR (400 MHz, $CDCl_3$) *δ ppm* (**Figure 2**): 7.5-6.9 (**H_{ar}**), 6.7 (ArC**H**=CH_2, focal group), 5.68 and 5.20 (ArCH=C**H_2**, focal group), 5.2-4.9 (C**H**-OCO-, **c'**), 4.08 (-C**H_2**-OCO-, **5**), 3.66 (-C**H_2**-OH, **5'**), 2.32 (-C**H_2**-COO-, **1** and **1'**), 1.70-1.50 (-C**H_2**-, **3, 3'** and **4, 4'**), 1.40 (-C**H_2**-, **2** and **2'**) and 3.85-0.96 (PSOH backbone overlapped by PCL signals); ^{13}C NMR (100.6 MHz, $CDCl_3$) *δ ppm*: 173.8 (C=O), 64.6 (-**C**H_2-OCO-, **5**), 62.8 (-**C**H_2-OH, **5'**), 34.7 (-**C**H_2-COO-, **1'**), 34.6 (-**C**H_2-COO-, **1**), 32.8 (-**C**H_2-, **4'**), 28.5 (-**C**H_2-, **4**), 26.0 (-**C**H_2-, **3**), 25.7 (-**C**H_2-, **3'**), 25.1 (-**C**H_2-, **2'**) and 24.8 (-**C**H_2-, **2**); FTIR (ATR) (cm^{-1}): 3500 (OH st), 3010 (arC-H st), 2950-2900 (C-H st), 1723 (C=O st), 1200-1140 (C-O-C st as/s).

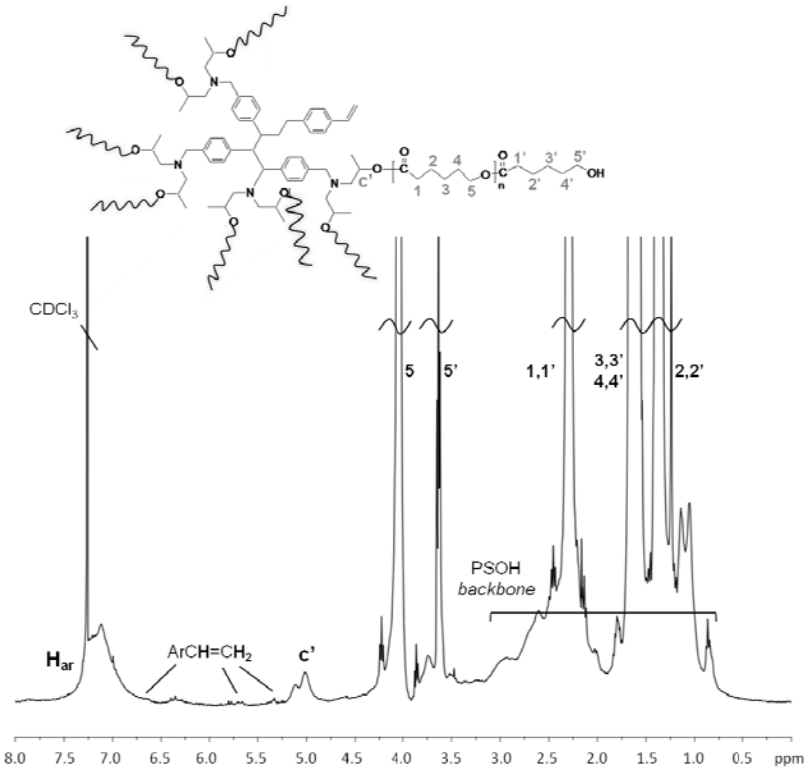

Figure 2 ^{1}H NMR spectra of the multiarm star copolymer synthesized (PSOH-*b*-PCL) in $CDCl_3$. (The drawn structure possesses one PCL arm for simplicity)

The yield, average molecular weights and thermal data of the star obtained are given in **Table 1.**

Table 1 Data of the multiarm star copolymer PSOH-*b*-PCL synthesized in this study

Entry	[ε-CL:OH]	*Yield*[a] [%]	$\overline{M}_{n,exp1}$ (g/mol)[b]	$\overline{M}_{n,exp2}$ (g/mol)[c]	$\frac{\overline{M}_w}{\overline{M}_n}$ [c]	$\overline{DP}_{arm}$ [d]	T_g[e] (ºC)	Δh_m[e] (J/g)	T_m[e] (ºC)	$T_{2\%}$[f] (ºC)
PS	-	52	5,100	3,900	3.22	-	82	-	-	131
PSOH	-	86	7,900	5,300	1.31	-	77	-	-	248
PSOH-*b*-PCL	10:1	98	79,900	16,600	1.62	10.5	42	64.9	50.3	272

a. Determined gravimetrically.
b. $\overline{M}_n$ determined by ^{1}H or ^{13}C NMR.
c. $\overline{M}_n$ and molecular weight dispersity were determined by SEC-RI with THF as solvent.
d. Degree of polymerization ($\overline{DP}_{arm}$) was determined by ^{13}C NMR in quantitative conditions.
e. Data obtained from the second DSC scan at 10 ºC/min.
f. Temperature of the onset of degradation under N_2 at 10 ºC/min.

Preparation of epoxy thermosets

The mixtures were prepared by adding the required amount of PSOH-*b*-PCL into the epoxy resin and gently heating until it was dissolved and the solution became clear. Then, 3 phr (part per hundred parts of mixture) of 1MI was added and the resulting solution was stirred and cooled down to -10 ºC to prevent polymerization. Mixtures containing 5 - 10 wt.% (by weight) of PSOH-*b*-PCL were prepared. The compositions of the formulations studied are detailed in **Table 2.**

Characterization

^{1}H NMR and ^{13}C NMR measurements were carried out at 400 MHz and 100.6 MHz, respectively, in a Varian Gemini 400 spectrometer. Benzene-d_6, dichloromethane (CD_2Cl_2), DMSO-d_6 and $CDCl_3$ were used as solvents for NMR measurements. For internal calibration, the solvent signals were used: δ (^{1}H) = 7.16, 5.32, 2.50 and 7.26; δ (^{13}C) = 128.06, 54.00, 39.52 and 77.16 ppm, respectively. Quantitative ^{13}C NMR experiments were recorded using a delay time between sampling pulses equal to 8 s and the sequence inverse gated decoupling.

The FTIR spectra were collected in a spectrophotometer FTIR-680PLUS from JASCO with a resolution of 4 cm^{-1}. This device was equipped with an attenuated-total-reflection accessory with a diamond crystal (Golden Gate heated single-reflection diamond ATR, Specac-Teknokroma).

The determination of the molecular weight was performed on an Agilent 1200 series system equipped with an Agilent 1100 series refractive-index (RI) detector using tetrahydrofuran (THF) as eluent in combination with PLgel 3-μm MIXED-E, PLgel 5-μm MIXED-D and PLgel 20-μm MIXED-A columns in series. The calibration of this SEC analysis was performed with poly(styrene) standards. The flow rate employed was 1.0 mL/min.

Calorimetric analyses were carried out on a Mettler dynamic scanning calorimetry DSC-822e thermal analyzer. Samples of ~ 5 mg in weight were placed

in aluminum pans under nitrogen atmosphere. The calorimeter was calibrated using an indium standard (heat flow calibration) and an indium-lead-zinc standard (temperature calibration).

The synthesized polymers were heated from – 50 to 150 ºC with a heating rate of 10 ºC/min, cooled down to – 100 ºC with a cooling rate of – 10 ºC/min and then heated again to 150 ºC at the same heating rate. Δh_m, T_m and T_g values were obtained from the second heating curves. Thermal data are collected in **Table 1**.

Non-isothermal curing experiments were performed from 20 to 250 ºC at heating rates of 2, 5, 10, and 15 ºC/min to determine the reaction heat and the kinetic parameters. In non-isothermal curing process the degree of conversion by DSC (α_{DSC}) was calculated as follows:

$$\alpha_{DSC} = \frac{\Delta H_T}{\Delta H_{dyn}} \quad (1)$$

where ΔH_T is the heat released up to a temperature T, obtained by integration of the calorimetric signal up to this temperature, and ΔH_{dyn} is the total reaction heat associated with the complete conversion of all reactive groups.

The glass transition temperatures (T_gs) of the completed cured materials were determined, by means of a second scan at 20 ºC/min, as the temperature of the half-way point of the jump in the heat capacity when the material changed from glassy to the rubbery state under N_2 atmosphere and the error is estimated to be ~ ± 1 ºC.

The kinetic triplet [pre-exponential factor, activation energy and kinetic model] of the curing process was determined using integral isoconversional nonisothermal kinetic analysis, Kissinger-Akahira-Sunose equation, combined with the Coats-Redfern procedure. Details of the kinetic methodology are given in previous publications [23,24].

Thermogravimetric analyses were carried out in a Mettler TGA/SDTA851e/LF/1100 thermobalance. Samples with an approximate mass of 8 mg were degraded between 30 and 800 ºC at a heating rate of 10 ºC/min in N_2 (100 cm^3/min measured in normal conditions).

Thermal-dynamic-mechanical analyses (DMTA) were carried out with a TA Instruments DMTA 2980 analyzer. The samples were cured isothermally in a mould at 120 ºC for 1.5 h and then post-cured for 1 h at 150 ºC. Three-point bending was performed on prismatic rectangular samples (10 x 5 x 1.5 mm^3). The apparatus operated dynamically at 3 ºC/min from 30 to 220 °C at a frequency of 1 Hz.

Rheological measurements were carried out in the parallel plates (geometry of 25 mm) mode with an ARG2 rheometer (TA Instruments, UK, equipped with a Peltier system). Complex viscosity (η^*) of the pre-cured mixtures were recorded as

function of angular frequency (0.1–100 rad/s) stating a constant deformation of 50 % at 80 ºC.

The gelation time was determined by setting the device in time sweep and multiwave oscillation mode. Experiments were performed isothermally at 80 ºC. Because the viscosity of the system changes significantly during the curing process, a control program was used in which the oscillation amplitude diminishes with an increase in the applied stress. By doing so, the curing process can be characterized in the whole range of conversion. Gel time was taken as the point where tan δ is independent of frequency [25]. The conversion at gelation (α_{gel}) was determined by stopping the rheology experiment at gelation and performing a subsequent dynamic DSC scan of the gelled sample.

The topography of the specimens metalized with gold was observed with a Jeol JSM 6400 with a resolution of 3.5 nm.

Transmission electron microscopy (TEM) was performed with a Jeol 1011 microscope. The film of the PSOH-*b*-PCL was prepared dissolving the star polymer with THF and subsequently removing it at 50 ºC during 24 h. Then, the film was cut using an ultramicrotome at room temperature and observed without staining.

Results and discussion

Synthesis of PSOH-b-PCL star

The synthesis of the copolymer star was conducted in three consecutive synthetic steps as depicted in **Scheme 1**.

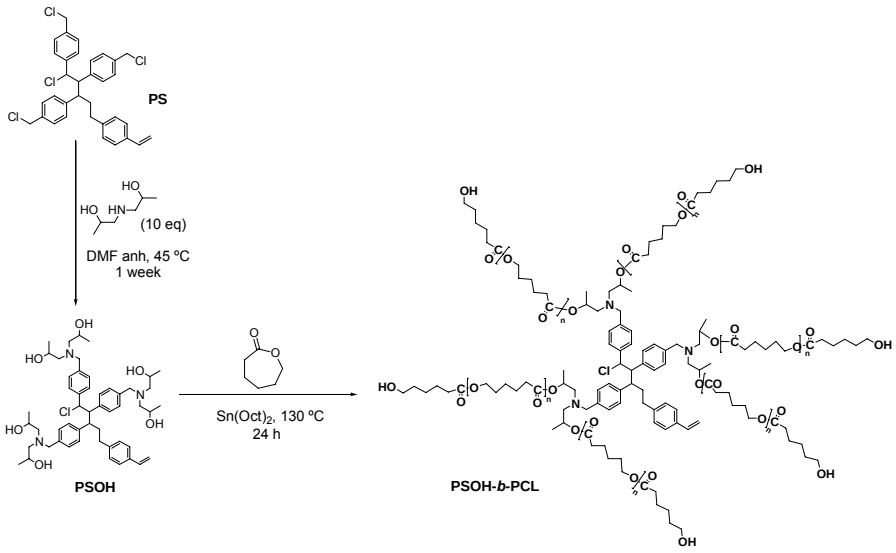

Scheme 1 Synthetic route to the multiarm star copolymer PSOH-b-PCL

Journal of Polymer Science, Part A: Polymer Chemistry **2011**, 49, 4639 – 4649

First, hyperbranched PS was prepared via SCVP using controlled activator generated by electron-transfer atom-transfer radical polymerization (AGET/ATRP) according to a previously published procedure [13]. The data of the PS prepared are collected in **Table 1**. The structural characterization was done by NMR and FTIR spectroscopy. **Figure 1** (**a**) shows the ^{1}H NMR spectrum of PS, where two main groups of signals of PS appear at 7.3–6.5 and 3.0–1.2 ppm corresponding to aromatic protons and to methine and methylene groups in the backbone units, respectively. The complex signals centered at about 4.6 and 4.2 ppm can be assigned to the methine and methylene protons of linear and terminal units having a chlorine atom. The three small signals at 6.7, 5.6 and 5.1 ppm can be attributed to the vinyl group of the focal unit. The degree of polymerization and the molar mass were obtained from the area of the signal of the aromatic protons and the area of the peak of the vinyl group (spectrum in CD_2Cl_2). The *DB* was found to be 0.36 and it was determined from the signals at 4.6 and 4.2 ppm in the ^{1}H NMR spectra of PS registered in C_6D_6 and CD_2Cl_2 [13].

By TGA the low thermal stability of PS was demonstrated, since at temperatures above 125 ºC a loss of mass can be observed due to the HCl elimination.

The second step in the synthesis of the star was the transformation of the chlorine groups to hydroxyls. To do that, we took advantage of the higher nucleophilic capacity of amines in comparison to hydroxyls that can substitute chlorine groups in benzylic positions. We selected bis(2-hydroxypropyl)amine (DIPA) since it is a secondary amine which can introduce two secondary hydroxyl groups per each substituted chlorine. The first evidence of the successful modification was the increased solubility of the modified polymer in polar solvents such as MeOH or DMSO. By means of ^{1}H NMR spectroscopy (**Figure 1** (**b**)), it could be proved that practically all the chlorine groups were successfully substituted without the concurrence of side reactions. In the spectrum, new signals appear at 4.5 ppm (OH protons) and at 3.9–3.1 ppm methine and methylene protons of the substituted linear and terminal PS units (**e** and **d**) overlapped with the methine proton of the new introduced moiety (**c**). The methylene protons of the aminoalcohol introduced (**b**) appear overlapped to the methine and methylene signals of the PS backbone. Finally, we can see at 0.98 ppm the signal corresponding to the methyl protons of the new introduced moiety (**a**).

The degree of modification achieved (90 %) was calculated by the ratio between the area of the peak corresponding to the aromatic protons ($\mathbf{H_{ar}}$) and the area of the peak due to the six protons of methyl groups (signal **a**). The complete modification could not be achieved possibly due to the steric hindrance existing for chlorine groups linked to methine carbons of the PS units.

In **Table 1**, average molar masses obtained by ^{1}H NMR and SEC-RI are collected. Some differences can be observed between the molar mass dispersity values of PS and PSOH. This fact could be attributed to the precipitation process over distilled water after the modification reaction, which leads to fractionation. The

number of hydroxyl groups per molecule of PSOH (N_{OH}) was determined from the ^{1}H NMR molecular weight, assuming two hydroxyl groups per modified unit, which results in an average of 60.

The high degree of modification leads to an increased thermal stability of the polymer, which becomes thermally stable up to 230 ºC. Moreover, the glass transition temperature seems to be slightly influenced after the modification since it is reduced by 5 ºC in comparison with the nonmodified polymer (PS).

For synthesizing the multiarm star poly(styrene)-*block*-poly(ε-caprolactone) we selected the cationic ring-opening polymerization of ε-caprolactone taking as macroinitiator the HBP prepared before (PSOH). The selected ratio of ε-caprolactone (ε-CL) to initiating hydroxyl groups in the feed was 10. The used synthetic procedure was similar to the one described by Burgath *et al.* [16].

The chemical structure of PSOH-*b*-PCL could be confirmed by quantitative ^{1}H and ^{13}C NMR analysis. In **Figure 2**, the assignment of the proton signals of the spectrum of PSOH-*b*-PCL is presented. The signals corresponding to PSOH core are visible as the signals corresponding to aromatic protons (7.9–6.5 ppm) and methine, methylene and methyl protons appearing between 3.7 and 0.7 ppm. The presence of the signal **c'** at 5 ppm due to the methine proton directly linked to PCL chain should be noted. The signals of the methylene protons of the PCL chain (**1-5** and **1'-5'**) overlap with the signals of the PSOH backbone. The vinylic focal unit is still visible in the spectrum.

The degree of polymerization of PCL arms ($\overline{DP}_{arm}$) was calculated from the ^{13}C NMR spectrum, registered under quantitative conditions, by dividing the areas of peak **5** (I_5) by peak **5'** ($I_{5'}$) and adding a terminal unit.

$$\overline{DP}_{arm} = \frac{I_5}{I_{5'}} + 1 \qquad (2)$$

The partial overlapping of the proton signals **5** and **5'** with the signals corresponding to the protons of the core in the ^{1}H NMR spectrum prevents the evaluation by this technique. The characterization data listed in **Table 1** show that the experimental value $\overline{DP}_{arm}$ of 10.5 was somewhat higher than the expected one ($\overline{DP}_{arm}$ = 10). This fact could be explained within complete initiation through each secondary hydroxyl group of PSOH which leads to slightly longer PCL arms. From $\overline{DP}_{arm}$ and the average number of PCL arms per molecule, it is possible to calculate the molecular weight of the multiarm star obtained, as follows:

$$\overline{M}_{n,exp1} = \overline{M}_{PSOH} + [N_{OH} \cdot \overline{DP}_{arm} \cdot M_{\varepsilon-CL}] \qquad (3)$$

Journal of Polymer Science, Part A: Polymer Chemistry **2011**, 49, 4639 – 4649

where $\overline{M}_{PSOH}$ is the molar mass of PSOH core, N_{OH} the average number of hydroxyl initiating sites, $\overline{DP}_{arm}$ is the degree of polymerization of PCL arms and $M_{\varepsilon-CL}$ is the molecular weight of ε-CL.

Comparing the molecular weight data of PSOH-*b*-PCL obtained by NMR and SEC-RI one can appreciate that the SEC value is considerably lower. This phenomenon has been observed in several works related with star polymers and can be explained by the fact that the molecular weights of star polymers are usually underestimated by this technique because of using linear standards [26].

The obtained PSOH-*b*-PCL showed a good thermostability up to 270 ºC. Moreover, the calorimetric dynamic sweep revealed a secondary transition centered at 42 ºC and a melting endotherm from PCL arms at 50.3 ºC, which indicates the partial crystalline character of the PCL arms.

Figure 3 shows the TEM picture of an unstained film of the PSOH-*b*-PCL star. As we can see, there is a clear phase separation due to the presence of poly(styrene) regions (dark spots) embedded in the poly(ε-caprolactone) matrix.

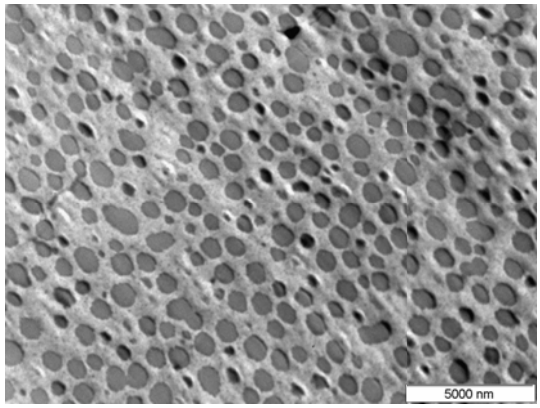

Figure 3 TEM image of the unstained film sample of neat PSOH-*b*-PCL

Study of the curing of DGEBA with different proportions of PSOH-b-PCL

1MI was selected as anionic initiator to perform the curing of DGEBA modified formulations. The amount of 1MI was kept constant for all the formulations at 3 phr. The composition of the formulations is given in **Table 2** with the calorimetric data and kinetic parameters determined by DSC. From the calorimetric data we can state that on increasing the proportion of the star copolymer, the global enthalpy diminishes since smaller epoxy fraction exists in the formulation. However, both modified formulations reach complete curing because they show practically the same enthalpy per epoxy equivalent as the neat formulation which is considered completely cured.

Table 2 Composition and calorimetric data of DGEBA/1MI mixtures with different percentages of PSOH-*b*-PCL

Formulation[a] (wt.%)	initiator/ epoxy	OH/ epoxy	Δh (J/g)	Δh^b (kJ/ee)	T_g^c (ºC)	E_a^d (kJ/mol)	ln A^e (s^{-1})	$k_{120\,ºC}$ x 10^{3f} (s^{-1})
0	0.066	0.041	503	92	167	56.2	12.7	3.85
PSOH-*b*-PCL								
5	0.070	0.048	441	85	134	59.0	12.3	2.90
10	0.074	0.056	427	86	111	59.4	12.2	2.83

a. % by weight of multiarm star copolymer.
b. Enthalpy value per equivalent of epoxy group.
c. Glass transition temperature obtained by DSC. Second scan after dynamic curing at 20 ºC/min.
d. Values of activation energies at 50 % of conversion were evaluated by isoconversional nonisothermal procedure.
e. Values of pre-exponential factor for A_2 kinetic model with $g(\alpha)=[-ln(1-\alpha)]^{1/2}$ determined at 120 ºC.
f. Values of rate constant at 120 ºC calculated using the Arrhenius equation.

On increasing the proportion of PSOH-*b*-PCL star in the material the T_g of the material decreases as PCL arms act as a plasticizer of the epoxy matrix. However, they keep a reasonably high value which allows using those materials as coatings at high temperature.

Figure 4 shows the calorimetric curves recorded at 10 ºC/min of neat DGEBA/1MI and DGEBA/PSOH-*b*-PCL/1MI formulations. A slight shift of the exotherms to high temperatures on adding the star modifier can be observed, but the shape of the curves does not change significantly. Similar results were obtained in a previous paper where a poly(glycidol)-*b*-poly(ε-caprolactone) star was used as modifier [17].

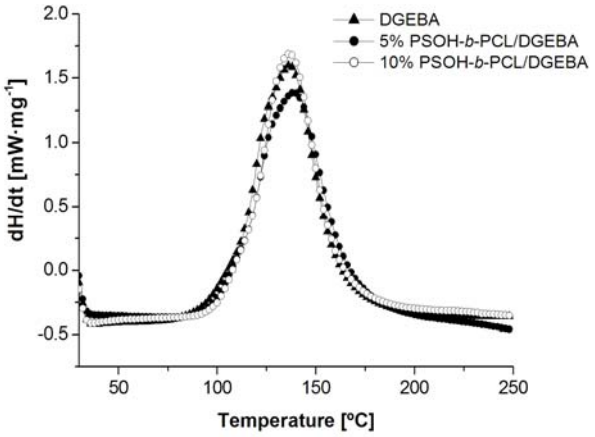

Figure 4 DSC scanning curves of the curing of neat DGEBA/1MI formulation and DGEBA/1MI containing 5 and 10 wt.% of PSOH-*b*-PCL at a heating rate of 10 ºC/min

The kinetic parameters of the curing process were calculated and the values are collected in **Table 2**. The addition of the reactive star copolymer leads to a slight increase of the activation energy, which is in accordance with the slight global retarding effect observed and the requirement of higher temperatures to proceed with the curing process. The constant rate calculated reflects the retarding effect on adding the modifier.

Journal of Polymer Science, Part A: Polymer Chemistry **2011**, 49, 4639 – 4649

By infrared spectroscopy (FTIR-ATR), the curing process could also be studied following the disappearance of the absorption at 913 cm^{-1}. In **Figure 5**, the plot of epoxy conversion against time at 120 and 150 ºC for the formulations studied is depicted. At both temperatures, a higher reactivity of the neat formulation is observed. However, 120 ºC is not enough to reach complete curing of the neat, and especially of the modified formulations. No significant effect of the proportion of star in the mixture on the kinetics can be observed at 120 ºC. This effect becomes more evident at 150 ºC. At this temperature, complete curing is achieved for the three formulations.

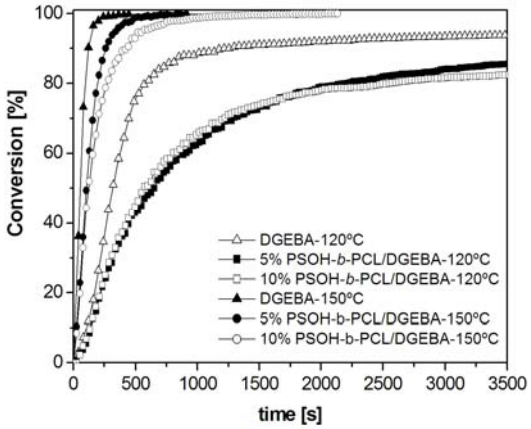

Figure 5 Conversion of epoxide against time of neat DGEBA/1MI formulation and DGEBA/1MI containing 5 and 10 wt.% of PSOH-*b*-PCL at 120 and 150 ºC from FTIR data

In previous work on anionic curing of epoxy resins, we observed an acceleration of the curing process and an increase of the final conversion of epoxide groups on increasing the proportion of hydroxyl groups in the curing mixture [4,27]. However, on adding the star polymer, the concentration of epoxy groups decreases and this fact can explain the observed deceleration.

Rheological characteristics of the formulations

Gel time is a valuable technological parameter in thermosetting coatings, because before gelation the reactive mixture can be easily applied. After gelation, the material loses its mobility and stress appears because of the shrinkage that generally accompanies the curing process. **Table 3** collects the gelation time and the conversion at the gel point for the formulations studied. On adding the star modifier to the formulation, both time and conversion increase. The great increase in the α_{gel} on adding the modifier should be noted, although no dependence with its proportion could be noticed. Anionic homopolymerization as a chain-growth process shows a lower conversion at gelation than a step-growth process. As has been generally studied, the conversion at gelation is defined by the kinetic chain length (KCL) [28,29]. Factors capable to reduce the KCL, such as high hydroxyl content or high initiator concentration, are the responsible for the increased conversion at the gel point (**Table 3**) [30]. This is because they favor the chain-transfer processes,

which leads to increase the number of polymer chains and therefore reduces the chain length and consequently the conversion at gelation.

Table 3 Gelation, TGA and DMTA data obtained from DGEBA/1MI thermosets containing different proportions of multiarm star copolymer PSOH-*b*-PCL

Formulation[a] (wt.%)	t_{gel} (min)	α_{gel}[b] (%)	$T_{\tan\delta}$[c] (ºC)	E'[d] (MPa)	T_{onset}[e] (ºC)
0	26.9	34	187	101	356
PSOH-*b*-PCL					
5	27.6	68	169	91	330
10	28.6	65	154	107	334

a. Percentage by weight of multiarm star copolymer.
b. Determined as the conversion reached by rheometry and DSC tests at 10 ºC/min.
c. Temperature of maximum of the tan δ at 1 Hz.
d. Relaxed modulus determined at the $T_{\tan\delta}$ +30 ºC.
e. Temperature of the onset decomposition on the TGA data at 10 ºC/min calculated for a 5 % of weight loss.

By rheological experiments the complex viscosity of the mixtures at 80 ºC was determined on varying the angular frequency, as it is shown in **Figure 6**.

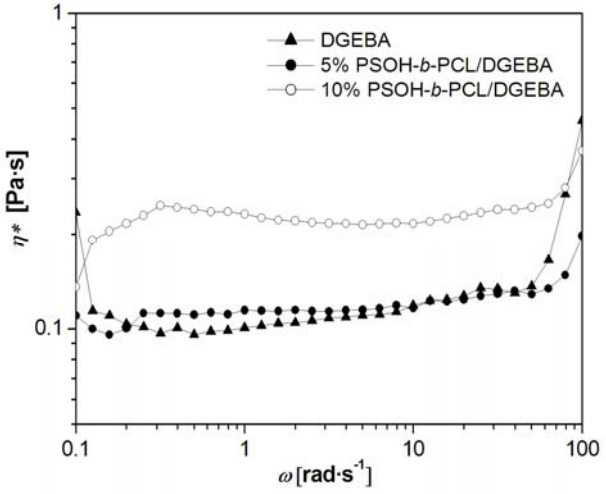

Figure 6 Complex viscosity (η^*) against angular frequency (ω) at 80 ºC for neat DGEBA/1MI and DGEBA/1MI containing 5 and 10 wt.% of PSOH-*b*-PCL

All formulations show a Newtonian behavior and little differences among them. In a previous article, we reported that the addition of multiarm star-shaped polymers did not increase the prepolymer viscosity and it was even decreased [17]. In this study, the addition of 5 wt.% of PSOH-*b*-PCL does not affect the processability of the mixture but the addition of 10 wt.% slightly increases the viscosity. However, in both cases, this characteristic does not exceed 0.5 Pa·s which is necessary to allow flowing through the mould in some industrial processes [31]. This positive behavior proves the great potential of star-shaped polymer as rheological modifiers.

Journal of Polymer Science, Part A: Polymer Chemistry **2011**, 49, 4639 – 4649

Thermal and thermomechanical properties of the thermosets obtained

The materials obtained were characterized by DMTA. The tan *δ* plot against temperature for all materials is represented in **Figure 7** and **Table 3** collects the thermomechanical data.

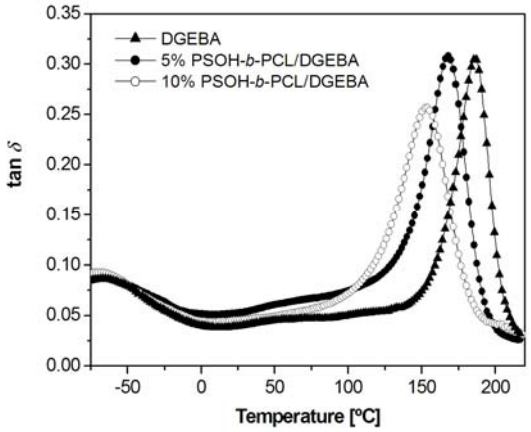

Figure 7 Tan *δ* against temperature at 1 Hz for the thermosets obtained

As we can see, the curves are unimodal and quite narrow but little differences can be observed in the width of the curve since it increases slightly on increasing the proportion of modifier which can be due to a less homogeneous character of the material. In addition, tan *δ* value decreases on adding the modifier which is in accordance with the behavior observed by DSC.

In terms of phase separation, we can state that no relaxations were observed at low temperature, which could indicate the complete solubility of PSOH-*b*-PCL in DGEBA facilitated by the PCL arms, the soluble block.

From the values of the modulus after relaxation no systematic tendency on increasing the proportion of the star copolymer can be stated, maybe due to the special behavior in the rubbery state of this architecture.

The thermal stability of the materials obtained was investigated by thermogravimetry and the data are collected in **Table 3**. The initial decomposition temperature of the modified thermosets slightly decreases which can be related to the presence of ester groups in the PCL arms, which can undergo a *β*-elimination process leading to the breakage of the polymeric network.

Characterization by SEM

The topography of neat DGEBA (**a**) and DGEBA modified thermosets with a 5 wt.% (**b**) and a 10 wt.% of PSOH-*b*-PCL (**c**) has been investigated by SEM and the microphotographs are collected in **Figure 8**.

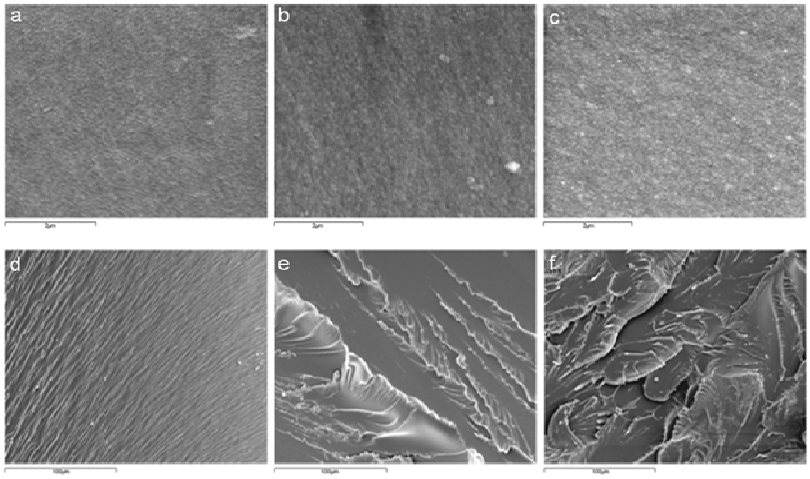

Figure 8 SEM micrographs of the surface topography of the following materials cured 1.5 h at 120 ºC and post-cured 1 h at 150 ºC: **a**) DGEBA/1MI; **b**) 5 wt.% PSOH-*b*-PCL/DGEBA/1MI; **c**) 10 wt.% PSOH-*b*-PCL/DGEBA/1MI and their respective fracture under liquid nitrogen: **d**), **e**) and **f**)

From the surface of the nonmodified material, we cannot observe the presence of well-defined particles or phase separation. However, a special patterned roughness is visible which can be generated during the fast curing process that occurs when 1MI is used as anionic initiator. Comparing the nonmodified material surface with the one of the thermosets containing PSOH-*b*-PCL, a higher roughness appears in the latter. In these micrographs (**b** and **c**), the surface has a more pronounced roughness based on nanosized grains distributed over all the material. This special effect is observed for both star contents but when a 10 wt.% of modifier is added these grains increase from 15 - 25 nm (with a 5 wt.% of star) to 30 - 40 nm in size. The nanopatterned organization of the modified star thermosets can be attributed to the presence of the star copolymer which can change the curing process in the surrounding of the star molecule. The observation of these materials by TEM did not show any defined morphology but a complete homogeneous appearance was observed, even in stained materials, which accounts for a nanograined morphology without nanophase separation. It has been reported that chain-wise polymerizations are intrinsically inhomogeneous since the increase of molecular weight of the polymer chains is not as regular as in polycondensations and the inhomogeneities formed become fixed by the crosslinks [25b].

Journal of Polymer Science, Part A: Polymer Chemistry **2011**, 49, 4639 – 4649

From the micrographs of the morphologies of the cryo-fractured materials (**Figure 8**), it can be appreciated that the neat epoxy material (**d**) appears as a smooth glassy surface with a high density of long unidirectional cracks. When the material contains 5 or 10 wt.% of PSOH-*b*-PCL a different fracture is observed since high expanded cracks appear (**e** and **f**) which could be an indication of a more tough fracture in comparison with the neat thermoset. The presence of a rougher nanostructured surface could be responsible for the improvement of the matrix yielding and a subsequent toughness.

Conclusions

A multiarm star copolymer (PSOH-*b*-PCL) with an average number of PCL arms per molecule of 60 has been prepared. 4-CMS was polymerized by ATRP and the terminal chlorines were substituted by a nucleophilic reaction to give the hydroxyl-ended derivative (PSOH). PSOH has been used as a macroinitiator core to polymerize *ε*-caprolactone by means of cationic ring-opening polymerization so as to obtain the star copolymer.

This star polymer was used as modifier in the curing of DGEBA by 1MI as an anionic initiator. The addition of this modifier to the reactive mixture slightly retarded the curing and increased the gelation time and the conversion at the gel point. It is expected that all these facts allow reducing the formation of internal stresses on curing.

From the point of view of the processability, the addition of the synthesized star to DGEBA formulations did not significantly increase the viscosity in comparison to the neat formulation.

The addition of PSOH-*b*-PCL modifiers to the formulation allowed maintaining the homogeneous appearance of the materials but a nanograined morphology could be observed. Increasing the proportion of modifier the grains increased in size. Moreover, the observation of the cryo-fracture put in evidence the changes in the ductile characteristics increasing it with the proportion of modifier.

Thus, one can conclude that PSOH-*b*-PCL star-like topology is a suitable modifier for epoxy resins enhancing toughness without affecting negatively the curing process and processability.

Acknowledgements

The authors from the Universitat Rovira i Virgili and Universitat Politècnica de Catalunya would like to thank MICINN (Ministerio de Ciencia e Innovación) and FEDER (Fondo Europeo de Desarrollo Regional) (MAT2008-06284-C03-01 and MAT2008-06284-C03-02) and to the Comissionat per a Universitat i Recerca de la Generalitat de Catalunya (2009-SGR-1512). All the authors thank to the Germany-Spanish collaboration program (HA2007-0022, DAAD PPP D/07/13493) for their financial support. M.M. acknowledges the grant FI-DGR 2009 from the Catalonian Government and the mobility fellowship from MICINN. Ms. Ulrike Georgi and Mr. Frank Däbritz are gratefully acknowledged for their useful advices in the synthesis of hyperbranched PS.

References

[1] May CA, editor. *Epoxy resins. Chemistry and technology.* Marcel Dekker, New York, **1988**, p.1-284.
[2] Petrie, E.M. *Epoxy adhesive formulations.* McGraw-Hill, New York, **2006**.
[3] Cicala, G., Recca, A. Polym. Eng. Sci. **2008**, 48, 2382-2388.
[4] Morell, M.; Fernández-Francos, X.; Ramis, X., Serra, A. Macromol. Chem. Phys. **2010**, 211, 1879-1889.
[5] Bagheri, R.; Marouf, B.T.; Pearson, R.A. J. Macromol. Sci., Part C: Polym. Rev. **2009**, 49, 201-225.
[6] Ruiz-Pérez, L.; Royston, G.J.; Fairclough, J.P.A. Ryan, A.J. Polymer **2008**, 49, 4475-4488.
[7] Meng, Y.; Zhang, X.H.; Du, B.Y.; Zhou, B.X.; Zhou, X.; Qi, G.R. Polymer **2011**, 52, 391-399.
[8] Kanaoka, S.; Sawamoto, M.; Higashimua, T. Macromolecules **1991**, 24, 2309-2313.
[9] Blencowe, A; Tan, J.F.; Goh, T.K.; Qiao, G.G. Polymer **2009**, 50, 5-32.
[10] Chen, Y.; Shen, Z.; Barriau, E.; Krautz, H.; Frey, H. Biomacromolecules **2006**, 7, 919-926.
[11] Lin, Y.; Liu, X.; Dong, Z.; Li, B.; Chen, X.; Li, Y.S. Biomacromolecules **2008**, 9, 2629-2636.
[12] Morell, M.; Ramis, X.; Voit, B.; Serra, A.; Lederer, A .J. Polym. Sci., Part A: Polym. Chem. **2011**, 49, 3138-3151.
[13] Komber, H.; Georgi, U.; Voit, B. Macromolecules **2009**, 42, 8307–8315.
[14] Weimer, M.W.; Fréchet, J.M.J.; Gitsov, I. J. Polym. Sci., Part A: Polym. Chem. **1998**, 36, 955–970.
[15] Georgi, U.; Erber, M.; Stadermann, J.; Abulikemu, M.; Komber, H.; Lederer, A.; Voit, B. J. Polym. Sci., Part A: Polym. Chem. **2010**, 48, 2224–2235.
[16] Burgath, A.; Sunder, A.; Neuner, I.; Mülhaupt, R.; Frey, H. Macromol. Chem. Phys. **2000**, 201, 792-797.
[17] Morell, M.; Lederer, A.; Ramis, X.; Voit, B.; Serra, A. J. Polym. Sci., Part A: Polym. Chem. **2011**, 49, 2395-2406.
[18] Guo, Q.; Groeninckx, G. Polymer **2001**, 42, 8647-8655.
[19] Fan, W.; Wang, L.; Zheng, S. Macromolecules **2009**, 42, 327-336.
[20] Hameed, N., Guo, Q.; Hanley, T.; Mai, Y.W. J. Polym. Sci., Part B: Polym. Phys. **2010**, 48, 790-800.
[21] Morell, M.; Ramis, X.; Ferrando, F; Serra, A. Polymer **2011**, 52, 4694-4702.
[22] Hölter, D.; Burgath, A.; Frey, H. Acta Polymer **1997**, 48, 30-35.
[23] Ramis, X.; Salla, J.M.; Mas, C.; Mantecón, A.; Serra, A. J. Appl. Polym. Sci. **2004**, 92, 381–393.
[24] Ramis, X.; Salla, J.M.; Cadenato, A.; Morancho, J.M. J. Thermal. Anal. Calorim. **2003**, 72, 707-718.
[25] Pascault, J.P., Sautereau, H., Verdu, J., Williams, R.J.J., *Thermosetting Polymers*, Marcel Dekker, New York, **2002**, (a) p. 188, (b) p. 222.
[26] Shen, Z.; Chen, Y.; Barriau, E.; Frey, H. Macromol. Chem. Phys. **2006**, 207, 57-64.
[27] Fernández-Francos, X.; Cook, W.D.; Serra, A.; Ramis, X.; Liang, G.G.; Salla, J.M. Polymer **2010**, 51, 26-34.
[28] Dusek, K.; Lunak, S.; Matejka, L. Polym. Bull. **1982**, 7, 145-152.
[29] Miller, D.R.; Valles, E.M.; Macosko, C.W. Polym. Eng. Sci. **1979**, 19, 272-283.
[30] a) Dell'Erba, I.E.; Williams, R.J.J. Polym. Eng. Sci. **2006**, 46, 351-359. b) Ooi, S.K.; Cook, W.D.; Simon, G.P.; Such, C.H. Polymer **2000**, 41, 3639-3649. c) Ricciardi, F.; Romanchick, W.A.; Joullie, M.M. J. Polym. Sci. Polym. Chem. Ed. **1983**, 21, 1475-1490. d) Rozenberg, B.A. Adv. Polym. Sci. **1986**, 75, 113-165.
[31] Corcione, C.E.; Frigione, M. Polym. Test. **2009**, 28, 830-835.

CAPÍTOL V

Síntesi de polímers estrella mitjançant ATRP i el seu ús com a modificants del DGEBA

UNIVERSITAT ROVIRA I VIRGILI
NOUS TERMOESTABLES EPOXÍDICS MODIFICATS AMB ESTRUCTURES DENDRÍTIQUES DE TIPUS HIPERRAMIFICAT I ESTRELLA
Mireia Morell Bel
DL:T. 155-2012

V.1 INTRODUCCIÓ

Els polímers estrella també poden ser obtinguts per polimerització radicalària emprant com a nucli un HBP. Per mitjà d'aquest mètode es poden obtenir una gran varietat d'estructures doncs existeix un elevat nombre de monòmers polimeritzables per via radicalària. De totes maneres, els polímers estrella contenint un nombre elevat de braços no es poden obtenir per polimerització radicalària convencional degut a l'elevada probabilitat que el sistema gelifiqui com a resultat de l'elevat nombre de reaccions de terminació entre les cadenes de les diferents molècules (*star-star* coupling). A més a més, és impossible controlar la longitud dels braços ja que l'etapa de propagació és molt ràpida. Finalment, l'etapa d'iniciació és lenta la qual cosa no permet iniciar simultàniament totes les cadenes i aquestes poden presentar una longitud diferent fent que l'estructura perdi definició.

Degut als inconvenients que presenta la polimerització radicalària convencional és necessari recòrrer a sistemes radicalaris controlats els quals redueixin el nombre de reaccions de terminació, presentin una etapa de propagació més lenta i una iniciació ràpida per assegurar el creixement homogeni de totes les cadenes. Entre ells, el ATRP (*atom transfer radical polymerization*) és un dels sistemes més emprats recentment per l'obtenció de noves topologies polimèriques complexes.

Els principis fonamentals de la polimerització per ATRP clàssica són els següents [1]:

1- L'etapa d'iniciació és molt ràpida i per tant instantàniament s'inicien totes les cadenes.

2- Existeix un equilibri dinàmic on els radicals en propagació (P_n*) són ràpidament transferits per mitjà d'un procés de desactivació (amb una constant de velocitat de desactivació, $\mathbf{k_{deact}}$) a través d'espècies X, les quals solen ser radicals estables com ara nitròxids o espècies organometàl·liques. Un cop aquests es troben en l'estat latent, es poden tornar a activar (amb una constant de velocitat d'activació, $\mathbf{k_{act}}$) espontàniament o tèrmicament, en presència d'un catalitzador apropiat restituint així els centres actius. El procés d'activació/desactivació establert, on sempre $\mathbf{k_{deact}} > \mathbf{k_{act}}$, es mostra a l'**Esquema V-1**.

[1] Braunecker, W.A.; Matysjaszewski, K. *Controlled/living radical polymerization: Features, developments, and perpectives* Prog. Polym. Sci. **2007**, 32, 93-146.

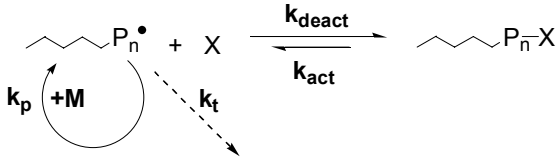

Esquema V-1 Processos involucrats en un sistema de polimerització radicalària controlada

3- Els radicals a més a més de poder propagar-se (k_p) poden reaccionar entre ells mitjançant l'anomenat procés de terminació (k_t). De totes maneres, aquest últim procés es veu cada cop menys afavorit a mida que passa el temps al contrari amb el que passa en la polimerització radicalària convencional. Cada terminació produeix una acumulació irreversible d'espècies inactives que no poden continuar reaccionant. El fet que la seva concentració augmenti progressivament amb el temps junt amb que la concentració de radicals sigui cada cop més baixa, redueix la probabilitat de que la terminació tingui lloc.

4- Els catalitzadors més emprats solen ser compostos de metalls de transició (Mt^n, on Mt^n: Cu(I), Fe(II), Co(II), entre d'altres) els quals poden expandir la seva esfera de coordinació i incrementar el seu estat d'oxidació incorporant un lligant complexant (L, on L: lligands multidentats nitrogenats) i un contra-ió (halògen) que pot formar un enllaç covalent o iònic amb el metall central.

5- El complex del metall de transició format (Mt^n/L) és el responsable de trencar l'enllaç homolític alquil-halògen de l'iniciador (R-X, on X: Cl, Br, I) per generar un radical orgànic (R*) el qual pot propagar (k_p), reaccionar amb un altre radical per terminació (k_t) o desactivar-se (k_{deact}) formant una espècie latent Mt^{n+1}X/L degut que el centre catalític veu incrementat el seu estat d'oxidació per incorporació de l'àtom halògen (contra-ió).

L'obtenció de polímers per ATRP permet controlar extraordinàriament la composició, l'estructura i la funcionalitat. Tanmateix, presenta un inconvenient important ja que cal eliminar l'oxigen i altres espècies oxidants presents al medi abans d'afegir el catalitzador el qual està en el seu estat d'oxidació més baix. Algunes estratègies que permeten fer front a aquesta limitació, es basen en l'ús del metall en el seu estat d'oxidació més alt (estable) i d'espècies formadores de radicals com ara, el AIBN (2,2'-azobis-2-metilpropionitril), capaces de reduir el metall i convertir-lo en actiu, sense necessitat de treballar en atmòsfera inert. De totes maneres, aquesta aproximació també presenta un inconvenient quan és

emprada per obtenir copolímers de bloc, ja que l'espècie generadora de radicals fa que creixin inevitablement cadenes d'homopolímer impurificant el producte [2].

Una alternativa, és l'utilització d'un agent reductor, com ara el $Sn(Oct)_2$ (2-etilhexanoat d'estany), sense capacitat per formar radicals. D'aquesta manera, la reducció del centre metàl·lic es pot fer in-situ, amb presència d'oxigen i sense formació d'homopolímer. A l'**Esquema V-2** es mostra l'actuació del $Sn(Oct)_2$ com agent reductor en un sistema de polimerització per ATRP. Aquesta estratègia és coneguda com a AGET/ATRP (*activator generated by electron transfer for atom transfer radical polymerization*) i és molt emprada tant en polimeritzacions apròtiques com en sistemes aquosos com en miniemulsió [3]. Val a dir que l'agent reductor es fa servir en quantitats estequiomètriques respecte al catalitzador.

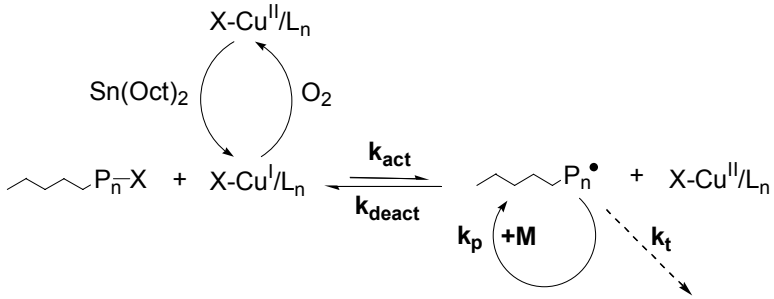

Esquema V-2 Mecanisme de polimerització per AGET/ATRP emprant $Sn(Oct)_2$ com agent reductor

En el present capítol, es descriu l'obtenció de polímers estrella amb braços de poli(metil metacrilat) a través de AGET/ATRP o poli(estirè) mitjançant ATRP clàssica, emprant el poliglicidol hiperramificat contenint grups 2-bromoisobutiril terminals per tal de poder ser emprat com a macroiniciador per ATRP.

V.1.1 Polímers estrella amb nucli hiperramificat obtinguts per polimerització radicalària controlada (ATRP) a través del mètode "*core-first*"

Com s'ha comentat anteriorment, els polímers estrella contenint un nombre elevat de braços no es poden obtenir per polimerització radicalària convencional degut a l'elevat nombre de reaccions de terminació entre les cadenes de les diferents estrelles, també conegut com *star-star coupling*. Per tant, el ATRP és una

[2] a) Jakubowski, W.; Matyjaszewski, K. *Activator generated by electron transfer for atom transfer radical polymerization* Macromolecules **2005**, 38, 4139-4146. b) Pintauer, T.; Matyjaszewski, K. *Atom transfer radical addition and polymerization reactions catalyzed by ppm amounts of copper complexes* Chem. Soc. Rev. **2008**, 37, 1087-1097.
[3] a) Oh, J.K.; Dong, H.; Zhang, R. Matyjaszewski, K. *Preparation of nanoparticles of double-hydrophilic PEO-PHEMA block copolymers by AGET ATRP in inverse miniemulsion* J. Polym. Sci., Part A: Polym. Chem. **2007**, 45, 4764-4772. b) Georgi, U.; Erber, M.; Stadermann, J.; Abulikemu, M.; Komber, H.; Lederer, A.; Voit, B. *New approaches to hyperbranched poly(4-chloromethylstyrene) and introduction of various functional end groups by polymer-analogous reactions* J. Polym. Sci., Part A: Polym. Chem. **2010**, 48, 2224-2235.

de les tècniques més eficients en l'obtenció d'aquest tipus d'estructures tant per la via "*arm-first*" [4], com per la de "*core-first*" [5].

Un dels primers treballs en descriure l'obtenció de polímers estrella per la via "*core-first"* emprant com a nucli un polímer hiperramificat va ser el de Maier *i col.* [5b] on es va polimeritzar per ATRP metil metacrilat (MA), emprant com a sistema catalític CuBr/*N,N,N',N'',N''*-pentametildietilentriamina (PMDETA). En aquest cas, el nucli era un poliglicidol hiperramificat prèviament modificat amb el bromur de 2-bromoisobutiril. Val a dir que tot i obtenir estructures ben definides, amb un promig de 45 – 55 braços de PMA i una baixa polidispersitat (1.25 – 2.50), la conversió màxima a la qual varen arribar, sense perill de gelificació, no superava el 35 %.

Més tard, Shen *i col.* [6], varen obtenir emprant el mateix nucli hiperramificat, polímers estrella contenint un promig entre 17 i 108 braços de poli(*tert*-butil acrilat) (P*t*BA) a través de ATRP. En aquest cas, al augmentar el nombre de braços i la conversió el control de la polimerització era cada cop més difícil i la polidispersitat augmentava considerablement.

Al mateix temps, Chen *i col.* [7], van aconseguir polimeritzar 2-hidroxietil metacrilat (HEMA) emprant diferents poliglicidols hiperramificats de diferent pes molecular i contenint entre 56 i 90 grups iniciadors (2-bromoisobutiril). El sistema catalític emprat, en aquest cas, va ser CuCl/2,2'-bipiridil (Bpy). Després d'optimitzar el procediment es va poder assolir conversions de fins el 79 % en aquells polímers amb un promig de 56 braços de PHEMA i del 37 % en aquells contenint uns 90 braços, mantenint la polidispersitat per sota de 2 en tots els casos.

Altres treballs portats a terme per Kowalczuck *i col*., descriuen la polimerització de tBA o estirè (St) a partir de diferent tipus de nuclis hiperramificat com ara el *p*-iodometilestirè [8] o bé un poli(arile-oxindole) hiperramificat prèviament modificat amb grups 2-bromoisobutiril terminals [9].

---

[4] a) Gao, H.; Matyjaszewski, K. *Synthesis of functional polymers with controlled architecture by CRP of monomers in the presence of cross-linkers: From stars to gels* Prog. Polym. Sci. **2009**, 34, 317-350. b) Blencowe, A.; Tan, J.F.; Goh, T.K.; Qiao, G.G. *Core cross-linked star polymers via controlled radical polymerization* Polymer, **2009**, 50, 5-32.
[5] a) Heise, A.; Hedrick, J.L.; Frank, C.W.; Miller, R.D. *Starlike block copolymers with amphiphilic arms as models for unimolecular micelles* J. Am. Chem. Soc. **1999**, 121, 8647-8648. b) Maier, S.; Sunder, A.; Frey, H.; Mülhaupt, R. *Synthesis of poly(glycerol)-block-poly(methyl acrylate) multi-arm star polymers* Macromol. Rapid Commun. **2000**, 21, 226-230.
[6] Shen, Z.; Chen, Y.; Barriau, E.; Frey, H. *Multi-arm star poly(glycerol)-block-poly(tert-butyl acrylate) and their respective multi-arm poly(acrylic acid) stars* Macromol. Chem. Phys. **2006**, 207, 57-64.
[7] Chen, Y.; Shen, Z.; Barriau, E.; Kautz, H.; Frey, H. *Synthesis of multiarm star poly(glycerol)-block-poly(2-hydroxyethyl methacrylate)* **2006**, 7, 919-926.
[8] a) Kowalczuk-Bleja, A.; Trzebicka, B.; Komber, H.; Voit, B.; Dworak, A. *Controlled radical polymerization of p-(iodomethyl)styrene-a route to branched and star-like structures* Polymer, **2004**, 45, 9-18. b) Kowalczuk-Bleja, A.; Sierocka, B.; Muszynszki, J.; Trzebicka, B.; Dworak, A. *Core-shell polyacrylate and poly styrene-block-polyacrylate stars* Polymer **2005**, 46, 8555-8564.
[9] Kowalczuk, A.; Vandendriessche, A.; Trzebicka, B.; Mendrek, B.; Szeluga, U.; Cholewinski, G.; Smet, M.; Dworak, A.; Dehaen, W. *Core-shell nanoparticles with hyperbranched poly(arylene-oxindole) interiors* J. Polym. Sci., Part A: Polym. Chem. **2009**, 47, 1120-1135.

També es van obtenir polímers estrella contenint braços de diferent estructura polimèrica a partir de ATRP i altres tècniques de polimerització radicalària controlada, aplicades consecutivament. En els treballs més recents descrits per Huang *i col.*, s'aconseguia obtenir polímers a partir de poliglicidol hiperramificat braços de diferent estructura polimèrica com ara, poliestirè (PS) i poli(àcid acrílic) (PAA) [10] o bé braços constituïts per copolímers de bloc com ara, poliestirè-*b*-poli(òxid d'etilè) (PS-*b*-PEO) [11]. En ambdós treballs es polimeritzava l'estirè emprant CuBr/Bpy com a sistema catalític. El nombre promig de braços per molècula estava entre els 60 i els 210. Tanmateix per portar a terme les reaccions de polimerització controladament, sense perill de *star-star coupling*, en tots els casos s'havia de limitar la conversió del monòmer a valors per sota del 20 %.

[10] Liu, C.; Zhang, Y.; Huang, J. *Well-defined star polymers with mixed-arms by sequential polymerization of atom transfer radical polymerization and reverse addition-fragmentation chain transfer on a hyperbranched polyglycerol core Macromolecules* **2008**, 41, 325-331.
[11] Liu, C.; Pan, M.; Zhang, Y.; Huang, J. *Preparation of star block copolymers with polystyrene-block-poly(ethylene oxide) as side chains on hyperbranched polyglycerol core by combination of ATRP with atom transfer nitroxide radical coupling reaction* J. Polym. Sci., Part A: Polym. Chem. **2008**, 46, 6754-6761.

UNIVERSITAT ROVIRA I VIRGILI
NOUS TERMOESTABLES EPOXÍDICS MODIFICATS AMB ESTRUCTURES DENDRÍTIQUES DE TIPUS HIPERRAMIFICAT I ESTRELLA
Mireia Morell Bel
DL:T. 155-2012

V.2

SYNTHESIS, CHARACTERIZATION AND RHEOLOGICAL PROPERTIES OF MULTIARM STARS WITH POLY(GLYCIDOL) CORE AND POLY(METHYL METHACRYLATE) ARMS BY AGET ATRP

Mireia Morell, Brigitte Voit, Xavier Ramis, Àngels Serra, Albena Lederer

Journal of Polymer Science, Part A: Polymer Chemistry ***2011****, 49, 3138 – 3151*

UNIVERSITAT ROVIRA I VIRGILI
NOUS TERMOESTABLES EPOXÍDICS MODIFICATS AMB ESTRUCTURES DENDRÍTIQUES DE TIPUS HIPERRAMIFICAT I ESTRELLA
Mireia Morell Bel
DL:T. 155-2012

Journal of Polymer Science, Part A: Polymer Chemistry **2011**, 49, 3138 – 3151

SYNTHESIS, CHARACTERIZATION, AND RHEOLOGICAL PROPERTIES OF MULTIARM STARS WITH POLY(GLYCIDOL) CORE AND POLY(METHYL METHACRYLATE ARMS BY AGET/ATRP

Mireia Morell,[1] Brigitte Voit,[2] Xavier Ramis,[3] Àngels Serra,[1]Albena Lederer[2]

[1] Department of Analytical and Organic Chemistry, University Rovira i Virgili, C/ Marcel·lí Domingo s/n, Tarragona 43007, Spain.
[2] Leibniz-Institut für Polymerforschung Dresden, Hohe Strasse 6, Dresden 01069, Germany.
[3] Thermodynamics Laboratory, ETSEIB University Politècnica de Catalunya, C/ Av. Diagonal 647, Barcelona 08028, Spain.

Abstract

Well-defined multiarm star block copolymers poly(glycidol)-*b*-poly(methyl methacrylate) (PGOHBr-*b*-PMMA$_x$) with an average number of PMMA arms of 85, 55 and 45 have been prepared. The *core*-first approach has been selected as the methodology using atom transfer radical polymerization (ATRP) of MMA from an activated hyperbranched poly(glycidol) as the core. These activated hyperbranched macroinitiators were prepared by esterification of hyperbranched poly(glycidol) (PGOH) with 2-bromoisobutyryl bromide. The effect of monomer/initiator ratio, catalyst concentration, time, temperature, and solvent on the growing of the arms has been studied in detail in order to optimize the process and to diminish the radical-radical coupling.

The final products and intermediates were characterized by means of size exclusion chromatography (SEC), nuclear magnetic resonance (NMR) and Fourier transform-infrared (FTIR) spectroscopy. The length of PMMA arms was determined by SEC after cleavage of ester bond linked to PGOH core. Glass transition temperature (T_g), thermal stability and rheological properties of the multiarm star copolymers were also studied. Finally, tapping mode atomic force microscopy (TMAFM) allowed the clear visualization of nano-sized particles (80 - 200 nm) corresponding to individual star molecules.

Keywords: AGET ATRP; copolymer; hyperbranched poly(glycidol); PMMA; star polymers

Introduction

Nowadays multiarm star polymers have an important relevance as advanced polymer materials due to their special bulk and solution properties [1,2].

The improvement of the controlled/living radical polymerization allows for well-tuned characteristics of the final product without using difficult synthetic methodologies.

Two major strategies have been employed for their preparation: the “core-first” approach which involves the living polymerization from a multifunctional core [3,4], and the “arm-first” approach, which consists in linking reactive polymer chains to a functionalized core or to a small amount of bifunctional vinyl compounds capable to crosslink [5]. Among them, the “core-first” strategy established itself as the most effective for the preparation of well-defined star polymers.

As well-defined star polymers cannot be prepared by means of conventional free radical polymerization, a large variety of star polymers have been synthesized

by ionic polymerization procedures [6]. Unfortunately, these approaches are only applicable for a limited number of monomers and are sensitive to impurities.

In recent years, several procedures for the controlled or "living" radical polymerization have been developed [7-10]. Among these methods, atom transfer radical polymerization (ATRP), which uses among others Cu (I) as catalyst, is of considerable efficiency to obtain star-shaped architectures involving a large variety of styrene or acrylate monomers [11-14]. Activator generated by electron transfer (AGET) ATRP together with activator regenerated by electron transfer (ARGET) ATRP are improved approaches. They lead to a reduction of the preparation time needed in the degassing procedure due to the use of a latent copper (II) precursor which is *in situ* reduced to active Cu (I) species. Moreover, the reducing agent employed is also capable of removing dissolved oxygen from the system, but the greater advantage is that it permits reducing the copper concentrations down to only 10 - 50 ppm during the polymerization while controlling molecular weight and molecular-weight distribution of linear polymers or block copolymers [15-17].

For the preparation of larger amounts of well-defined star polymers with a large number of arms, dendrimers as cores are not suitable due to their rather complicated and expensive synthesis. For that reason, hyperbranched polymers can be considered as good candidates to be employed as multifunctional core structures. Among them, hyperbranched poly(glycidol) (PGOH) with low molecular-weight distribution, obtained via ring-opening anionic polymerization is one of the most employed macroinitiators [3,11,18].

Hyperbranched poly(glycidol) has demonstrated to be a good choice as a core molecule since it combines several remarkable features, including a polyether backbone, multiple hydroxyl groups, hydrophilic character and excellent biocompatibility [18,19].

Although the synthesis of dendrimers have been attached by living radical polymerization following simple methodologies, nowadays, only few reports involve the synthesis of well-defined star polymers with a number of arms larger than 40 per core unit [20,21]. This fact is the result of the dramatic increase of radical-radical coupling probability with the increasing arm number during the polymerization. Frey and coworkers [11], reported the synthesis of multiarm star polymers from 17 to 108 poly(*tert*-butyl acrylate) arms on a hyperbranched poly(glycidol) core. They stated that coupling side reactions are always present when the arm number exceeds 66 and the only way to avoid them is to limit the monomer conversion to 30 %. This statement agrees with previous observations reported by Gnanou and coworkers [12].

Poly(methyl methacrylate) (PMMA) is an important polymer due to its variety of applications such as bone cements, dental moulds or adhesives [22,23]. To our knowledge, up to now only few papers reported the synthesis of star-like poly(methyl methacrylate) structures and they possess only 3 to 20 arms per molecule [24-27]. Matyjaszewski *et al.* [28], have recently obtained star-like block

copolymers with 10 or 20 arms based on poly(*n*-butyl acrylate)-*b*-poly(methyl methacrylate) using short linear multifunctional initiators by classic ATRP. However, they observed a partial star coupling when the number of arms increased despite of limiting the polymerization conversion down to 40 %.

From the point of view of application, multiarm star copolymers as high-molecular-weight macromolecules, with controlled architecture, represent an ideal starting point because of their potential application in intramolecular engineering, in mechanical performance, as crystallization modulators and also as viscosity modifiers due to their inherent "molecular softness" [29]. To date, the rheological characterization of multiarm star copolymers obtained by ATRP employing the core-first approach has not been reported. Therefore, the aim of the present work has been the synthesis of well-defined multiarm star poly(glycidol)-*block*-poly(methyl methacrylate) copolymers with a number of arms in the range of 45 - 85 by AGET ATRP and their characterization. We have complemented the study with the thermal and linear rheological behaviour of the multiarm star copolymers in the melt state, relating their characteristics (i) with the number of arms per molecule and (ii) with the molecular weight of the arms in order to uncover the optimal architecture which possesses the lower melt shear viscosity for the required application. Furthermore, the morphology of the corresponding star molecules has been studied by means of tapping mode atomic force microscopy (TMAFM).

Experimental

Materials

Glycidol (96 %) was distilled under reduced pressure and stored over molecular sieve at 2 - 5 ºC, dioxane was dried over calcium hydride and subsequently distilled and methyl methacrylate (MMA, 99 %) was passed through basic alumina column to remove the radical inhibitor. Trimethylolpropane (TMP) (97 %), potassium methylate solution (25 % v/v in methanol), $CuBr_2$ (99 %), *N,N,N',N',N''*-pentamethyldiethylene triamine (PMDETA, 99 %), tin(II) 2-ethylhexanoate ($Sn(Oct)_2$, 98 %), 2-bromoisobutyryl bromide (98 %), anhydrous pyridine, anhydrous anisole and anhydrous DMF were used without further purification. All these chemicals were purchased from Sigma-Aldrich.

All other reagents and solvents were purchased from Scharlab. Dialysis tubes based on regenerated cellulose membrane (MWCO 2,000 g/mol) were acquired from Roth.

Synthesis of ATRP macroinitiators

Hyperbranched poly(glycidol) (PGOH, $\overline{M_n}$ (^{1}H NMR) 7,900 g/mol with an average of 107 hydroxyl group per molecule) was prepared according to already published procedures [19], and dried under vacuum during 2 days at 50 ºC.

^{1}H NMR (400 MHz, DMSO-d_6) *δ ppm*: 4.8-4.3 (O**H**), 3.8-3.2 (C**H**O/C**H**OH/C**H$_2$**O/C**H$_2$**OH, poly(glycidol) backbone), 1.28 (C**H$_2$**, TMP in the PGOH) and 0.81 (C**H$_3$**, TMP in the PGOH); ^{13}C NMR (100.6 MHz, DMSO-d_6,) *δ ppm*: 80.9-80.0 (**C**H linear unit), 79.0-78.0 (**C**H dendritic unit), 74.0-72.8 (**C**H$_2$ linear unit), 72.5-70.6 (**C**H$_2$/**C**H terminal and dendritic unit), 69.6-68.4 (**C**H linear unit), 63.9-63.1 (**C**H$_2$ terminal unit) and 61.5-61.0 (**C**H$_2$ linear unit); FTIR (ATR) (cm^{-1}): 3370 (OH), 1170-980 (C-O-C st as); $\overline{M_n}$ (SEC-LS) = 10,500 g/mol, $\overline{M_w}/\overline{M_n}$ = 1.48.

The signal assignment and the degree of branching (DB) of PGOH, according to the Frey's definition, were determined according to a previous publication [30]. DB was 0.49, calculated from ^{13}C NMR signal intensities obtained under quantitative conditions.

Macroinitiators with variation in number of initiating sites, PGOHBr$_x$ for ATRP were prepared as reported previously [3], by esterification of hyperbranched PGOH with 2-bromoisobutyryl bromide to different extent. All the macroinitiators were additionally purified by dialysis against chloroform in case of PGOHBr$_{85}$ and PGOHBr$_{55}$ or methanol for PGOHBr$_{45}$ during 3 days to completely remove low molecular weight impurities.

(**A**) **PGOHBr$_{85}$** and (**B**) **PGOHBr$_{55}$** possess an average number of 85 and 55 2-bromoisobutyryl groups per molecule, respectively, which correspond to a degree of modification of 80 and 52 %, respectively. The degree of modification was calculated by ^{1}H NMR spectroscopy of previously acidified samples with deuterated trifluoroacetic acid (TFA-d$_1$) to remove the remaining hydroxyl group signals from the signal region which is used to determine the signal intensity of the backbone protons.

^{1}H NMR (400 MHz, $CDCl_3$) *δ ppm*: 5.4-5.0 (m, C**H**-OOC-C(CH$_3$)$_2$-Br), 4.6-4.0 (m, C**H$_2$**-OOC-C(CH$_3$)$_2$-Br), 4.0-3.2 (m, C**H$_2$**/C**H** PGOH core), 1.95 (s, CH$_2$/CH-OOC-C(C**H$_3$**)$_2$-Br), 1.43 (CH$_3$-C**H$_2$**- TMP in the PGOH core) and 0.87 (C**H$_3$**-CH$_2$-TMP in the PGOH core); ^{13}C NMR (100.6 MHz, $CDCl_3$) *δ ppm*: 171 (**C**=O), 79.2-62.3 (**C**H$_2$/**C**H PGOH core and **C**H$_2$/**C**H-OOC-C(CH$_3$)$_2$-Br), 56.4-54.7 (CH$_2$/CH-OOC-**C**(CH$_3$)$_2$-Br) and 30.5 (CH$_2$/CH-OOC-C(**C**H$_3$)$_2$-Br); FTIR (ATR) (cm^{-1}): 1733 (C=O), 1310 (CH$_3$, *γ*), 1210-1030 (C-O-C, st as). $\overline{M_n}$ (^{1}H NMR, PGOHBr$_{85}$) = 20,600 g/mol and $\overline{M_n}$ (^{1}H NMR, PGOHBr$_{55}$) = 16,100 g/mol.

Journal of Polymer Science, Part A: Polymer Chemistry **2011**, 49, 3138 – 3151

(**C**) **PGOHBr$_{45}$** has an average number of 45 2-bromoisobutyryl groups per molecule which corresponds to a degree of modification of 42 %, calculated from samples acidified with deuterated trifluoroacetic acid (TFA-d_1).

^{1}H NMR (400 MHz, DMSO-d_6) *δ ppm*: 5.4-4.8 (m, C**H**-OOC-C(CH$_3$)$_2$-Br), 4.5-3.9 (m, C**H$_2$**-OOC-C(CH$_3$)$_2$-Br), 3.9-3.2 (m, C**H$_2$**/C**H** PGOH core), 1.90 (s, CH$_2$/CH-OOC-C(C**H$_3$**)$_2$-Br), 1.27 (CH$_3$-C**H$_2$**- TMP in the PGOH core) and 0.79 (C**H$_3$**-CH$_2$- TMP in the PGOH core); ^{13}C NMR (100.6 MHz, DMSO-d_6) *δ ppm*: 171 (**C**=O), 77.8-60.6 (**C**H$_2$/**C**H PGOH core and **C**H$_2$/**C**H-OOC-C(CH$_3$)$_2$-Br), 57.2-56.7 (CH$_2$/CH-OOC-**C**(CH$_3$)$_2$-Br) and 30.3 (CH$_2$/CH-OOC-C(**C**H$_3$)$_2$-Br); FTIR (ATR) (cm^{-1}): 3700-3100 (OH), 1732 (C=O), 1270 (CH$_3$, *γ*), 1190-1030 (C-O-C, st as). $\overline{M_n}$ (^{1}H NMR, PGOHBr$_{45}$) = 14,600 g/mol.

Synthesis of PGOH-b-PMMA$_x$ multiarm star copolymer

The synthesis is exemplified for entry 12 of **Table 1**. PGOHBr$_{45}$ (0.5 g, 0.034 mmol, 1.54 mmol of bromine atoms), 15 g of MMA (154 mmol), 15 mL of anhydrous anisole, 0.325 mL of PMDETA (1.54 mmol) and 0.172 g of CuBr$_2$ (0.77 mmol) were placed in a three-necked round flask and degassed by one freeze-pump-thaw cycle. Then 0.112 mL of Sn(Oct)$_2$ (0.347 mmol) was added to the solution mixture under argon and the flask was immersed in an oil bath thermostated at 50 ºC. After 40 min the reaction was stopped by immersing the flask into liquid nitrogen. The crude product was dissolved in THF and passed through a silica gel column to remove the copper complex. The samples were precipitated twice in 10-fold excess *n*-hexane, filtered and dried at 50 ºC under vacuum for two days.

^{1}H NMR (400 MHz, CDCl$_3$) *δ ppm*: 4.9 (m, C**H**-OOC-C(CH$_3$)$_2$-PMMA$_x$, PGOHBr core), 4.5-3.9 (m, C**H$_2$**-OOC-C(CH$_3$)$_2$-PMMA$_x$, PGOHBr), 3.7 (s, -COOC**H$_3$**, PMMA end group), 3.5 (s, -COOC**H$_3$**, PMMA backbone), 2.1-1.4 (m, -C**H$_2$**-, PMMA backbone), 1.2 (s, -C**H$_3$**, isotactic PMMA), 1.0 (s, -C**H$_3$**, atactic PMMA) and 0.8 (s, -C**H$_3$**, syndiotactic PMMA); ^{13}C NMR (100.6 MHz, CDCl$_3$) *δ ppm*: 177 (**C**=O), 54 (**C**H$_2$, PMMA backbone), 51.7 (-COO**C**H$_3$, PMMA backbone), 44.3 (quaternary **C**, PMMA backbone), 19.0 and 16.6 (-**C**H$_3$, PMMA backbone); FTIR (ATR) (cm^{-1}): 1727 (C=O), 1220-1080 (C-O-C, st as).

Cleavage of PMMA arms of the multiarm star copolymer

One-hundred milligram of multiarm star was dissolved in 20 mL of THF. 20 mL of a NaOH solution ($6\cdot10^{-3}$ M in MeOH) were added and the solution was refluxed at 80 ºC overnight. After neutralizing the solution with 1 M HCl and evaporating to dryness, the cleaved arms were analyzed by SEC.

Characterization

^{1}H NMR and ^{13}C NMR measurements were carried out at 400 MHz and 100.6 MHz, respectively, on a Varian Gemini 400 spectrometer. CDCl$_3$ and DMSO-d_6 were used as solvents for all NMR measurements. For internal calibration the

solvent signals were used: δ (^{13}C) = 77.16 ppm, δ (^{1}H) = 7.26 ppm for $CDCl_3$ and δ (^{13}C) = 39.52 ppm, δ (^{1}H) = 2.50 ppm for DMSO-d_6. Quantitative ^{13}C NMR experiments were recorded using a delay time between sampling pulses equal to 8 seconds and inverse gated proton decoupling.

^{1}H NMR T_2 relaxation measurements were carried out at 298 K on a Bruker Avance III 600 spectrometer operating at a proton frequency of 600.20 MHz using a 5 mm CPTCI triple resonance (^{1}H, ^{13}C, ^{31}P) gradient cryoprobe. The spectral width was 13 ppm and a total of 16 transients were collected into 64K data points for each ^{1}H spectrum. A recycling delay time of 8 seconds was applied between scans to ensure correct quantification. Exponential line broadening of 0.3 Hz was applied before Fourier transformation. T_2-edited ^{1}H spectra were performed using the Carr-Purcell-Meiboom-Gill sequence (*2) (or CPMG pulse) of spin-spin T_2 relaxation filter with a time filter that ranges from 40.7 to 1220 ms. In order to compare with ^{1}H-NMR T_2 unedited spectra, acquisition parameters were maintained in all experiments. The frequency spectra were phased, baseline corrected and then calibrated (TMS, 0.0 ppm) using TopSpin software (version 2.1, Bruker). T_2 relaxation times were determined using the described procedure [31].

The FTIR spectra were collected in a spectrophotometer FTIR-680PLUS from JASCO with a resolution of 4 cm^{-1}. This device was equipped with an attenuated-total-reflection accessory with a diamond crystal (Golden Gate heated single-reflection diamond ATR, Specac-Teknokroma).

The determination of molecular weights, molecular weight distributions and radius of gyration ($R_{g,z}$) were carried out on a modular build SEC-system on an Agilent 1200 series pump coupled with a multiangle laser light scattering (MALLS) detector Tristar MiniDawn (Wyatt Technology) and Knauer RI detector in combination with a PolarGel-M-column (Polymer Laboratories) in DMAc mixed with 3 g·L^{-1} LiCl. The evaluations of the molecular weights and radius of gyration were made using software ASTRA 4.9 (Wyatt Technology). Complete mass recovery was assumed leading to the dn/dc values from the SEC-MALLS measurement interpretation. The dn/dc values were well reproducible and complete mass recovery was found from the linear molar weight / elution volume plot. The dn/dc of the hyperbranched polyglycidol was found to be 0.11 dL/g and for the PGOH-*b*-PMMA$_x$ stars of 0.055 to 0.065 dL/g depending on the number of PMMA arms. The radius of gyration ($R_{g,z}$) was estimated by the mean square radius using the Zimm's method.

The determination of the molecular weight of the PMMA arms was performed on an Agilent 1200 series system equipped with an Agilent 1100 series refractive-index (RI) detector using THF as eluent in combination with PLgel 3 μm MIXED-E, PLgel 5 μm MIXED-D and PLgel 20 μm MIXED-A columns in series. The calibration of this SEC analysis was performed with poly(methyl methacrylate) standards. The flow rate employed was 1.0 mL/min in both equipments.

Gas chromatography was used to determine the monomer conversion by analysis in a 6890 gas chromatograph and a 5973 inert mass spectrometer, using a HP-5MS capillary column (30 m, 0.25 mm, 0.25 μm), all from Agilent Technologies

Journal of Polymer Science, Part A: Polymer Chemistry **2011**, 49, 3138 – 3151

(Palo Alto). Carrier gas was 99.999 % pure helium at a flow rate of 1 mL/min. Injected volume was 1 μL of sample in split mode, with an split ratio of 10:1. The injector was set at a temperature of 220 ºC, and the oven temperature of GC was initially held at 40 ºC for 5 minutes, and then raised to 150 ºC at a rate of 15 ºC/min. The total chromatographic analysis time was of 12.33 min. The mass spectrometer acquired data in scan mode with an m/z interval from 35 to 200. Methyl methacrylate was quantified by target ion (69, 100 %) and identified by two qualifier ions (100, 48 % and 41, 97 %) and retention time (2.98 min). External calibration was performed by analysing diluted methacrylate commercial standards, freshly prepared in chloroform at the moment of calibration. Five calibration levels were used, at amounts ranging between 50 and 1000 ppm. Calibration curves showed good linearity, with a determination coefficient (r^2) of 0.998. Samples diluted in chloroform were analysed in the same conditions than the standards.

Calorimetric analyses were carried out on a Mettler DSC-822e thermal analyzer. Samples of ~ 25 mg in weight were placed in aluminum pans under nitrogen atmosphere. The calorimeter was calibrated using an indium standard (heat flow calibration) and an indium-lead-zinc standard (temperature calibration). The glass transition temperatures (T_gs) were determined by means of a second scan at 10 ºC/min as the temperature of the half-way point of the jump in the heat capacity under N_2 atmosphere.

TGA analyses were carried out in a Mettler TGA/SDTA851e/LF/1100 thermobalance. Samples with an approximate mass of 8 mg were degraded between 30 and 800 ºC at a heating rate of 10 ºC/min in N_2 (100 cm^3/min measured in normal conditions).

Measurements were carried out in the parallel plates (geometry of 25 mm) mode with an ARG2 rheometer (TA Instruments, UK, equipped with a Peltier system). All of them were performed in the linear viscoelastic regime determined by previous strain sweeps. Storage modulus (G'), loss modulus (G'') and complex viscosity (η^*) were recorded as function of frequency (0.01-100 Hz) stating a constant deformation of 1 4% at 130 ºC. PGOH-*b*-$PMMA_x$ star copolymers powders (1 g) were stabilized by 1 % of Irganox®, dissolved in 5 mL of DMF and molded into a clear glass capsule. Films were obtained after evaporation of solvent at 50 ºC during 24 hours.

Because the storage modulus at intermediate frequencies was not constant, the “plateau” modulus was estimated by applying the loss tangent minimum criterion. G_N^0 was taken as G' at the frequency where ($\tan \delta = G''/G'$) is minimum in the “plateau” range,

$$G_N^0 = G' \mid_{\tan \delta \rightarrow \min} \quad (1)$$

The observation of single macromolecules was done by drop-casting (solution of 2 mg/L of polymer in THF) onto freshly cleaved mica surface. The samples were dried at room temperature and observed using an Agilent 5500 AFM/SPM

microscope (Agilent Technologies Inc.) in the tapping mode. The measurements were performed in air using Si cantilevers with a nominal spring constant and resonance frequency of 3 N/m and 75 kHz respectively. Height and phase images were taken at a tip velocity of 1.5 lines/s.

Results and discussion

Hyperbranched poly(glycidol) (PGOH) was prepared according to previously published procedures by anionic polymerization of glycidol employing as initiator trimethylolpropane (TMP) and potassium methylate [19].

Subsequently, the hydroxyl groups of PGOH were partially modified by esterification with 2-bromoisobutyryl bromide to generate three ATRP macroinitiators with an average number of 45, 55 and 85 of bromine sites and with molecular weights varying from 14,600 to 20,600 g/mol. Finally, MMA was polymerized from them to obtain the multiarm copolymers by means of AGET ATRP. The synthetic pathway is depicted in **Scheme 1**.

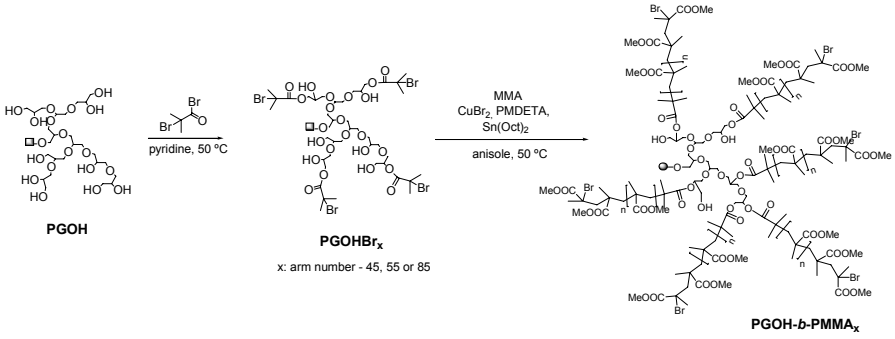

Scheme 1 Synthetic route to multiarm star copolymers PGOH-b-PMMA$_x$

Synthesis of multiarm star poly(glycidol)-block-poly(methyl methacrylate)

AGET ATRP on the macroinitiators was performed employing $CuBr_2$/PMDETA as catalytic system. A stoichiometric amount of reducing agent, namely, tin (II) 2-ethylhexanoate ($Sn(Oct)_2$) was employed, because of its capacity to reduce the catalytic complex. This polymerization system takes place without free radical formation and therefore avoids homopolymerization [15,32].

Up to now, the synthesis of linear PMMA by ATRP has been successfully attempted in bulk [33], apolar solvents as anisole or even with extremely polar solvents as DMF or poly(ethylene glycol) at temperatures between 70 and 110 ºC [34,35]. Taking into account these previous results, we firstly performed the reactions in anisole at 80 ºC. As it can be seen in **Table 1**, all the polymerizations conducted at this temperature were uncontrolled and for all macroinitiators star-star coupling (entries 5 and 9, $\overline{M_w}/\overline{M_n}$ = 9.84 and 5.09 respectively) or gelation (entries 10 and 11) occurred.

Journal of Polymer Science, Part A: Polymer Chemistry **2011**, 49, 3138 – 3151

Table 1 Experimental conditions and molecular weight data of PGOH-*b*-PMMA$_x$ multiarm star copolymers using AGET ATRP

Entry	[M][a]:[I][a]:[$CuBr_2$][b]	*T* (ºC)	*Time* (min)	*Conv.*[c] (%)	$\overline{M}_{n,theoric}$[d] (g/mol)	$\overline{M}_{n,SEC-LS}$[e] (g/mol)	$\overline{M}_w/\overline{M}_n$[e]	$R_{g,z}$[f] (nm)
PGOH-*b*-PMMA$_{85}$								
5	100:1:0.5	80	30	40	360,600	422,700	9.84	116
7	100:1:0.5	50	90	65	573,100	413,400	2.05	16
8	100:1:0.5	50	180	88	768,600	760,700	1.70	38
PGOH-*b*-PMMA$_{55}$								
9	100:1:0.5	80	60	82	467,100	892,000	5.09	127
PGOH-*b*-PMMA$_{45}$								
10	100:1:0.5	80	10	gel	-	-	-	-
11	300:1:0.5	80	15	gel	-	-	-	-
12	100:1:0.5	50	40	42	205,400	186,500	1.79	23
13	100:1:0.5	50	50	66	313,400	324,500	2.20	-
14[g]	100:1:0.4	50	10	gel	-	-	-	-

a. [M] and [I] are, respectively, the monomer and initiator concentrations.
b. Polymerization conditions: L: PMDETA; I is the initiating site of PGOHBr$_x$; [$CuBr_2$]:[L]=0.5:1; [$Sn(Oct)_2$]:[$CuBr_2$]=0.22; solvent: anisole, $V_{anisole}$:V_{MMA} = 1:1.
c. Conversion determined by gas chromatography.
d. $\overline{M}_{n,theoric}$ was determined as: ([M]:[I]) x M(MMA) x Br x conversion) + $\overline{M}_n$ (PGOHBr$_x$).
e. $\overline{M}_n$ and PDI of star copolymers were measured by SEC-MALLS with DMAc as solvent.
f. Radius of gyration ($R_{g,z}$) determined by MALLS.
g. [CuCl]:[L]=1:2; solvent:DMF; V_{DMF}:V_{MMA}=0.25:1; [$CuBr_2$]=6.5·10^{-2} M.

Unexpectedly, employing the same experimental conditions, gelation occurred at short reaction times (within 10 minutes) for 45-arm macroinitiator, whereas it did not happen with the higher modified initiators. This can be explained according to the previous observation that in the preparation of star polymers with less poly(*tert*-butyl acrylate) arms the fastest polymerizations occurred [11]. This fast reaction could in our case lead to gelation. In order to control the reaction, we set the feed ratio of MMA to initiating sites to 300:1 (entry 11) but again it was not possible to suppress the radical-radical coupling due to the fast polymerization rate. To obtain well-defined multiarm PMMA stars it was necessary to decrease the reaction temperature to 50 ºC while maintaining the feed ratio MMA to initiating sites at 100:1. In these conditions, the molecular-weight distribution values of the obtained 45- or 85-arm PMMA stars could be controlled in the range of 1.70-2.20 (entries 7, 8, 12 and 13) driving the reaction to maximum conversion values of 88 %. It is worth to mention that the 45-arm macroinitiator had an initial limited solubility in the reaction mixture when anisole was used as solvent. Therefore, initially we performed the polymerization in DMF (0.25:1 v/v, DMF:MMA) with $CuBr_2$ as deactivating agent and CuCl as catalyst at 50 ºC (entry 14) to solubilize it and make the initiation step easier. However, DMF as polar solvent changes the balance of Cu(I)/Cu(II) equilibrium resulting in an increase in the overall rate of polymerization which led to crosslinking in only few minutes [36]. Thus, DMF was replaced by anisole (entries 12 and 13). Despite of being initially insoluble, the solubility increased when a certain number of initiating sites of the macroinitiator started to polymerize MMA. After this induction period, the polymerization solution became fully homogeneous.

Structural characterization of PGOH-b-PMMA$_x$

The obtained hyperbranched poly(glycidol) (PGOH) cores, macroinitiators and multiarm copolymers with 45, 55 or 85 PMMA arms were characterized by ^{1}H NMR. In **Figure 1** (**a**) and (**b**) ^{1}H NMR spectra of poly(glycidol) core before and after 42 % of modification with 2-bromoisobutyril bromide are shown.

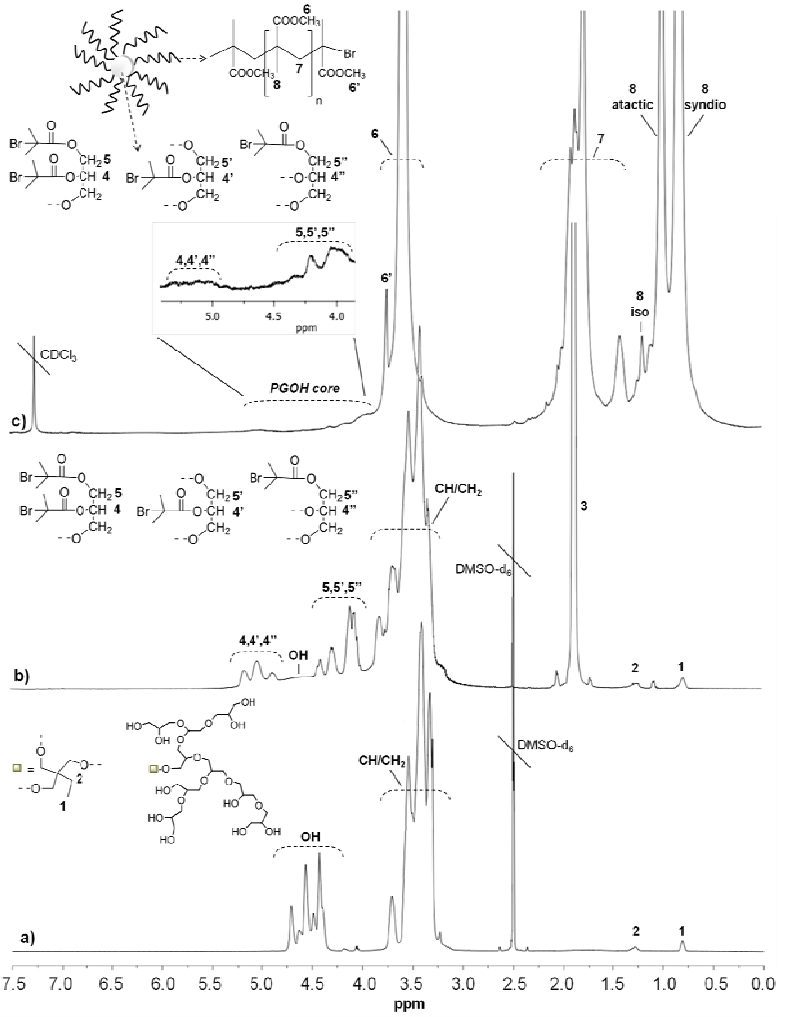

Figure 1 ^{1}H NMR spectra of **a**) PGOH in DMSO-d_6, **b**) PGOHBr$_{45}$ in DMSO-d_6 and **c**) star copolymer PGOH-*b*-PMMA$_{45}$ in $CDCl_3$ (entry 13 in **Table 1**)

As it can be seen in the spectrum (**a**)**,** the main signal of hyperbranched poly(glycidol) appears at 3.8 - 3.2 ppm and corresponds to the five protons (1-5) of methine and methylene groups in the repeating unit. There is also a complex signal centered at about 4.5 ppm corresponding to the hydroxyl groups and two small signals at 1.28 and 0.81 ppm that can be attributed to the TMP core. From the ratio

Journal of Polymer Science, Part A: Polymer Chemistry **2011**, 49, 3138 – 3151

of integral area corresponding to the five protons of PGOH repeating unit and the integral area from methyl group of TMP core, we obtained the degree of polymerization, which nearly corresponds to the number of hydroxyl groups per molecule. After the esterification reaction (spectrum **b**), some new signals appear in the region from 5.4 to 3.9 ppm, due to the shift on the methine and methylene protons produced by the modification reaction of primary and secondary hydroxyl groups. In the spectrum we can also see the signal at 1.90 ppm, assigned to the six methyl protons of the 2-bromoisobutyryl group. The remaining OH groups are visible as a broad signal centered at ~ 4.5 ppm and after acidification with TFA-d_1 the integral area from esterified units is reduced due to downfield shift of this signal. Therefore, the achieved degree of modification was calculated by integration of the signals in the region 5.4 - 3.2 ppm (methine and methylene protons of esterified and non-esterified units) and the signal at 1.90 ppm (methyl protons of the esterified unit) from the sample acidified with TFA-d_1. Therefore, the number of bromine sites (*Br*) was determined using the average molecular weight of PGOH ($\overline{M_n}$ PGOH), the molecular weight of a repeating unit (*M(R.U.)*) and the degree of modification (*D.M.*), as follows:

$$Br = \frac{\overline{M}_n PGOH}{M\,(R.U.)}\, xD.M. \qquad (2)$$

In **Figure 1** (**c**) the spectrum of the PGOH-*b*-$PMMA_{45}$ (entry 13 in **Table 1**) is shown. The high molecular weight of arms and their high number led to the broadening of PGOHBr signals due to the lack of mobility of this core structure and the resulting shorter relaxation time in comparison with PMMA arms. PMMA signals appear at 3.7 ppm (OCH_3), 2.1 - 1.4 ppm (methylene protons in the chain) and 1.2, 1.0 and 0.8 ppm, corresponding to the triads of the methyl protons. All PMMA copolymers obtained showed the same tacticity which was about 60 % syndiotactic, 30 % atactic and 10 % isotactic triads corresponding to the typical PMMA tacticity obtained by conventional radical polymerization [37]. In addition, a small broad signal at 4.9 ppm and a broad shoulder from 4.5 - 3.9 ppm, partially overlapped with the signal of -OCH_3 from PMMA arms, appear also in the spectrum. In order to elucidate their origin, a spin-spin relaxation (T_2) experiment was performed. By this technique, the segmental motion on the picosecond time scale can be deduced. Low mobility regions possess smaller rotational diffusivity and shorter T_2 spin-spin relaxation times, which leads to broader spectral lines in comparison with regions with higher mobility [38]. Therefore, it is possible to apply editing spectra techniques, based on the differences in T_2, to the structural characterization of multiarm star copolymers due to the existence of two parts: a core with restricted motions and arms with higher mobility.

In **Figure 2** the unfiltered ^{1}H NMR spectrum (**a**) and the edited spectrum (**b**) after application of a CPMG filter (1220 ms) are shown.

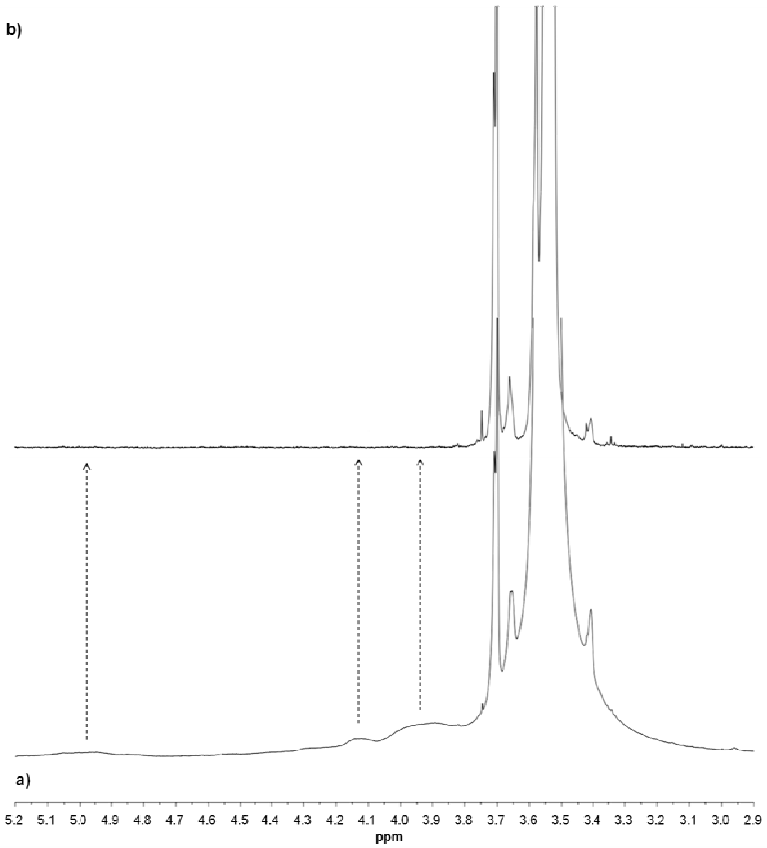

Figure 2 Region of the ^{1}H NMR from 2.9 to 5.2 ppm of multiarm star copolymer PGOH-*b*-$PMMA_{45}$ (entry 13, **Table 1** in $CDCl_3$) spectra: **a**) unedited reference spectrum and **b**) T_2-edited after a CPMG filter (1220 ms) spectrum

The application of this strategy led to the indirect detection of the PGOH core because the broad signals are disappearing when the filter is used. After removing the core signals, the spectrum shows only the part with less restricted mobility, which corresponds to the PMMA arms. T_2 relaxation times were determined from the signal at 4.5 - 3.9 ppm (corresponding to PGOH core) and the signal at 3.7 ppm (corresponding to the PMMA arms) and were found to be 47 and 250 ms, respectively. These values confirm that the broad signals observed correspond to PGOHBr core while PMMA arms appear as sharper signals in the spectrum. With this technique it has been possible indirectly to prove the copolymer structure of these stars.

^{13}C NMR spectral data of all these polymers further confirm the structure and are given in the experimental part with their assignments.

Journal of Polymer Science, Part A: Polymer Chemistry **2011**, 49, 3138 – 3151

The structural characterization of PGOH-*b*-PMMA$_x$ has also been performed by FTIR. As an example, FTIR spectra of PGOH, PGOHBr$_{45}$ and PGOH-*b*-PMMA$_{45}$ are shown in **Figure 3**.

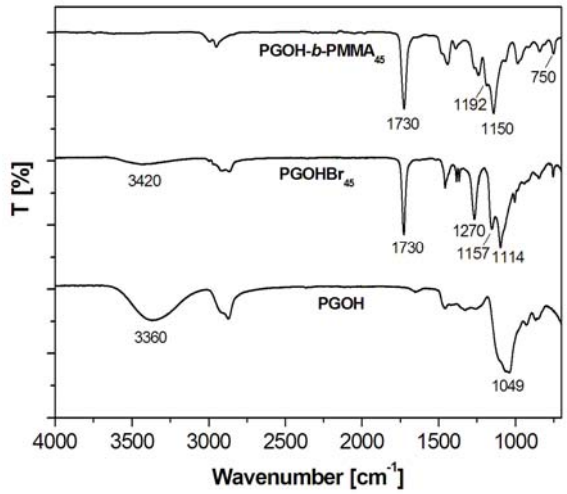

Figure 3 FTIR (ATR) spectra of PGOH, PGOHBr$_{45}$ and star copolymer PGOH-*b*-PMMA$_{45}$ (entry 13 in **Table 1**)

The successful partial modification of PGOH is evidenced by the remaining hydroxyl group signal centered at 3420 cm^{-1} and by the carbonyl signal that appears at 1730 cm^{-1} corresponding to C=O stretching vibration. The spectrum of the PGOH-*b*-PMMA$_{45}$ star only shows the absorbances corresponding to the poly(methyl methacrylate) arms, because of the low proportion of poly(glycidol) in the whole structure.

Average molecular weights of the macroinitiators ($\overline{M_n}$ PGOHBr$_x$) were determined using the number of active sites in the macroinitiator (*Br*) and the following equation:

$$\overline{M_n}\,(PGOHBr_x) = \left[N\,(Br)\,x\,M\,(BriB) + \overline{M_n}\,(PGOH)\right] - N\,(Br)\,x\,M\,(H) \qquad (3)$$

where *M (BriB)* is the molecular weight of the 2-bromoisobutyryl group, $\overline{M_n}$ PGOH is the molecular weight of polyglycidol and *M (H)* is the atomic weight of a proton.

Average molecular weights of the synthesized stars were determined by SEC coupled with light-scattering detector (MALLS). The values obtained are collected in **Table 1**. The calculated molecular weights from the conversion reached ($\overline{M}_{n,theoric}$) lay generally above than those determined experimentally which can be rationalized by the impossibility of the complete monomer conversion caused by the increased reaction viscosity and the high risk of gelation. Exceptions are entry 5 and 9 which show values higher than theoretically expected due to very broadly distributed

molecular weight. As can be also observed the MMA consumption employing the 45-arm macroinitiator appeared to be higher in a shorter period of time than using the 85-arm macroinitiator which is in accordance to the suggested fastest polymerization occurred in the preparation of star polymers with fewer arms. Generally, at 50 ºC it is possible to drive the reaction at high monomer conversion without gelation.

From the radius of gyration ($R_{g,z}$) determined by MALLS (**Table 1**) we observed that the stars with broad molecular-weight distribution (entries 5 and 9 in **Table 1**) show dimensions higher than 100 nm in comparison to narrowly molecular weight distributed molecules which have a $R_{g,z}$ lower than 23 nm. The reason for these discrepancies is the existence of ultra high molecular weight species in the distribution of entries 5 and 9 corresponding to weight average molecular weights higher than 10^6 g/mol.

In order to further investigate the copolymer nature of the stars, the cleavage of the arms was performed in a similar way to that described by Xue *et al.* [24]. The cleaved arms were analyzed by SEC-RI with PMMA standards. The values are collected in **Table 2**.

Table 2 Molecular weight data of PMMA arms and multiarm star copolymers calculated from them

Entry	$\overline{M}_n$ SEC-RI[a] Arms (g/mol)	$\overline{M}_w/\overline{M}_n$ [a] Arms	$\overline{M}_{n,calc}$ [b] Stars (g/mol)
PGOH-*b*-PMMA$_{85}$			
5	8,800	1.11	768,600
7	5,100	1.13	454,100
8	6,100	1.12	539,100
PGOH-*b*-PMMA$_{55}$			
9	13,200	1.07	742,100
PGOH-*b*-PMMA$_{45}$			
12	3,300	1.09	164,900
13	5,400	1.18	257,600

a. Arms cleavage was performed in NaOH $6 \cdot 10^{-3}$ M/MeOH at 80 ºC during 24 h. $\overline{M}_n$ and PDI were measured by SEC-RI with THF as solvent and PMMA standards.

b. $\overline{M}_{n,calc}$ was determined as: [*N*(Br) x $\overline{M}_n$ (arms)] + $\overline{M}_n$ (PGOHBr$_x$).

The molecular weights of the multiarm copolymers were also calculated from these values multiplied by the number of arms. They are collected in the same table and fit reasonably well with the ones values experimentally obtained by SEC-MALLS with the exception of the broadly distributed stars (entries 5 and 9). This fact indicates a good agreement between the number of initiating sites of each macroinitiator and the number of arms grown during the polymerization for sample **7** and **8** and **12** and **13**.

Figure 4 shows the molecular weight distribution curve of PGOH and the star copolymers prepared at different temperatures.

Journal of Polymer Science, Part A: Polymer Chemistry **2011**, 49, 3138 – 3151

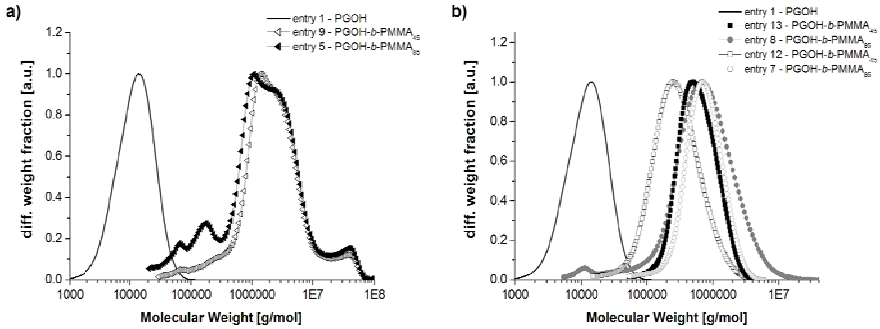

Figure 4 Molar mass distribution curves of star copolymer PGOH-*b*-PMMA$_x$ obtained **a**) at 80 ºC and **b**) at 50 ºC

Figure 4 (**a**) allows concluding that the copolymers obtained at 80 ºC have not a well-defined star structure. Partial star-star coupling occurred during the polymerization by means of radical-radical reaction between arms of different molecules. This fact could be also proved by the appearance of a small peak at very high molecular weight. In addition, the shape of the main curve is not unimodal and a shoulder appears in both curves. On the contrary, the shape of the molecular weight distribution curve in **Figure 4** (**b**), obtained from star copolymers prepared at 50 ºC, has a symmetrically distributed, monomodal appearance, which indicates the well-defined nature of the stars prepared under these conditions.

Thermal characterization of PGOH-b-PMMA$_x$

The origin of glass transition in nonlinear polymers is strongly influenced by the number and the chemical structure of the functional end groups, the degree of branching and the chemical structure of the repeating unit [39,40]. Actually, in case of multiarm star copolymers using a hyperbranched polymer as core it does not exist any evidence that the appearance of two second order transitions could be related to the core and to the arms. Kowalczuk-Bleja *et al.* [41], studied the T_gs of stars with a hyperbranched poly(styrene) core and linear poly(styrene) or poly(styrene-*co*-*tert*-butyl acrylate) arms, identifying two different transitions - the one at lower temperature was attributed to the movement of the undisturbed star arms and the one at higher temperature to the motion of the whole star. The same research group [42], described star copolymers based on hyperbranched poly(arylene-oxindole) core possessing 28 poly(*tert*-butyl acrylate) arms. In this work, they observed a decrease in the T_g of the hyperbranched core from 250 ºC to 160 ºC by increasing the arm length, while the T_g of the arms remained at the same temperature in comparison with the linear poly(*tert*-butyl acrylate) analog. The decrease of the T_g was attributed to the motion of the entire star polymer and not to changes in the flexibility of the core, caused by the arms.

The T_g plots of PGOH and our synthesized multiarm star copolymers are represented in **Figure 5**.

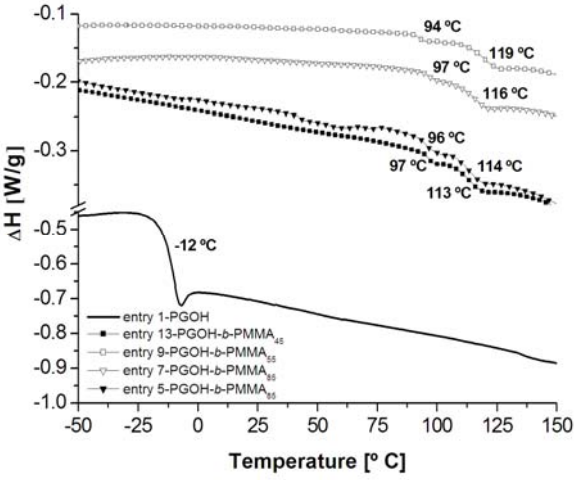

Figure 5 DSC plots at 10 ºC/min of PGOH and star copolymers PGOH-*b*-PMMA$_x$ with 45, 55 and 85 poly(methyl methacrylate) arms

The thermograms were obtained in a second heating scan after eliminating the thermal history. As it can be seen for all copolymers, two second order transitions were observed. The first one appears at about 95 ºC and the second one at 115 ºC. As the PGOH core has a very low T_g at – 12 ^{o}C, it is obvious that the transition of an undisturbed core can no longer be detected. Thus, according to the previous publications mentioned earlier, the two transitions could be explained as a result of two different motions presented in the whole structure. The one at lower temperature corresponds to the more flexibilized regions of arms caused by the soft core and the second one, at higher temperature reflects the translational movement of undisturbed arms.

The thermal stability of the star copolymers was analyzed by thermogravimetry in nitrogen atmosphere and compared to that of PGOH core and macroinitiator. **Figure 6** shows the differential curves of the weight loss against temperature for PGOH, PGOHBr$_{45}$ and PGOH-*b*-PMMA$_{45}$.

Journal of Polymer Science, Part A: Polymer Chemistry **2011**, 49, 3138 – 3151

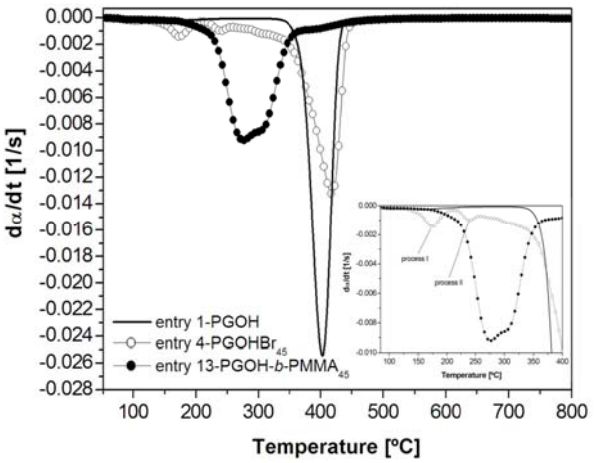

Figure 6 TGA derivative curves at 10 ºC/min in N_2 atmosphere of PGOH, $PGOHBr_{45}$ and star copolymer PGOH-*b*-$PMMA_{45}$

In **Table 3** all the thermal data are collected. The thermal degradation behaviors of PGOH, $PGOHBr_{45}$ and PGOH-*b*-$PMMA_x$ copolymer appear quite different. The thermal degradation of PGOH takes place in one step with the highest rate of degradation at 404 ºC which can be explained by the thermal degradation of the ether linkages which are rather stable. In addition, a practically inappreciable weight loss is observed at 120 ºC, attributable to a slight loss of water from the hydroxyl groups. $PGOHBr_{45}$ also presents one degradation step, but the presence of bromoisobutyril esters reduces the degradation temperature to 276 ºC. More complex is the degradation behavior of the star copolymers, which show three different peaks at temperatures between 160-210 ºC (I), 220-300 ºC (II) and 340-430 ºC (III).

Table 3 Thermal and rheological properties of the core, macroinitiator ($PGOHBr_{45}$) and PGOH-*b*-$PMMA_x$ multiarm star copolymers

Entry	T_1[a] (ºC)	T_2[a] (ºC)	T_3[a] (ºC)	$\omega_{crossover}$[b] (rad·s^{-1})	G_N^{0}[c] (Pa)
PGOH	-	-	404	6.28	13
$PGOHBr_{45}$					
4	-	276	-	-	-
PGOH-*b*-$PMMA_{85}$					
5	196	289	403	5.04	220.000
7	174	239	419	90.02	176.000
PGOH-*b*-$PMMA_{55}$					
9	161	270	404	4.96	518.000
PGOH-*b*-$PMMA_{45}$					
13	162	285	407	25.95	451.000

a. Maximum temperature of the different degradation processes by TGA. Experiments performed at 10 ºC/min in N_2 atmosphere.
b. Crossover value between *G'* and *G''* modulus determined at 130 ºC.
c. Storage modulus (*G'*) applying the loss tangent minimum criterion ($G^0_N = G'$⌉ $\tan\delta \rightarrow$ min) at 130 ºC.

Norman *et al.* [43], studied the thermal degradation of PMMA obtained by ATRP which resulted in three steps of degradation at 170, 270 and 410 ºC. They attributed the first step to the scission of head-to-head linkages and/or to the loss of methyl halide as end groups in this type of polymerization. The second process was described as the degradation of unsaturated end groups whereas the third and main degradation step involves the saturated PMMA backbone random scission. The degradation profiles obtained for the star synthesized by us are generally in agreement with the above referred study. However, the second process can be also originated from the degradation of the hyperbranched polyether core, because the temperature of this second process coincides with the main degradation of the macroinitiator.

Rheological behaviour of PGOH-b-PMMA$_x$

The topology of the molecules influences the melt dynamic response, resulting in different rheological behaviour. For star polymers the theory suggests that arms escape from their confining tubes not by reptation, which is suppressed by the immobilization of branching points, but by a process of arm retraction [44].

Table 3 collects the crossover values of *G'* and *G''* ($\omega_{crossover}$) and the storage modulus (G_N^0) of the corresponding star copolymers. As it can be seen, the crossover moves to lower frequencies with increasing molecular weight of the arms (entries 5 and 7), but it seems to be unaffected by the number of arms (entries 7 and 13). This is a typical feature of star branched polymers which occurs due to the different relaxation mechanism of arms which has been observed in other related works [38,45].

The growing of PMMA arms on the PGOH core leads to a clear increase in the storage modulus, but any systematic relationship of this property with the number of arms or their molecular weight cannot be deduced.

The development of the complex viscosity (η^*) as a function of angular frequency at 130 ºC of the star copolymers is shown in **Figure 7**.

The complex viscosity of multiarm star copolymer possessing 85 arms is lower than the value of the star with 45 arms (entries 7 and 13). Both stars have approximately the same length of arms. This fact can be related to the increase of the structure compactness which reduces the hydrodynamic volume and leads to a decrease of the complex viscosity. Furthermore, if we vary the molecular weight of arms while keeping the number of arms constant (entries 7 and 5) we can observe that the star with longer arms (8,800 g/mol, entry 5) possesses a higher complex viscosity than the one with 5,100 g/mol (entry 7). This is a result of the increased "linear-like" polymer behaviour which favours the entanglements between molecules and derives in an increased complex viscosity. From this result we can conclude that the processability of multiarm copolymers can be optimized increasing the number of arms and keeping the length of the arms as short as possible.

Journal of Polymer Science, Part A: Polymer Chemistry **2011**, 49, 3138 – 3151

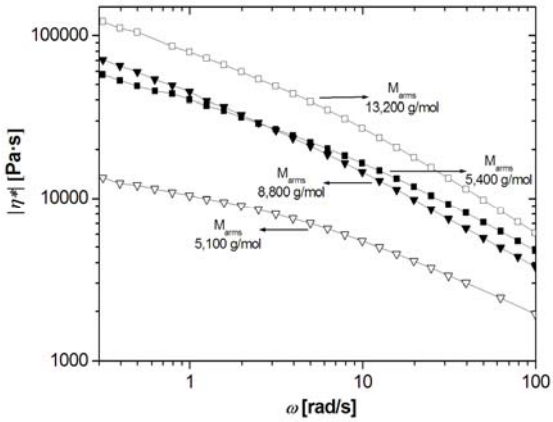

Figure 7 Complex viscosity (η^*) versus angular frequency (ω) at 130 ºC of PGOH-*b*-$PMMA_{85}$ (entries 5 and 7), PGOH-*b*-$PMMA_{55}$ (entry 9) and PGOH-*b*-$PMMA_{45}$ (entry 13) in **Table 1**

TMAFM Visualization of PGOH-b-$PMMA_x$

In order to obtain information on the morphologies of the synthesized multiarm star copolymers, tapping-mode atomic force microscopy (TMAFM) was used to observe the dry state of the molecules on mica surfaces. The copolymers were drop-cast from THF solution with concentration of 2 mg/mL and dried onto mica surfaces at room temperature for 15 minutes. **Figure 8** shows the TMAFM height images, size distribution and profiles of two PGOH-*b*-$PMMA_x$ stars.

This method does not allow observing the arm-branch morphology due to the high number of arms per molecule; however, single molecules can be clearly recognized. **Figures 8** (**a**) **and** (**b**) show the morphology of multiarm copolymer with 45 PMMA arms. With increasing the number of arms per molecule to 85, **Figures 8** (**c**) and (**d**)**,** one can deduce that the molecules increase in size and thickness. From the size distribution histograms it is possible to observe that PGOH-*b*-$PMMA_{45}$ appears, mostly, as single unconnected molecules showing diameters in the range from 80 to 150 nm. On the other hand, PGOH-*b*-$PMMA_{85}$ shows mainly molecular sizes between 100 and 200 nm and also several particles higher than 200 nm are present. This fact can be explained by the increase of the aggregating effect when the length of the arms increases due to the arm entangling.

Comparing the dimensions in the dried state with those in solution ($R_{g,z}$ values in **Table 1**) it is possible to observe a significantly smaller size of the molecules in solution for the stars with 85 and 45 PMMA arms. This fact can be explained with a more disc like shape of dried multiarm stars and the arms stretch out on the mica surface; therefore they show larger dimensions in the *x*-directions and a small diameter in the *y*-direction. Moreover, it can be noticed that with increasing number of arms per molecule, considering molecules with nearly the same molecular-weight distribution, the dimensions increase in accordance with TMAFM observations.

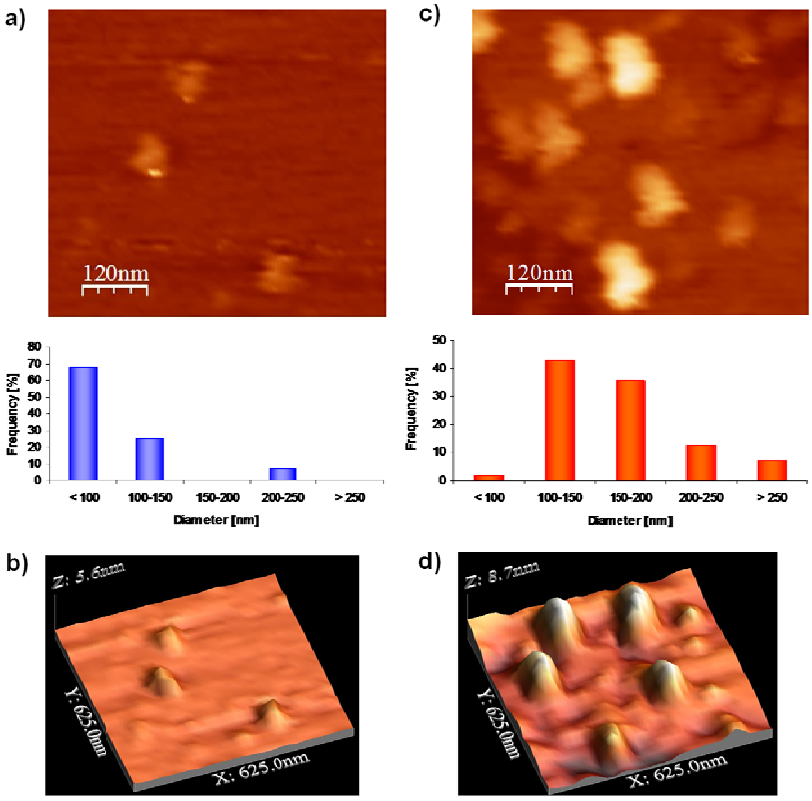

Figure 8 TMAFM height mode images and size distribution of (45 - 70 particles measured) of: PGOH-*b*-PMMA$_{45}$ (entry 13, **Table 1**) (**a** and **b**) and PGOH-*b*-PMMA$_{85}$ (entry 8, **Table 1**) (**c** and **d**)

Conclusions

Multiarm star copolymers based on hyperbranched poly(glycidol) core with 45, 55 and 85 PMMA arms were synthesized by core-first AGET/ATRP. Molecular weight characterization of the corresponding star copolymers and the cleavage of the arms indicate ATRP initiation efficiency from nearly all initiating sites. PMMA stars of relatively narrow molecular-weight distribution were thus obtained setting the reaction temperature at 50 ºC. By these conditions, the maximum monomer conversion reached was 88 % without gel formation.

The study of the thermal properties of the corresponding star copolymers revealed two second order transitions as a result of two different motions present in the whole star structure and a rather low thermal stability due to chain scission processes in the PMMA arms.

By rheometry, it could be concluded that multiarm copolymers with higher number of arms and shorter length arms led to decrease of the complex viscosity which indicates a better processability in the melt dynamic state.

Journal of Polymer Science, Part A: Polymer Chemistry **2011**, 49, 3138 – 3151

The isolated star molecules were visualized by tapping mode AFM proving the existence of nano-sized particles (80 - 200 nm) corresponding to individual well-defined star molecules.

Acknowledgements

The authors from the Universitat Rovira i Virgili and Universitat Politècnica de Catalunya would like to thank MICINN (Ministerio de Ciencia e Innovación) and FEDER (Fondo Europeo de Desarrollo Regional) (MAT2008-06284-C03-01 and MAT2008-06284-C03-02) and to the Comissionat per a Universitat i Recerca de la Generalitat de Catalunya (2009-SGR-1512). All the authors thank to the Germany-Spanish collaboration program (HA2007-0022, DAAD PPP D/07/13493) for their financial support. M.M. acknowledges the grant FI-DGR 2009 from the Catalonian Government and the mobility fellowship from MICINN. Miguel Ángel Rodríguez and Ramon Guerrero are gratefully acknowledged for the NMR T_2 relaxation measurements and Hartmut Komber for its useful discussion concerning the NMR characterization and interpretation.

References

[1] Roovers, J.; Zhou, L.; Toporowski, P.M.; Zwan, M.; Iatrou, H.; Hadjichristidis, N. Macromolecules **1993**, 26, 4324-4331.
[2] Islam, M.T.; Archer, J.; Archer, L.A. Macromolecules **2001**, 34, 6438-6449.
[3] Maier, S.; Sunder, A.; Frey, H.; Mülhaupt, R. Macromol. Rapid Commun. **2000**, 21, 226-230.
[4] Gao, H.; Matyjaszewski, K. Macromolecules **2008**, 41, 1118-1125.
[5] Xia, J.; Zhang, X.; Matyjaszewski, K. Macromolecules **1999**, 32, 4482-4484.
[6] Hirao, A.; Hayashi, M.; Loykulnant, S.; Sugiyama, K.; Woog Ryu, S.; Haraguchi, N.; Matsuo, A.; Higashihara, T. Prog. Polym. Sci. **2005**, 30, 111-182.
[7] Ouchi, M.; Terashima, T.; Sawamoto, M. Chem. Rev. **2009**, 111, 4963-5050.
[8] Percec, V.; Guliashvili, T.; Ladislaw, J.S.; Wistrand, A.; Stjerndahl, A.; Sienkowska, M.J.; Monteiro, M.J.; Sahoo, S. J. Am. Chem. Soc. **2006**, 128, 14156-14165.
[9] Rosen, B.M.; Percec, V. Chem. Rev. **2009**, 109, 5069-5119.
[10] Braunecker, W. A.; Matyjaszewski, K. Prog. Polym. Sci. **2007**, 32, 93-146.
[11] Chen, Y.; Shen, Z.; Barriau, E.; Krautz, H.; Frey, H. Biomacromolecules **2006**, 7, 919-926.
[12] Angot, S.; Shanmugananda, K.; Taton, D.; Gnanou, Y. Macromolecules **1998**, 31, 7218-7225.
[13] Schmitz, C.; Keul, H.; Möller, M. Eur. Pol. J. **2009**, 45, 2529-2539.
[14] Jankova, K.; Bednarek, M.; Hvilsted, S. J. Polym. Sci., Part A: Polym. Chem. **2005**, 43, 3748-3759.
[15] Jakubowski, W.; Matyjaszewski, K. Macromolecules **2005**, 38, 4139-4146.
[16] Min, K.; Jakubowski, W.; Matyjaszewski, K. Macromol. Rapid Commun. **2006**, 27, 594-598.
[17] Mueller, L.; Jakuboswski, W.; Tang, W.; Matyjaszewski, K. Macromolecules **2007**, 40, 6464-6472.
[18] Knischka, R.; Lutz, P.J.; Sunder, A.; Mülhaupt, R.; Frey, H. Macromolecules **2000**, 33, 315-320.
[19] Wilms, D.; Stiriba, S.E.; Frey, H. Acc. Chem. Res. **2010**, 43, 129-141.
[20] Sienkowska, M.J.; Rosen, B.M.; Percec, V. J. Polym. Sci., Part A: Polym. Chem. **2009**, 47, 4130-4140.
[21] Rosen, B.M.; Lligadas, G.; Hahn, C.; Percec, V. J. Polym. Sci., Part A: Polym. Chem. **2009**, 47, 3940-3948.

[22] Farrar, D.F.; Rose, J. Biomaterials **2001**, 22, 3005-3013.
[23] Pascual, B.; Vázquez, B.; Gurruchaga, M.; Goñi, I.; Ginebra, M. P.; Gil, F. J.; Planell, J. A.; Levenfeld, B.; San Román, J. Biomaterials **1996**, 17, 509-516.
[24] Xue, L.; Agarwal, U.S.; Zhang, M.; Staal, B.B.P.; Müller, A.H.E.; Bailly, C.M.E.; Lemstra, P.J. Macromolecules **2005**, 38, 2093-2100.
[25] Heise, A.; Hedrick, J.L.; Trollsas, M.; Miller, R.D.; Frank, C.W. Macromolecules **1999**, 32, 231-234.
[26] Jeon, H.J.; Youk, J.H.; Ahn, S.H.; Choi, J.H.; Cho, K.S. Macromol. Res. **2009**, 17, 240-244.
[27] Haddleton, D.M.; Heming, A.M.; Jarvis, A.P.; Khan, A.; Marsh, A.; Perrier, S.; Bon, S.A. F.; Jackson, S.G.; Edmonds, R.; Kelly, E.; Kukulj, D.; Waterson, C. Macromol. Symp. **2000**, 157, 201-208.
[28] Nese, A.; Mosnácek, J.; Juhari, A.; Ae, Y.J.; Koynov, K.; Kowalewski, T.; Matyjaszewski, K. Macromolecules **2010**, 43, 1227-1235.
[29] (a) Schultz, D.N.; Glass, J.E.E.; Polymers as Rheology Modifiers; ACS Symposium Series 462; American Society: Washington, DC, **1991**; (b) Gao, C.; Yan, D. Prog. Polym. Sci. **2004**, 29, 183-275; (c) Zhang, M.; Estournes, C.; Bietsch, W.; Muller, A.H.E. Adv. Funct. Mater. **2004**, 14, 871-882.
[30] Kainthan, R.K.; Muliawan, E.B.; Hatzikiriakos, S.G.; Brooks, D.E. Macromolecules **2006**, 39, 7708-7717.
[31] Friebolin, H. *Basic One-and Two-Dimensional NMR Spectroscopy*. 4th ed, Wiley-VCH, Weinheim, **2005**, p.173-177.
[32] Pintauer, T.; Matyjaszewski, K. Chem. Soc. Rev. **2008**, 37, 1087-1097.
[33] Kwak, Y.; Matyjaszewski, K. Macromolecules **2008**, 41, 6627-6635.
[34] Zhang, H.; Schubert, U.S. Macromol. Rapid Commun. **2005**, 25, 1225-1230.
[35] Hu, Z.; Shen, X.; Qiu, H.; Lai, G.; Wu, J.; Li, W. Eur. Pol. J. **2009**, 45, 2313-2318.
[36] Perrier, S.; Armes, S.P.; Wang, X.S.; Malet, F.; Haddleton, D.M. J. Polym. Sci., Part A: Polym. Chem. **2001**, 39, 1697-1707.
[37] Fuchs, K.; Friedrich, C.; Weese, J. Macromolecules **1996**, 29, 5893-5901.
[38] Dreiss, C.A.; Cosgrove, T.; Benton, N.J.; Kilburn, D.; Ashraf Alam, M.; Schmidt, R.G.; Gordon, G.V. Polymer **2007**, 48, 4419-4428.
[39] Tande, B.; Wagner, N.; Kim, Y. Macromolecules **2003**, 36, 4619-4623.
[40] Khalyavina, A.; Schallausky, F.; Komber, H.; Al Samman, M.; Radke, W.; Lederer, A. Macromolecules **2010**, 43, 3268-3276.
[41] Kowalczuk-Bleja, A.; Sierocka, B.; Muszynski, J.; Trzebicka, B.; Dworak, A. Polymer **2005**, 46, 8555-8564.
[42] Kowalczuk, A.; Vandendriessche, A.; Trzebicka, B.; Mendrek, B.; Szeluga, U.; Cholewinski, G.; Smet, M.; Dworak, A.; Dehaen, W. J. Polym. Sci., Part A: Polym. Chem. **2009**, 47, 1120-1135.
[43] Norman, J.; Moratti, S.C.; Slark, A.T.; Irvine, D.J.; Jackson, A.T. Macromolecules **2002**, 35, 8954-8961.
[44] Lee, J.H.; Orfanou, K.; Driva, P.; Iatrou, H.; Hadjichristdis, N.; Lohse, D.J. Macromolecules **2008**, 41, 9165-9178.
[45] Erwin, B.M.; Cloitre, M.; Gauthier, M.; Vlassopoulos, D. Soft Matter **2010**, 6, 2825-2833.

V.3

NEW IMPROVED THERMOSETS OBTAINED FROM DIGLYCIDYLETHER OF BISPHENOL A AND A MULTIARM STAR COPOLYMER BASED ON HYPERBRANCHED POLY(GLYCIDOL) CORE AND POLY(METHYL METHACRYLATE) ARMS

Mireia Morell, Xavier Ramis, Francesc Ferrando, Àngels Serra

Macromolecular Chemistry and Physics, In press (DOI: 10.1002/macp.201100497)

UNIVERSITAT ROVIRA I VIRGILI
NOUS TERMOESTABLES EPOXÍDICS MODIFICATS AMB ESTRUCTURES DENDRÍTIQUES DE TIPUS HIPERRAMIFICAT I ESTRELLA
Mireia Morell Bel
DL:T. 155-2012

Macromolecular Chemistry and Physics, *In press (DOI: 10.1002/macp.201100497)*

NEW IMPROVED THERMOSETS OBTAINED FROM DIGLYCIDYLETHER OF BISPHENOL A AND A MULTIARM STAR COPOLYMER BASED ON HYPERBRANCHED POLY(GLYCIDOL) CORE AND POLY(METHYL METHACRYLATE) ARMS

Mireia Morell,[1] Xavier Ramis,[2] Francesc Ferrando,[3] Àngels Serra[1]

[1] Department of Analytical and Organic Chemistry, Universitat Rovira i Virgili, C/ Marcel·lí Domingo s/n, Tarragona 43007, Spain.
[2]Thermodynamics Laboratory, ETSEIB Universitat Politècnica de Catalunya, Av. Diagonal 647, Barcelona 08028, Spain.
[3] Department of Mechanical Engineering, Universitat Rovira i Virgili, C/ Països Catalans, 26, Tarragona 43007, Spain.

Abstract

A well-defined multiarm star copolymer, hyperbranched poly(glycidol)-*b*-poly(methyl methacrylate) (PGOH-*b*-PMMA), with an average number of 85 arms per molecule was used as a modifier in the curing of diglycidylether of bisphenol A (DGEBA) using 1-methyl imidazole (1MI) as anionic initiator. The effect of the polymer topology on the curing and gelation processes was studied by dynamic scanning calorimetry (DSC) and rheometry. The addition of the PGOH-*b*-PMMA to the resin left the complex viscosity (η^*) practically unaltered. The addition of the star-shaped modifier decreased the shrinkage after gelation in reference to that measured in the curing of the neat resin. The study of the materials by dynamic thermomechanical analysis (DMTA) showed an only relaxation process in the pure DGEBA and modified thermosets. Electronic microscopy (SEM) evidenced a nanograined morphology for all the modified materials suggesting a nanostructuration associated with the nucleation of modifier rich star domains. The addition of the star-like modifier led to an improvement on the mechanical characteristics such as the impact strength and microhardness in comparison to the neat material.

Keywords: star polymers; hyperbranched polymers; epoxy resin; anionic polymerization; thermosets

Introduction

Chemically induced phase separation (CIPS) is one of the methodologies used to improve the fracture toughness by promoting biphasic nanostructured morphology. In this process, the morphology develops during curing from an initial homogenous mixture [1-3]. Using block copolymers, one of the blocks is previously insoluble or phase separates during curing while the other remains soluble. In this case, the nanostructured morphology originated is mainly explained from the nanoparticles of the segregated block fixed by the soluble block to the epoxy resin [4].

Another possibility to origin nanostructured thermosets is to take benefit of the heterogeneities generated during the curing process. Although epoxy resins are described as three-dimensional network with a regular structure, the truth is that the curing process is not a perfect process and in some points of the mixture the crosslinking reaction proceeds faster generating a non-homogeneous matrix [5]. Epoxy networks obtained by homopolymerization of epoxy resins by using curing

initiators are intrinsically inhomogeneous materials favoring the appearance of nanostructured morphologies. The curing agent, the type of catalyst (if necessary), their concentrations, the different mechanisms that can compete during curing, the temperature and time of curing are parameters which influence the final morphology. Moreover, the use of linear- or dendritic modifiers has also proved to play an important role on it [3,6,7].

Hyperbranched polymers, as dendritic polymers, could substitute linear polymers as modifiers of epoxy resins due to their relative low melt viscosity, their better solubility and its capacity of improving toughness without negatively affecting the glass transition temperature (T_g) of the final materials [8-11].

Additionally to hyperbranched polymers, multiarm star copolymers can also be considered as a new class of modifiers for epoxy resins [12]. We have recently studied the use of a multiarm star-shaped block copolymer based on hyperbranched poly(styrene) core and poly(ε-caprolactone) arms obtained by the "core first" approach. Formulations of this modifier with DGEBA using 1-methyl imidazole as anionic initiator were cured and the characteristics of the materials were determined [13]. The results obtained were very promising in terms of processability and toughness improvement since the observation of the fracture of the modified materials by electronic microscopy (SEM) showed a more ductile appearance with a nanograined topology composed of particles of size from 15 to 40 nm completely interconnected. However, no mechanical properties were evaluated.

Poly(methyl methacrylate) (PMMA) is a common polymer used to modify epoxy resins. Nevertheless, some discrepancies appear in reference to its capacity of phase-separate during the curing process. Some studies established that PMMA was soluble with DGEBA in all proportions but for the most of hardeners it became phase-separated during curing before gelation [14-16]. In contrast, some others stated that this block remained soluble before and after curing [17,18]. However, the responsible facts of this different behavior are still not clear.

Taking all of this into account, in the present work we propose the use of a well-defined multiarm star copolymer, poly(glycidol)-*b*-poly(methyl methacrylate) (PGOH-*b*-PMMA), as modifier of DGEBA in order to set up the topology effect on the curing and gelation processes, rheological behavior and the final properties of the materials. Moreover, we will pay attention on the morphology of PGOH-*b*-PMMA modified DGEBA thermosets and the role that PMMA block plays on it.

Experimental section

Materials

Glycidol (96 %) was distilled under reduced pressure and stored over molecular sieve at 2 - 5 ºC, dioxane was dried over calcium hydride and subsequently distilled and methyl methacrylate (MMA, 99 %) was passed through

basic alumina column to remove the radical inhibitor. Trimethylolpropane (TMP) (97 %), potassium methylate solution (25 % v/v in methanol), $CuBr_2$ (99 %), *N,N,N',N',N''*-pentamethyldiethylenetriamine (PMDETA, 99 %), tin(II) 2-ethylhexanoate ($Sn(Oct)_2$, 98 %), 2-bromoisobutyryl bromide (98 %), anhydrous pyridine, anhydrous anisole and 1-methyl imidazole (1MI, 99 %) were used without further purification. All these chemicals were purchased from Sigma-Aldrich. All other reagents and solvents were purchased from Scharlab.

Diglycidylether of bisphenol A (DGEBA) Epikote Resin 827 was provided by Shell Chemicals (epoxide equivalent weight (EEW) = 182.1 g/eq, n = 0.082).

Preparation of multiarm star poly(glycidol)-b-poly(methyl methacrylate) (**Scheme 1**)

A well-defined multiarm star copolymer based on poly(glycidol)-*b*-poly(methyl methacrylate) (PGOH-*b*-PMMA) was synthesized employing as the core a hyperbranched poly(glycidol) obtained by anionic ring-opening polymerization of glycidol [19], with an average number of hydroxyl initiating sites of 100 - 110 per molecule. Subsequently, the hydroxyl groups of PGOH were modified by esterification with 2-bromoisobutyryl bromide to generate an ATRP (atom transfer radical polymerization) macroinitiator with an average number of 85 bromine sites per molecule determined from the degree of modification by ^{1}H NMR. Finally, methyl methacrylate (MMA) was polymerized from the activated groups to obtain the corresponding multiarm copolymer by means of AGET/ATRP (activator generated by electron transfer/atom transfer radical polymerization). The detailed synthetic procedure and the characterization of this multiarm star copolymer are described in a previous publication [20].

$\overline{M_n}$ (SEC-MALLS) = 413,000 g/mol, $\overline{M_w} / \overline{M_n}$ = 2.05; T_g (DSC) = 97 and 116 ºC and $T_{2\%}$ (TGA) = 239 ºC (2 % of mass loss).

Preparation of epoxy thermosets

The mixtures were prepared by adding the required amount of PGOH-*b*-PMMA into the epoxy resin and gently heating until it was dissolved and the solution became clear. Then, 5 phr (part per hundred parts of mixture) of 1MI was added and the resulting solution was stirred and cooled down to - 10 ºC to prevent polymerization. Mixtures containing 5 – 10 wt.% (by weight) of PGOH-*b*-PMMA were prepared. A neat formulation with DGEBA and 5 phr of 1MI was prepared to compare with the modified formulations. The compositions of the formulations studied are detailed in **Table 1.**

Characterization

Calorimetric analyses were carried out on a Mettler DSC-822e thermal analyzer. Samples of approximately 5 mg in weight were placed in aluminum pans under nitrogen atmosphere. The calorimeter was calibrated using an indium

standard (heat flow calibration) and an indium-lead-zinc standard (temperature calibration).

PGOH-*b*-PMMA was heated from – 50 to 150 ºC with a heating rate of 10 ºC/min, cooled down to – 100 ºC with a cooling rate of – 10 ºC/min and then heated again to 150 ºC at the same heating rate. T_g value was obtained from the second heating curve.

Non-isothermal curing experiments were performed from 30 to 250 ºC at heating rates of 2, 5, 10, and 15 ºC/min to determine the reaction heat and the kinetic parameters. In non-isothermal curing process the degree of conversion by DSC (α_{DSC}) was calculated as follows:

$$\alpha_{DSC} = \frac{\Delta H_T}{\Delta H_{dyn}} \quad (1)$$

where ΔH_T is the heat released up to a temperature T, obtained by integration of the calorimetric signal up to this temperature and ΔH_{dyn} is the total reaction heat associated with the complete conversion of all reactive groups obtained dynamically.

The kinetic triplet [pre-exponential factor, activation energy and kinetic model] of the curing process was determined using integral isoconversional non-isothermal kinetic analysis, Kissinger-Akahira-Sunose equation, combined with the Coats-Redfern procedure. Details of the kinetic methodology are given in previous publications [21,22].

Thermogravimetric analyses were carried out in a Mettler TGA/SDTA851e/LF/1100 thermobalance. Samples with an approximate mass of 8 mg were degraded between 30 and 800 ºC at a heating rate of 10 ºC/min in N_2 (100 cm^3/min measured in normal conditions).

Dynamic mechanical analyses were carried out with a TA Instruments DMA Q800. The samples were cured isothermally in a mould at 120 ºC for 1.5 h and then post-cured for 1 h at 150 ºC. Three-point bending at 1 Hz was performed at 3 ºC/min, from 40 ºC to 250 ºC on prismatic rectangular samples (20 x 5 x 1.5 mm^3).

Rheological measurements were carried out in the parallel plates (geometry of 25 mm) mode with an ARG2 rheometer (TA Instruments, UK, equipped with a Peltier system). The gelation time was determined by setting the device in time sweep and multiwave oscillation mode. Experiments were performed isothermally at 80 ºC. Because the viscosity of the system changes significantly during the curing process, a control program was used in which the oscillation amplitude diminishes with an increase in the applied stress. By doing so, the curing process can be characterized in the whole range of conversion. Gel time was taken as the point where tan δ is independent of frequency [23]. The conversion at gelation (α_{gel}) was

Macromolecular Chemistry and Physics, *In press (DOI: 10.1002/macp.201100497)*

determined by stopping the rheology experiment at gelation and performing a subsequent dynamic DSC scan of the gelled sample.

Complex viscosity (η^*) of the pre-cured mixtures was recorded as function of angular frequency (0.1 – 30 rad/s) stating a constant deformation of 50 % at 80 ºC.

Microhardness was measured with a Wilson Wolpert (Micro- Knoop 401MAV) device following the ASTM D1474-98 (2002) standard procedure. For each material 10 determinations were made with a confidence level of 95 %. The Knoop microhardness (HKN) was calculated from the following equation:

$$HKN = L / A_p = L / l^2 \cdot C_p \quad (2)$$

where, L is the load applied to the indenter (0.025 Kg), A_p is the projected area of indentation in mm^2, l is the measured length of long diagonal of indentation in mm, C_p is the indenter constant (7.028×10^{-2}) relating l^2 to A_p. The values were obtained from 10 determinations with the calculated precision (95 % of confidence level).

The impact test was performed at room temperature by means of an Izod 5110 impact tester, according to ASTM D 4508-05 (2008) using rectangular samples (25 x 12 x 2 mm^3). The pendulum employed had a kinetic energy of 1 J.

The fracture area of the specimens after impact tests metalized with gold was observed with a Jeol JSM 6400 with a resolution of 3.5 nm.

Results and discussion

Hyperbranched poly(glycidol) (PGOH) was prepared according to previously published procedures by anionic polymerization of glycidol employing as initiator trimethylolpropane (TMP) and potassium methylate. Subsequently, the hydroxyl groups of PGOH were partially modified by esterification with 2-bromoisobutyryl bromide to generate an ATRP macroinitiator. Finally, MMA was polymerized from it to obtain the multiarm copolymer by means of AGET ATRP. The reaction was conducted under the same conditions as described in a previous work (entry 7, **Table 1**) [20]. The synthetic pathway is depicted in **Scheme 1**.

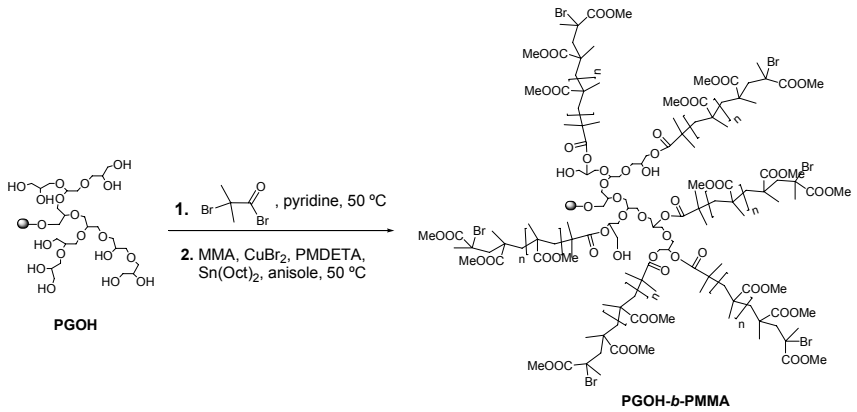

Scheme 1 Synthetic route to multiarm star copolymer PGOH-*b*-PMMA

From the molar-mass distribution curves of PGOH core and the PGOH-*b*-PMMA multiarm star copolymer (**Figure 1**) it is possible to appreciate that the growing of MMA through an ATRP process has been done under controlled conditions since it shows a symmetrical distribution with a monomodal appearance, which indicates the well-defined nature of the star polymer.

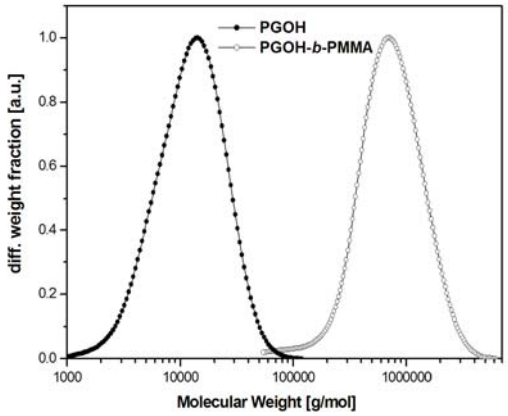

Figure 1 Molar mass distribution of PGOH and the corresponding star copolymer (PGOH-*b*-PMMA) determined by SEC-LS in DMAc

Therefore, the resulting multiarm star obtained possesses a high molar mass ($\overline{M_n}$ = 413,000 g/mol) constituted by a hyperbranched poly(glycidol) core with an average molecular weight of 10,500 g/mol and 80 - 90 poly(methyl methacrylate) arms with a degree of polymerization of about 50 MMA. The chemical structure of the multiarm star was proved by NMR spectroscopy according to a previous publication [20].

Curing of DGEBA with different proportions of PGOH-b-PMMA

Differential scanning calorimetry was used to investigate the evolution of the anionic curing process using 5 phr of 1-methyl imidazole (1MI) as initiator (0.61 mmol of initiator per gram of mixture). The calorimetric data of the formulations studied and their compositions are collected in **Table 1**.

Table 1 Composition and calorimetric data of DGEBA/1MI mixtures with different percentages of PGOH-*b*-PMMA

Formulation[a] (wt.%)	epoxy/ initiator[b]	epoxy/ OH[b]	Δh (J/g)	Δh[c] (kJ/ee)	T_{max}[d] (ºC)	E_a[e] (kJ/mol)	ln A[f] (s^{-1})	$k_{150\,ºC}$ x 10^{3}[g] (s^{-1})
0	9.0	24.40	638	116.1	132	60	12.89	15.25
PGOH-*b*-PMMA								
5	8.6	24.39	457	87.6	128	63	13.90	19.01
10	8.1	24.38	432	87.4	129	61	13.77	16.52

a. % by weight of multiarm star copolymer.
b. Equivalent ratio (ratio between mol of functional groups) of the formulations.
c. Enthalpy value per equivalent of epoxy group.
d. Temperature of the maximum of the exotherm.
e. Values of activation energies at 50 % of conversion were evaluated by isoconversional non isothermal procedure.
f. Values of pre-exponential factor for A_2 kinetic model with $g(\alpha)=[-ln(1-\alpha)]^{1/2}$.
g. Values of rate constant at 150 ºC calculated using the Arrhenius equation.

From the values of enthalpy per gram we can see that they diminish on adding the star modifier in 5 and 10 wt.%, due to the fact that epoxy content is decreased. In addition, the enthalpy per epoxy equivalent is slightly lower in the formulations containing PGOH-*b*-PMMA but there is not much variation with the proportion of modifier. The same behaviour was observed in a previous work in which the addition of a multiarm star leads to a reduction of the enthalpy evolved during curing, although the value is independent of the proportion of modifier [24]. This seems to indicate that the conversion of epoxy groups is slightly lower for the modified formulations, although epoxy band at 910 cm^{-1} is not visible in the FTIR spectra of the cured materials. The overlapping with some endothermic processes cannot be discarded.

The kinetic parameters of the curing process were calculated and are collected in **Table 1**. There are no much differences in the activation energies at a conversion of 50 % and it remained constant during the curing process. The values of constant rate at 150 ºC agree with the evolution observed during curing for the formulations studied and with the slightly accelerative effect exerted by PGOH-*b*-PMMA on curing at high conversions.

Figure 2 shows the exothermic curves (**a**) and the plot of conversion against temperature (**b**) for the studied formulations.

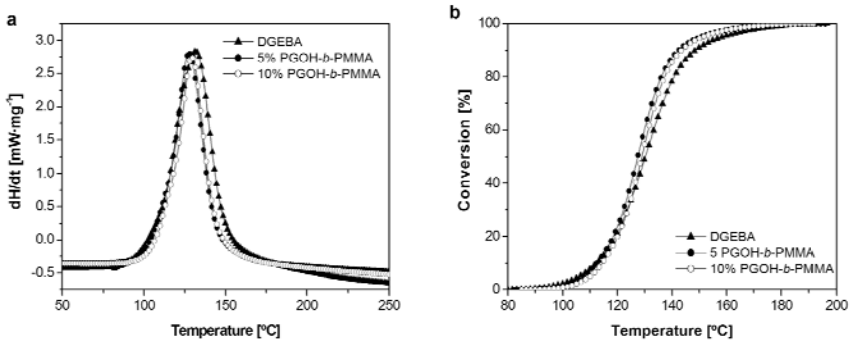

Figure 2 DSC scanning curves (**a**) and conversion degree (**b**) against temperature of the curing of DGEBA and DGEBA containing 5 and 10 wt.% of PGOH-*b*-PMMA at a heating rate of 10 ºC/min

The addition of the star modifier does not change substantially the shape of the exotherm. However, the curves of the formulations containing PGOH-*b*-PMMA appear narrower than the pure resin.

In terms of the curing rate, it can be seen from **Figure 2** (**b**) that the addition of modifier slightly accelerates the curing process at conversions above 0.2, but not in a regular way. Thus, the addition of 5 wt.% of modifier produces a more notable effect. There are some facts that can influence the curing kinetics of these formulations. On the one side, the addition of modifier increases the viscosity of the mixture, which retards the reaction because of an immobilizing effect of the reactive species in the mixture. On the other side, on increasing the percentage of modifier the initiator proportion per epoxy group increases, which should lead to an increased reactivity. Both factors could influence in a contrary way the kinetic behaviour of the curing process, explaining the non-regular reactivity order observed when the conversion is higher than 0.2.

Rheological and gelation properties of the formulations

Multiarm star-branched polymers are interesting topologies since they present less entanglements in solution compared to linear analogs with the same molecular weight which leads to lower viscosity values [25,26].

By rheological experiments the complex viscosity of the pre-cured mixtures without initiator at 80 ºC was determined on varying the angular frequency, as it is shown in **Figure 3**.

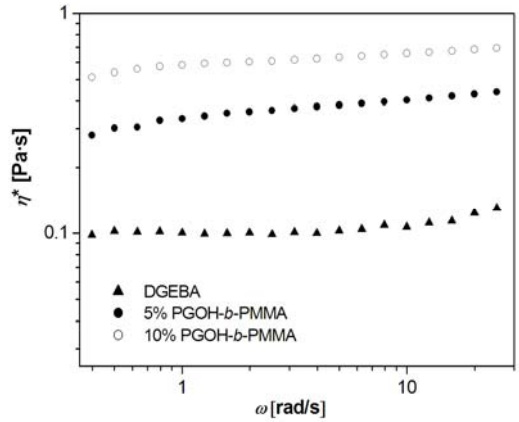

Figure 3 Complex viscosity (η^*) against angular frequency (ω) at 80 ºC for neat DGEBA and DGEBA containing 5 and 10 wt.% of PGOH-*b*-PMMA

We can observe that the addition of 5 or 10 wt.% of the star copolymer to the reactive mixture slightly increases the viscosity values in comparison to pure DGEBA but not much in comparison to what happens when a linear polymer is added [25]. Thus it can be stated that the use of multiarm star topologies as modifiers is beneficial since a low pre-polymer viscosity is necessary for coatings applications.

Gelation parameters were also determined at 80 ºC by rheometry and they are collected in **Table 2**.

Table 2. Gelation, TGA and DMTA data obtained from DGEBA/1MI thermosets containing different proportions of multiarm star copolymer PGOH-*b*-PMMA

Formulation[a] (wt.%)	t_{gel} (min)	α_{gel}[b] (%)	$T_{\tan\delta}$[c] (ºC)	E'[d] (MPa)	T_{onset}[e] (ºC)
0	20.5	52	178	96.3	368
PGOH-*b*-PMMA					
5	21.5	28	158	53.2	354
10	23.4	32	156	64.1	338

a. % by weight of multiarm star copolymer.
b. Determined as the conversion reached by rheometry at 80 ºC and DSC tests at 10 ºC/min.
c. Temperature of maximum of the tan δ at 1 Hz.
d. Relaxed modulus determined at the $T_{\tan\delta}$ + 30 ºC.
e. Temperature of the onset decomposition on the TGA data at 10 ºC/min calculated for a 5 % of weight loss.

The gelation times are practically of the same order and slightly increase with the proportion of PGOH-*b*-PMMA. Conversion at the gel point (α_{gel}) decreases significantly on adding the star modifier but this decrease is not influenced by the proportion of the star. The lower conversion at the gel point can be explained if the modifier reacts, introducing a high multifunctionality in the system by the star topology with a high number of chain ends. This fact can derive in a cross-linked network at low epoxy conversion values. It should be noticed that there are bromoisobutyryl groups as chain ends of the star which could react with the

alkoxides formed by attack of the imidazole initiator to the epoxy ring. Alkoxide could lead to a nucleophilic substitution of the bromine in the activated *α*-position of the final carbonylic unit of bromoisobutyryl groups, connecting covalently the star to the epoxy matrix. In related works, we observed the contrary effect [24,13], that is the conversion at the gelation increases on adding a star shaped polymer. However, in that cases the star copolymers employed possessed hydroxyl groups at the end of the arms, which can undergo chain-transfer processes with alkoxides of activated polymer chains resulting in an increased number of growing chains. This fact accounts for a reduction of the kinetic chain length which leads to the subsequent higher conversion at the gel point whereas the covalent linkage of the modifier to the matrix has the contrary effect by inactivation of the growing chains [27].

Thermal and thermomechanical properties of the thermosets obtained

The materials obtained were characterized by DMTA. The tan *δ* and storage modulus (*E'*) plots against temperature for all the materials are represented in **Figure 4** (**a**) and (**b**) respectively, and the thermomechanical data collected in **Table 2**.

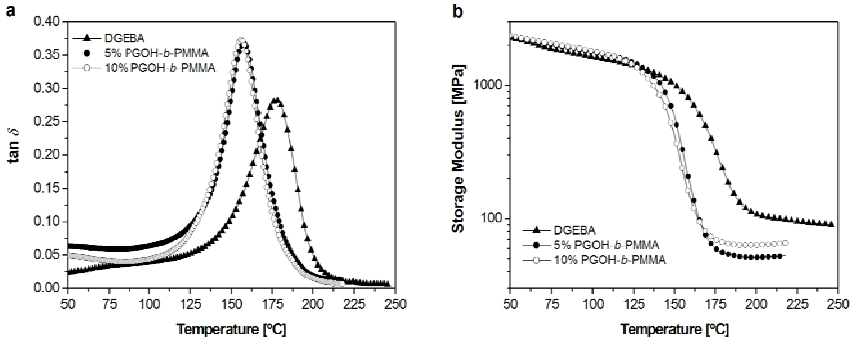

Figure 4 Tan *δ* (**a**) and storage modulus (*E'*) (**b**) against temperature at 1 Hz for the thermosets obtained

As we can see, all of tan *δ* curves are unimodal. This fact evidences the homogeneous character of the modified materials. The addition of star modifier decreases the tan *δ* value but this decrease is not affected by the proportion of the star since the material containing a 10 wt.% of PGOH-*b*-PMMA shows a temperature of tan *δ* similar to the one with a 5 wt.%. The height of the relaxation curves for star modified materials is greater than for the pure DGEBA thermoset which could be explained by a decrease of the crosslinking degree.

In **Figure 4** (**b**) can be appreciated that star modified thermosets possess a lower modulus after relaxation than pure DGEBA. This parameter is affected by the interpenetrating degree of the arms caused by the star topology. However, comparing both modified materials, the one containing a 10 wt.% of PGOH-*b*-PMMA show a higher modulus than the one with 5 wt.%. This fact could be

rationalized on the basis of the inherent rigidity of PMMA arms forming part of the special star topology which help maintaining the thermomechanical properties once the material has reached the rubbery state. A similar behavior in the trend of the moduli in the rubbery state was observed in epoxy thermosets modified with star copolymer with poly(styrene) arms [28].

The thermal stability of the materials obtained was investigated by thermogravimetry and the data are collected in **Table 2**. The modified thermosets show a slightly lower thermal stability than the unmodified thermoset. As we can see in **Figure 5**, the degradation curve shows an only process, due to the similar stability of C-O and C-C bonds of the epoxy matrix and PMMA arms, respectively.

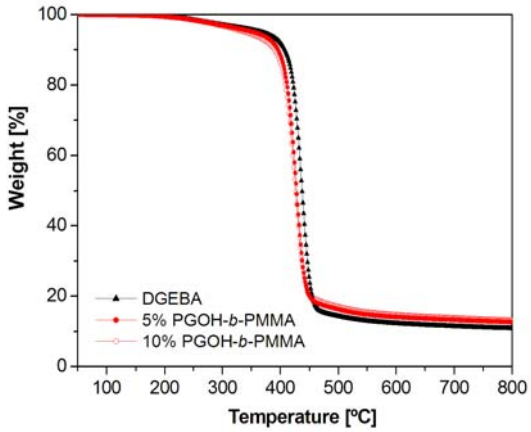

Figure 5 Thermogravimetric curves at 10 ºC/min in N_2 atmosphere of thermosetting materials obtained from DGEBA and DGEBA containing different proportions of PGOH-*b*-PMMA

Mechanical properties of the modified thermosets

Hyperbranched polymers (HBPs) have been widely studied in terms of toughness enhancers for epoxy resins and they could demonstrate their beneficial effect on this property [8,9,29]. However, until now not many data are available concerning the effect of multiarm star polymers as modifiers for epoxy resins on the impact strength [25].

The effect of adding PGOH-*b*-PMMA to the formulations in the impact strength is shown in **Figure 6** (**a**).

The values correspond to the energy consumption of the material in preventing crack propagation. It is possible to observe that the modification of DGEBA with the star copolymer improves this value in comparison with the neat material. The maximum improvement is reached for the modified thermoset containing a 10 wt.% of PGOH-*b*-PMMA since a 140 % of enhancement in reference to the neat material is obtained. The superior increase in toughness of multiarm star-modified thermosets obtained in the present study could be explained by the higher capacity of the arms of the star to interpenetrate into the epoxy

network and also to the special nanograined morphology observed by electron microscopy which will be commented below, but a lower degree of crosslinking achieved should be also considered.

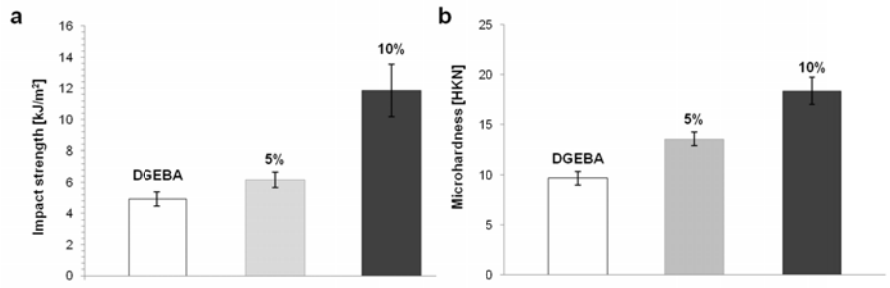

Figure 6 Impact strength (**a**) and microhardness (**b**) for the thermosets obtained

Microhardness measurements are very useful in rating coatings on rigid substrates for their resistance to mechanical abuse, such as that produced by blows, gouging and scratching. This property, generally, is related to the final mechanical properties of the material: elongation at break and strength at break. In materials presenting high values of these properties, the microhardness should be also high. As we can see in **Figure 6** (**b**), all modified materials have a higher hardness value because of the rigidity caused by the addition of the PMMA arms of the star. Again, the maximum improvement is reached for the modified thermoset containing a 10 wt.% of PGOH-*b*-PMMA since a 75 % of enhancement in reference to the neat material is obtained.

Morphology and fractography by SEM

The morphology of the surfaces of neat DGEBA (**a**) and DGEBA modified thermosets with a 5 wt.% (**c**) and a 10 wt.% of PGOH-*b*-PMMA (**e**) has been investigated by SEM and the micrographs are collected in **Figure 7**.

In the surface of the non-modified material (micrograph **a**) we cannot observe the presence of well-defined particles or phase-separation. However, a patterned roughness is visible which can be generated during the fast curing process that occurs when 1MI is used as anionic initiator. Comparing the non-modified material surface with the one of the thermosets containing PGOH-*b*-PMMA a higher roughness appears in the latter. In these micrographs (**c** and **e**), the surfaces present nanosized grains distributed all over the material. This special effect is observed for both star contents but when a 10 wt.% of modifier is added, these grains increase from 10-20 nm (with a 5 wt.% of star) to 60 - 80 nm in size, although bigger particles are also visible. In a previous work [20] we have determined the size of the stars in DMAc solution by light-scattering technique, which was approximately of 16 nm. Thus, the size of the grains is in accordance to the size of the molecule when the proportion of the star in the material is of 5 wt.%. When a higher proportion of modifier is present in the formulation aggregation of star molecules giving grains of a greater size can occur. However, the

nanopatterned appearance of the modified star thermosets could be also attributed to the effect of the star copolymer which could modify the curing process in the surrounding of the star molecule. It has been reported, that chain-wise polymerizations are intrinsically inhomogeneous since the increase of molecular weight of the polymer chains is not as regular as in polycondensations and the inhomogeneities formed become fixed by the crosslinks [23]. This behavior was also observed in a previous work regarding the DGEBA modification with a multiarm star based on a hyperbranched poly(styrene) core and poly(*ε*-caprolactone) arms [13]. In that study no mechanical properties were evaluated although the observation of the cryofracture also evidenced more ductile characteristics on increasing the proportion of star copolymer in the material.

From the micrographs of the fractures of the impacted materials (**Figure 7**), it can be appreciated that the neat epoxy material (**b**) appears as a smooth glassy surface with long unidirectional cracks. When the material contains 5 or 10 wt.% of PGOH-*b*-PMMA a different fracture is observed since high expanded cracks appear with river line pattern (**d** and **f**) which could be an indication of a more tough fracture in comparison with the neat thermoset. Therefore, the presence of a rougher nanostructured surface can be the responsible for the improvement of the matrix yielding and the subsequent increased toughness observed although the lower crosslinking density produced by the presence of the multiarm star structure cannot be discarded.

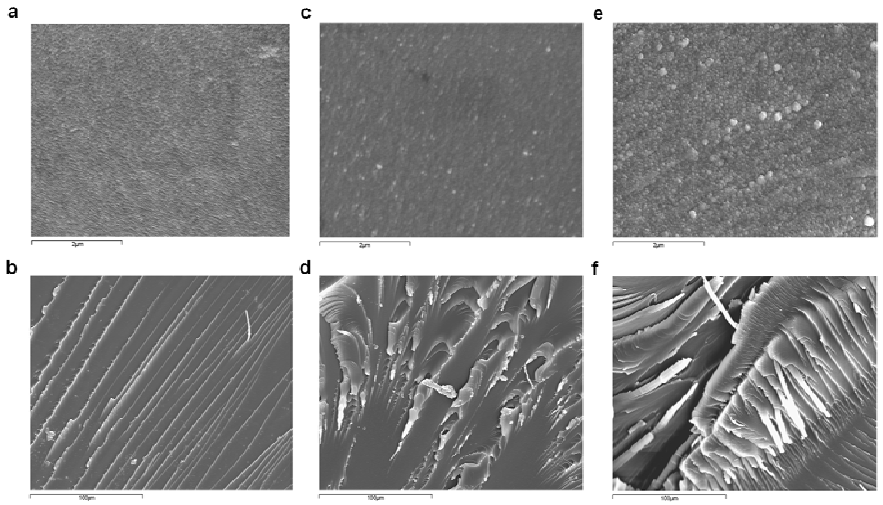

Figure 7 SEM micrographs of the morphology of surfaces of the following materials cured 1.5 h at 120 ºC and post-cured 1 h at 150 ºC: **a**) DGEBA; **c**) 5 wt.% PGOH-*b*-PMMA/DGEBA; **e**) 10 wt.% PGOH-*b*-PMMA/DGEBA; and the corresponding impacted surfaces: **b**) DGEBA; **d**) 5 wt.% PGOH-*b*-PMMA/DGEBA; **f**) 10 wt.% PGOH-*b*-PMMA/DGEBA

Conclusions

A multiarm star copolymer poly(glycidol)-*b*-poly(methyl methacrylate) (PGOH-*b*-PMMA) with an average number of PMMA arms per molecule of 85 was used as modifier for DGEBA resin cured anionically by 1-methyl imidazole. The addition of this modifier to the reactive mixture slightly accelerates the curing at conversions above 0.2.

The addition of the star copolymer slightly increased the viscosity of the DGEBA formulations and it is possible to state that the star topology does not worsen the processability of the neat DGEBA when added in a 5 wt.%.

Temperatures of the maximum of tan δ of the modified materials were lower than that of the neat DGEBA but higher than 150 ºC in all cases. The modulus in the rubbery state decreases on adding the star copolymer indicating a lower degree of crosslinking.

Impact strength was improved on adding PGOH-*b*-PMMA and the highest enhancement was obtained when a 10 wt.% of PGOH-*b*-PMMA was added to the formulation. Microhardness followed the same tendency and again, the best improvement was obtained for the thermosets with the highest star copolymer content studied.

The addition of PGOH-*b*-PMMA modifiers to the formulation allowed maintaining the homogeneous appearance of the materials but a nanograined morphology could be observed. On increasing the proportion of modifier the grains increased in size. The fracture surface changed from brittle to ductile on adding the modifier, especially when it was added in a 10 wt.%.

Thus, one can conclude that multiarm PGOH-*b*-PMMA star-like modifier is very suitable for epoxy resins enhancing toughness without harmfully affecting the curing, processability and thermomechanical characteristics.

Acknowledgements

The authors from the Universitat Rovira i Virgili and Universitat Politècnica de Catalunya would like to thank MICINN (Ministerio de Ciencia e Innovación) and FEDER (Fondo Europeo de Desarrollo Regional) (MAT2011-27039-C03-01 and MAT2011-27039-C03-02) and to the Comissionat per a Universitat i Recerca de la Generalitat de Catalunya (2009-SGR-1512). M.M. acknowledges the grant FI-DGR 2009 from the Catalonian Government.

References

[1] Frigione, M.E.; Mascia, L.; Acierno, D. Eur. Polym. J. **1995**, 31, 3649-3659.
[2] Ruiz-Pérez, L.; Royston, G.J.; Fairclough, J.P.A. Ryan, A.J. Polymer **2008**, 49, 4475-4488.
[3] Mezzenga, R.; Plummer, C.J.G.; Boogh, L.; Månson, J.A.E. Polymer **2001**, 42, 305-317.
[4] Pascault, J.P., Williams, R.J.J. *Epoxy Polymers.* Wiley-VCH, Weinheim, **2010**; Chapter 8, p. 237.
[5] Kaelble, D.H., Moacanin, J., Gupta, A. *Epoxy resins. Chemistry and Technology.* May, C.A., ed., Marcel Dekker, New York, **1988**, Chapter 6, p. 608.

[6] Remiro, P.M.; Marieta, C.; Riccardi, C.C.; Mondragon, I. Polymer **2001**, 42, 9909-9914.
[7] Guo, Q.; Habrard, A.; Park, Y.; Halley, P.J.; Simon, G.P. J. Polym. Sci., Part B: Polym. Phys. **2006**, 44, 889-899.
[8] Xu, G.; Shi, W.; Gong, M.; Yu, F.; Feng, J. Polym. Adv. Technol. **2004**, 15, 639-644.
[9] Yang, J.P.; Chen, Z.K.; Yang, G.; Fu, A.Y.; Ye, L. Polymer **2008**, 49, 3168-3175.
[10] Fu, J.F.; Shi, L.Y.; Yuan, S.; Zhong, Q.D.; Zhang, D.S.; Chen, Y.; Wu, J. Polym. Adv. Technol. **2008**, 19, 1597-1607.
[11] Karger-Kocsis, J.; Fröhlich, J.; Gryshchuk, O.; Kautz, H.; Frey, H.; Mülhaupt, R. Polymer **2004**, 45, 1185-1195.
[12] Meng, Y.; Zhang, X.H.; Du, B.Y.; Zhou, B.X.; Zhou, X.; Qi, G.R. Polymer **2011**, 52, 391-399.
[13] Morell, M.; Foix, D.; Lederer, A.; Ramis, X.; Voit, B.; Serra, A. J. Polym. Sci., Part A: Polym. Chem. **2011**, 52, 4694-4702.
[14] Zucchi, I.A.; Galante, M.J.; Williams, R.J.J. Polymer **2005**, 46, 2603-2609.
[15] Maiez-Tribut, S.; Pascault, J.P.; Soulé, E.R.; Borrajo, J.; Williams, R.J.J. Macromolecules **2007**, 40, 1268-1273.
[16] Blanco, M.; López, M.; Kortaberria, G.; Mondragon, I. Polym. Int. **2010**, 59, 523-528.
[17] Dean, J.M.; Verghese, N.E.; Pham, H.Q.; Bates, F.S. Macromolecules **2003**, 36, 9267-9270.
[18] Fan, W.; Zheng, S. Polymer **2008**, 49, 3157-3167.
[19] Sunder, A.; Hanselmann, R.; Frey, H.; Mülhaupt, R. Macromolecules **1999**, 32, 4240-4246.
[20] Morell, M.; Ramis, X.; Voit, B.; Serra, A.; Lederer, A .J. Polym. Sci., Part A: Polym. Chem. **2011**, 49, 3138-3151.
[21] Ramis, X.; Salla, J.M.; Mas, C.; Mantecón, A.; Serra, A. J. Appl. Polym. Sci. **2004**, 92, 381-393.
[22] Ramis, X.; Salla, J.M.; Cadenato, A.; Morancho, J.M. J. Thermal. Anal. Calorim. **2003**, 72, 707-718.
[23] Pascault, J.P., Sautereau, H., Verdu, J., Williams, R.J.J., *Thermosetting Polymers*, Marcel Dekker, New York, **2002**.
[24] Morell, M.; Lederer, A.; Ramis, X.; Voit, B.; Serra, A. J. Polym. Sci., Part A: Polym. Chem. **2011**, 49, 2395-2406.
[25] Morell, M.; Ramis, X.; Ferrando, F; Serra, A. Polymer **2011**, 52, 4694-4702.
[26] Higashihara, T.; Hayashi, M.; Hirao, A. Prog. Polym. Sci. **2011**, 36, 323-375.
[27] Fernández-Francos, X.; Cook, W.D.; Serra, A.; Ramis, X.; Liang, G.G.; Salla, J.M. Polymer **2010**, 51, 26-34.
[28] Morell, M.; Fernández-Francos, X.; Gombau, J.; Lederer, A.; Ramis, X.; Voit, B.; Serra, A. Prog. Org. Coat. *In press*, (DOI: 10.1016/j.porgcoat.2011.09.001).
[29] Fröhlich, J.; Kautz, H.; Thomann, R.; Frey, H.; Mülhaupt, R. Polymer **2004**, 45, 2155-2164.

UNIVERSITAT ROVIRA I VIRGILI
NOUS TERMOESTABLES EPOXÍDICS MODIFICATS AMB ESTRUCTURES DENDRÍTIQUES DE TIPUS HIPERRAMIFICAT I ESTRELLA
Mireia Morell Bel
DL:T. 155-2012

V.4

MULTIARM STAR POLY(GLYCIDOL)-*block*-POLY(STYRENE) AS MODIFIER OF ANIONICALLY CURED DIGLYCIDYLETHER OF BISPHENOL A THERMOSETTING COATINGS

Mireia Morell, Xavier Fernández-Francos, Jordi Gombau, Francesc Ferrando, Albena Lederer, Xavier Ramis, Brigitte Voit, Àngels Serra

Progress in Organic Coatings, In press (DOI: 10.1016/j.porgcoat.2011.09.001)

UNIVERSITAT ROVIRA I VIRGILI
NOUS TERMOESTABLES EPOXÍDICS MODIFICATS AMB ESTRUCTURES DENDRÍTIQUES DE TIPUS HIPERRAMIFICAT I ESTRELLA
Mireia Morell Bel
DL:T. 155-2012

Progress in Organic Coatings, *In press* (DOI: 10.1016/j.porgcoat.2011.09.001)

MULTIARM STAR POLY(GLYCIDOL)-*block*-POLY(STYRENE) AS MODIFIER OF ANIONICALLY CURED DIGLYCIDYLETHER OF BISPHENOL A THERMOSETTING COATINGS

Mireia Morell,[1] Xavier Fernández-Francos,[1] Jordi Gombau,[1] Francesc Ferrando,[2] Albena Lederer,[3] Xavier Ramis,[4] Brigitte Voit,[3] Angels Serra[1]

[1] Department of Analytical and Organic Chemistry, University Rovira i Virgili, C/ Marcel·lí Domingo s/n, Tarragona 43007, Spain.
[2] Department of Mechanical Engineering, Universitat Rovira i Virgili, C/ Països Catalans, 26, Tarragona 43007, Spain.
[3] Leibniz-Institut für Polymerforschung Dresden, Hohe Strasse 6, Dresden 01069, Germany.
[4] Thermodynamics Laboratory, ETSEIB University Politècnica de Catalunya, C/ Av. Diagonal 647, Barcelona 08028, Spain.

Abstract

Well-defined multiarm star copolymer poly(glycidol)-*b*-poly(styrene) (PGOH-*b*-PS) with an average number of PS arms per molecule of 85 has been prepared. The core first approach has been selected as the methodology using atom transfer radical polymerization (ATRP) of styrene to grow the arms from an activated hyperbranched poly(glycidol) as core. This activated hyperbranched macroinitiator was prepared by esterification of hyperbranched poly(glycidol) (PGOH) with 2-bromoisobutyryl bromide.

PGOH-*b*-PS was used to modify diglycidylether of bisphenol A coatings cured by anionic ring-opening mechanism using 1-methyl imidazole as the initiator. The kinetics of the curing process, studied by dynamic scanning calorimetry (DSC), was not much affected when PGOH-*b*-PS was added to the formulation. By rheometry the effect of this new polymer topology on the complex viscosity (η^*) of the reactive mixture was analyzed. The phase-separation of the modified coatings was proved by dynamic thermomechanical analysis (DMTA) and electronic microscopy (SEM and TEM) showing nano- or microphase separation as a function of the modifier content. The addition of this star polymer led to increase in the rigidity in terms of Young's modulus and in the microhardness in comparison to neat DGEBA.

Keywords: star polymers; hyperbranched; epoxy resin; anionic polymerization; thermosets

Introduction

Epoxy resins are known to be commonly used as thermosetting coating materials due to their excellent thermal and mechanical properties [1-3]. It has been observed that the formation of micro- or nanostructures in epoxy thermosets improves the overall properties without reducing the crosslinking degree of the epoxy matrix [4,5].

One of the possibilities employed to generate self-assembled structures is to start using a block copolymer completely miscible in the reactive mixture. In this case, phase separation of one of the blocks is achieved during the crosslinking polymerization while the other one remains miscible at high degree of conversion. This methodology has been commonly applied employing diblock, triblock or tetrablock linear copolymers [6]. Another alternative to the formation of

nanostructures in thermosets consists in the pre-selfassembly of block copolymers where the precursors of thermosets act as the selective solvents. The subsequent curing process preserves the formed nanophases in the matrix [7]. It has been reported that the size of these phases can be adjusted tuning the concentration of the modifier in the pre-cured mixture [8].

Additionally to linear block copolymers, multiarm stars can also be considered as a new class of modifier for epoxy resins capable of generating self-assembled matrices [9]. Using this strategy, Meng *et al.* obtained nanostructured diglycidylether of bisphenol A (DGEBA) thermosets using core-crosslinked stars (CCS) based on poly(styrene) core with poly(ethylene oxide) or poly(styrene)-*b*-poly(ethylene oxide) arms both synthesized by the "arm first" approach. The non-reactive end groups of the arms hinder the chemical incorporation of the star copolymers into the epoxy matrix [10,11]. We reported in a recent study the use of a hydroxyl-terminated multiarm star copolymer poly(styrene)-*b*-poly(ε-caprolactone), obtained by the "core first" approach strategy to modify DGEBA coatings. In that case, no evidence of clear nanophase separation of the star copolymer was obtained but a nanograined morphology was observed [12]. Therefore, different morphologies can be fixed depending on several factors: (i) the initial miscibility of the star copolymer in the epoxy resin, (ii) the reactivity of the multiarm star with the epoxy resin and (iii) the homogeneity of the pure thermosetting matrix mainly caused by the type of curing initiator employed.

In the present paper we describe the synthesis of a multiarm star block copolymer based on poly(glycidol)-*b*-poly(styrene) (PGOH-*b*-PS) by the "core first" approach [13-15]. To obtain it, we firstly synthesized hyperbranched poly(glycidol) which was subsequently activated by reaction with 2-bromoisobutyryl bromide. This activated hyperbranched polymer was used as macroinitiator to grow poly(styrene) arms by means of atom transfer radical polymerization (ATRP) to obtain the corresponding multiarm star copolymer.

Star polymer topology has proved to show some advantages over other modifiers such as linear or hyperbranched polymers. It offers a lower precursor polymer viscosity than the linear analogs because they behave like dense colloidal hairy particles making the arm relaxation by reptation difficult [16-18]. This characteristic is of main importance in coatings technology.

In the present work we propose the use of the synthesized multiarm star copolymer (PGOH-*b*-PS) as modifier of DGEBA thermosets cured anionically. The selection of PS arms aims to reach phase separated morphologies, because of their low reactivity and low compatibility in epoxy thermosets. Our goal is to investigate its influence on the curing process, the pre-polymer viscosity and the possible phase-separation on curing. Moreover, the effect of the polymer architecture and the phase separation on the mechanical properties will be discussed.

Experimental

Materials

Glycidol (96 %) was distilled under reduced pressure and stored over molecular sieves at 2 - 5 ºC, dioxane was dried over calcium hydride and subsequently distilled and styrene (St, 98 %) was passed through basic alumina column to remove the radical inhibitor. Trimethylolpropane (TMP) (97 %), potassium methylate solution (25 % v/v in methanol), CuBr (98 %), 2,2'-bipyridyl (Bpy, 99 %), 2-bromoisobutyryl bromide (98 %), anhydrous pyridine and 1-methyl imidazole (1MI, 99 %) were used without further purification. All these chemicals were purchased from Sigma-Aldrich.

All other reagents and solvents were purchased from Scharlab. Dialysis tubes based on regenerated cellulose membrane (MWCO 2,000 g/mol) were acquired from Roth. Diglycidylether of bisphenol A (DGEBA) Epikote Resin 827 was provided by Shell Chemicals (epoxide equivalent weight (EEW) = 182.1 g/eq, n = 0.082).

Synthesis of ATRP macroinitiator

Hyperbranched poly(glycidol) (PGOH, $\overline{M_n}$ (^{1}H NMR) 7,900 g/mol with an average of 100-110 hydroxyl groups per molecule) was prepared according to already published procedures [19,20] and dried under vacuum during 2 days at 50 ºC.

^{1}H NMR (400 MHz, DMSO-d_6) δ *ppm*: 4.8-4.3 (O**H**), 3.8-3.2 (C**H**O/C**H**OH/C**H$_2$**O/C**H$_2$**OH, poly(glycidol) backbone), 1.28 (C**H$_2$**, TMP in the PGOH) and 0.81 (C**H$_3$**, TMP in the PGOH); FTIR (ATR) (cm^{-1}): 3370 (OH), 1170-980 (C-O-C st as); $\overline{M_n}$ (SEC-MALLS) = 10,500 g/mol, $\overline{M_w}$ / $\overline{M_n}$ = 1.48; T_g (DSC) = -12 ºC and $T_{2\%}$ (TGA) = 373 ºC (2 % of mass loss).

The signal assignment and the degree of branching (DB) of PGOH, according to the Frey's definition, were determined according to a previous publication [21]. DB was 0.49, calculated from ^{13}C NMR signal intensities obtained under quantitative conditions.

The ATRP macroinitiator was prepared as reported previously by esterification of hyperbranched PGOH, previously synthesized, with 2-bromoisobutyryl bromide [14,22]. It was additionally purified by dialysis against chloroform during 3 days to completely remove low molecular weight impurities. The modified polymer possessed an average number of 85 2-bromoisobutyryl groups per molecule which correspond to a degree of modification of 80 %. The degree of modification was calculated by ^{1}H NMR spectroscopy of acidified sample with deuterated trifluoroacetic acid (TFA-d_1) to remove the remaining hydroxyl group signals from the signal region which is used to determine the signal intensity of the backbone protons.

^{1}H NMR (400 MHz, $CDCl_3$) *δ ppm*: 5.4-5.0 (m, C**H**-OOC-C$(CH_3)_2$-Br), 4.6-4.0 (m, C**H$_2$**-OOC-C$(CH_3)_2$-Br), 4.0-3.2 (m, C**H$_2$**/C**H** PGOH core), 1.95 (s, CH_2/CH-OOC-C(C**H$_3$**)$_2$-Br), 1.43 (CH_3-C**H$_2$**- TMP in the PGOH core) and 0.87 (C**H$_3$**-CH_2-TMP in the PGOH core); FTIR (ATR) (cm^{-1}): 1730 (C=O, st), 1170-980 (C-O-C st as); $\overline{M_n}$ (^{1}H NMR, $CDCl_3$) = 20,600 g/mol; T_g (DSC) = - 5 ºC and $T_{2\%}$ (TGA) = 278 ºC (2 % of mass loss).

Synthesis of PGOH-b-PS multiarm star copolymer

ATRP macroinitiator (0.25 g, 0.012 mmol, 1.02 mmol of bromine atoms), 34 g of styrene (325 mmol) and 0.16 g of Bpy (1.02 mmol) were placed in a 100 mL three-necked round flask and degassed by three freeze-pump-thaw cycles. Then, 0.15 g of CuBr (1.02 mmol) were added to the solution mixture under argon and the flask was immersed in an oil bath thermostated at 90 ºC. After 5.5 hours, the mixture was cooled down with liquid nitrogen, dissolved in 25 mL of THF. The reaction mixture was passed over neutral alumina to remove the copper compounds. The polymer was precipitated in cold ethanol twice to remove residual monomer, filtered and dried at 50 ºC under vacuum for 24 h. The signal assignments were in accordance to those described in a previous article [15].

^{1}H NMR (400 MHz, $CDCl_3$) *δ ppm*: 7.4-6.3 (PS backbone, **H$_{ar}$**), 4.7-4.4 (C**H**, PS ending group, **c**), 3.8-2.6 (C**H**/C**H$_2$**, PGOH backbone), 2.2-1.1 (C**H**/C**H$_2$**, PS backbone, **b**), 1.0-0.67 (C**H$_3$**, **a**); FTIR (ATR) (cm^{-1}): 3080 (arC-H, st), 2950-2890 (C-H, st), 1731 (C=O), 1220-1090 (C-O-C, st as); $\overline{M_n}$ (SEC-MALLS) = 190,700 g/mol, $\overline{M_w}/\overline{M_n}$ = 1.78; T_g (DSC) = 89 ºC and $T_{2\%}$ (TGA) = 224 ºC (2 % of mass loss).

Preparation of epoxy thermosets

The mixtures for curing through anionic ring-opening mechanism were prepared by adding the required amount of PGOH-*b*-PS, previously dissolved in dichloromethane, into the epoxy resin. Subsequently, solvent was eliminated under reduced pressure and dried under vacuum at 50 ºC during 12 h until the solution became clear. Then, 5 phr (parts of initiator per hundred parts of mixture) of 1-methyl imidazole (1MI) were added and the resulting solution was stirred and cooled down to - 10 ºC to prevent polymerization. Mixtures containing 2–5 wt.% (by weight) of PGOH-*b*-PS were prepared. The compositions of the formulations studied are detailed in **Table 1**.

Preparation of the epoxy coatings

The coating samples were prepared from liquid formulations, using prismatic rectangular PTFE moulds, of different sizes, placed between two metal sheets like a sandwich. The system was previously placed in the oven at 120 ºC. Afterwards, the mixture was introduced through it, filling the PTFE mould cavity. Finally, the system was introduced again in the oven and the sample was cured at 120 ºC during 1.5 hours and post-cured at 150 ºC an hour.

Characterization

^{1}H NMR and ^{13}C NMR measurements were carried out at 400 MHz and 100.6 MHz, respectively, on a Varian Gemini 400 spectrometer. $CDCl_3$ and DMSO-d_6 were used as solvents for all NMR measurements. For internal calibration the solvent signals were used: δ (^{13}C) = 77.16 ppm, δ (^{1}H) = 7.26 ppm for $CDCl_3$ and δ (^{13}C) = 39.52 ppm, δ (^{1}H) = 2.50 ppm for DMSO-d_6. Quantitative ^{13}C NMR experiments were recorded using a delay time between sampling pulses equal to 8 s and inverse gated proton decoupling.

The FTIR spectra were collected in a spectrophotometer FTIR-680PLUS from JASCO with a resolution of 4 cm^{-1}. This device was equipped with an attenuated-total-reflection accessory with a diamond crystal (Golden Gate heated single-reflection diamond ATR, Specac-Teknokroma).

The determination of molecular weights and molecular weight distributions were carried out on a modular build SEC-system on an Agilent 1200 series pump coupled with a multi-angle laser light scattering (MALLS) detector Tristar MiniDawn (Wyatt Technology) and Knauer RI detector in combination with a PolarGel-M-column (Polymer Laboratories) in DMAc mixed with 3 $g{\cdot}L^{-1}$ LiCl at a flow rate of 1mL/min. Astra 4.9 Software (Wyatt, USA) was used for evaluation of the results.

Calorimetric analyses were carried out on a Mettler DSC-822e thermal analyzer. Samples of approximately 5 mg in weight were placed in aluminum pans under nitrogen atmosphere. The calorimeter was calibrated using an indium standard (heat flow calibration) and an indium-lead-zinc standard (temperature calibration).

PGOH, the ATRP macroinitiator and the corresponding multiarm star polymer (PGOH-*b*-PS) were heated from – 50 to 150 ºC with a heating rate of 10 ºC/min, cooled down to – 100 ºC with a cooling rate of – 10 ºC/min and then heated again to 150 ºC at the same heating rate. T_g values were obtained from the second heating curves.

Non-isothermal curing experiments were performed from 30 to 250 ºC at heating rates of 10 ºC/min to determine the reaction heat and the kinetic parameters. In non-isothermal curing process the degree of conversion by DSC (α_{DSC}) was calculated as follows:

$$\alpha_{DSC} = \frac{\Delta H_T}{\Delta H_{dyn}} \quad (1)$$

where ΔH_T is the heat released up to a temperature T, obtained by integration of the calorimetric signal up to this temperature, and ΔH_{dyn} is the total reaction heat associated with the complete conversion of all reactive groups.

Thermogravimetric analyses were carried out in a Mettler TGA/SDTA 851e/LF/1100 thermobalance. Samples of the synthesized polymers and the complete cured materials with an approximate mass of 8 mg were degraded between 30 and 800 ºC at a heating rate of 10 ºC/min in N_2 (100 cm^3/min measured in normal conditions).

Dynamic mechanical analyses were carried out with a TA Instruments DMA Q800. The samples were cured isothermally in a mould at 120 ºC for 1.5 h and then post-cured for 1 h at 150 ºC. Single cantilever bending at 1 Hz was performed at 3 ºC/min, from 40 ºC to 250 ºC on prismatic rectangular samples (20 x 5 x 1.5 mm^3). Young's modulus was determined from the slope of a stress-strain curve recorded at 3 N/min from 0 to 18 N.

Rheological measurements were carried out in the parallel plates (geometry of 25 mm) mode with an ARG2 rheometer (TA Instruments, UK, equipped with a Peltier system).

Complex viscosity (η^*) of the pre-cured mixtures was recorded as function of angular frequency (0.1 – 50 rad/s) stating a constant deformation of 50 % at 80 ºC.

Microhardness was measured with a Wilson Wolpert (Micro-Knoop 401MAV) device following the ASTM D1474-98 (2002) standard procedure. For each material 10 determinations were made with a confidence level of 95 %. The Knoop microhardness (HKN) was calculated from the following equation:

$$HKN = L / A_p = L / l^2 \cdot C_p \quad (2)$$

where L is the load applied to the indenter (0.025 Kg), A_p is the projected area of indentation in mm^2, l is the measured length of long diagonal of indentation in mm, C_p is the indenter constant (7.028 x 10^{-2}) relating l^2 to A_p. The values were obtained from 10 determinations with the calculated precision (95 % of confidence level). The samples used were prismatic rectangular (20 x 5 x 1.5 mm^3) previously cured isothermally at 120 ºC for 1.5 h and then post-cured for 1 h at 150 ºC.

The impact test was performed at room temperature by means of an Izod 5110 impact tester, according to ASTM D 4508-05 (2008) using rectangular samples (25 x 12 x 2 mm^3). The pendulum employed had a kinetic energy of 0.56 J.

The fracture area of the specimens for impact tests was observed with an environmental scanning electron microscope (SEM) model Jeol JSM 6400 with a resolution of 3.5 nm.

Transmission electron microscopy (TEM) was performed with a Jeol 1011 microscope. The samples of the neat and modified PGOH-*b*-PS thermosets were prepared using an ultra microtome at room temperature and observed without previous staining.

Results and discussion

Synthesis and characterization of multiarm star poly(glycidol)-block-poly(styrene)

Hyperbranched poly(glycidol) (PGOH) was prepared according to previously published procedures by anionic polymerization of glycidol employing trimethylolpropane (TMP) as initiator [19,20]. Subsequently, the hydroxyl groups of PGOH were modified by esterification with 2-bromoisobutyryl bromide to generate an ATRP macroinitiator with an average number of 85 bromine sites per molecule. The NMR signal assignments and the quantification of bromine initiating sites were done in accordance to a previous article [14,22]. Finally, styrene was polymerized from the activated groups to obtain the corresponding multiarm copolymer by means of ATRP. The reaction was conducted under the same conditions as described by Liu *et al.* [15]. The synthetic pathway is depicted in **Scheme 1**.

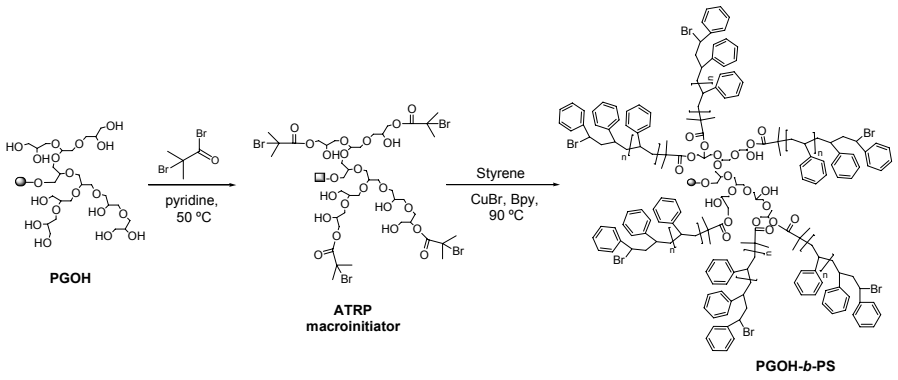

Scheme 1 Synthetic route to multiarm star copolymer PGOH-*b*-PS

In **Figure 1** the ^{1}H NMR spectrum of PGOH-*b*-PS is shown. As it can be seen, the main signals observed at 2.2-1.1 ppm (**b**) and 7.4-6.3 ppm ($\mathbf{H_{ar}}$) correspond to styrene repeating units of PS arms. The signal of the methyl protons of 2-bromoisobutyryl group introduced in the PGOH core is shifted to higher field, as a result of the styrene polymerization, from 1.95 ppm to 1.0-0.67 ppm (**a**) because of the change of the carbon-bromine bond to carbon-carbon bond of the tertiary carbon. Moreover, the methine proton of the styrene ending group (**c**) linked to a bromine atom appears between 4.7 and 4.4 ppm. The high molecular weight of PS arms and their high number lead to the broadening of PGOH signals (centered at

3.1 ppm) due to the lack of mobility of this core structure and the resulting shorter relaxation time in comparison with PS arms.

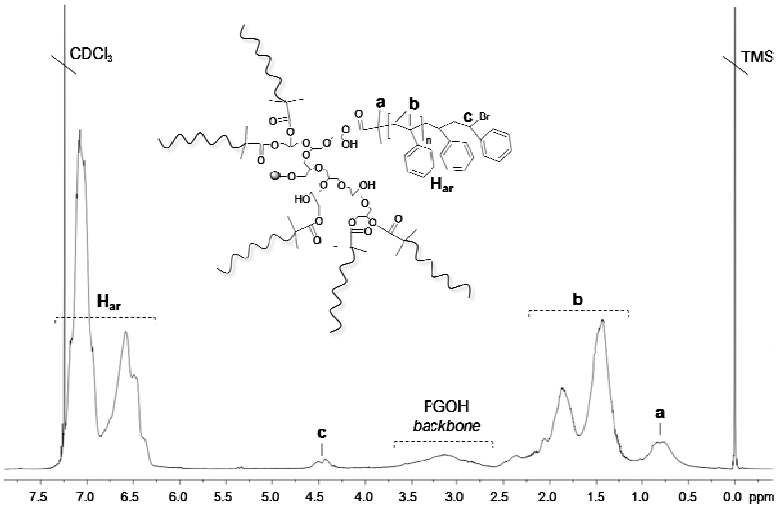

Figure 1 ^{1}H NMR spectra of the multiarm star copolymer synthesized (PGOH-*b*-PS) in $CDCl_3$. (The drawn structure possesses one PS arm for simplicity)

From the molar-mass distribution curves of PGOH core and the PGOH-*b*-PS multiarm star copolymer (**Figure 2**) one can appreciate that ATRP process has been done under controlled conditions since it shows a symmetrical distribution with a monomodal appearance, which indicates the well-defined nature of the polymer sample.

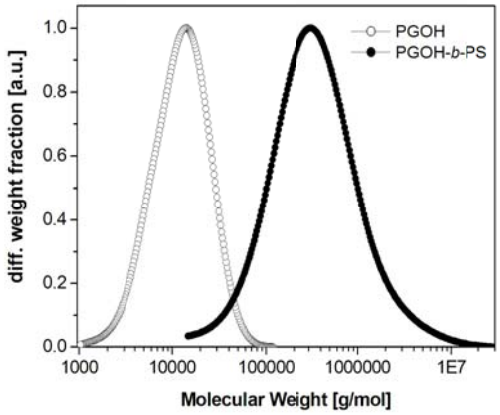

Figure 2 Molar mass distribution curves of PGOH core and the corresponding star copolymer PGOH-*b*-PS obtained by SEC-LS in DMAc

Therefore, the resulting multiarm star copolymer obtained possesses a high average molar mass ($\overline{M_n}$ = 190,700 g/mol) based on a hyperbranched poly(glycidol) core with an average molecular weight of 10,500 g/mol with an

average number of polystyrene arms of 85 and a degree of polymerization of about 20 styrene units per arm.

Study of the curing process by DSC

Differential scanning calorimetry was used to investigate the evolution of the anionic curing process using 5 phr 1-methyl imidazole (1MI) as the initiator. **Table 1** collects the calorimetric data of the formulations studied and their compositions in terms of the ratio between epoxy groups and initiatior (epoxy/initiator) and epoxy groups and hydroxyl groups from the DGEBA pre-polymer (epoxy/OH).

Table 1 Composition and enthalpy data of DGEBA/1MI mixtures with different percentages of PGOH-*b*-PS

PGOH-*b*-PS[a] (wt.%)	epoxy/ initiator	epoxy/ OH	Δ*h* (J/g)	Δ*h*[b] (kJ/ee)
0	9.0	24.4	638	116.1
2	8.8	24.1	483	94.0
5	8.5	23.8	460	92.1

a. % by weight of multiarm star copolymer.
b. Enthalpy value per equivalent of epoxy group.

From the values of enthalpy per gram we can see that they diminish on adding the star modifier (in 2 and 5 wt.%), due to the fact that the epoxy content is lowered. In addition, the enthalpy per epoxy equivalent is slightly lower in the formulations containing PGOH-*b*-PS but there is not much variation with the proportion of modifier.

Figure 3 shows the plot of conversion against temperature for all the studied formulations. The addition of the modifier slightly accelerates the curing process but not in a regular way.

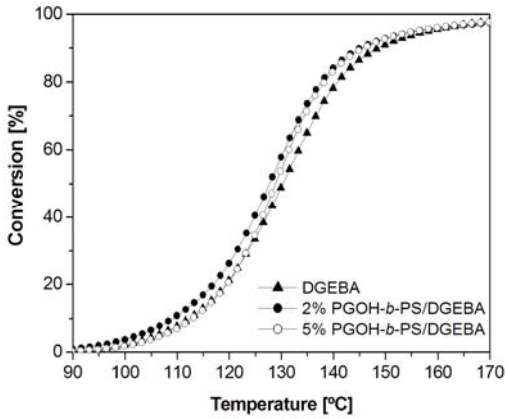

Figure 3 Conversion degree against temperature of the curing of DGEBA/1MI and DGEBA/1MI containing 2 and 5 wt.% of PGOH-*b*-PS at a heating rate of 10 ºC/min by DSC

There are some facts that can influence the curing kinetics of these formulations. On the one side, on increasing the percentage of modifier the initiator proportion per epoxy group increases, which should lead to an increased reactivity. On the other side, the addition of modifier increases slightly the viscosity of the mixture, which makes it difficult for the reaction to take place. Both factors could influence in a contrary way the kinetic behaviour of the curing process, explaining the non-regular reactivity order observed. However, the addition of this modifier to the reactive mixture did not affect, in a high extent, the curing process since no chemical incorporation of the star copolymer can be expected.

Evolution of complex viscosity (η) by rheometry*

Multiarm star-branched polymers compared to linear analogs with the same molecular weights present less entanglements in solution which leads to lower viscosity values [23]. Therefore, this topology is especially interesting for our purposes since coating technology requests low pre-polymer viscosities.

By rheological experiments the complex viscosity of the mixtures at 80 ºC was determined on varying the angular frequency, as it is shown in **Figure 4**.

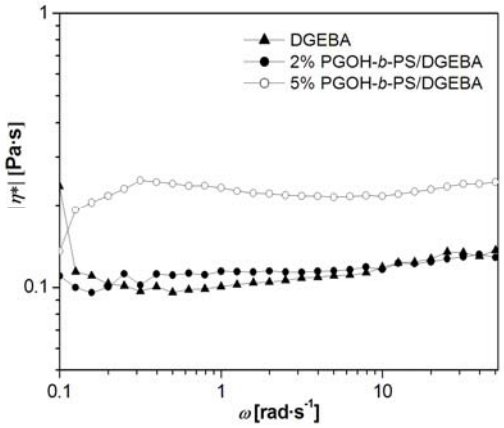

Figure 4 Complex viscosity (*η**) against angular frequency (*ω*) at 80 ºC for DGEBA/1MI and DGEBA/1MI containing 2 and 5 wt.% of PGOH-*b*-PS

All formulations show a Newtonian behavior in this range of frequencies. Moreover, we can see that on addition of 2 wt.% of the star polymer to the reactive mixture the viscosity values did not change at all compared to pure DGEBA and also addition of 5 wt.% of the star polymer led only to a slight increase. This fact evidences that the use of star shaped polymers does not worsen the processability of the pure epoxy resin even though a very high molar mass component has been added.

Progress in Organic Coatings, *In press* (DOI: 10.1016/j.porgcoat.2011.09.001)

Thermomechanical properties of the thermosets obtained

The materials obtained were characterized by DMTA. The tan *δ* and storage modulus (*E'*) plots against temperature for all the materials are represented in **Figure 5** and the thermomechanical data collected in **Table 2**.

Table 2 TGA, DMTA and mechanical properties data obtained from DGEBA/1MI thermosets containing different proportions of multiarm star copolymer PGOH-*b*-PS

	DMTA		TGA		Mechanical Properties[f]	
PGOH-*b*-PS[a] (wt.%)	$T_{\tan\delta}$[b] (ºC)	E'[c] (MPa)	T_{onset}[d] (ºC)	T_{max}[e] (ºC)	Young's Modulus (GPa)	Microhardness HKN
0	178	96.3	368	437	1.8 (0.1)	13.5 (0.5)
2	159	56.4	346	427	2.0 (0.1)	17.8 (0.7)
5	163	75.5	340	430	2.7 (0.0)	20.4 (0.3)

a. % by weight of multiarm star copolymer.
b. Temperature of maximum of the tan *δ* at 1 Hz.
c. Relaxed modulus determined at the $T_{\tan\delta}$ + 40 ºC.
d. Temperature of the onset decomposition on the TGA data at 10 ºC/min calculated for a 5 % of weight loss.
e. Temperature of the maximum rate of decomposition.
f. Standard deviations are shown in parentheses.

As we can see in **Figure 5** (**a**), the tan *δ* curves of neat DGEBA and DGEBA modified with PGOH-*b*-PS are unimodal, but the modified materials show a small relaxation, which is detected at around 90 ºC. This relaxation is more pronounced for the material containing 5 wt.% of the star copolymer. On increasing the proportion of star modifier, tan *δ* peak decreases. This fact is in accordance with the higher intensity of the relaxation curves observed for the modified materials which can be related to a lower crosslinking degree. This means that there is no complete phase separation and the partial solubility of the star in the epoxy matrix leads, according to the Fox equation [24], to a lower T_g.

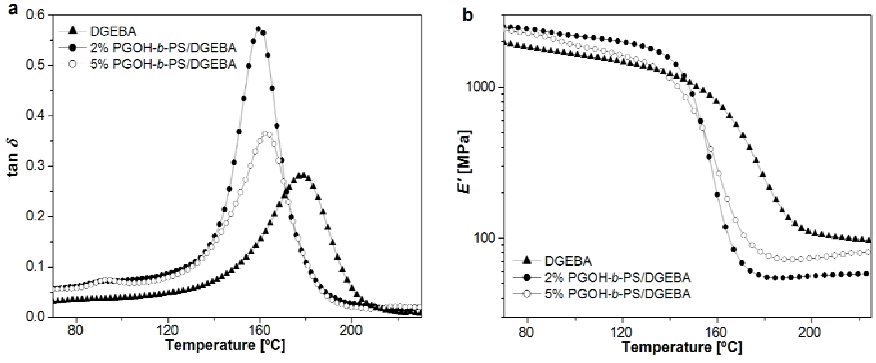

Figure 5 Tan *δ* (**a**) and storage modulus (*E'*) (**b**) against temperature at 1 Hz for the thermosets obtained

In **Figure 5** (**b**) the decrease of the modulus after relaxation on adding the modifier can be appreciated. This parameter is affected by the degree of crosslinking and the distance between crosslinks, which is higher for PGOH-*b*-PS

modified thermosets since star molecules prevent the formation of crosslinking points. However, a non-regular behaviour is observed again in this parameter, since 5 wt.% of modifier leads to a higher value of modulus than thermoset with a 2 wt.%. This could be related to the better solubility of the star in the matrix, when it is added in a low proportion as it will be discussed below.

Micrography by SEM and TEM of the materials obtained

In **Figure 6** the morphology of the samples can be observed by SEM and TEM. By means of both techniques a phase separation of PGOH-*b*-PS from the epoxy matrix can be appreciated for the modified materials in comparison to the neat thermoset (**a** and **b**), especially for the one containing 5 wt.% of modifier (**e** and **f**). More precisely, for the later material numerous polymer particles are observed with sizes varying from 1.0 to 1.5 μm. For the material containing 2 wt.% of PGOH-*b*-PS (**c** and **d**) we can observe that the disperse phase is formed as smaller particles (from 200 to 500 nm) and in a number which is not proportional to the amount of modifier introduced. From the evaluation of the area of the particles in the modified thermosets, we can evaluate that when 2 wt.% of PGOH-*b*-PS is used less than 1 % of it separates from the matrix, whereas in the material containing a 5 wt.% of the modifier a nearly complete segregation is observed. The differences in the phase separation agrees with the fact that the thermoset with 5 wt.% of PGOH-*b*-PS shows in DMTA a more pronounced relaxation corresponding to PS dispersed phase and a higher modulus of relaxation in the rubbery state.

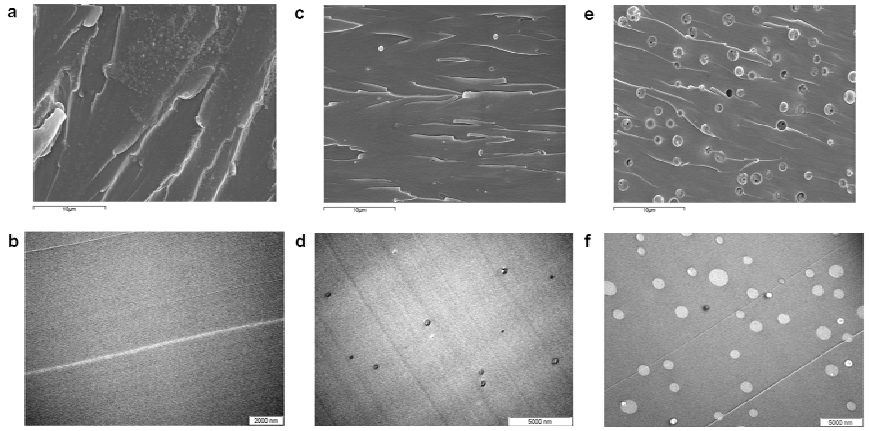

Figure 6 Electron micrographs for surfaces of the following materials: **a** (SEM, scale bar = 10 μm) and **b** (TEM, scale bar = 2000 nm) of DGEBA/1MI; **c** (SEM, scale bar = 10 μm) and **d** (TEM, scale bar = 5000 nm) of 2 wt.% PGOH-*b*-PS/DGEBA/1MI; **e** (SEM scale bar = 10 μm) and **f** (TEM, scale bar = 5000 nm) of 5 wt.% PGOH-*b*-PS/DGEBA/1MI

Moreover, no chemical bonding between particles and epoxy matrix can be assumed due to the unlikely chemical incorporation into the matrix of the star copolymer, mostly ended with bromine groups. This fact supports the small effect

observed by DSC on the curing process when DGEBA was modified with 2 - 5 wt.% of PGOH-*b*-PS.

Thermal stability of the materials

The thermal stability of the thermosetting coatings was investigated by thermogravimetry in nitrogen atmosphere and the data are collected in **Table 2**. The modified thermosets show a lower thermal stability than the neat thermoset, which can be attributed to the low thermal stability of the star polymer obtained by ATRP which involves the loss of hydrobromic acid [25] that could accelerate the random scission of polyether network structure.

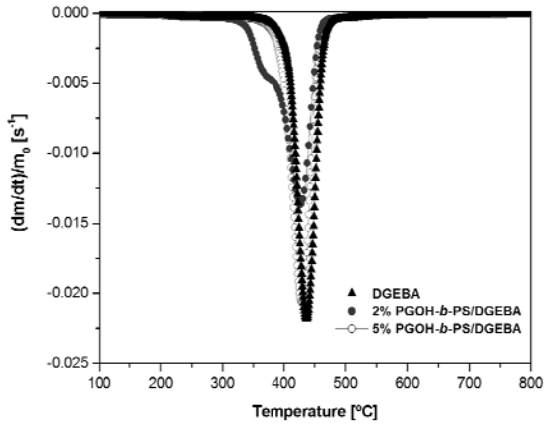

Figure 7 TGA derivative curves at 10 ºC/min in N_2 atmosphere of pure DGEBA and PGOH-*b*-PS modified DGEBA thermosets

From the derivative of the thermogravimetric curves (**Figure 7**) it is possible to observe that the modified coatings present a slightly faster degradation process in comparison with the neat one. It is important to note that the thermoset modified with 2 wt.% of PGOH-*b*-PS clearly shows a different behavior in comparison to the neat thermoset and the modified one with 5 wt.% of the star polymer. This fact could be rationalized by the partial solubility of PGOH-*b*-PS into the epoxy matrix before and after the curing process which results in mixed properties of the thermoset coming from the star copolymer and the epoxy resin. This behavior is in accordance with the scarcely phase separated particles observed by microscopy. In contrast, the material containing 5 wt.% of PGOH-*b*-PS shows a high similarity in material properties to the neat material due to the phase separated nature where the main component is the epoxy resin.

Mechanical properties

In **Table 2** the values of the Young's modulus obtained by DMTA and microhardness of the coatings studied are collected. As it can be seen, on increasing the proportion of the star copolymer the material stiffness increases,

since PS particles can reinforce the epoxy matrix at room temperature due to the glassy characteristics of this polymer.

Microhardness measurements are very useful in rating coatings on rigid substrates for their resistance to mechanical abuse, such as that produced by blows, gouging and scratching [26]. As we can see, the addition of star copolymer slightly increases this property in reference to pure cured DGEBA.

In terms of toughness improvement it is important to mention that no advances were observed on the impact strength comparing the modified PGOH-*b*-PS thermosets with the neat material (2.46 ± 0.62 kJ/m^2) and even this parameter decreased when the proportion of modifier is increased from 2 wt.% (0.69 ± 0.20 kJ/m^2) to 5 wt.% (0.66 ± 0.09 kJ/m^2). It is known that poly(styrene) is a commodity polymer with an inherent macroscale brittleness [27,28] but we expected that the use of a star architecture and the generation of micro or nano-phase separation would play a positive role in this property. The increased stiffness of the modified thermosets can also account for their lower toughness characteristics.

Conclusions

A multiarm star copolymer poly(glycidol)-*b*-poly(styrene) (PGOH-*b*-PS) with an average number of PS arms per molecule of 85 was prepared by the core-first strategy and the growth of the arms by ATRP. The high molar mass star copolymer ($\overline{M_n}$ = 190,700 g/mol) showed a relatively narrow molecular-weight distribution which proved its well-defined nature.

The star polymer was used as modifier in the curing of DGEBA by 1-methyl imidazole as an anionic initiator. The addition of this modifier to the reactive mixture did not affect the curing process since no chemical incorporation of the star copolymer was expected.

From the point of view of the processability, the addition of the high molar mass star polymer to DGEBA formulations did not significantly increase the viscosity in comparison to the neat formulation, which is very adequate for coating application.

The addition of PGOH-*b*-PS modifier to DGEBA allowed obtaining nano (2 wt.% PGOH-*b*-PS) or micro (5 wt.% PGOH-*b*-PS) phase separated morphologies.

The mechanical characterization allowed stating that on increasing the proportion of modifier the Young's modulus and microhardness increased. However, no improvements were observed in the impact strength.

Acknowledgements

The authors from the Universitat Rovira i Virgili and Universitat Politècnica de Catalunya would like to thank MICINN (Ministerio de Ciencia e Innovación) and FEDER (Fondo Europeo de Desarrollo Regional) (MAT2008-06284-C03-01 and MAT2008-06284-C03-02) and to the Comissionat per a Universitat i Recerca de la Generalitat de Catalunya (2009-SGR-1512). All

the authors thank to the Germany-Spanish collaboration program (HA2007-0022, DAAD PPP D/07/13493) for their financial support. M.M. acknowledges the grant FI-DGR 2009 from the Catalonian Government and the mobility fellowship from MICINN.

References

[1] May CA, editor. *Epoxy resins. Chemistry and technology.* Marcel Dekker, New York, **1988**, Chapter 1.
[2] Petrie, E.M. *Epoxy adhesive formulations.* McGraw-Hill, New York, **2006**.
[3] Pascault, J.P., Williams, R.J.J. *Epoxy Polymers. New Materials and Innovations,* Pascault, J.P., Williams R.J.J., editors, Wiley-VCH, Weinheim, **2010**, Chapter 1.
[4] Meng, F.; Xu, Z.; Zheng, S. Macromolecules **2008**, 41, 1411-1420.
[5] Maiez-Tribut, S.; Pascault, J.P.; Soulé, E.R.; Borrajo, J.; Williams, R.J.J. Macromolecules **2007**, 40, 1268-1273.
[6] Ruiz-Pérez, L.; Royston, G.J.; Fairclough, J.P.A. Ryan, A.J. Polymer **2008**, 49, 4475-4488.
[7] Bagheri, R.; Marouf, B.T.; Pearson, R.A. J. Macromol. Sci., Part C: Polym. Rev. **2009**, 49, 201-225.
[8] Lipic, P.M.; Bates, F.S.; Hillmyer, M.A. J. Am. Chem. Soc. **1998**, 120, 8963-8970.
[9] Meng, Y.; Zhang, X.H.; Du, B.Y.; Zhou, B.X.; Zhou, X.; Qi, G.R. Polymer **2011**, 52, 391-399.
[10] Kanaoka, S.; Sawamoto, M.; Higashimua, T. Macromolecules **1991**, 24, 2309-2313.
[11] Blencowe, A; Tan, J.F.; Goh, T.K.; Qiao, G.G. Polymer **2009**, 50, 5-32.
[12] Morell, M.; Foix, D.; Lederer, A.; Ramis, X.; Voit, B.; Serra, A. J. Polym. Sci., Part A: Polym. Chem. **2011**, 52, 4694-4702.
[13] Burgath, A.; Sunder, A.; Neuner, I.; Mülhaupt, R.; Frey, H. Macromol. Chem. Phys. **2000**, 201, 792-797.
[14] Morell, M.; Ramis, X.; Voit, B.; Serra, A.; Lederer, A .J. Polym. Sci., Part A: Polym. Chem. **2011**, 49, 3138-3151.
[15] Liu, C.; Zhang, Y.; Huang, J. Macromolecules **2008**, 41, 325-331.
[16] Morell, M.; Ramis, X.; Ferrando, F; Serra, A. Polymer **2011**, 52, 4694-4702.
[17] Erwin, B.M.; Cloitre, M.; Gauthier, M.; Vlassopoulos, D. Soft Matter **2010**, 6, 2825-2833.
[18] Lee, J.H.; Orfanou, K.; Driva, P.; Iatrou, H.; Hadjichristdis, N.; Lohse, D.J. Macromolecules **2008**, 41, 9165-9178.
[19] Sunder, A.; Hanselmann, R.; Frey, H.; Mülhaupt, R. Macromolecules **1999**, 32, 4240-4246.
[20] Kautz, H.; Sunder, A.; Frey, H. Macromol. Symp. **2001**, 163, 67-73.
[21] Kainthan, R.K.; Muliawan, E.B.; Hatzikiriakos, S.G.; Brooks, D.E. Macromolecules **2006**, 39, 7708-7717.
[22] Maier, S.; Sunder, A.; Frey, H.; Mülhaupt, R. Macromol. Rapid Commun. **2000**, 21, 226-230.
[23] Higashihara, T.; Hayashi, M.; Hirao, A. Prog. Polym. Sci. **2011**, 36, 323-375.
[24] Morell, M.; Fernández-Francos, X.; Ramis, X., Serra, A. Macromol. Chem. Phys. **2010**, 211, 1879-1889.
[25] Zhang, C.H.; Li, J.G.; Zhang, J.; Zhang, L.Y.; Li, H.Y. Polym. Adv. Technol. **2010**, 21, 710-719.
[26] Nielsen, L.E., Landel, R.F. *Mechanical Properties of Polymers and Composites*. 2nd ed., Marcel Dekker, New York, **1994**, p. 362.
[27] Donald, A.M.; Kramer, E.J. Polymer **1982**, 23, 1183-1188.
[28] Hasan, O.A.; Boyce, M.C. Polymer **1993**, 34, 5085-5092.

UNIVERSITAT ROVIRA I VIRGILI
NOUS TERMOESTABLES EPOXÍDICS MODIFICATS AMB ESTRUCTURES DENDRÍTIQUES DE TIPUS HIPERRAMIFICAT I ESTRELLA
Mireia Morell Bel
DL:T. 155-2012

CAPÍTOL VI

Conclusions

UNIVERSITAT ROVIRA I VIRGILI
NOUS TERMOESTABLES EPOXÍDICS MODIFICATS AMB ESTRUCTURES DENDRÍTIQUES DE TIPUS HIPERRAMIFICAT I ESTRELLA
Mireia Morell Bel
DL:T. 155-2012

1. The addition of hyperbranched poly(ester-amide)s to DGEBA/MTHPA systems in the presence of tertiary amine as a catalyst leads to the covalent incorporation of the HBP structure to the network, which produces a reduction of the global shrinkage, but specially of the shrinkage after gelation. This effect is more pronounced on increasing the molecular weight of HBP. The incorporation of ester groups to the network reduces the thermal stability and some of the modified thermosets can be classified as reworkable. The addition of S1200 to the formulation leads to an increase in toughness, Young's modulus and microhardness of the corresponding modified thermosets. The thermoset containing a 10 wt.% of H30000 is the one with the best mechanical characteristics of the materials modified with HBPs obtained from hexahydrophthalic anhydride. The improvements achieved in these modified materials are not accompanied by a worsening of the thermomechanical characteristics, and even an increase in the glass transition temperature is reached.

2. A new hyperbranched poly(amino-ester) (PAE) has been synthesized by means of a coupled-unsymmetric monomer methodology. The addition of PAE to DGEBA in the presence of 1-methyl imidazole as anionic initiator leads to the chemical incorporation of HBP to the network by a transfer chain reaction mechanism. The global shrinkage is notably reduced on adding the HBP modifier and there is a progressive improvement of thermal reworkability on increasing its proportion.

3. Multiarm stars with poly(glycidol) core and poly(*ε*-caprolactone) arms of different length (3,000 or 1,000 g/mol) have been obtained by the core-first strategy using ring opening polymerization. The addition of these modifiers to DGEBA with 1-methyl imidazole as initiator increases the gelation time and the conversion at the gel point. Global shrinkage is notably reduced on adding these modifiers, being the effect more pronounced on adding the star with long arms. Moreover, the addition of the star modifiers does not worsen significantly the processability of the reactive mixture and even it is improved on adding a 5 wt.% of the star with short arms.

4. In the curing of DGEBA initiated by $Yb(OTf)_3$, the addition of the poly(glycidol)-*b*-poly(*ε*-caprolactone) multiarm star with short arms leads to improvements in impact strength and shrinkage after gelation. On comparing with a linear poly(*ε*-caprolactone) analog, much better processability and mechanical characteristics are obtained with the star topology.

5. The synthesis of a new multiarm star based on HBP poly(styrene) core and poly(*ε*-caprolactone) arms has been carried out, by a three step synthetic pathway that includes: the polymerization of *p*-(chloromethyl) styrene by AGET/ATRP, the substitution of terminal chlorine groups to obtain the hydroxyl-ended derivative and finally, the polymerization of *ε*-caprolactone by cationic ring-opening. The addition of this modifier to DGEBA in anionic curing produces an increase in both the

conversion and time of gelation. Furthermore, the viscosity of the reactive mixture is not much increased by the addition of the star modifier. The materials obtained show, by SEM observation, a different morphology than the neat material, with a rougher nanograined appearance, which can be the responsible of the matrix yielding.

6. A set of multiarm star copolymers with different number of arms, from 45 to 85, based on a hyperbranched poly(glycidol) core and poly(methyl methacrylate) arms has been successfully synthesized by AGET/ATRP. After optimizing the polymerization conditions, well-defined structures with a narrow molar mass dispersity are obtained, reaching a high monomer conversion and avoiding star-star coupling. It is observed by AFM, that on increasing the number of arms, the size of the individual molecules increases from 80 to 200 nm. Moreover, it has been put in evidence that the higher the number of arms and the shorter their lengths the lower the complex viscosity in the melt state, which accounts for a higher compactness of the structure and a lower entanglement of the arms.

7. The poly(glycidol)-*b*-poly(methyl methacrylate) star showing the best rheological characteristics, has been used as a modifier in the anionic curing of DGEBA. The impact strength and microhardness of the thermosets experiment a regular improvement with the proportion of modifier, without dropping down their thermomechanical characteristics. This can be explained in the basis of the nanograined morphologies observed by SEM. The size of the particles increases on increasing the proportion of the star copolymer in the reactive mixture.

8. By ATRP, a multiarm star copolymer poly(glycidol)-*b*-poly(styrene) with an average number of PS arms per molecule of 85 has been prepared. Subsequently, it has been used to modify DGEBA anionic thermosets. In these materials, nano- or microphase separation is observed according to the proportion of the star modifier. Despite of the increase in microhardness and Young's modulus, no improvement in impact resistance is observed, which can be explained by the inherent fragile characteristics of PS.

ANNEXOS VII

UNIVERSITAT ROVIRA I VIRGILI
NOUS TERMOESTABLES EPOXÍDICS MODIFICATS AMB ESTRUCTURES DENDRÍTIQUES DE TIPUS HIPERRAMIFICAT I ESTRELLA
Mireia Morell Bel
DL:T. 155-2012

VII.1 ACRÒNIMS I SÍMBOLS

α	grau de conversió
$\alpha_{shrinkage}$	grau de contracció
A	factor pre-exponencial o absorbància
AFM	microscòpia de forces atòmiques
AGET	activador generat per transferència electrònica
ATRP	polimerització radicalària per transferència atòmica
BDMA	*N,N*-benzildimetilamina
Bpy	2,2'-bipiridina
***ε*-CL**	*ε*-caprolactona
4-CMS	4-clorometilestirè
CTE	coeficient d'expansió tèrmica
D	coeficient de difusió
δ	desplaçament químic (ppm) o desfasament entre la tensió i la deformació
dα/dt	velocitat de reacció o conversió
DB	grau de ramificació
DGEBA	diglicidilèter de bisfenol A
D.M.	grau de modificació
$\overline{DP}$	grau de polimerització promig
dh/dt	velocitat d'alliberament de calor durant un procés
DIPA	diisopropanolamina
DMF	*N*,*N*-dimetilformamida
DMTA	anàlisi termodinamomecànica
DSC	calorimetria diferencial d'escombrat
DMSO	dimetilsulfòxid
ε	absortivitat o deformació aplicada
E	mòdul de rigidesa/elasticitat
E'	mòdul d'emmagatzematge/elàstic
E''	mòdul de pèrdues
E_a	energia d'activació d'un procés
EEW	equivalent en pes d'epoxi
f(α)	funció diferencial del model cinètic d'un procés
FTIR-ATR	espectroscòpia d'infraroig amb transformada de Fourier – reflectança atenuada total
G'	mòdul d'emmagazematge/elàstic
G''	mòdul de pèrdues
g(α)	funció integral del model cinètic d'un procés
GC	cromatografia de gasos
h	gap (distància entre plats)

Δh	calor alliberada durant un procés
HBP	polímer hiperramificat
HHPA	anhídrid *cis*-hexahidroftàlic
I	intensitat
I.S.	resistència a l'impacte
I.W.	absorció d'aigua
k	constant de velocitat d'un procés
KCL	longitud de cadena cinètica
KHN	nombre de duresa Knoop
L	longitud o gruix
$\overline{M}_n$	pes molecular promig en nombre
$\overline{M}_w$	pes molecular promig en pes
$\frac{\overline{M}_w}{\overline{M}_n}$	polidispersitat (PDI o D)
MALLS	dispersió de llum làser multiangular
MeOH	metanol
M.H.	microduresa
1MI	1-metilimidazole
MMA	metil metacrilat
MTHPA	anhídrid metiltetrahidroftàlic
η^*	viscositat complexa
NMR	espectroscòpia de ressonància magnètica nuclear
N_{OH}	nombre hidroxíl·lic
OTf	trifluorometansulfonat
PAE	poli(amino-ester) hiperramificat
phr	parts d'iniciador per cent parts de mescla de monòmers
PCL	poli(*ε*-caprolactona)
PGOH	poliglicidol hiperramificat
PMDETA	*N,N,N',N',N''*-pentametildietilentriamina
PMMA	poli(metil metacrilat)
PS	poli(*p*-clorometilestirè) hiperramificat o poliestirè lineal (braços en un polímer estrella)
PSOH	poli(*p*-clorometilestirè) hiperramificat modificat amb grups hidroxil terminals
ρ	densitat
R	constant del gasos ideals
R_g	radi de gir
RI	índex de refracció
ROP	polimerització per obertura d'anell
R.U.	unitat repetitiva
σ	tensió aplicada

SA	anhídrid succínic
SCVP	autopolicondensació vinílica
SEC	cromatografia d'exclusió per tamany
SEM	microscòpia electrònica d'escombrat
S_{gel}	contracció després de la gelificació
Sn(Oct)$_2$	2-etilhexanoat d'estany
St	estirè
T	temperatura
T_2	temps de relaxació spin-spin
t	temps
TEM	microscòpia electrònica de transmissió
TGA	anàlisi termogravimètrica
THF	tetrahidrofurà
TIPA	triisopropanolamina
TMA	anàlisi termomecànica
TMP	trimetilolpropà
T_g	temperatura de transició vítria
ω	freqüència angular
wt.%	percentatge en pes

UNIVERSITAT ROVIRA I VIRGILI
NOUS TERMOESTABLES EPOXÍDICS MODIFICATS AMB ESTRUCTURES DENDRÍTIQUES DE TIPUS HIPERRAMIFICAT I ESTRELLA
Mireia Morell Bel
DL:T. 155-2012

VII.2 PUBLICACIONS INCLOSES A LA TESI

Morell, M.; Ramis, X.; Ferrando, F.; Serra, A. *New improved thermosets obtained from diglycidylether of bisphenol A and a multiarm star copolymer based on hyperbranched poly(glycidol) core and poly(methyl methacrylate) arms.* Macromolecular Chemistry and Physics. In press (DOI: 10.1002/macp.201100497).

Morell, M.; Fernández-Francos, X.; Gombau, J.; Ferrando, F.; Lederer, A.; Ramis, X.; Voit, B.; Serra, A. *Multiarm star poly(glycidol)-block-poly(styrene) as modifier of anionically cured diglycidylether of bisphenol A thermosetting coatings.* Progress in Organic Coatings. In press (DOI: 10.1016/j.porgcoat.2011.09.001)

Morell, M.; Foix, D.; Lederer, A.; Ramis, X.; Voit, B.; Serra, A. *Synthesis of a new multiarm star polymer based on hyperbranched poly(styrene) core and poly(ε-caprolactone) arms and its use as reactive modifier of epoxy thermosets.* Journal of Polymer Science, Part A: Polymer Chemistry **2011**, 49, 4639-4649.

Morell, M.; Ramis, X.; Ferrando, F.; Serra, A. *Effect of polymer topology on the curing process and mechanical characteristics of epoxy thermosets modified with linear or multiarm star poly(ε-caprolactone).* Polymer **2011**, 52, 4694-4702.

Morell, M.; Voit, B.; Ramis, X.; Serra, A.; Lederer, A. *Synthesis, characterization, and rheological properties of multiarm stars with poly(glycidol) core and poly(methyl methacrylate) arms by AGET ATRP.* Journal of Polymer Science, Part A: Polymer Chemistry **2011**, 49, 3138-3151.

Morell, M.; Lederer, A.; Ramis, X.; Voit, B.; Serra, A. *Multiarm star poly(glycidol)-block-poly(ε-caprolactone) of different arm lengths and their use as modifiers of diglycidylether of bisphenol A thermosets.* Journal of Polymer Science, Part A: Polymer Chemistry **2011**, 49, 2395-2406.

Morell, M.; Fernández-Francos, X.; Ramis, X.; Serra, A. *Synthesis of a new hyperbranched polyaminoester and its use as a reactive modifier in anionic curing of DGEBA thermosets.* Macromolecular Chemistry and Physics **2010**, 211, 1879-1889.

Morell, M.; Erber, M.; Ramis, X.; Ferrando, F.; Voit, B., Serra, A. *New epoxy thermosets modified with hyperbranched poly(ester-amide) of different molecular weight.* European Polymer Journal **2010**, 46, 1498-1509.

Morell, M.; Ramis, X.; Ferrando, F.; Yu, Y.; Serra, A. *New improved thermosets obtained from DGEBA and a hyperbranched poly(ester-amide).* Polymer **2009**, 50, 5374-5378.

VII.3 PUBLICACIONS RELACIONADES AMB LA TESI

Morell, M.; Fernández-Francos, X.; Ramis, X.; Serra, A. *Kinetic study by FTIR and DSC on the thermal curing of DGEBA/MTHPA system catalyzed with different type of initiators.* En preparació.

Foix, D.; Khalyavina, A.; Morell, M.; Voit, B.; Lederer, A.; Ramis, X.; Serra, A. *Influence of the degree of branching of a hyperbranched polyester used as reactive modifier in epoxy thermosets.* Macromol. Mat. Eng. **2011**. In press (DOI: 10.1002/mame.201100078).

Santiago, D.; Morell, M.; Fernández-Francos, X.; Serra, A.; Salla, J.M.; Ramis, X. *Influence of the end groups of hyperbranched poly(glycidol) on the cationic curing and morphology of diglycidylether of bisfenol a thermosets.* React. Funct. Polym. **2011**, 71, 380-389.

VII.4 PARTICIPACIÓ A CONGRESSOS

Autors: Serra, A.; Morell, M.; Foix, D.; Lederer, A.; Ramis, X.; Voit, B.
Pòster: "Synthesis of a new multiarm star polymer based on hyperbranched poly(styrene) core and poly(*ε*-caprolactone) arms and its use as reactive modifier of epoxy thermosets."
Congrés: 9th Advanced Polymers via Macromolecular Engineering.
Lloc/Data: Cappadocia (Turquia), del 5 al 8 de Setembre del 2011.

Autors: Morell, M.; Lederer, A.; Ramis, X.; Voit, B.; Serra, A.
Comunicació oral: "Anionic crosslinking of mixtures of diglycidylether of bisphenol a with multiarm star poly(glycidol)-*b*-poly(*ε*-caprolactone) of different arm lengths."
Congrés: European Polymer Congress 2011.
Lloc/Data: Granada (Espanya), del 26 de Juny al 1 de Juliol del 2011.

Autors: Morell, M.; Komber, H.; Ramis, X.; Voit, B.; Serra, A.; Lederer, A.
Pòster: "Synthesis of multiarm star polymers based on hyperbranched poly(glycidol) with poly(methyl methacrylate), poly(styrene) and poly(*ε*-caprolactone) arms."
Congrés: Macro2010 43rd IUPAC World Polymer Congress.
Lloc/Data: Glasgow (Escòcia), del 11 al 16 de Juliol del 2010.

Autors: Morell, M.; Ramis, X.; Ferrando, F.; Serra, A.
Comunicació oral: "Nuevos materiales termoestables con base epoxi modificados con poli(ester-amidas) hiperramificadas."
Congrés: 5ª reunión de jóvenes investigadores en polímeros (JIP 2010).
Lloc/Data: Calella de Palafrugell (Espanya), del 2 al 6 de Maig del 2010.

Autors: Morell, M.; Erber, M.; Ramis, X.; Ferrando, F.; Salla, J.M.; Voit, B.; Serra, A.
Pòster: "Influence of the molecular weight of a poly(ester-amide) hyperbranched polymer on the characteristics of modified epoxy thermosets."
Congrés: 8th Advanced Polymers via Macromolecular Engineering.
Lloc/Data: Dresden (Alemanya), del 4 al 7 d'Octubre del 2009.

Autors: Morell, M.; Mantecón, A.; Ramis, X.; Serra, A.
Pòster: "Obtención de un poli(*β*-aminoester) hiperramificado polihidroxílico y su utilización como modificante reactivo de DGEBA."
Congrés: 11ª Reunión del Grupo especializado en Polímeros (GEP 2009).
Lloc/Data: Valladolid (Espanya), del 20 al 24 de Setembre del 2009.

Autors: Morell, M.; Yu, Y.; Ramis, X.; Salla, J.M.; Ferrando, F.; Mantecón, A.; Serra, A.
Pòster: "New thermosets from DGEBA and poly(ester-amide) hyperbranched polymers cured with methyltetrahydrophthalic anhydride."
Congrés: Frontiers in Polymer Science.
Lloc/Data: Mainz (Alemanya), del 7 al 9 de Juny del 2009.

VII.5 ESTADES INTERNACIONALS

Centre de destí: Leibniz-Institut für Polymerforschung Dresden e.V. (Dresden, Alemanya).
Període: del 14 de Setembre al 15 de Novembre de 2009 i del 14 de Gener al 5 d'Abril del 2010.

UNIVERSITAT ROVIRA I VIRGILI
NOUS TERMOESTABLES EPOXÍDICS MODIFICATS AMB ESTRUCTURES DENDRÍTIQUES DE TIPUS HIPERRAMIFICAT I ESTRELLA
Mireia Morell Bel
DL:T. 155-2012